THE DESIGN, IMPLEMENTATION, AND ASSESSMENT OF STUMBLE RECOVERY BEHAVIORS FOR ROBOTIC LOWER-LIMB PROSTHESES AND EXOSKELETONS

By

Maura E. Eveld

Dissertation

Submitted to the Faculty of the

Graduate School of Vanderbilt University

in partial fulfillment of the requirements

for the degree of

DOCTOR OF PHILOSOPHY

in

Mechanical Engineering

August 31, 2022

Nashville, Tennessee

Committee:

Karl Zelik, Ph.D.

Michael Goldfarb, Ph.D.

Gerasimos Bastas, Ph.D.

David Braun, Ph.D.

Eric Barth, Ph.D.

ACKNOWLEDGMENTS

To start, I would like to wholeheartedly thank Dr. Zelik and Dr. Goldfarb for their invaluable mentorship throughout my Ph.D. journey. Dr. Zelik's investment in me was clear from the start, and his guidance along the way helped me to be a better engineering researcher and scientific communicator. Dr Goldfarb's unwavering support and constant willingness to help, from reframing a research question to troubleshooting a controller, helped me grow both intellectually and technically. Together, they have curated a remarkably intelligent, curious, hardworking, collaborative, and inclusive research team, and that is no doubt a testament to their dedicated and encouraging mentorship styles.

I would also like to thank the rest of my dissertation committee: Dr. Bastas, Dr. Barth, and Dr. Braun. They not only provided thoughtful and impactful feedback on my dissertation work, but also offered genuine interest in and concern for my experience at Vanderbilt, which made my time here all the more positive.

Next, I owe immense gratitude to all members of CREATe: students, postdocs, and staff – past and present. I feel so lucky to have researched alongside this group of brilliant, supportive, question-asking, answer-seeking, fun-appreciating colleagues, mentors, and friends. They made this experience an unforgettable one.

Of course, this dissertation work simply would not have been possible without the commitment of many study participants. Their willingness to spend hours in the lab for experiments, as well as their crucial, informative feedback throughout the process, ultimately drove these innovations, and I am so appreciative of their investment.

I must also acknowledge my undergraduate experiences that led me down this research path. As an undergraduate researcher at the University of Notre Dame's Tissue Mechanics Lab, I drew inspiration from weekly lab meetings, seeing for the first time the importance (and excitement) of asking relevant research questions, conducting thoughtful experiments, and disseminating meaningful results. As an experimental biomechanics intern at the Johns Hopkins University Applied Physics Lab, I witnessed the rewards of performing involved, rigorous experiments with purpose, drive, and humor – and with that the true value of teamwork.

I also had tremendous support outside of the research space, for which I am immensely thankful. The friendships I have made in Nashville turned this city into a home. And the support of my friends and family from Notre Dame, St. Louis, and Kansas City did not go unnoticed.

I would like to specifically thank my immediate family, whose steadfast encouragement, kindness, and advocacy has never faded. I am deeply grateful.

Lastly, I would like to acknowledge my funding sources, the National Institutes of Health and the National Science Foundation Graduate Research Fellowship, that enabled this research and my research experience.

TABLE OF CONTENTS

LIST OF TABLES

LIST OF FIGURES

CHAPTER 1

Introduction

1.1 Stumble Recovery: A gap in robotic lower-limb wearable assistive device development

Assistive technology (i.e., devices intended to assist or augment human performance from rehabilitation to industrial settings) is a rapidly growing field and market. Lower-limb wearable assistive devices such as prostheses and exoskeletons (Fig. 1.1) have shown promise as a means for individuals to regain independence, rehabilitate weaknesses, decrease injury risk, or augment performance [125].

Figure 1.1: Examples of lower-limb wearable assistive devices. From left to right, Berkeley Lower Extremity Exoskeleton (BLEEX) [128], Parker Indego, Ottobock C-Leg, Michigan Open-Source Robotic Leg [3]

Initially, research for these devices focused on optimizing the design and control for proper assistance during level-ground walking, often the primary task of their intended use; however, in order for these devices to be safe and ultimately adopted in the real world, they need to be functional and robust for all aspects of daily life. Thus there have been recent efforts to direct research towards more non-steady state daily tasks such as turning, walking on uneven terrain or slopes, responding to unexpected disturbances or perturbations, and transitions among these activities [91]. In order to truly be useful, it is crucial that lower-limb wearable assistive devices demonstrate effectiveness and safety in these environments outside the lab.

An unexpected perturbation that is of primary concern is the event of a stumble, which is a major cause of falls and subsequent injury [117, 4]. In this work, a stumble is defined as the event in which the foot unexpectedly encounters an obstacle in swing phase, which requires a corrective response to clear the obstacle and recover without falling. Examples of stumbles (Fig. 1.2) abound in daily life (e.g., encountering an uneven sidewalk on a walk, flooring variations in the home, a child's toy on the floor, etc.) and the workplace (e.g., contacting cord covers, warehouse obstacles, rippled carpets, etc.). Moreover, stumbles are an eventuality for both prosthesis and exoskeleton users, but a safe, beneficial response in this scenario has not been properly explored for either device.

1.1.1 Prostheses

1.1.1.1 Motivation for stumble recovery research for prostheses

The transfemoral prosthesis user population (i.e., individuals with an amputation or congenital defect such that their lower limb ends above the knee joint) experiences a substantially high fall rate compared to the healthy population [53,

Figure 1.2: Daily-life stumble scenarios

95, 114, 46, 49]. This not only leads to higher injury incidence and medical costs, but also incurs psycho-social burdens such as fear of falling and loss of confidence, which ultimately affects physical fitness, community engagement, and overall well-being [68, 65, 53, 49]. Therefore addressing stumble recovery for transfemoral prosthesis users could have a transformative impact on this population.

While retrospective studies provide this fall prevalence data, it is important to understand what specific factors lead to falls for this population. A few studies have analyzed stumble recovery for transfemoral prosthesis users, and there is evidence that both prosthetic-side and sound-side stumbles need to be addressed [17, 108, 48]. However, limitations in study design and inconsistent results from previous works motivate further investigation. The field would benefit from a more comprehensive understanding of the specific deficiencies that lead to falls for this population in order to inform potential interventions.

1.1.1.2 Current state of prosthetic technology for stumble recovery

Transfemoral prosthesis users are typically prescribed prosthetic knees that are energetically passive, and as such lack the power at the knee and ankle joints exhibited by the biological limb. These devices achieve swing phase motion using the double-pendulum inertial mechanics of the swing limb driven by the thigh motion of the user. Such functionality necessarily requires a low-impedance knee joint during swing, which make the devices particularly susceptible to swing-phase perturbations. Furthermore, swing-stance transitions and stance-phase support are both more compromised than in the healthy limb, therefore making them more susceptible to stance knee buckling in the case when full knee extension is not achieved prior to heel-strike.

There have been some attempts to incorporate stumble responses into prosthetic knees. For example, with the rise of microprocessor-controlled knees (i.e., knees with onboard sensors and microcontrollers that can change passive knee parameters in real-time) came added stumble response functionality. For example, the Ottobock C-Leg increases flexion resistance during the extension portion of swing phase so that the knee can safely be loaded in the event of a stumble [7]. Indeed, several studies have shown the C-Leg performs better with respect to stumble perturbations and fall risk [11, 7, 8, 41, 46, 12]. However, studies thus far have used a rope-tug procedure during swing extension to simulate a trip, which may not accurately represent a stumble since there is no physical obstacle to clear; furthermore, falls and compensation techniques were still reported in these studies. Regardless, microprocessor-controlled knees still cannot provide any active response as a healthy biological limb would both during and following a stumble perturbation.

In order to provide some of the powered behaviors exhibited by the healthy knee joint, many researchers have turned to powered prosthetic devices, which have the potential to address the deficiencies of typically prescribed passive knees. Indeed, active flexion and extension provided by powered prosthetic knees [56, 58, 3] have been shown to be beneficial for walking, stair climbing, and other activities of daily living. In fact, there are currently two powered prosthetic knees on the market (Ossur PowerKnee and Reboocon Bionics IntelLeg Knee). However, research in the area of stumble recovery for powered prosthetic knees is limited. While many works have investigated methods for perturbation detection and recovery strategy selection without implementation in an actual device [55, 126], and a few

have implemented responses with limited testing in an able-bodied adaptor [115], successful implementation of active stumble recovery behaviors with a transfemoral prosthesis user has not yet been reported.

Furthermore, to date there has been no development of potential prosthetic interventions that mitigate the effects of stumbles to the sound limb. Investigations into the response of transfemoral prosthesis users to sound-side stumbles, insights into what may improve their recovery rate, and testing of such interventions is a wholly unexplored area of stumble recovery that is crucial for ultimately reducing fall risk for this population.

1.1.1.3 Open questions considered in this work

- How do transfemoral prosthesis users respond to stumbles?
- What deficiencies in these responses lead to falls?
- What interventions might improve stumble recovery?
- Can introducing powered stumble recovery behaviors into prosthetic knees improve responses and/or mitigate falls?

1.1.2 Exoskeletons

1.1.2.1 Motivation for stumble recovery research for exoskeletons

Incorporating stumble recovery behaviors into lower-limb exoskeletons may serve two crucial purposes. To start, it may mitigate falls that would have otherwise been caused by the exoskeleton itself. Without an incorporated stumble response, existing mechanical or control features of an exoskeleton (e.g., added weight, joint impedance, or restrictive controller) might limit the ability of the exoskeleton user to react adequately to an unexpected stumble. This is especially concerning for individuals using these devices as walking aids (e.g., stroke survivors, post-polio patients, spinal cord injury patients, elderly patients), as they may be particularly unable to compensate for these constraints due to muscle weakness or neurological impairment.

Aside from the potential fall risk induced by the exoskeleton itself, many populations experience a high fall risk regardless of exoskeleton use and could benefit from external stumble recovery assistance. Falls are a major cause of injury for many patient groups (e.g., stroke survivors [45], older adults [33], and post-polio patients [66]) due to muscle weakness, delayed reaction times, decreased range of motion, among other causes. Robotic lower-limb exoskeletons, therefore, have the potential to improve recovery in the event of a stumble by providing active assistance to the lower limbs.

1.1.2.2 Current state of exoskeleton technology for stumble recovery

The response of exoskeletons during stumble events has received little attention to date. Nevertheless, this field is growing rapidly, with lower-limb exoskeletons encompassing a wide range of designs (e.g., multi or single joint, unilateral vs. bilateral), control strategies (e.g., gait trajectory, model-based, adaptive oscillator-based, fuzzy) and applications (e.g., load carrying augmentation, healthy participant assistance, impaired participant assistance, paraplegic patient assistance) [124]. Many recent review papers have highlighted the lack of an appropriate response to stumbles as a knowledge gap in the field and a crucial barrier for widespread adoption [105, 91, 39, 124, 13]. To date only one paper has studied individuals while stumbling in an exoskeleton; however, no active, stumble-specific controller was implemented; rather, the conditions of continuing assistance or stopping assistance were investigated [1]. Moreover, exoskeleton stumble recovery behaviors have yet to be explored or tested as (1) a safety mechanism for existing users or (2) a stumble recovery intervention for those at high fall risk.

1.1.2.3 Open questions considered in this work

- How should a stumble be detected?
- What type of active assistance should be provided following a stumble, and how is that decision made?
- Will the human accept active, external device behavior?
- Can introducing powered stumble recovery behaviors improve responses and/or mitigate falls?

1.1.3 Using the healthy adult stumble recovery response to inform devices: what we know and what we need to know

Healthy adults rarely fall. A recent study reports the healthy adult population's fall rate to be just 0.37 falls per person per year [120]. This low fall rate is due to the healthy adult's ability to react to an unexpected stumble with a coordinated, corrective stepping response to avoid a fall. Therefore, the successful stumble recovery response of healthy individuals can and should inform interventional device behavior.

Many works have characterized stumble recovery for healthy adults [38, 102, 24, 107, 15]. Upon contact with an obstacle, the individual performs one of three primary recovery strategies (Fig. 1.3): In the elevating strategy, the tripped limb elevates up and over the obstacle, clearing the obstacle in the same step. In the lowering strategy, the tripped limb lowers to the ground posterior to the obstacle to terminate the step, and the contralateral limb subsequently completes a recovery step; the tripped limb then clears the obstacle in the following step. In the delayed lowering strategy, the tripped limb initially elevates, but ultimately elevation is abandoned and the limb is lowered posterior to the obstacle akin to the lowering strategy. Researchers have termed the recovery limb as the limb that takes the primary recovery step and the support limb as the stance limb during the recovery step. For the elevating strategy, the tripped limb that elevates over the obstacle is the recovery limb, and the stance limb during the elevating step is the support limb. For the lowering and delayed lowering strategies, the tripped limb that lowers is the support limb, and the contralateral stepping limb is the recovery limb. Ultimately, an individual needs to restore trunk control (arrest forward angular momentum induced by perturbation) with a sufficient and timely stepping response in order to recover successfully [38, 37]. Previous works have highlighted the role of both the recovery limb and the support limb in recovery success [86, 88].

Although the three primary recovery strategies used by healthy adults have been well characterized in previous works, the basis upon which each is selected is unknown [101, 30, 107]. How to decide which recovery strategy to perform (stumble recovery strategy identification) is a knowledge gap in the field and has crucial implications for prosthesis and exoskeleton interventions. Since elevating and lowering strategies involve the opposite tripped-limb reaction (hip and knee flexion for elevating, hip and knee extension for lowering), a prosthesis or exoskeleton that provides stumble recovery assistance in theory needs to make the proper decision. Filling this knowledge gap could potentially be beneficial not only by providing a better physiological understanding of human stumble recovery, but also by providing a basis upon which to design stumble recovery controllers, informing sensor selection and algorithm design.

1.1.3.1 Open questions considered in this work

- How do healthy adults select stumble recovery strategy?
- What factors of the perturbation contribute to this decision?
- To what extent is the decision unique?
- How could a healthy adult decision model inform device interventions?

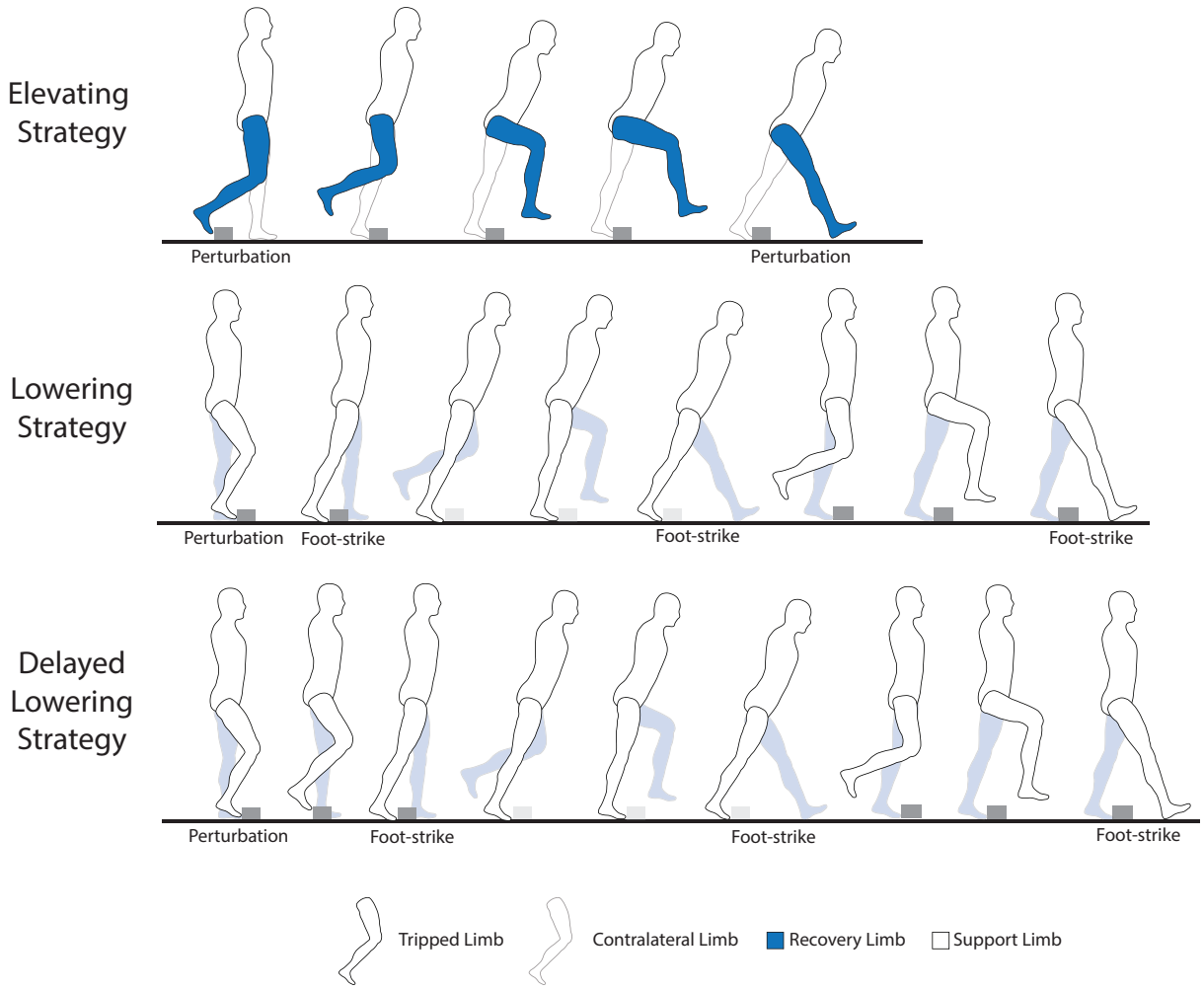

Figure 1.3: Diagram of the three primary stumble recovery strategies.

1.1.4 State of the experimental study of stumble recovery

Addressing the many open questions and knowledge gaps introduced here requires the systematic, experimental study of stumble recovery in a lab setting to properly characterize responses and test interventions. In order to elicit authentic responses to stumbles akin to a real-world stumble event, the stumble needs to be realistic (i.e., involve a physical obstacle to clear), unexpected (i.e., the individual does not have any auditory, visual, or tactile cues that the perturbation is coming), and targetable (i.e., can be introduced at specific points during the gait cycle), all while allowing for kinematic/kinetic analysis. Though various stumble perturbation systems have been designed and implemented and improved the study of stumble recovery [102, 15, 38, 24, 107], none have comprehensively addressed all four aforementioned goals.

1.1.5 Overarching Scope

The goal of this dissertation work is to examine the potential efficacy of implementing stumble recovery behaviors in robotic lower-limb prostheses and exoskeletons, particularly for purposes of reducing fall risk for wearers. This endeavor requires addressing several preliminary knowledge gaps, such as experimental stumble system design, healthy adult recovery strategy selection, and impaired population stumble response characterization. Thus this scope of work

will address crucial blind spots in the fields of prosthetic and exoskeleton technology, ultimately to improve users' stumble recovery and reduce fall risk for these populations.

1.2 Dissertation Contributions

1.2.1 Summary

This dissertation addresses several of the aforementioned knowledge gaps in the field of stumble recovery in order to ultimately propose and test robotic lower-limb wearable assistive device interventions to reduce fall risk. First, a stumble perturbation system was designed, built, and validated in order to reliably, repeatedly, and safely study stumble recovery for healthy and impaired populations (Chapter 2). The subsequent work can be viewed in two parallel tracks, one associated with a robotic lower-limb exoskeleton and one with a robotic lower-limb prosthesis as stumble recovery interventions.

In the first track, the biomechanical dataset from the seven-participant validation in Chapter 2 was leveraged in order to elucidate the healthy adult stumble recovery strategy selection process with a machine learning approach (Chapter 3), thus informing fall-prevention interventions. Using insights from the healthy adult stumble recovery strategy characterization and selection model in Chapters 2 and 3, a preliminary stumble recovery controller for a powered knee exoskeleton was designed, implemented, and validated a with one healthy adult (Chapter 4, Part 1). The stumble detection and recovery strategy identification algorithms were refined in a subsequent work and validated with a five-participant exoskeleton stumble experiment (Chapter 4, Part 2). Then, the effect of knee exoskeleton assistance on the impaired recovery responses of three healthy individuals (Chapter 4, Part 3) was explored in a separate stumble experiment.

In the second track, the sound-side stumble responses of six transfemoral prosthesis users wearing their prescribed prosthesis were characterized in order to understand the stumble recovery deficiencies of this population and suggest potential interventions (Chapter 5). One of the interventions suggested, a powered knee prosthesis, was tested for sound-side (Chapter 6, Part 1) and prosthetic-side (Chapter 6, Part 2) stumbles with a subset of those transfemoral prosthesis users. These contributions are diagrammed in Fig. 1.4.

1.2.2 Chapter 2 Contributions

The primary contribution of this chapter is the design, implementation, and validation of a new stumble perturbation system that can be used to experimentally study stumble recovery in a lab setting. The experimental study of stumble recovery for healthy and impaired individuals is crucial to better understanding the reflexive mechanisms that help prevent falls and the deficiencies in some populations (or devices) that might increase fall risk. While previous systems have been developed for this purpose, they fall short in meeting one or more of the four ideal characteristics of a stumble system: perturbations (1) are akin to a stumble in real life (i.e., obstacle disrupting the foot in swing phase), (2) are unexpected by participants, (3) can be targeted to a specific point in the gait cycle, and (4) allow for kinematic and kinetic evaluation. The system presented in this work was shown to meet all four criteria. First, the system involves a custom obstacle delivery apparatus that releases a steel block onto the treadmill, which serves as the obstacle that must be encountered and cleared to recover. Second, the ramp design as well as sensory occlusion techniques used in the experimental protocol ensure that the perturbation is unexpected, which was validated in a perception study with seven healthy participants. Third, the system involves a predictive targeting algorithm that controls the timing of the perturbation to the foot during swing phase, with a mean targeting accuracy of 25 ms (6.2% of swing phase). The system was implemented with seven healthy adult participants, collecting motion capture and ground-reaction forces and computing joint-level kinematics and kinetics.

Overall, the stumble perturbation system was shown to be effective in eliciting realistic stumbles and preventing anticipation by the participants, an improvement over previous systems. Furthermore, the accurate targeting allows for efficient data collection that minimizes mistrials and thus allows for fewer participants or time spent collecting data as compared to previous studies. Also of note, the kinematic data collected was sufficiently similar to responses reported in previous overground studies, validating the use of the treadmill in this setup. Finally, this work was

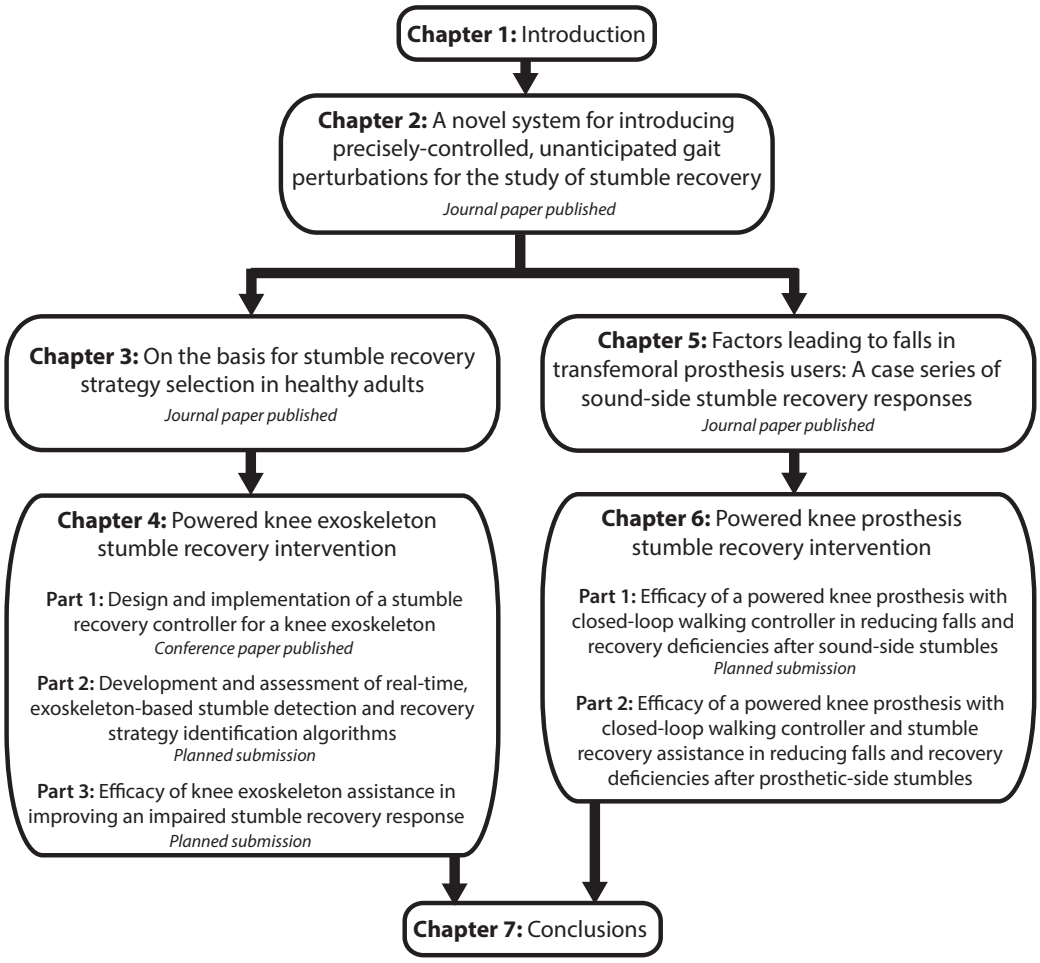

Figure 1.4: Dissertation outline

published as an article titled "A novel system for introducing precisely-controlled, unanticipated gait perturbations for the study of stumble recovery" in the Journal of NeuroEngineering and Rehabilitation in 2019. Of note, the obstacle delivery apparatus CAD file and predictive targeting algorithm were provided with the open-access publication so that the system can be recreated by other researchers. Additionally, this work was leveraged to draft an American Society for Testing Materials (ASTM) International Standard Test Method titled "Standard Test Method for Evaluating Exoskeleton Fall Risk due to Stumbling" which was published in July 2022.

1.2.3 Chapter 3 Contributions

The primary contribution of this chapter is a stumble recovery strategy selection model that uses dynamic factors of the human body during the stumble event to predict strategy with substantially improved accuracy relative to the conventional swing percentage criterion. Although the three primary recovery strategies used by healthy adults have been well characterized in previous works, the basis upon which each is selected was unknown. The convention has been to associate strategy selection with the swing percentage at which the perturbation occurs, but previous studies have shown that this metric does not comprehensively determine strategy selection, and additionally its measurement in real-time is based on many assumptions that lose accuracy as individuals vary movement patterns.

Thus in this work the goal was to identify a set of real-time, physical measurements that better explain strategy selection in order to inform potential assistive device interventions and physiological understanding. Specifically, a set of biomechanical measurements at/after the perturbation from the seven-participant stumble experiment described in Chapter 2 were considered in a two-stage classification structure to find the set of features that best explained the strategy selection process. The proposed model yielded 99% and 94% classification accuracies in strategy selection for Stages 1 and 2, respectively, compared to 94% and 85.6% with the swing percentage model.

Overall, this work is the first model to address stumble recovery strategy selection in healthy adults and provides a set of features that predict strategy selection with substantially higher accuracy than swing percentage. Notably, the use of real-time measurable features in this model (that do not require assumptions of a stationary gait required for estimating swing percentage) not only provides insights into the human physiological response, but also points to real-time signals that can be monitored for various fall-prevention interventions, such as wearables during a stumble recovery training protocol or onboard interventional assistive devices such as prostheses or exoskeletons. This work was published as an article entitled "On the basis for stumble recovery strategy selection in healthy adults" in the American Society of Mechanical Engineers (ASME) Journal of Biomechanical Engineering in 2021.

1.2.4 Chapter 4 Contributions

1.2.4.1 Part 1

The primary contribution of Part 1 of Chapter 4 is the preliminary design, implementation, and validation of a stumble recovery controller for a knee exoskeleton. While research and development of lower-limb exoskeletons have been on the rise in the past decade, the focus of design and control has been for steady-state activities such as walking; as such, these devices do not consider or account for common unexpected disturbances such as tripping over obstacles. Addressing this event is crucial for safety and thus adoption of exoskeletons as daily-use devices on the factory floor or in the rehabilitation clinic. Therefore, this work presents a stumble recovery controller for a knee exoskeleton that detects a stumble perturbation, selects an anticipated recovery strategy, and provides appropriate recovery assistance. Of note, the recovery strategy selection leverages work in Chapter 3 by repeating the feature selection methods for an abbreviated set of potential measurements (only signals that could be accessed by the exoskeleton), and fits the set of features that best modeled strategy selection from the seven-participant dataset to a logistic regression model that was implemented onboard the device for real-time strategy selection. The knee exoskeleton was tested on a single adult participant, with results showing successful perturbation detection, strategy selection, and some improvements in recovery kinematics relative to alternate control approaches of maintaining walking assistance or disabling walking assistance following perturbation.

Overall, this work presents the first active lower-limb exoskeleton stumble recovery controller, and it is the first study to show that a device can act in concert with the healthy individual's reflexive strategy decision. Of note, this controller can be readily implemented in any lower-limb exoskeleton with control of the knee joint, potentially improving the safety and adoption of existing and future devices. This work was published as a conference paper titled "Design and implementation of a stumble recovery controller for a knee exoskeleton" for the 2021 IEEE/RSJ International Conference on Intelligent Robots and Systems (IROS 2021).

1.2.4.2 Part 2

The primary contribution of Part 2 of Chapter 4 is the development of real-time exoskeleton-based stumble detection and stumble recovery identification algorithms with validation on a new, five-participant dataset of stumbles. Though results from Part 1 suggest efficacy in terms of perturbation detection and strategy selection for one participant, it was important that the approach be tested on multiple individuals to robustly assess its performance in acting in concert with the individual's reflexive response. Five healthy adults were recruited for a stumble experiment while wearing the knee exoskeleton unassisted to collect sensor data on which to develop and test the algorithms, which resulted in 109 stumbles and 109 normal swing phases. The stumble detection algorithm used thresholds on frequency content and acceleration magnitude from IMU data to detect swing-phase obstacle perturbations with 100% accuracy and no false positives with an average detection delay of 18 ms. The recovery strategy identification algorithm further

modified the approach from Part 1, ultimately using logistic regression equations with data from three sensor signals to predict recovery strategy with 96% classification accuracy.

Overall, this work presents the first stumble detection algorithm that uses data from a single IMU to detect obstacle perturbations throughout swing phase with 100% accuracy and no false positives within the typical human response muscle latency for stumbles. Likewise, this work presents the first recovery strategy identification algorithm to use real-time sensor data from a separate test set and achieve 96% classification accuracy for obstacle perturbations throughout swing phase. As in Part 1, these algorithms can be readily implemented on any lower limb exoskeleton with a thigh IMU and knee encoder, offering a critical first step in the development of exoskeletons that are robust to stumble perturbations. This work will be submitted to a peer-reviewed journal or conference.

1.2.4.3 Part 3

The primary contribution of Part 3 of Chapter 4 is the first demonstration of exoskeleton knee assistance as a stumble recovery intervention to decrease fall risk. While previous works studying stumble recovery had highlighted the role of the recovery limb in successfully performing the elevating strategy, interventions thus far had focused on training; moreover, exoskeleton assistance had never been explored after stumbles. In this work three healthy adult participants were first impaired using leg weights attached to their shank, with stumble experiments validating that the weights indeed impeded their recovery limb kinematics (local effect) and increased overall fall risk (global effect). Then, knee exoskeleton assistance (i.e., active flexion and extension after the perturbation) was tested as an intervention, and was shown to improve recovery limb kinematics and reduce fall risk.

Overall, this work is the first to show knee exoskeleton assistance as a successful intervention to improve an impaired stumble recovery response, with many promising future applications to reduce fall risk for fall-prone populations and improve the safety and adoption of lower-limb exoskeletons. This work will be submitted to a peer-reviewed journal or conference.

1.2.5 Chapter 5 Contributions

The primary contribution of this work is a case-series characterization of sound-side stumble responses to obstacle perturbations in early, mid, and late swing phase for six transfemoral prosthesis users of various ages and prosthesis types. While retrospective studies highlight the high fall rate of transfemoral prosthesis users compared to healthy adults, studies that actually analyze the response of transfemoral prosthesis users to stumbles are limited. Previous studies presented limited analysis with respect to side tripped, participant age, prosthesis type, and swing percentage of perturbation; in fact, only one short communication has reported stumbles to the sound limb without handrails. Thus the aim of this study was to address these knowledge gaps in sound-side stumble recovery. Specifically, a high fall rate was reported, with five out of six participants falling at least once, and stumbles in mid swing resulting in the most falls. Participant age corresponded to higher fall rate, while prosthesis type did not. Transfemoral prosthesis users recovered with similar strategies to that of healthy control data, but with exaggerated trunk flexion, thigh abduction, and arm motion. Falls were attributed to deficiencies in lower-limb kinematics that led to more trunk flexion, trunk flexion velocity, and less anterior foot positioning relative to the body's center of mass.

Overall this work provides a comprehensive characterization of sound-side stumble responses for six transfemoral prosthesis users and consequently suggests several interventions that may benefit prosthesis users. On the sound side, muscle strength and motor skill training and/or exoskeleton assistance may help facilitate the elevating strategy. On the prosthetic side, muscle strength and motor skill training and/or powered prosthetic knee assistance may help initiate and complete swing phase, limit buckling, and provide counteracting torques in stance to reduce forward angular momentum. This work is currently in press as an article entitled "Factors leading to falls in transfemoral prosthesis users: A case series of sound-side stumble recovery responses" at the Journal of NeuroEngineering & Rehabilitation.

1.2.6 Chapter 6 Contributions

The primary contribution of Chapter 6 is the analysis of the efficacy of a powered knee intervention for stumble recovery for transfemoral prosthesis users. While previous characterizations of transfemoral prosthesis user stumble recovery suggested that powered behaviors might improve responses to both sound-side and prosthetic-side stumbles, a powered prosthesis intervention had never been tested for this population. In Part 1, a closed-loop walking controller is tested as an intervention for sound-side stumbles; this served to benefit prosthesis users by reducing falls in mid-swing as well as reducing trunk motion (i.e., fall risk) and thigh motion (i.e., compensation techniques) during recoveries. In Part 2, active stumble recovery responses along with the closed-loop walking controller were tested as an intervention for prosthetic-side stumbles; after training, this served to benefit prosthesis users by enabling the elevating strategy after early swing stumbles as well as reducing trunk motion and thigh abduction during recoveries.

Overall this work provided a critical first step in exploring and testing powered prosthesis interventions for stumble recovery and yielded many important insights and directions for future work. The sound-side intervention (Part 1) will be submitted as a short communication to a peer-reviewed journal.

1.2.7 Contribution Deliverables

1.2.7.1 First-author journal papers

Eveld, M. E., King, S. T., Zelik, K. E and Goldfarb, M. (2022) Efficacy of a powered knee prosthesis with closed-loop walking controller in reducing falls and recovery deficiencies after sound-side stumbles. Planned submission as Short Communication.

Eveld, M. E., King, S. T., Zelik, K. E and Goldfarb, M. (2022) Factors leading to falls in transfemoral prosthesis users: A case series of sound-side stumble recovery responses. J NeuroEngineering & Rehabilitation. In Press.

Eveld, M. E., King, S. T., Vailati, L. G., Zelik, K. E and Goldfarb, M. (2021) On the basis for stumble recovery strategy selection in healthy adults. J. Biomech Eng. doi:10.1115/1.4050171.

Eveld, M. E., King, S. T., Martínez, A., Zelik, K. E and Goldfarb, M. (2019). A novel system for introducing precisely-controlled, unanticipated gait perturbations for the study of stumble recovery. J NeuroEngineering & Rehabilitation. 16(1), 69. (Co-first author with Shane King)

1.2.7.2 First-author conference papers

Eveld, M. E., King, S. T., Zelik, K. E and Goldfarb, M. (2022) Efficacy of knee exoskeleton assistance in improving an impaired stumble recovery response. Planned submission.

Eveld, M. E., King, S. T., Zelik, K. E and Goldfarb, M. (2022) Development and assessment of real-time, exoskeleton-based stumble detection and recovery strategy identification algorithms. Planned submission.

M. Eveld, S. King, K. Zelik and M. Goldfarb. (2021) Design and implementation of a stumble recovery controller for a knee exoskeleton. 2021 IEEE/RSJ International Conference on Intelligent Robots and Systems (IROS), pp. 6196-6203, doi: 10.1109/IROS51168.2021.9636879.

1.2.7.3 Second-author journal papers

King, S. T., Eveld, M. E., Zelik, K. E and Goldfarb, M. (2022) Efficacy of a powered knee prosthesis with stumble recovery assistance in reducing falls and recovery deficiencies after prosthetic-side stumbles. Planned Submission.

King, S. T., Eveld, M. E., Zelik, K. E and Goldfarb, M. (2022) Design and validation of powered knee stumble recovery controller. Planned submission.

King, S. T., Eveld, M. E., Zelik, K. E and Goldfarb, M. (2022) Transfemoral prosthesis user responses to prosthetic-side stumbles: a Case Series. Planned submission.

1.2.7.4 First-author conference presentations

Eveld, M. E., King, S. T., Zelik, K. E. and Goldfarb, M. Addressing stumble recovery for transfemoral prosthesis users. World Congress of Biomechanics (Virtual), July 2022. Oral Presentation.

Eveld, M. E., King, S. T., Zelik, K. E. and Goldfarb, M. Transfemoral prosthesis user stumble recovery responses for both limbs across swing phase. International Society of Biomechanics (Virtual) Conference, July 2021. Poster Presentation.

Eveld, M. E., King, S. T., Zelik, K. E. and Goldfarb, M. Stumble recovery strategies for healthy individuals and transfemoral prosthesis users. American Society of Biomechanics (Virtual) Conference, August 2020. Poster Presentation.

Eveld, M.E., King, S. T., Zelik, K. E., and Goldfarb, M. Aerial Phase during Stumble Recovery: Causes, Effects, and Implications. Mid-South Biomechanics Conference, February 2020, Memphis, TN, USA. Oral Presentation.

Eveld, M. E., King, S. T., Martinez, A., Zelik, K. E. and Goldfarb, M. Stumble recovery: Strategies, kinematics and kinetics as a function of foot perturbation timing during swing phase. ISB/ASB Conference, August 2019, Calgary, Canada. Oral Presentation.

1.2.7.5 Second-author conference presentations

King, S. T., Eveld, M. E., Zelik, K. E. and Goldfarb, M. A case series of early swing perturbation recovery strategies in transfemoral prosthesis users. International Society of Biomechanics (Virtual) Conference, July 2021. Oral Presentation.

King, S. T., Eveld, M. E., Vailati, L. G., Zelik, K. E. and Goldfarb, M. Development and evaluation of a powered knee stumble recovery controller for transfemoral prosthesis users. American Society of Biomechanics (Virtual) Conference, August 2020. Poster Presentation.

King, S. T., Eveld, M. E., Martinez, A., Zelik, K. E. and Goldfarb, M. Development of a novel gait perturbation system for the study of stumble recovery. ISB/ASB Conference, August 2019, Calgary, Canada. Poster Presentation.

King, S. T., Eveld, M. E., Martinez, A., Zelik, K. E. and Goldfarb, M. Development of a novel gait perturbation system for the study of stumble recovery. Mid-South Biomechanics Conference, February 2019, Memphis, TN, USA. Oral Presentation.

1.2.7.6 Reports

Standard Test Method for Evaluating Exoskeleton Fall Risk due to Stumbling. American Society for Testing & Materials (ASTM) International. July 2022.

1.2.7.7 Additional academic contributions not discussed in dissertation

Eveld, M. E., Lamers, E. P., and Zelik, K. E. (2019) Subject-Specific Responses to an Adaptive Ankle Prosthesis during Incline Walking. J Biomechanics. 95: 109273. (Co-first author with E.P. Lamers)

Walking with Ossur ProprioFoot on Level Ground, Incline/Decline and Stair Ascent/Descent. Collaboration with Ossur. Industry Report. November 2017.

Eveld, M. E., Wolfe, A.E., Cruz, J.P., Sifuentes, N.J., Ausec, B.N., Zelik, K.E., McDonald, K.A. Task-specific device use in paediatric prosthesis users. 12th Australasian Biomechanics Conference (ABC12) Conference, December 2021, Adelaide, SA, Australia. Oral Presentation.

Eveld, M.E., Teater, R.H., Matijevich, E.S., King, S.T., Ziemnicki, D.M., Nurse, C.A., Zelik, K.E. Pivoting to virtual outreach efforts for K-12 students: A comparison of two approaches. Orthopaedic Research Society (ORS) Annual Meeting, February 2022, Tampa, FL, USA. Oral Presentation. (Co-first author with R.H. Teater)

Eveld, M. E., Lamers, E. P., and Zelik, K. E. Effects of an Adaptive Prosthesis on Level and Sloped Walking for Transtibial Prosthesis Users. American Congress of Rehabilitation Medicine, September 2018, Dallas, TX, USA. Oral Presentation.

Lamers, E. P., Eveld, M. E., and Zelik, K. E. Effects of an Adaptive Ankle Prosthesis on Level and Sloped Walking. American Society of Biomechanics Annual Conference, August 2018, Rochester, MN, USA. Poster Presentation.

CHAPTER 2

A novel system for introducing precisely-controlled, unanticipated gait perturbations for the study of stumble recovery

2.1 Chapter Summary

The experimental study of stumble recovery is essential to better understanding reflexive mechanisms that help prevent falls as well as deficiencies in fall-prone populations. This study would benefit from a system that can introduce perturbations that: 1) are realistic (e.g., obstacle disrupting the foot in swing phase), 2) are unanticipated by subjects, 3) are controllable in their timing, and 4) allow for kinematic and kinetic evaluation. A stumble perturbation system was designed that consists of an obstacle delivery apparatus that releases an obstacle onto a force-instrumented treadmill and a predictive targeting algorithm which controls the timing of the perturbation to the foot during swing phase. Seven healthy subjects were recruited to take part in an experimental protocol for system validation, which consisted of two sub-experiments. First, a perception experiment determined whether subjects could perceive the obstacle as it slid onto the treadmill belt. Second, a perturbation experiment assessed the timing accuracy of perturbations relative to a target percent swing input by the experimenter. Data from this experiment were then used to demonstrate that joint kinematics and kinetics could be computed before and after the perturbation. Out of 168 perception trials (24 per subject), not a single obstacle was perceived entering the treadmill by the subjects. Out of 196 perturbation trials, 190 trials successfully induced a stumble event, with a mean targeting accuracy, relative to the desired percent swing, of 25 ms (6.2% of swing phase). Joint kinematic and kinetic results were then computed for three common stumble recovery strategies and shown to be qualitatively consistent with results from prior stumble studies conducted overground. The stumble perturbation system successfully introduced realistic obstacle perturbations that were unanticipated by subjects. The targeting accuracy substantially reduced mistrials (i.e., trials that did not elicit a stumble) compared to previous studies. This accuracy enables stumble recovery to be studied more systematically as a function of when the perturbation occurs during swing phase. Lastly, joint kinematic and kinetic estimates allow for a comprehensive analysis of stumble recovery biomechanics.

2.2 Introduction

Falls due to tripping are a common cause of injury [117, 57]. The experimental study of tripping (i.e., stumbling) and the subsequent recovery response in healthy and impaired people is essential to better understanding reflexive mechanisms that help prevent falls and the deficiencies in some populations that increase the proclivity for falls. Such studies are an important element of developing interventions that can reduce the likelihood or severity of falls, particularly in impaired populations.

An effective experimental system for studying stumble recovery would ideally have several characteristics. First, it should be able to introduce a perturbation to elicit a stumble. This perturbation should be delivered in a realistic manner. As such, the perturbation should be applied to the foot during swing phase using a three-dimensional object which must be cleared by the swing foot in order to recover, analogous to stumble events in daily life (e.g., stumbling on an uneven sidewalk or a toy on the floor). A perturbation of this nature is hereafter referred to as an obstacle perturbation. Second, the system should be capable of introducing repeated, unanticipated perturbations so that multiple responses can be characterized as a function of the experimental conditions and analyzed statistically. The repeated presentation of perturbations, however, is challenging because eliciting an authentic stumble response (i.e., a reflexive response) relies on the subject not anticipating each perturbation (i.e., the subject receiving no sensory cues indicating when or where the perturbation will occur). Third, the timing of the perturbation should be controllable, such that it can be targeted within a specific window of the gait cycle (i.e., to perturb the foot at different portions of swing phase). Controllable timing of the perturbation minimizes the number of mistrials in an experiment and allows for a more thorough analysis of stumble recovery responses. Fourth, the experimental system should enable measurement of kinematics and kinetics on both the perturbed (ipsilateral) and contralateral limbs before, during, and after the stumble in order to

effectively assess recovery biomechanics.

Several systems have been developed to produce stumbles in human gait, including overground floor-deployable obstacle perturbations (e.g.[86, 25, 24, 17, 81, 82, 79, 118, 87, 88, 55, 38, 97], overground rope-blocking (e.g. [11])), treadmill-based belt-deployable obstacle perturbations (e.g., [100, 102, 101, 103]), treadmill-based rope-blocking (e.g. [108, 106, 107, 109]), and treadmill-based belt-speed perturbations (e.g. [30, 16, 47, 126, 104, 121]). Although these systems can each be effective in causing a person to stumble, each also entails some limitations with respect to the aforementioned desired characteristics of a system for studying stumble recovery. For instance, overground floor-deployable obstacle perturbations are an effective means of emulating the described conditions for obstacle perturbations, but are limited by constrained walkway length. In this type of setup, subjects are frequently aware of the nominal location of the perturbation, and as such introducing a large number of perturbations in an unexpected manner has been challenging. As described in [81], to avoid the possibility of subject anticipation, 79 subjects were recruited, each to be stumbled once; however, only 61 subjects were successfully stumbled, resulting in unusable data from 18 subjects. Further, it can be difficult to ensure a large number of strides between the initiation of walking and the introduction of the perturbation due to limited walkway lengths. Finally, in previous studies, the relative phasing between the subject and the obstacle has been determined by the subject at the start of the walkway, and once established, the timing of the perturbation has been difficult to control. Overground rope-blocking perturbations entail similar limitations due to walkway length, do not emulate a physical obstacle which must be cleared, and may complicate kinetic analysis due to the rope applying a force to the foot before and after the perturbation [10].

Other researchers have employed treadmill-based systems which largely address the challenges of limited walkway length associated with overground setups. Treadmill-based setups enable a large number of perturbations in a given session, provide an assurance of steady-state walking prior to the perturbation, and allow for better control of perturbation timing with respect to swing percentage. However, neither rope-blocking nor belt-speed perturbations recreate an obstacle perturbation due to the lack of a physical object to clear. Also, in the case of belt-speed perturbations, the perturbation is not applied to the swing foot, introducing both mechanical and sensory differences relative to an obstacle perturbation. The belt-deployable obstacle approach, as employed in [100, 102, 101, 103], most closely resembles the ideal system characteristics detailed above. This previous system used an electromagnet to release an obstacle from a small height above the treadmill belt. However, a subject was easily able to detect when an obstacle was released onto the belt through the impulsive vibration produced by the impact, which introduced the potential for anticipatory responses. In [102, 101], the authors describe circumventing this issue by using a metal rod to strike the treadmill at irregular intervals, in order to disorient the subject as to which impact preceded the impending perturbation. This tactic may decrease the likelihood of an anticipatory response from the subject, but may not completely eliminate it. Further, the repeated impacts confound the calculation of kinetics prior to the perturbation.

It should be noted that of all the stumble studies previously described, only two have presented joint-level kinetic data. Ipsilateral limb kinetics were reported in [25], and contralateral limb kinetics were reported in [87]. The lack of reported joint-level kinetic data is likely due to the challenge of reliably measuring force and moment data in several of the aforementioned systems associated with stumble experimentation.

In this paper, the authors describe the design and methodology of a novel stumble perturbation system that 1) provides an obstacle perturbation (i.e., one similar to stumble events encountered in daily life), 2) enables introduction of repeated perturbations while eliminating the subject's ability to perceive the obstacle's entry and thus anticipate the events, 3) provides controllable timing of the perturbation, and 4) enables calculation of joint-level kinematics and kinetics before, during, and after the perturbation. The proposed system is based on and improves upon the system presented by [100, 102, 101, 103]. However, the one described here precludes subjects from perceiving the deployment of the obstacle, is able to time the perturbation to within 2.5% of the stride cycle, and enables straightforward computation of joint kinetics using conventional inverse dynamics techniques. This paper describes the design of the system and employs it to collect kinematic and kinetic data on seven healthy subjects in order to confirm that the four aforementioned objectives are met. Apparatus design files and targeting algorithm scripts are included with the supplemental material such that other researchers can reproduce the experimental system for the study of stumble recovery.

2.3 Methods

2.3.1 Stumble Perturbation System

The stumble perturbation system consists of (i) an obstacle delivery apparatus that inconspicuously releases an obstacle onto a split-belt force-instrumented treadmill, and (ii) a predictive targeting algorithm which controls the timing of the perturbation. The major components of the system are illustrated in Fig. 2.1.

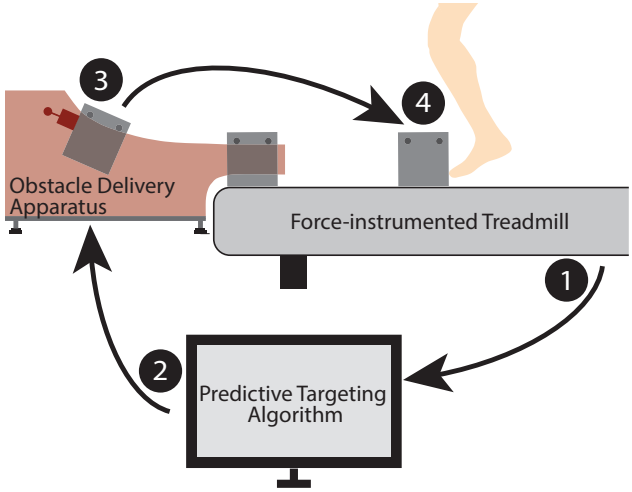

Figure 2.1: Schematic of the stumble perturbation system. The subject walks on the instrumented treadmill. Ground reaction forces and moments are collected (1) and used to calculate the center of pressure under the foot, which is then used to detect gait events. These gait events are used to calculate the time at which the obstacle should be released using the predictive targeting algorithm (2). At this time the electromagnet turns off (3) and releases the obstacle onto the treadmill such that a perturbation is introduced (4) at the desired percent of swing phase.

2.3.1.1 Obstacle Delivery Apparatus Design

As with the system described in [100, 102, 101, 103], the essential mechanism of inducing a stumble is based on introducing a weighted obstacle onto a treadmill belt. The obstacle used in this study was a 16 kg (35 lb) block of steel, chosen to ensure minimal movement relative to the treadmill belt during a stumble compared to previous designs which used a 2.2 kg (5 lb) obstacle [100, 102, 101, 103]. The obstacle measures 20 cm wide, 12.5 cm long, and 7.5 cm high (8.125" x 5" x 3"). Firm foam padding of 1.25 cm in thickness (0.5") is adhered to the front and bottom of the obstacle to protect the subject's toes and the treadmill belt, respectively. Note that while this specific weight and shape were used for this study, an obstacle of any given weight and various shapes could be used in its place depending on the objective of the experiment. The system's functionality is independent of the obstacle's weight and shape, within certain bounds of size and form-factor.

Additionally, deployment of the obstacle onto the belt without perception necessitates that the obstacle be transferred to the belt with minimal impulse, which requires that the obstacle be deployed with near-zero vertical velocity, and horizontal velocity that approximates the treadmill belt speed. Any substantial variation from these velocities will result in a noticeable force impulse on the treadmill due to the change in obstacle momentum, which will be perceptible to the user, as was the case in previous designs [102, 101] and evident in the authors' pilot testing.

In order to deploy the 16 kg obstacle with minimal impulse, a ramp-based obstacle delivery apparatus (Fig. 2.2) was designed to deploy the obstacle onto the treadmill belt, as illustrated in Fig. 1, at near-zero vertical velocity and at a prescribed, adjustable horizontal velocity in order to match a given belt speed. The ramp consists of an acrylic track attached to an aluminum frame with adjustable, vibration-damping feet. The obstacle is held at a given point along the ramp via an electromagnet, which is held by a rod located by a pair of holes in the ramp (Fig. 2.2). When released via computer control (discussed subsequently), the obstacle rolls down the ramped track on a set of flanged roller bearings

mounted on shoulder bolts threaded into each corner of the obstacle (Fig. 2) and then onto the front of the treadmill belt (Fig. 2.1). Note that a large, padded bin was used to catch the obstacle on the posterior end of the treadmill. The initial height of the center of mass of the obstacle determines the horizontal velocity at exit, and thus the ramp includes multiple starting points for the obstacle (i.e., multiple initial heights) in order to approximate a range of treadmill belt speeds. The starting height can additionally be fine-tuned via a threaded interface between the electromagnet and the rod to more precisely match a given belt speed. While any curve that is tangent to the treadmill belt at the exit could be employed, in order to simplify and improve the timing algorithm, a tautochrone curve [84] was implemented, which has been shown to have two desired features for this application. For a mass without friction in a constant gravitational field, a tautochrone curve: 1) provides the fastest path between two points, and 2) provides a constant time of travel, regardless of the starting point. These features respectively: 1) minimize the delay between obstacle release and the perturbation, which reduces associated predictive error, and 2) enable multiple belt speeds while considering only a single, fixed ramp travel time in the algorithm.

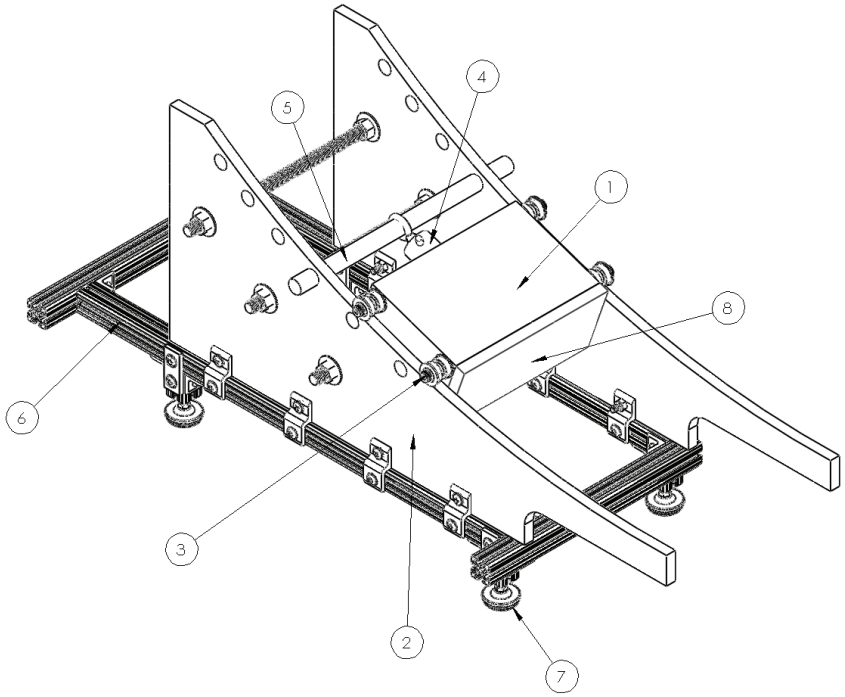

Figure 2.2: Obstacle delivery apparatus. A steel block (1) rests on an acrylic track (2) via flanged bearing stacks (3). The block is held in place by an electromagnet (4), whose position is determined by the height of the metal rod (5). The track is mounted to an aluminum frame (6) with adjustable, vibration-damping feet (7). Foam (8) is adhered to the front and bottom of the block to protect the subject's toes and reduce the impulsive loading on the treadmill, respectively.

2.3.1.2 Predictive Targeting Algorithm

A predictive targeting algorithm was developed so the system could elicit precisely timed perturbations during a given stride, in order to: 1) reduce the proportion of mistrials (e.g., in [81, 102], where 23% and 39% of attempts failed to elicit a stumble, respectively), and 2) enable a more precise study of the variation in response mechanics as a function of when the perturbation occurs during swing phase. The targeting algorithm assumes the use of a lateral split-belt, force-instrumented treadmill. The control flow information is illustrated in Fig. 2.3. Note that both a left and right obstacle delivery apparatus were used for the human subject experiment described here, but each is independent (i.e., only requires kinetic signals from the side to be perturbed) and therefore the algorithm is described in the context of a single obstacle delivery apparatus. The predictive targeting algorithm is initialized with

a desired percent swing at which the perturbation should occur. At the next toe-off event after the obstacle release is triggered by the experimenter, the algorithm calculates a time delay ($t_{release}$) such that the perturbation will occur at the desired percent of swing phase. The desired percent of swing phase corresponds to a point in space and time after toe-off, hereafter referred to as the targeted perturbation point and the targeted perturbation time, respectively. The algorithm requires real-time measurement of the two sagittal plane forces (vertical and anterior-posterior (AP) ground reaction forces (GRF)) and the one sagittal plane moment (mediolateral ground reaction moment (GRM)) from the instrumented treadmill. These kinetic signals are used to calculate the AP center of pressure (CoP) which is then used to detect gait events. The detected gait events are used to determine the timing of the release of the obstacle to achieve a perturbation at the desired percent of swing phase. The specific algorithm by which the appropriate time delay is calculated is described below. The key measurements and variables used in the algorithm are defined in Fig. 4. For the implementation described here, the force and moment signals were sampled at 1 kHz and filtered with a 1st order low-pass filter with a cut-off frequency of 30.5 Hz. Additionally, an experimentally determined 90 N threshold was used on the vertical GRF to reduce noise in the CoP signal near heel-strike and toe-off. Below this threshold the CoP signal was zeroed. Also note, as indicated in Fig. 2.4, the sagittal plane forces and moment are measured by the instrumented treadmill with respect to a coordinate frame, which is provided by the treadmill manufacturer (Bertec, Columbus, USA).

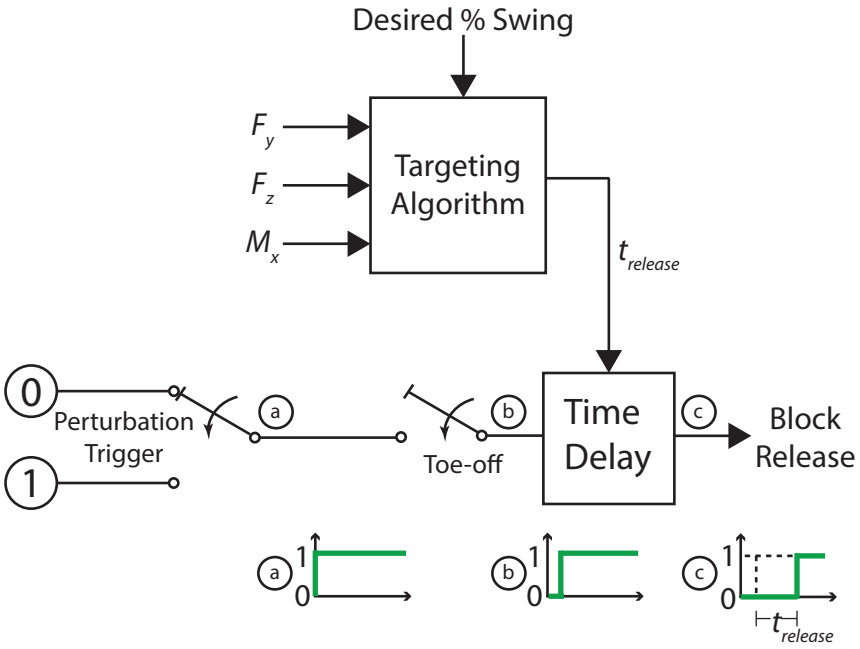

Figure 2.3: Predictive targeting algorithm control flow diagram. The targeting algorithm receives the desired percent swing input from the experimenter and the Fy, Fz, and Mx signals from the instrumented treadmill. Once the experimenter triggers a perturbation (a), the system waits until the next toe-off event (b), then passes to the time delay block where the time delay, $t_{release}$, is received from the Targeting Algorithm. The system then releases the obstacle following the time delay (c) which results in a targeted perturbation during the subject's swing phase. The unit step plots indicate the obstacle release signal at each point in the flow diagram: (a) indicates the immediate switch to high at the time of the trigger, (b) indicates the delay of the switch due to the time between the trigger and the subsequent toe-off, and (c) represents the added algorithmically-computed time delay before the obstacle is released. Note that $t_{release}$ is calculated in Eqs. (1) – (10).

The targeting algorithm assumes a uniform periodic motion (i.e., treadmill velocity is constant and the subject's position on the treadmill does not change substantially between time of release and time of perturbation). The time delay $t_{release}$ signifies when the obstacle should be released by the electromagnet in order to perturb the subject at a desired percent of swing phase. The time delay $t_{release}$ is calculated at a specified toe-off as a function of several component times, illustrated in Fig. 2.4, as:

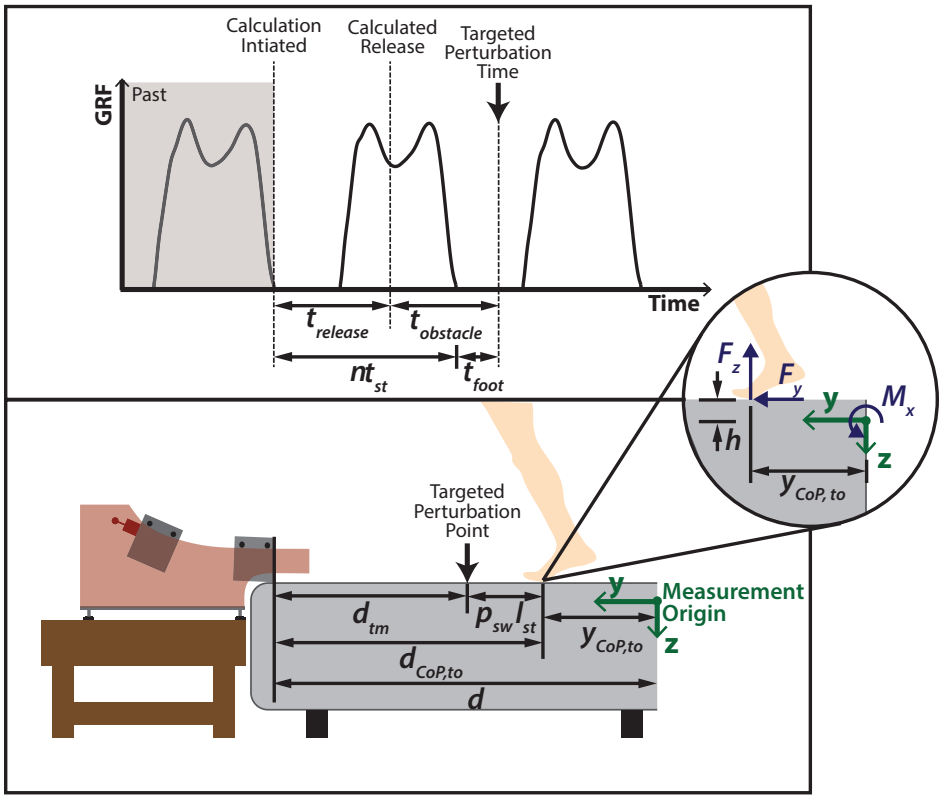

Figure 2.4: Schematic depicting variables used in the predictive targeting algorithm. The algorithm calculates the release time ($t_{release}$) such that the obstacle contacts the subject's foot at the desired time in swing phase. The time domain variables (top) and position domain variables (bottom) depicted here are used in Eqs. (1) – (10).

$$t_{release} = nt_{st} + t_{foot} - t_{obstacle} \tag{2.1}$$

where t_{st} is the average stride time, t_{foot} is the time required for the foot to travel from toe-off position to the targeted perturbation point, $t_{obstacle}$ is the time required for the obstacle to travel from its initial position on the ramp to the targeted perturbation point, and n is the smallest integer that makes $t_{release} \geq 0$. The component times in (2.1) are computed as follows. The time $t_{obstacle}$ is defined by:

$$t_{obstacle} = t_{tm} + t_{ramp} \tag{2.2}$$

where t_{ramp} is the time required for the obstacle to travel down the ramp to its point of entry on the treadmill belt and t_{tm} is the time required for the obstacle to travel on the treadmill belt from its point of entry on the treadmill to the targeted perturbation point. The time t_{ramp} is a constant due to the nature of the tautochrone curve and thus is independent of the starting position of the obstacle on the ramp. Although this time can be estimated analytically, it was determined experimentally to account for frictional effects. The time t_{tm} is given by:

$$t_{tm} = \frac{d_{tm}}{v_{tm}} \tag{2.3}$$

where v_{tm} is the treadmill belt velocity, assumed to be constant, and d_{tm} is the distance the obstacle must travel on the treadmill to the targeted perturbation point, which is calculated as:

$$d_{tm} = d_{CoP,to} - p_{sw} l_{st} \tag{2.4}$$

where $d_{CoP,to}$ is the computed distance from the obstacle's point of entry on the treadmill to the CoP at the toe-off event, p_{sw} is the targeted percent of swing phase (converted to a decimal) which is provided as an experimenter input into the algorithm, and l_{st} is the computed average stride length (see Fig. 2.4). In this equation, the computed distance d_{CoP},to is given by:

$$d_{CoP,to} = d - y_{CoP,to} \tag{2.5}$$

where d is the AP positional offset between the obstacle's point of entry on the treadmill and the force plate origin (Fig. 2.4), and $y_{CoP,to}$ is the distance from the AP CoP of the ipsilateral foot at toe-off to the force plate origin, which is given by calculating y_{CoP} at the time of toe-off using:

$$y_{CoP} = \frac{F_y h + M_x}{F_z} \tag{2.6}$$

where h is the vertical positional offset between the belt surface and force plate origin, F_y is the AP GRF, F_z is the vertical GRF, and M_x is the mediolateral GRM (Fig. 2.4).

The stride length in (2.4) is computed as a moving average of the previous 10 stride lengths, each of which is calculated as the difference of the AP CoP at heel-strike and the prior toe-off:

$$l_{st} = y_{CoP,hs}(i) - y_{CoP,to}(i-1) \tag{2.7}$$

where i is the stride index, and $y_{cop,hs}$ and $y_{CoP,to}$ are the distances from the AP CoP signal to the force plate origin at heel-strike and toe-off, respectively. The heel-strike event is detected as an increase in the vertical GRF beyond the 90 N threshold, and heel-strike position is computed as the average of the first 10 non-zero samples of the AP CoP signal after the heel-strike event. The toe-off event is detected as a decrease in the vertical GRF below the threshold, and toe-off position is computed as the last 10 non-zero samples of the AP CoP signal prior to toe-off. Both of these CoP values are calculated using (2.6) at the time of their respective events. Stride time in (2.1) is the measured time between each successive ipsilateral heel-strike:

$$t_{st} = t_{hs}(i) - t_{hs}(i-1) \tag{2.8}$$

which is computed as a moving average of the past 10 stride times. Heel-strike time (t_{hs}) is the time of the heel-strike event, which is detected at the first non-zero sample of the AP CoP signal after swing phase.

The time t_{foot}, which is the time within the periodic cycle required for the foot to advance from the toe-off position to the targeted perturbation point, is given by:

$$t_{foot} = p_{sw} t_{sw} \tag{2.9}$$

where t_{sw} is the moving average of the previous 10 swing times, each of which is calculated as the time difference between heel-strike and the prior toe-off:

$$t_{sw} = t_{hs}(i) - t_{to}(i-1) \tag{2.10}$$

where toe-off time (t_{to}) is detected at the time of the last non-zero sample of the AP CoP signal during stance phase. Note that the calculation of swing time (t_{sw}) may be affected by the threshold set on the force signals, thus artificially increasing the value. In this implementation an experimentally determined scaling factor that was inversely proportional to the subject's average stride length was used to account for this effect of thresholding the GRF. As illustrated in Fig. 2.3, the time delay value calculated in (2.1) is computed at the toe-off event, using (2.2)-(2.10), to enable the experimenter to specifically target a perturbation at a desired percent of the swing phase. The computer-aided design (CAD) files for the obstacle delivery apparatus and scripts implementing the targeting algorithm are included in the supplemental material of this paper. The following section provides a validation of the experimental setup and algorithm.

2.3.2 Experimental Validation

A 7-subject study of stumble recovery responses in healthy subjects was conducted in order to validate the efficacy of the stumble perturbation system. The protocol for this study and data analysis methods are outlined respectively in the subsections below.

2.3.2.1 Experimental Protocol & Data Collection

Seven subjects participated, three females and four males (age: 23.6 yrs, height: 1.8 m, mass: 81.3 kg). All experimental protocols were approved by the Vanderbilt Institutional Review Board, and all subjects gave their written informed consent. Subjects walked on the treadmill at 1.1 m/s [102]. The handrails were removed so they could not be used as a recovery aid; however, a full-body harness with slackened safety rope was worn to prevent a true fall. To prevent subjects from hearing or seeing the obstacle being deployed, each subject listened to white noise via earbuds, wore noise-canceling headphones, and wore dribble goggles that occluded the inferior visual field. Each subject watched on-screen visual feedback to ensure a centered position on the treadmill and avoid crossing over to the contralateral force plate. As a distraction technique, subjects were instructed to count backwards aloud from an arbitrary number by intervals of seven [112] (i.e., perform Serial Sevens). Subjects were given several minutes to walk on the treadmill prior to testing in order to acclimate to the setup.

Various data were recorded during each trial, including GRF data, which were recorded under each foot at a sampling rate of 2 kHz via a lateral split-belt, force-instrumented treadmill (Bertec, Columbus, USA). Full-body kinematic data were collected via infrared motion capture at a sampling rate of 200 Hz, which included feet, shanks, thighs, pelvis, torso, upper arms, and forearms (Vicon, Oxford, GBR). The experimental protocol consisted of two sub-experiments. First, a perception experiment (hereafter referred to as Perception Trials) was performed to determine the extent to which subjects could perceive the deployment of the obstacles due to the potential introduction of vibrations to the treadmill, as this perception would induce an anticipatory response. Second, a perturbation experiment (hereafter referred to as Perturbation Trials) was performed to assess the timing accuracy of perturbations and quantify the kinematics and kinetics of the stumble recovery responses. In the Perception Trials, for each of the two belts, an obstacle delivery apparatus was aligned laterally on the treadmill belt to ensure that when the obstacle was released it would not contact the subject's foot (i.e., it would pass lateral to the foot path). Subjects walked for approximately 15 min while the obstacles were released 6 times per belt at approximately 20, 30, 40, 50, 60, and 70% of swing phase.

The subjects were asked to raise their hand on the respective side if or when they perceived the obstacle entering the treadmill.

Following the Perception Trials, each obstacle delivery apparatus was repositioned such that the obstacles, when released, would be in the line of progression of the subject's foot. During the Perturbation Trials, each subject was perturbed 14 times per lower limb, targeted from 10% to 75% of swing phase in 5% increments. The order of perturbations was randomized in terms of targeted percent swing, the number of strides prior to the perturbation (between 25 and 120) and the side perturbed (i.e., left vs. right). A video of representative stumbles from these trials is provided in the supplemental material.

Note that prior to each trial the subject was not informed when or on which side the obstacle would be released, and as such they did not know when or where to expect the perturbation. The instructions given to the subjects prior to the Perturbation Trials were as follows: 1) Watch the visual feedback on screen to ensure a centered position on the treadmill, 2) perform serial sevens out loud, and 3) when the perturbation occurs, try to recover and return to steady state walking. They were also informed that in the event of a fall (i.e., in which they were caught by the overhead harness), the treadmill would be stopped.

Additionally, 60 seconds of unperturbed walking data were collected before and after the set of 28 perturbations, and the Perception Trials were repeated after the Perturbation Trials to ensure subjects did not acclimate to the system.

2.3.2.2 Data Processing

GRF and motion capture data were filtered with a zero-phase, 3rd order, low-pass Butterworth filter with a cut-off frequency of 15 and 6 Hz, respectively. Next, inverse dynamics were computed using Visual3D (C-Motion, Germantown, USA) to estimate joint-level kinematics and kinetics for each trial. Additionally, the kinetic signal profile of the obstacle (i.e., the GRF and GRM profiles due to the obstacle as it travels across the treadmill from entry to exit) was obtained prior to the testing session (i.e., without a subject on the treadmill) and subsequently subtracted from the kinetic signals recorded during the Perturbation Trials. This removed the obstacle's contribution to the measured kinetic data.

Prior to analysis, unperturbed walking data were parsed by heel-strike into strides and normalized to 100% of the stride cycle. Perturbed strides were normalized such that the toe-off event matched that of the unperturbed walking strides (i.e., perturbed strides were normalized based strictly on the stance phase, which is devoid of the perturbation).

The percent swing at which the stumble actually occurred was calculated as:

$$P_{sw} = \frac{t_{pto}}{t_{sw,avg}} \tag{2.11}$$

where t_{pto} is the time the perturbation occurred relative to the preceding toe-off event, and $t_{sw,avg}$ is the average swing time of 25 strides prior to the perturbation. The perturbation event was determined as the instant at which the foot contacted the obstacle, which was identified via a transient peak in the AP GRF measured by the treadmill. The actual percentage of swing phase of the perturbation, P_{sw}, was then compared to the targeted percentage of swing phase of the perturbation, p_{sw}, to assess the accuracy of the system.

The responses of the subjects to each perturbation were divided into three stumble recovery strategies that have been defined in previous works: the elevating strategy [24, 38, 101, 107], lowering strategy [24, 101, 107], and delayed lowering strategy [101, 107]. The recovery strategy was determined by the trajectory of the perturbed foot after contact with the obstacle. For the elevating strategy, the perturbed foot lifts up and over the obstacle, landing anterior to the obstacle. For both the lowering and delayed lowering strategies, the perturbed foot lowers posterior to the obstacle. During the delayed lowering strategy, the perturbed foot lifts slightly before lowering posterior to the obstacle, while in the lowering strategy the perturbed foot shows no upward movement before lowering.

To demonstrate that the system enables calculation of joint-level kinematics and kinetics, hip, knee, and ankle angle and moment trajectories over the recovery period for each strategy were computed and shown for a single subject in Fig. 2.6 and Fig. 2.9. To briefly summarize group-level results, peak GRFs, trunk deflection and joint flexion angles, and joint flexion and extension moments were also computed and the inter-subject means of these metrics for each recovery strategy were determined.

These summary metrics served to 1) provide values with which to compare to previous overground studies as further validation that the system is able to provide realistic perturbations leading to authentic stumble recovery responses, and 2) present initial findings to show trends in magnitude and range of responses across different recovery strategies. Wilcoxon rank-sum tests ($\alpha = 0.05$) with a Holm-Bonferroni correction were used to determine statistical significance of these summary metrics, for each recovery strategy compared to the unperturbed control values.

2.4 Results

2.4.1 Subject Perception

Of the 168 obstacle deployments that occurred during the Perception Trials (12 pre-test and 12 post-test trials for 7 subjects), none were perceived by subjects.

2.4.2 Targeting Accuracy

The Perturbation Trials yielded 190 successful stumbles out of 196 attempted. Six trials were excluded due to the subject stepping onto the obstacle. Therefore, only 3% (6 of 196) of the trials were deemed mistrials. The authors note this failure rate is an order of magnitude lower than the overground experiments described in [81, 102].

Fig. 2.5 shows the targeted versus actual swing percentage corresponding to the 190 successful stumble perturbations. The mean absolute error was 6.2% of swing phase (or 2.5% of the stride cycle, assuming that swing phase is approximately 40% of the total stride cycle). This corresponds to an average error of approximately 25 ms based on the average swing time (0.41 s $\pm$ 0.027 s) from the 7 subjects.

2.4.3 Kinematics

The observed recovery strategies and associated movements measured for the 7 subjects were qualitatively consistent with those previously reported for healthy individuals [24, 101, 107]. In total, 126 elevating strategies, 23 lowering strategies, and 39 delayed lowering strategies were observed. Two anomalous trials were excluded, one due to the subject scuffing his toe during the recovery, and the other due to the subject falling during the attempted recovery (i.e., caught by the safety harness). Sagittal plane kinematic trajectories for each of these strategies for a single subject are shown in Fig. 2.6, while inter-subject ($N = 7$) mean peak joint angles and trunk deflection angle (i.e., the mean of each subject's average peak angle for each strategy) are given in Fig. 2.7.

For the elevating strategy (Fig. 2.6 top row), the subject exhibited an increase in ipsilateral hip and knee flexion immediately following the perturbation as the leg cleared the obstacle. The ankle showed initial plantarflexion as the foot contacted the obstacle; however, this was quickly followed by dorsiflexion as the foot crossed over the obstacle. The contralateral limb kinematics did not deviate substantially from the unperturbed trajectories. The subject's hip and knee flexion increased slightly in the step following the perturbation, along with a more substantial increase in ankle plantarflexion.

For the lowering strategy (Fig. 2.6 middle row), the subject exhibited ipsilateral hip extension after contact with the obstacle. In late swing phase, knee extension was exhibited as the foot lowered to the ground. There was slight ankle plantarflexion and initial knee flexion on the ipsilateral side as the foot impacted the obstacle. The ankle plantarflexion gave way to dorsiflexion before the foot hit the ground. In the following stride an increase in hip and knee flexion was

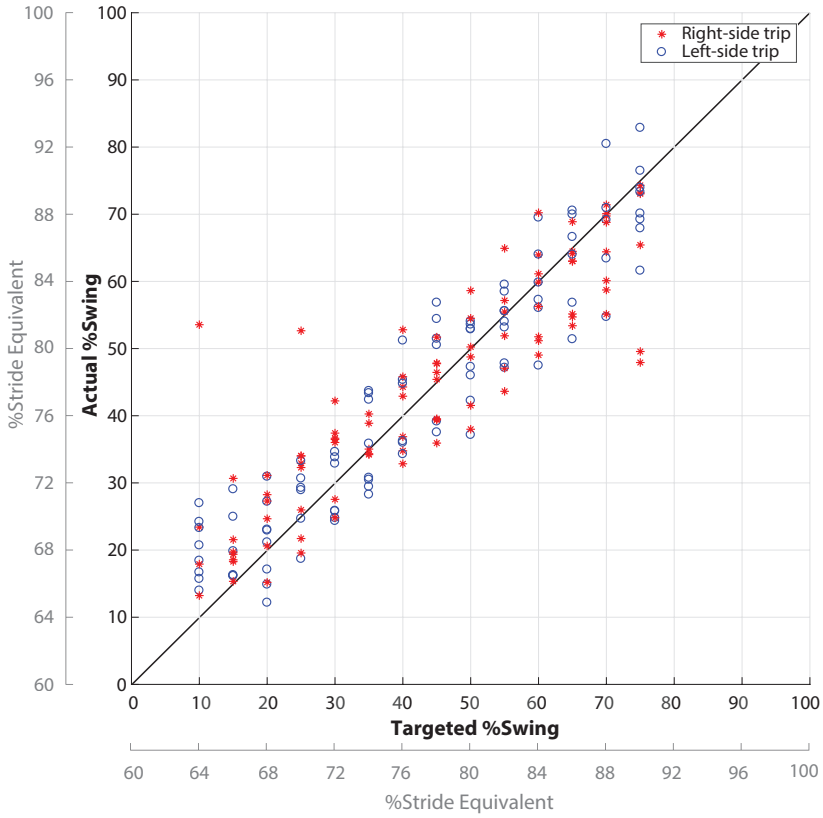

Figure 2.5: Targeted percent swing of perturbation versus the actual percent swing. Targeted percent swing is the input of the predictive targeting algorithm. Data are shown for 190 stumbles (28 trips per 7 subjects, excluding 6 mistrials). The mean absolute error of the system was 6.2% swing (2.5% stride), which corresponds to approximately 25 ms. An identity line is included to better visualize the system's accuracy. The stride equivalent axis assumes swing phase makes up 40% of the stride cycle.

seen while the ankle maintained a slight dorsiflexion as the foot cleared the obstacle. The contralateral side displayed increased hip flexion and knee flexion during the following swing phase.

For the delayed lowering strategy (Fig. 2.6 bottom row), the subject's response began with increased hip and knee flexion on the ipsilateral side, prior to switching to hip and knee extension as the foot was subsequently lowered to the ground. The ankle displayed initial plantarflexion as it contacted the obstacle before transitioning to dorsiflexion. In the next stride, an increase in hip and knee flexion and an increase in ankle dorsiflexion were observed as the foot cleared the obstacle. On the contralateral side, increased hip and knee flexion as well as ankle dorsiflexion were observed during the subsequent swing phase

To complement the single subject results, Fig. 2.7 shows averaged results across all subjects in this study for various kinematic metrics associated with each strategy. During the perturbed step, the elevating strategy exhibited the highest deviation from unperturbed walking in peak trunk deflection angle (16° greater), ipsilateral peak hip flexion angle (34° greater), ipsilateral peak knee flexion angle (42° greater), and ipsilateral peak ankle dorsiflexion angle (12° greater). For the stride following the perturbation, the delayed lowering response exhibited the greatest deviation from unperturbed walking in peak trunk deflection angle (23° greater), ipsilateral peak knee flexion angle (50° greater), and ipsilateral peak ankle dorsiflexion angle (6° greater). On the contralateral side, the lowering strategy yielded the greatest deviation from unperturbed walking peak knee flexion angle (28° greater), and peak ankle dorsiflexion angle (9° greater). Statistical significance for each metric compared to the unperturbed data is illustrated in Fig. 2.7.

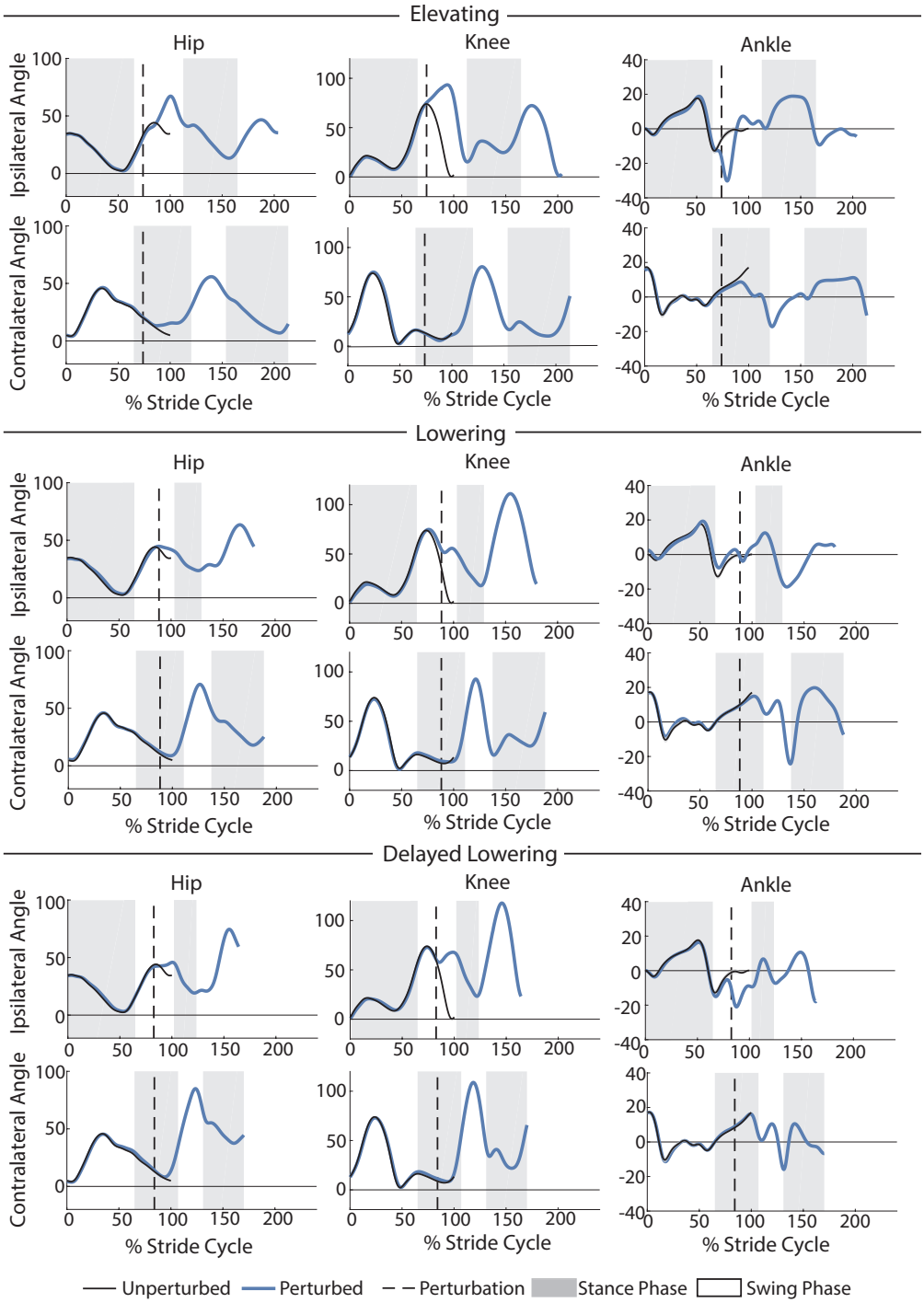

Figure 2.6: Kinematic trajectories of the hip, knee, and ankle. Depicted are the kinematic trajectories of the ipsilateral and contralateral limbs during an elevating, lowering, and delayed lowering strategy from a single subject. The trajectories were normalized to the toe-off of the unperturbed stride and extended accordingly. The unperturbed stride shown is the average of 25 strides prior to the perturbation. For the hip and knee, positive angles indicate joint flexion and negative angles indicate joint extension. For the ankle, positive angles indicate dorsiflexion and negative angles indicate plantarflexion. Angles are reported in degrees.

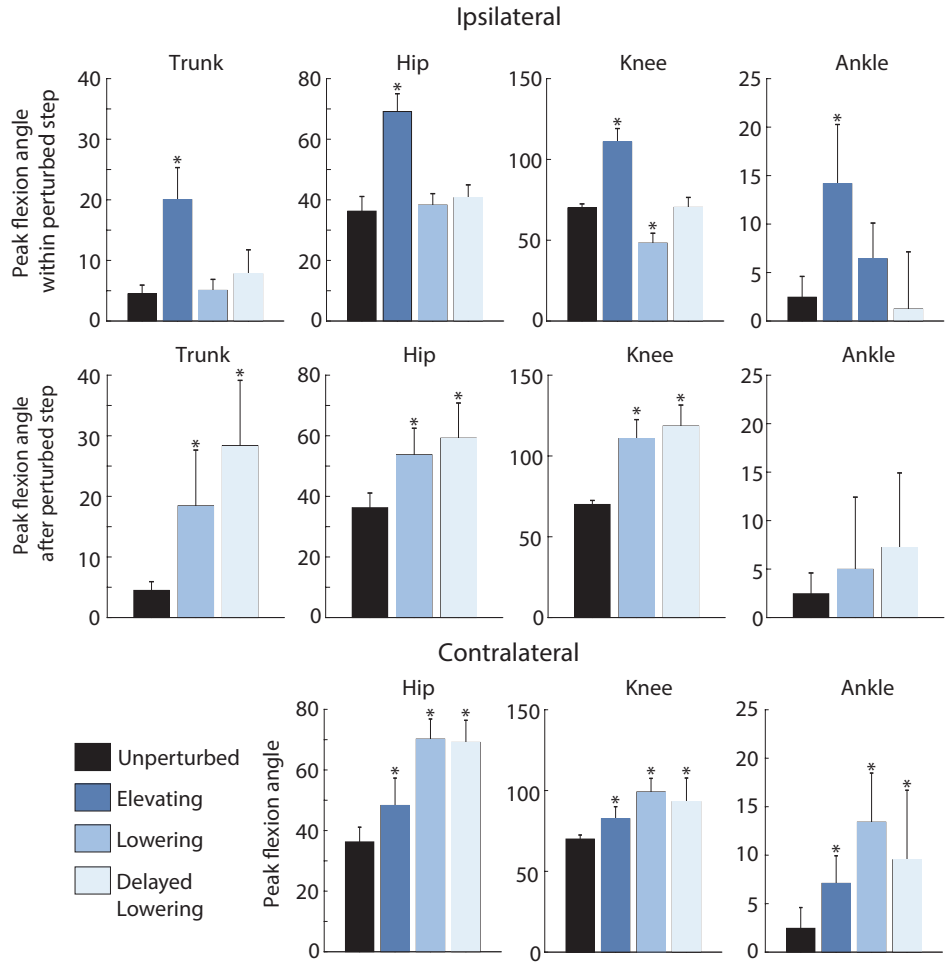

Figure 2.7: Peak joint and trunk deflection angles. Values are depicted for the elevating, lowering, and delayed lowering strategies on the ipsilateral and contralateral limbs. Each bar depicts the inter-subject ($N = 7$) mean of the average peak angles for each strategy, with standard deviation displayed as error bars. For the ipsilateral (perturbed) limb, peak joint flexion angle or trunk deflection angle within the perturbed step (before the perturbed foot contacts the treadmill after perturbation) and after the perturbed step (in the step following the perturbation) are reported. For the contralateral limb, peak joint flexion angle in the step following the perturbation are reported. For the ankle, flexion refers to dorsiflexion. The unperturbed values shown are the inter-subject mean of the 25-stride average prior to the perturbation. Angles are reported in degrees. For each metric, values that are significantly different from that of unperturbed walking are marked with an asterisk.

Fig. 2.8 compares summary metrics across all subjects in this study to the same metrics reported in previous overground studies, specifically those reported in [24, 38]. For the elevating strategy, the peak trunk deflection, hip flexion, knee flexion, and ankle dorsiflexion angles are qualitatively comparable to previous studies, although slightly larger. All metrics reported in both this paper and [24, 38] are significantly different from their respective unperturbed metrics for the elevating strategy. For the lowering strategy, trunk deflection angle during the perturbed stride was again qualitatively comparable to [24] (both this paper and [24] found no significant difference between this metric and that of the unperturbed stride). In the stride following the perturbation, trunk deflection angle is significantly different from that of the unperturbed stride for this paper and [24], though this paper reports slightly higher trunk deflection angle during the perturbed stride. Statistical significance for each metric compared to the unperturbed data for this paper and for [24, 38] is illustrated in Fig. 2.8.

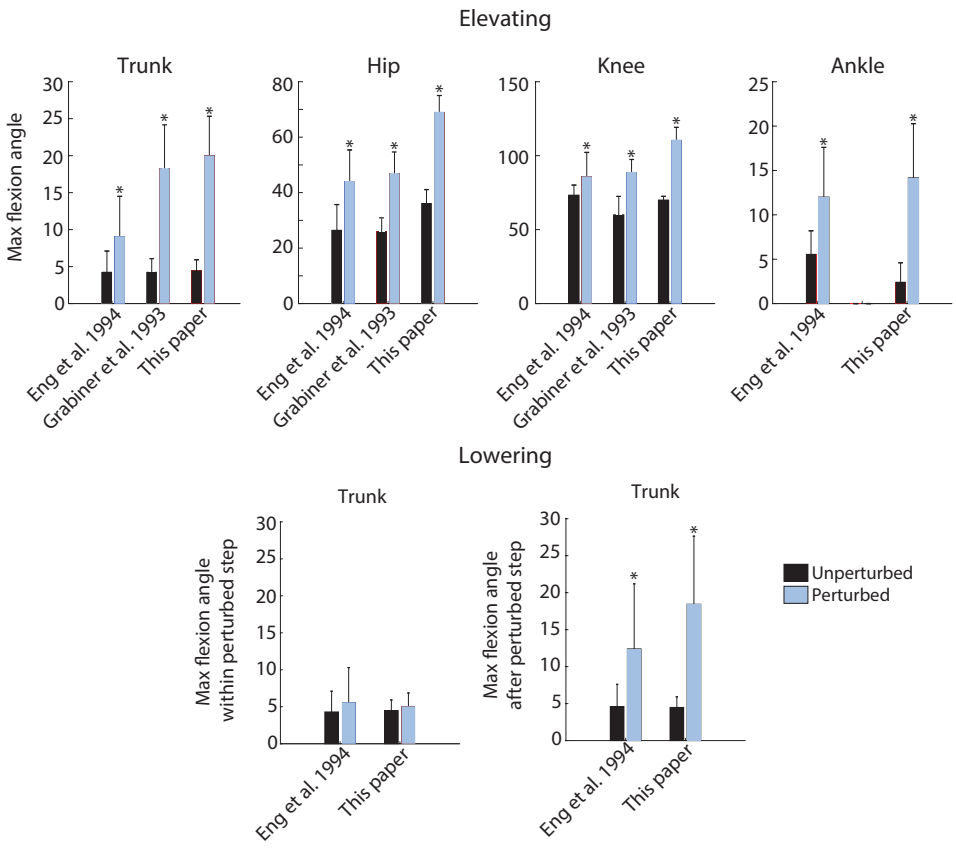

Figure 2.8: Peak joint angles for the elevating and lowering strategies. Results from this study as well as from previous works ([5, 32]) are reported. For this paper, the bars depict the inter-subject ($N = 7$) mean of the average peak angles for each strategy, with inter-subject standard deviation displayed as error bars. For [5], the bars depict the total average peak angle for each strategy ($n = 25$ stumbles for elevating, $n = 17$ stumbles for lowering, $n = 25$ for unperturbed control), with standard deviation displayed as error bars. For [32], the bars depict total average peak angles for the elevating strategy ($n = 42$ stumbles), with standard deviation displayed as error bars. For the elevating strategy, peak flexion angle is defined as the peak joint angles of the ipsilateral limb and peak trunk deflection angle during the swing phase of the recovery. For the lowering strategy, peak trunk deflection angle within perturbed step (before the perturbed foot contacts the treadmill after perturbation) and after perturbed step (in the step following the perturbation) are reported. For the ankle, flexion refers to dorsiflexion. The unperturbed values shown are the inter-subject mean of the 25-stride average prior to the perturbation. Angles are reported in degrees. Asterisks above bars indicate that the value is significantly different from the same metric for unperturbed walking.

2.4.4 Kinetics

Joint-level kinetics were computed for each of the strategies for both the ipsilateral and contralateral limbs. Sagittal-plane joint moments for each strategy from the same subject are shown in Fig. 2.9. Inter-subject mean peak kinetic metrics across all subjects for each strategy as well as unperturbed walking are given in Fig. 2.10. Although the system enables the estimation of joint-level kinetics as intended, in several trials the subject crossed over onto the contralateral belt during recovery which compromises the inverse dynamics calculations, or the obstacle moved relative to the treadmill belt after impact with the swing foot (which would require an additional correction algorithm, not yet implemented, in order to properly estimate inverse dynamics). Because of these factors, trials in which either event occurred were removed from the kinetic analysis. As such, for the contralateral foot 126 ($N = 7$) elevating strategies, 18 ($N = 7$) lowering strategies, and 22 ($N = 6$) delayed lowering strategies were included. For the ipsilateral foot 24

($N = 7$) elevating strategies, 2 ($N = 2$) lowering strategies, and 16 ($N = 6$) delayed lowering strategies were included.

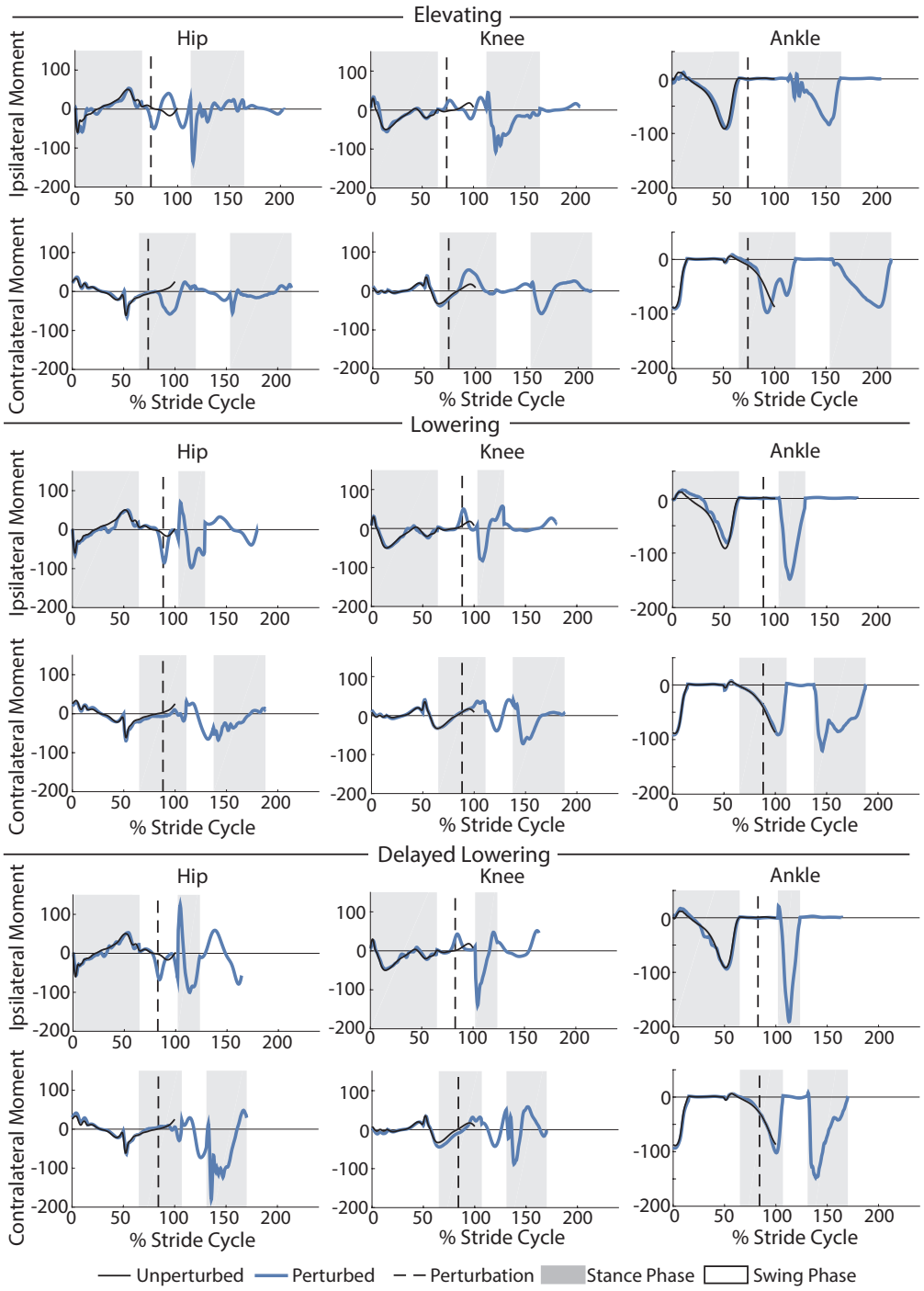

Figure 2.9: Kinetic trajectories of the hip, knee, and ankle. Depicted are the kinetic trajectories of the ipsilateral and contralateral limbs during an elevating, lowering, and delayed lowering strategy from a single subject. The trajectories were normalized to the toe-off of the normal stride and extended accordingly. The unperturbed stride shown is the average of 25 strides prior to the perturbation. For the hip and knee, positive moments indicate flexion moments and negative moments indicate extension moments. For the ankle, positive moments indicate dorsiflexion moments and negative moments indicate plantarflexion moments. Moments are reported in Newton-meters.

For the elevating strategy (Fig. 2.10 top row), the subject exhibited a semi-periodic ipsilateral hip moment oscillating between extension and flexion during swing before producing a large extension torque upon contact with the ground. The ipsilateral knee displayed similar behavior as it oscillated between flexion and extension moments in swing before exerting a large extension moment upon heel-strike. These hip and knee moment behaviors are qualitatively consistent with the findings of [25]. During stance as the ipsilateral limb elevated over the obstacle, the contralateral limb experienced an extension moment at the hip and flexion moment at the knee, which is qualitatively consistent with the results of [88].

For the lowering and delayed lowering strategies (Fig. 2.10 middle and bottom row respectively), the subject displayed very similar kinetic characteristics. After contact with the obstacle, the ipsilateral hip produced an extension moment before producing a flexion moment upon ground contact and then switching back to an extension moment in late stance. The ipsilateral knee demonstrated a flexion moment after contact with the obstacle before exhibiting an extension moment during early stance and switching to a flexion moment in late swing. The ipsilateral ankle demonstrated a large plantarflexion moment during stance after the perturbation. The contralateral limb initially exhibited a hip and knee flexion moment before entering swing phase and then exerted a large hip and knee extension moment on subsequent heel-strike.

Fig. 2.10 shows averaged data across all subjects in this study for various kinetic metrics associated with each strategy. On the ipsilateral side, the elevating strategy exhibited the greatest deviation from unperturbed walking in peak hip extension moment (1.2 Nm/kg greater), peak knee extension moment (1.4 Nm/kg greater), peak vertical GRF (8.7 N/kg greater) and peak AP GRF (1.3 N/kg greater). The delayed lowering strategy exhibited the greatest increase in peak ankle plantarflexion moment (0.9 Nm/kg greater) on the ipsilateral side. As the perturbed limb elevates, the contralateral limb showed increases in peak hip extension moment, peak knee flexion moment, peak ankle plantarflexion moment, and peak GRFs compared to unperturbed walking. In the stance phase after perturbation, lowering and delayed lowering strategies exhibited increases in peak joint moments and GRFs on the contralateral side, compared to that of unperturbed walking. Significance for each metric compared to the unperturbed data is illustrated in Fig. 2.10.

2.5 Discussion

The stumble perturbation system presented here provides a realistic obstacle perturbation to the swing foot, which both disrupts the foot's trajectory and requires the person to clear a physical obstacle in the course of recovery to avoid falling. The system is capable of introducing repeated perturbations in a targeted manner without subjects being able to perceive or anticipate the perturbation. The system was able to elicit the three stumble recovery strategies previously described in literature, and kinematic and kinetic results obtained were qualitatively consistent with behaviors observed in previously published overground studies of stumble (Fig. 2.8). Further, the system enables precise, controllable timing of the perturbation to within 25 ms, or 2.5% of the stride cycle (Fig. 2.5). Finally, the system allows for the collection of joint-level kinematic and kinetic data for both limbs before, during, and after the perturbation (Fig. 2.6 and Fig. 2.9). The obstacle delivery apparatus design and predictive targeting algorithm are detailed in a manner to enable replication of the system for those wishing to study stumble recovery.

This system has eliminated the introduction of detectable vibrations to the treadmill, as evidenced by the Perception Trials, in which no subject indicated any perception of the obstacle out of 168 trials. Note that the Perception Trials were performed both before and after the Perturbation Trials, indicating that the subjects did not acclimate to the system. Avoiding perception of the obstacle prior to perturbation is imperative for the stumble perturbation system, as any anticipation of the impending perturbation will alter the reflexive nature of the stumble recovery response and compromise the authenticity of the response.

The apparatus itself has removed the issue of inducing vibrations to the treadmill, and thus the subject's ability to feel the obstacle entering the treadmill. However, several other measures were taken experimentally to ensure that the subject was unaware of the obstacle's entry (similar to previous works [19]). First, though efforts were made to reduce the audible noise from the obstacle rolling down the ramp (e.g., greased roller bearings), it is impossible to make such an event completely silent. Thus, white noise and noise-cancelling headphones were used. Second, the inferior visual field-blocking goggles were necessary to avoid subject temptation of looking down at the apparatus. Lastly, the Serial Sevens task was not necessary to avoid detection, but rather was chosen as a distraction task, since

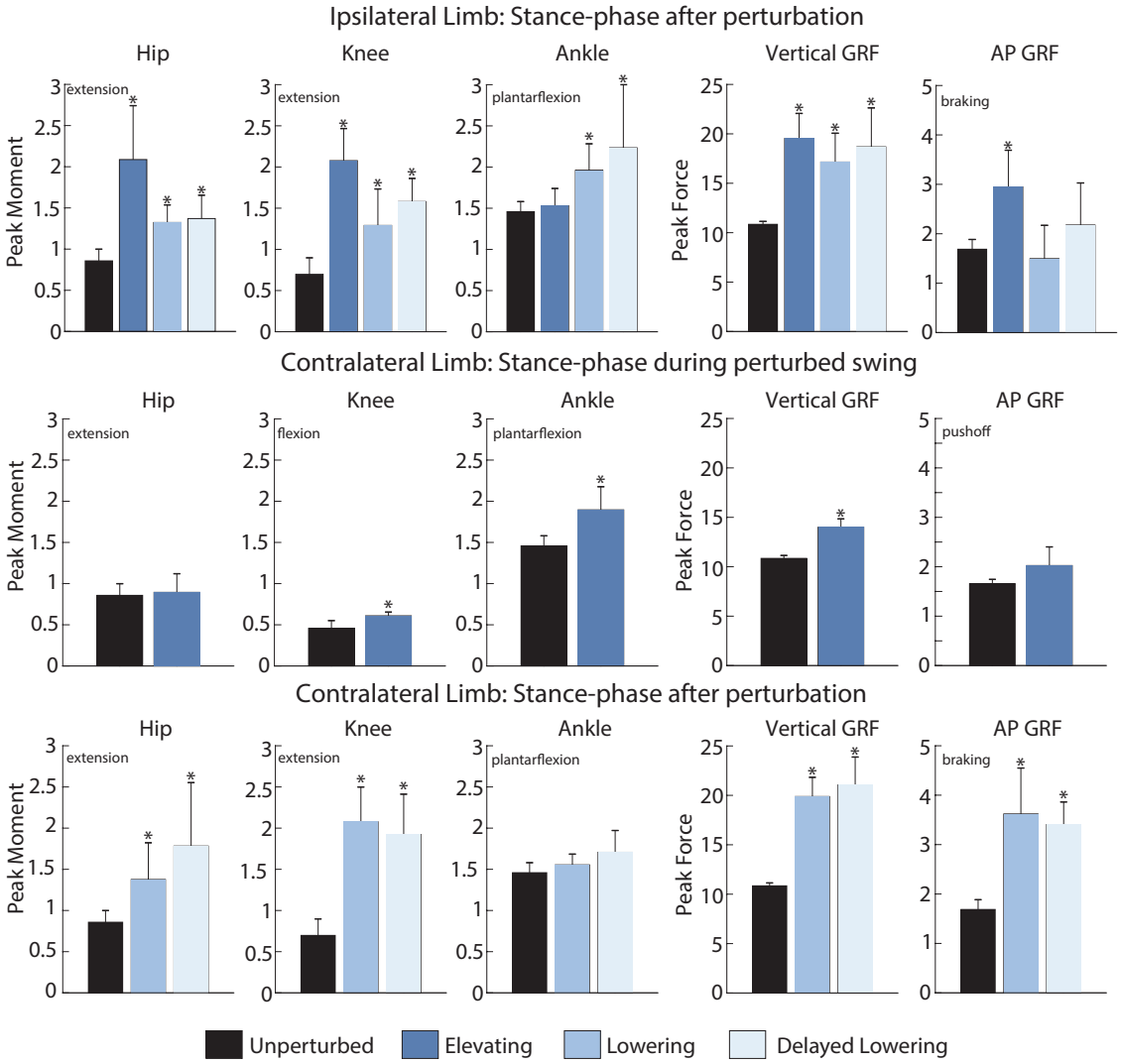

Figure 2.10: Peak joint moments and GRFs. Values are depicted for the elevating, lowering, and delayed lowering strategies on the ipsilateral and contralateral limbs. Each bar depicts the inter-subject mean of the average peak values for each strategy, with standard deviation displayed as error bars. The unperturbed values shown are inter-subject mean of the 25-stride average prior to perturbation. Moments are reported as Newton-meters/kilogram, and forces are reported as Newtons/kilogram. Asterisks above bars indicate that the value is significantly different from the same metric for unperturbed walking.

anticipation of stumble can alter the stumble response. The Serial Sevens task therefore was intended to distract and relax the subjects, in order to produce a more authentic stumble response.

The accuracy of the system in targeting specific times in swing phase helped to minimize mistrials and improve analytical resolution (Fig. 2.5). In this study, only 3% of trials were deemed mistrials (compared to [81, 102], in which 23% and 39% were mistrials, respectively). Minimizing mistrials is particularly important in the study of the stumble recovery response in populations with gait pathologies, for whom an excessive number of mistrials can lead to longer experiments, which can be physically taxing. Additionally, by ensuring the stumble perturbation system is accurate, a larger data set can be obtained without requiring as many sessions or as large of a subject pool.

The kinematic trends produced by the system (comparing unperturbed to perturbed strides) were qualitatively similar to those found in previous overground studies (Fig. 2.8), with the possible exception of peak hip flexion. The greater

difference between unperturbed and perturbed peak hip angle is likely attributable to the fact that this study employed a heavier obstacle resulting in a greater impedance perturbation than from obstacles employed in the studies by [24, 38]. The similarity shown between the system depicted in this article and previous overground systems is notable as it demonstrates that the treadmill-based gait perturbation system provides kinematically and kinetically similar responses to overground stumble. Note that because the treadmill belt velocity was held constant for each trial, no acceleration was applied to the subject and as such the treadmill can be treated as an inertial reference frame, just as the ground is for overground walking.

The system allowed for the first time the calculation of ipsilateral and contralateral joint-level kinetics before, during, and after the stumble event. Time series data for a single subject and a brief set of kinetic summary metrics for all subjects are presented (Fig. 2.9 and Fig. 2.10). The purpose of this paper was simply to demonstrate the capability of the system. A more comprehensive analysis and interpretation of stumble recovery kinetics warrants further study but is beyond the scope and objective of this paper. One important consideration for future work is that the obstacle did not always remain stationary upon foot contact. Rather, in approximately 60% the recorded trips, the obstacle rotated about the vertical or mediolateral axis during the stumble. This behavior was similarly reported in other studies [102], and is representative of many actual stumble events (i.e., stumbling over a rock or heavy object that may shift on the ground). Movement of the obstacle, however, must be accounted for in the kinetic computations. A method for doing so could be developed and implemented using motion capture markers on the obstacle; however, it was not presented here, and therefore the ipsilateral kinetic data presented here (Fig. 2.10) corresponds to only the trials in which the obstacle did not move (70 of the 190 trials).

Beyond the limitation in kinetic analysis, other limitations of this system include the predictive targeting algorithm's inability to respond to instantaneous changes in the subject's gait immediately prior to or after the release of the obstacle and the assumption of constant foot velocity during swing phase. The predictive nature of the system (due to the travel time of the obstacle being notably longer than that of the subject's foot) requires the system to take a moving average of several gait metrics which are used to determine the release time of the obstacle. Once the obstacle is released, the system cannot respond to deviations from the period motion, or belt location. Since the release occurs one to two strides prior to the perturbation, some deviations may occur, which are likely the limiting factor in determining targeting accuracy. Finally, the system's assumption of constant foot velocity (in its calculation of the travel time of the subject's foot) could also contribute to the slightly different levels of error in early and late swing (Fig. 2.5), since these regions are where this assumption is less robust.

The system's efficacy in producing realistic, unanticipated, and controllable perturbations to the swing foot while allowing for the measurement and calculation of joint-level kinetics and kinematics lends itself to several prevalent research applications. First, its targeting capabilities could provide insight into several unknowns regarding the biomechanics of stumble recovery for healthy individuals, such as when and why healthy individuals choose specific recovery strategies. Second, this system can be used to study individuals who are particularly susceptible to perturbations of the swing foot (e.g., transfemoral prosthesis users) to study how their strategies differ from healthy individuals, and ultimately how to inform better interventions (e.g., prostheses) to recover from such perturbations. Lastly, as proposed and described by others, this system could be used for fall training purposes [62]; however, the efficacy of using this apparatus as a training device to potentially reduce the incidence or severity of community falls is unknown.

2.6 Conclusion

The stumble perturbation system described in this paper was shown to be an effective means of inducing stumbles and evaluating recovery strategies during human walking. The system provided realistic obstacle perturbations and was also shown to prevent anticipation by the subjects due to the obstacle's imperceptible entry onto the treadmill. The accurate targeting demonstrated by the system enables efficient and systematic data collection, thus reducing the required subject sample size or the amount of time spent collecting data on each subject. The ability to collect kinematic and kinetic data for both the ipsilateral and contralateral lower limbs allows for versatile use of the system across a diverse range of studies. Finally, this work provides the necessary obstacle delivery apparatus CAD files and predictive targeting algorithm scripts such that this system could be recreated and adopted by other researchers studying stumble recovery.

CHAPTER 3

On the basis for stumble recovery strategy selection in healthy adults

3.1 Chapter Summary

Healthy adults employ one of three primary strategies to recover from stumble perturbations – elevating, lowering, or delayed lowering. The basis upon which each recovery strategy is selected is not known. Though strategy selection is often associated with swing percentage at which the perturbation occurs, swing percentage does not fully predict strategy selection; it is not a physical quantity; and it is not strictly a real-time measurement. The objective of this work is to better describe the basis of strategy selection in healthy individuals during stumble events, and in particular to identify a set of real-time measurable, physical quantities that better predict stumble recovery strategy selection, relative to swing percentage. To do this, data from a prior seven-participant stumble experiment was reanalyzed. A set of biomechanical measurements at/after the perturbation were taken and considered in a two-stage classification structure to find the set of measurements (i.e., features) that best explained the strategy selection process. For Stage 1 (decision between initially elevating or lowering of the leg), the proposed model correctly predicted 99.0% of the strategies used, compared to 93.6% with swing percentage. For Stage 2 (decision between elevating or delayed lowering of the leg), the model correctly predicted 94.0% of the strategies used, compared to 85.6% with swing percentage. This model uses dynamic factors of the human body to predict strategy with substantially improved accuracy relative to swing percentage, giving potential insight into human physiology as well as potentially better informing the design of fall-prevention interventions.

3.2 Introduction

People exhibit various balance recovery strategies in response to a stumble perturbation. The three primary responses to a perturbation in swing phase have been identified as (1) the elevating strategy, in which the foot lifts up and forward to clear the obstacle in the same step, (2) the lowering strategy, in which the foot lowers to the ground behind the obstacle and clears it in the following step, and (3) the delayed lowering strategy, in which the foot initially lifts up but subsequently lowers to the ground behind the obstacle before clearing it in the following step [101, 24]. The causal factors that underlie the selection of these recovery strategies are not well known. Better understanding the factors associated with strategy selection (i.e., the process by which a perturbation results in one of the three aforementioned recovery strategies), and particularly the information upon which this selection is based, may improve the design of interventions intended to mitigate the effect of stumble perturbations, especially for individuals at heightened fall risk (e.g., elderly individuals, stroke patients, and lower-limb prosthesis users).

Over the past several decades, the majority of stumble-related research has focused on three topics: experimental apparatus design, fall prediction, and recovery characterization. Regarding the first, various methods of eliciting stumbles in a lab setting have been presented and validated in order to study stumbling and the subsequent recovery or fall of healthy and impaired individuals. Methods include overground floor-deployable obstacle perturbations (e.g., [24]), overground rope-blocking (e.g., [11]), treadmill-based belt-deployable obstacle perturbations (e.g., [102, 50]), treadmill-based rope-blocking (e.g., [107, 30]), and electrical stimulation (e.g., [6]). Using these techniques, researchers have explored the risk factors for falls in various populations. Some studies investigate the effect of dynamic factors such as trunk flexion angle on recovery success [81, 118, 98, 18, 29, 111], while others consider demographics and physical characteristics such as age, sex, strength and gait pattern [82, 80, 79]. Other studies characterize the nature of recovery in healthy individuals, namely the elevating, lowering, and delayed lowering strategies. The focus of these studies include: the kinematics of the tripped limb for each recovery strategy [24, 102, 38], the reflexes involved in each recovery strategy [101, 24, 103, 100, 96, 119], the role of the support limb [87, 87], the role of arm movements [97], the mechanical modeling of recovery [15], and segmental energy changes in recovery strategies [31].

Although the kinematics and kinetics of the three primary recovery strategies have been characterized, the basis upon

which each is selected is not well established. The convention in prior literature is to associate stumble recovery strategy selection with the swing percentage at which the perturbation occurs. For example, it has been observed that elevating strategies are typically used following early-swing perturbations, while lowering strategies are typically used following late-swing perturbations (e.g., [24]). However, there is evidence that healthy individuals do not select a recovery strategy during a stumble event based upon swing percentage.

First, the accuracy with which swing percentage predicts strategy selection is limited, particularly in the mid-swing regime (i.e., 40-70% swing phase). Reference [101] introduced stumble perturbations to eight healthy individuals, targeted at early, mid, and late swing phase. The authors found that there was no clear swing percentage threshold that separated elevating from lowering strategies, concluding that the final strategy used was not simply a function of the swing percentage of the perturbation. Similarly, [30] introduced stumble perturbations of various durations and at various points in swing phase to five healthy individuals and concluded that the factors that led to the selection of a specific recovery strategy were unknown. Reference [107] also reported that perturbations during mid-swing can result in various recovery strategies, suggesting that other factors (besides swing percentage of perturbation) affect strategy selection. This idea was also highlighted in [93].

Second, swing percentage is neither a real-time measurement nor a physical quantity. Swing percentage is defined relative to the entire swing phase (time duration), which cannot be exactly known until the entire swing phase has been completed. Furthermore, swing percentage is not a direct physical measurement of the body's dynamic state at perturbation. Rather, a person (or device) who has stumbled must make a strategy selection in real-time, presumably based on sensing of one or more measurable quantities. Note that swing percentage can be estimated in real-time via measurement of at least one measurable proxy (e.g., ground reaction force), where the accuracy of the estimate depends on the degree of stationarity (i.e., invariant periodicity) and structural invariance (i.e., invariance in relationships between states). The accuracy of this real-time estimation therefore decreases as individuals change cadence or vary movement patterns. Thus there is ample motivation for exploring the extent to which real-time physical measurements (which do not require assumptions of stationarity or structural invariance) can provide improved accuracy relative to a phase variable (e.g., swing percentage).

A couple papers have investigated factors beyond swing percentage for strategy selection [106, 81]. Reference [106] investigated the effect of perturbation duration and limb tripped (i.e., left vs. right), in addition to swing percentage, on strategy selection. They found that swing percentage and perturbation duration significantly improved the prediction of their multinomial logistic regression model, and that limb tripped improved the prediction but not significantly. Reference [81] investigated the effect of forward hip velocity and speed and height of the swing ankle (in addition to swing percentage) on strategy selection. They found that the odds of employing a lowering strategy increased as swing ankle height decreased, and the odds increased as swing percentage increased, but recovery strategy was unrelated to the forward hip velocity or swing ankle speed. The delayed lowering strategy was not investigated.

This work builds upon this prior research, and specifically leverages a large experimental set of stumble data to offer insight into the nature of the strategy selection process, specifically by identifying a set (or sets) of factors that (i) are real-time measurable, physical quantities and (ii) predict strategy selection with better accuracy than using the traditional swing percentage input. The intent is to provide a better understanding of which physical factors may form the basis of strategy selection, giving potential insight into human physiology as well as informing the design of interventional devices such as prosthetic limbs.

3.3 Methods

In order to gain insight into which real-time measurable quantities best describe the outcomes observed in a prior study of healthy participant stumble perturbations, the problem was treated as a classification problem with a large number of possible measurable inputs, and with three output classes: Elevating, Lowering, and Delayed Lowering. The authors established a basic framework for the strategy selection process, based on foot trajectory timing. Next a set of potential model inputs was identified. Data from the prior stumble experiment were then processed and organized in such a way that the classification problem could be tested (i.e., features were extracted from the potential inputs as predictors, and data were organized into a set of potential features and corresponding output class for each trial). After several feature exploration steps, a feature selection process was implemented to obtain the final feature sets. Finally, classification

results using the final feature sets were compared to results using swing percentage of perturbation as the feature set (within the same selection framework). The following subsections enumerate: i) the stumble recovery experiment, ii) the strategy selection framework, iii) the set of potential model inputs, iv) the composition of datasets for each stage, v) feature exploration, vi) feature selection, and vii) model comparison.

3.3.1 Stumble Perturbation Experiment

In order to provide an extensive dataset upon which a stumble recovery strategy selection model could be constructed and tested, seven healthy participants (three female, four male, mean age: 23.6 yrs, mean height: 1.8 m, mean mass: 81.3 kg) were recruited in a prior study for a series of stumble perturbation experiments. The stumble perturbation system and protocol used are described in [50]. All experimental protocols were approved by the Vanderbilt Institutional Review Board, and all participants gave their written informed consent. Each participant experienced 14 unexpected obstacle perturbations to each limb, targeted between 10% and 75% swing phase in 5% increments, while walking on a treadmill at 1.1 m/s. Note that the obstacle perturbations were imperceptible to the participants prior to contact due to obstacle delivery apparatus design choices and sensory occlusion techniques, as detailed in [50]. This seven-participant, single-speed stumble experiment is hereafter referred to as Experiment A.

In order to better inform a potential dependence on walking speed, the experimental protocol was repeated for one of the seven participants (Participant 3) at two additional speeds. For these trials, the participant experienced a total of 13 obstacle perturbations at 0.8 m/s and 13 obstacle perturbations at 1.4 m/s, targeted between 10% and 75% swing phase. This single-participant, two-speed stumble experiment is hereafter referred to as Experiment B.

For all trials, ground reaction force (GRF) data were collected under each foot at 2 kHz via a force-instrumented split-belt treadmill (Bertec, Columbus, USA), in addition to full-body kinematic data (including foot, shank, thigh, pelvis, torso, upper arm, and forearm segments), which were recorded at 200 Hz via an infrared motion capture system (Vicon, Oxford, GBR). GRF and motion capture data were processed with a zero-phase, 3rd order, Butterworth low-pass filter at a cutoff frequency of 15 and 6 Hz, respectively. Inverse dynamics were computed using Visual3D (C-Motion, Germantown, USA) to estimate full-body kinematics and kinetics for each trial.

The swing percentage at which the stumble occurred was calculated as the time of perturbation relative to the preceding toe-off event divided by the average swing time of 25 strides prior to the perturbation. The perturbation event was determined as the instant at which the foot contacted the obstacle, which was identified via a transient peak in the anterior-posterior GRF measured by the treadmill.

The recovery strategy used for each stumble event was identified as Elevating, Lowering, or Delayed Lowering, as determined by the trajectory of the swing foot immediately after the perturbation as follows: in the Elevating strategy, the foot lifts up and over the obstacle after contact with the obstacle; in the Lowering strategy, the foot lowers to the ground behind the obstacle after contact with the obstacle; in the Delayed Lowering strategy, the foot initially elevates (i.e., shows some upward motion) before elevation is abandoned and the foot subsequently lowers to the ground without clearing the obstacle.

3.3.2 Strategy Selection Framework

Strategy selection was modeled using a two-stage process. During initial exploration, the response to the stumble perturbation was modeled as a one-stage process, in which at the time of perturbation one of the three responses (Elevating, Lowering, or Delayed Lowering) was selected. Upon further analysis of the data, however, it became clear that a two-stage process, as depicted in Fig. 3.1, is more representative of the observed stumble recovery strategy selection process. Figure 3.1(a) shows a representation of typical data for foot height immediately following the stumble perturbation. As observed in the trajectories, the data indicate two points of bifurcation that occur at two distinct points in time: at the instant of perturbation, and tens of milliseconds after the perturbation. The first time point corresponds to either Elevating vs. Lowering, while the second time point corresponds to either continuing to Elevate vs. abandoning the Elevating strategy in favor of Lowering (i.e., Delayed Lowering). As such, the selection process was modelled as a two-stage process, as diagrammed in Fig. 3.1(b). Existence of a two-stage decision process

is also supported by [101], which reports that the EMG signals during a Delayed Lowering strategy suggests that on-line afferent information during the recovery is incorporated into the response and may be used to alter the final stumble recovery strategy. References [103, 72, 22] support the existence of a two-stage muscle activity response to perturbations, and [92, 94] explore this concept further by introducing a secondary constraint during trip recovery. Thus, the Delayed Lowering strategy is modeled as a change in initial strategy rather than a strategy in itself. The authors note that the existence of a two-stage selection process, such as that proposed here, was further substantiated by improved accuracy of the models (see Supplementary Material Table D1 for results from alternate one-stage selection frameworks as a comparison). As such, model formulation was separated into two sequential classification problems: a first between Elevating vs. Lowering, and a second between Elevating vs. Delayed Lowering, each with a potentially distinct set of real-time inputs.

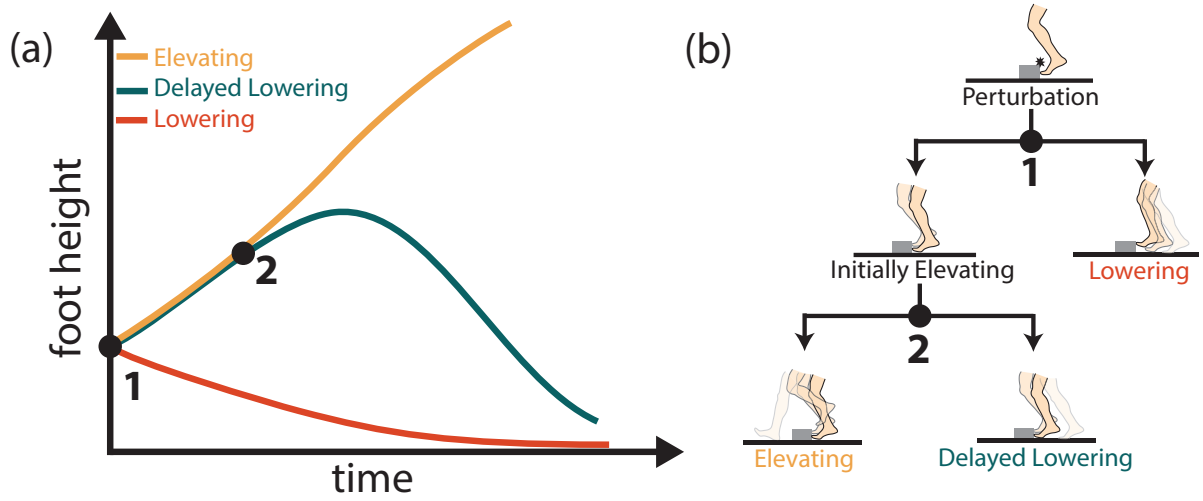

Figure 3.1: Representative plot of the foot's vertical trajectory for the first approximately 250 ms after a stumble perturbation (a), which motivates the two-stage selection process, diagrammed in (b). In the first stage, immediately after perturbation the individual initially either begins Elevating or Lowering; in the second stage, if the individual initially elevated, he/she either continues Elevating or abandons elevating and instead lowers (Delayed Lowering).

There are numerous classification algorithms that can be used for each stage in this model. In initial processing, multiple classification schemes were compared and all performed similarly; logistic regression was chosen based on its straightforward ability to report probability of membership in a certain class, which provides insight into the weight/confidence of each prediction, and its relative computational simplicity, which lends itself well to real-time implementation within embedded systems (e.g., for eventual implementation in interventional devices such as robotic prostheses).

3.3.3 Potential Model Inputs

To capture the body's configuration and body-mass-normalized kinetic state, the potential inputs included joint (internal) and segment (external) angles, joint and segment angular velocities, joint and segment angular accelerations, foot center-of-mass (COM) linear velocities and accelerations, body COM linear velocities and accelerations, as well as each foot's anterior-posterior position relative to the body center of mass (and corresponding derivatives). The quantities considered are illustrated in Fig. 3.2.

3.3.4 Composition of Datsets

Data from the stumble perturbation trials were treated as the classification problem discussed in the Strategy Selection Framework subsection. To start, two datasets were generated from Experiment A – one to test each stage.

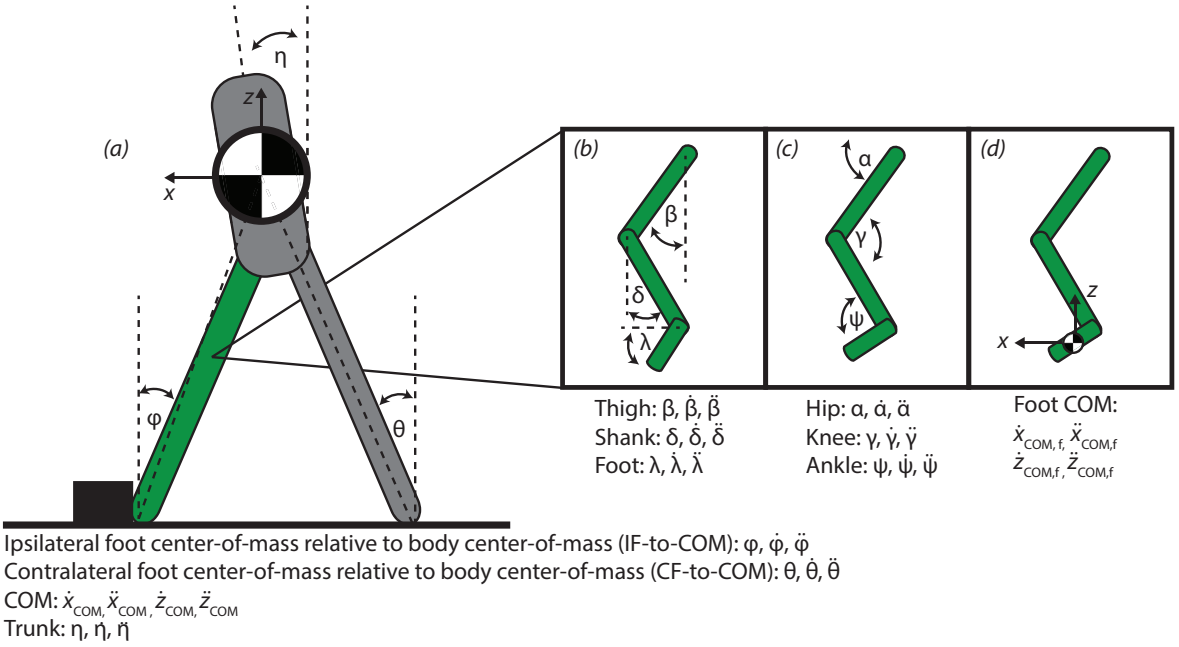

Figure 3.2: Diagram of the real-time measurable, physical quantities considered as potential inputs to the two-stage strategy selection model. The quantities capture (a) the whole-body configuration and body-mass-normalized kinetic states, (b) perturbed lower limb external configuration and body-mass-normalized kinetic states, (c) perturbed lower limb internal configuration and body-mass-normalized kinetic states, and (d) foot COM linear dynamics.

To test Stage 1 (see Fig. 3.1), each of the potential inputs was extracted for each trial at the instant of perturbation (hereafter referred to as features), and each trial was given the class tag Initially Elevating or Lowering (i.e., Elevating and Delayed Lowering strategies were labelled Initially Elevating while Lowering strategies were labeled Lowering). This dataset is hereafter referred to as Dataset A1, comprised of 35 features for each of the 188 relevant experimental trials.

To test Stage 2 (see Fig. 3.1), each of the potential inputs was extracted for all Initially Elevating trials (1) at the instant of perturbation and (2) 60 ms after the perturbation (hereafter referred to as features), and each of these trials was given the class tag Elevating or Delayed Lowering. The difference in each potential input from the instant of perturbation to 60 ms after the perturbation was also recorded and used as a feature. This dataset is hereafter referred to as Dataset A2, comprised of 105 features for each of the 165 relevant experimental trials. The 60-ms post-perturbation delay was chosen because it is sooner than the time-to-peak of the foot height trajectories of all Delayed Lowering strategies recorded (minimum: 90 ms, maximum: 200 ms; average: 128.7 +/- 28.2 ms) but long enough after the perturbation to allow for the integration of a new physiological reflex [101, 103].

As in Dataset A, all Experiment B trials were tagged as Initially Elevating or Lowering for Dataset B1, and all Initially Elevating trials were tagged as Elevating or Delayed Lowering for Dataset B2, and the corresponding set of features was generated for each trial. Features were standardized to zero-mean and unit-variance [43].

3.3.5 Feature Exploration

To gain an initial (and unsupervised) understanding of the information provided by the features for each stage, a Principal Component Analysis (PCA) was computed for the 35-feature set (Stage 1) and 105-feature set (Stage 2), which gives an estimate of the dimensionality of each feature set. Additionally, the Pearson's Linear Correlation

Coefficient was calculated for each feature against every other feature, which gives insight into the redundancy or interdependence of some features.

In order to understand the performance of each feature individually in explaining strategy selection, each feature was singularly considered as a feature subset. For Stage 1, each feature in Dataset A1 was fit to a logistic regression model with L2 (i.e., Ridge) regularization and cross-validated by participant [43]. Specifically, a model was fit to six participants' data and then tested on the remaining participant; this step was repeated seven times (until all trials had been tested). Initially Elevating was set as the reference class, such that for each trial, if the logistic regression model output a probability greater than 0.5, the trial was predicted as Initially Elevating; otherwise, it was predicted as Lowering. The probability and prediction for each trial were recorded. The percentage of trials that were predicted correctly (classification accuracy) was computed for each fold (which consisted of one participant's trials). After the seven iterations, the average of each participant's classification accuracy was computed and recorded as total classification accuracy. This process was performed for each of the following regularization strength (hyperparameter) values: 0.001, 0.01, 0.1, 1, 10, 100, 1000; the value that produced the highest total classification accuracy was used. For Stage 2, each individual feature in Dataset A2 was fit to a logistic regression model with L2 regularization and cross-validated by participant. Elevating was set as the reference class, such that for each trial, if the logistic regression model output a probability greater than 0.5, the trial was predicted as Elevating; otherwise, it was predicted as Delayed Lowering. This process was performed for each of the following regularization strength values: 0.001, 0.01, 0.1, 1, 10, 100, 1000; the value that produced the highest total classification accuracy was used.

3.3.6 Feature Selection

A wrapper method was used to find the subset of features that produced the highest total classification accuracy for each stage (i.e., the subset of features that best modeled the strategy selection process for Dataset A1, and then again for Dataset A2) [40]. Specifically, every combination of features for each stage (with a maximum number of features based on PCA results) was considered using the cross-validation procedure with hyperparameter tuning described in the previous subsection, and the subsets that produced the highest total classification accuracy were recorded for each stage.

In order to arrive at a final feature set for each stage, the feature subsets that best predicted strategy selection for 1.1 m/s trials (i.e., the feature subsets that resulted in the highest total classification accuracy from the wrapper method on Experiment A) were then tested to determine whether they also extended across walking speeds (i.e., also extended to Experiment B). Recall that Experiment B consisted of Participant 3 walking at two other walking speeds. In order to test the extent to which the feature sets identified in Experiment A also described Experiment B, each of the best performing subsets for Stage 1 was trained on Dataset A1, excluding data from Participant 3, and tested on Dataset B1 (Participant 3's data at other walking speeds related to Stage 1) for each of the regularization strength values. Likewise, each of the best performing subsets for Stage 2 was trained on Dataset A2, excluding data from Participant 3, and tested on Dataset B2 (Participant 3's data at other walking speeds related to the Stage 2) for each of the regularization strength values. Classification accuracy was recorded for each stage for each feature subset-hyperparameter combination, calculated as the percentage of correctly predicted trials in Datasets B1 and B2. The feature subsets for each stage that performed best on Datasets B1 and B2 were chosen as the final feature sets.

Logistic Regression model fitting and testing using the wrapper method with cross-validation and hyperparameter tuning were all performed in Python (Python 3.8, Amsterdam, NL) using the Scikit-learn module [83]. Preliminary data exploration was performed using the Orange Data Mining Toolbox [20].

3.3.7 Model Comparison

The classification results for the final feature sets for Stage 1 and Stage 2 were compared to the classification results for the feature set of swing percentage (using the same selection framework, classification algorithm, cross-validation process, and hyperparameter tuning) for Experiment A. Likewise, the classification results for training on Dataset A and testing on Dataset B using the final feature sets were compared to results using swing percentage as the feature set.

3.4 Results

3.4.1 Stumble Perturbation Experiment Results

In total, Experiment A elicited 126 Elevating strategies, 39 Delayed Lowering strategies, and 23 Lowering strategies. Note that six trials were excluded due to the participant stepping onto the obstacle (i.e., targeting error), and two trials were excluded due to anomalous recoveries (i.e., due to foot scuff and falling, which prevented these trials from being classified as one of the three defined recovery strategies). The breakdown of strategy used as a function of swing percentage of perturbation is depicted in Fig. 3.3.

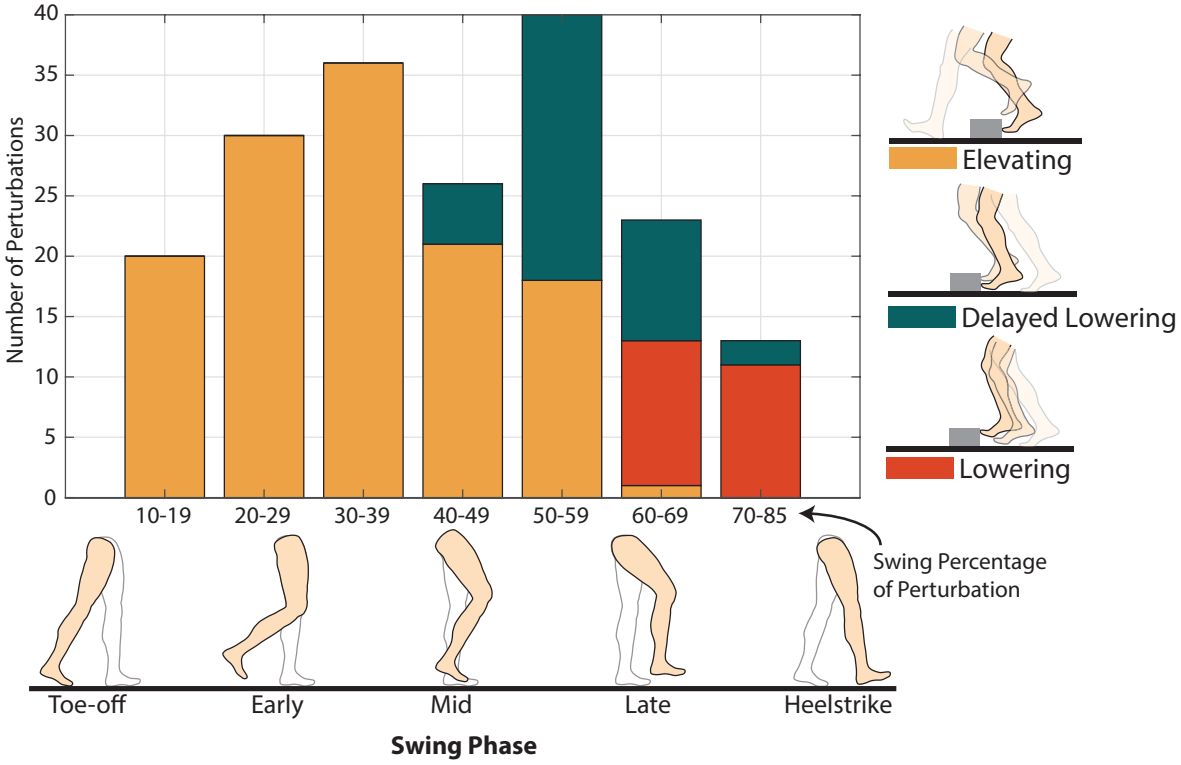

Figure 3.3: Breakdown of strategy used for each binned percentage of swing phase for Experiment A. In total there were 126 Elevating strategies, 39 Delayed Lowering strategies, and 23 Lowering strategies, depicted in the illustrations on the right.

Experiment B elicited a total of 8 Elevating, 3 Delayed Lowering, and 2 Lowering strategies at 0.8 m/s and 6 Elevating, 6 Delayed Lowering, and 1 Lowering strategy at 1.4 m/s. These results are expanded upon in Supplementary Material Fig. C1, which shows the breakdown of strategy used as a function of swing percentage of perturbation.

3.4.2 Feature Exploration Results

The PCA results indicated that approximately 80% of the variance of the Stage 1 set of features can be accounted for with three principal components, and 80% of the variance of the Stage 2 set of features can be accounted for with four principal components. Thus, four was set as the maximum number of features in a subset for the wrapper method described in Methods. To elaborate on the results of the PCA, Scree plots are reported in Supplementary Material Fig. A1. Correlation coefficients of every feature pair are given in the Supplementary Material Figs. A2 and A3 for reference.

Table 3.1: The final feature sets chosen for the model for each stage of the strategy selection process, with corresponding total classification accuracies from the cross-validation process for Datasets A1 and A2 (i.e., the average of the percentage of correctly predicted trials from each participant/fold). Note that the "+" indicates that the feature is the measurement taken 60 ms after perturbation, and the "Δ" indicates that the feature is the change in value from the instant of perturbation to 60 ms after the perturbation. Refer to Fig. 3.2 for diagrams depicting each physical quantity.

Dataset	Feature Set	Classification Accuracy
A1 (Stage 1)	CF-to-COM Angle (θ) Knee Angular Velocity ($\dot{\gamma}$) Body COM Vertical Velocity ($\dot{z}_{com}$) Foot Angular Acceleration ($\ddot{\lambda}$)	99.0%
A2 (Stage 2)	IF-to-COM Angular Acceleration ($\ddot{\phi}$) Shank Angular Acceleration ($\ddot{\delta}$) Knee Angle+ (γ+) Body COM Vertical Velocity Δ ($\dot{z}_{com\Delta}$)	94.0%

The feature that best predicted strategy selection alone for Stage 1 was hip angular velocity ($\dot{\alpha}$) with 96.3% classification accuracy, and for Stage 2 was ipsilateral foot to body COM (IF-to-COM) angle at perturbation (ϕ) with 88.3% classification accuracy. Notably, eight features individually outperformed swing percentage (93.7%) for Stage 1, and 13 features individually outperformed swing percentage (85.6%) for Stage 2. The classification accuracy of each individual feature for each stage is tabulated in Supplementary Material Tables A1 and A2 for reference.

3.4.3 Feature Selection Results

For Stage 1, using the wrapper method, four subsets of features (out of 59,500 possible subsets) produced a classification accuracy of 99.0% or higher. For Stage 2, 28 subsets of features (out of 4,973,150 possible subsets) produced a classification accuracy of 94.0% or higher. The final feature sets (i.e., the feature subsets for each stage that performed best when also testing on Dataset B) are reported in Table 3.1. Figures 3.4 and 3.5 further delineate the results for each stage with a) the confusion matrix of prediction results and b) scatter plots of the datasets as a function of inputs used. For reference, the classification results from remaining top performing subsets are tabulated in Supplementary Material Tables B1 and B2.

3.4.4 Model Comparison Results

The results from the two-stage strategy selection framework with final feature sets of real-time measurable, physical quantities (i.e., the final feature sets chosen as explained in Methods and reported in Table 3.1) will hereafter be referred to as the RTMM (real-time measurable model). The results from the same framework using swing percentage of perturbation as the feature set will hereafter be referred to as the SPM (swing percentage model).

Table 3.2 reports the classification accuracy results of the RTMM versus the SPM for each stage, as well as a composite accuracy for Dataset A. Specifically, the first two rows give the total classification accuracy from the cross-validation process for Datasets A1 and A2 (i.e., the average of the percentage of correctly predicted trials from each participant/fold). The composite accuracy (third row) was calculated by combining the Stage 1 and Stage 2 classification accuracies, weighted by the number of trials in each class. Table 3.3 reports the classification accuracy results of the RTMM versus the SPM for testing on Dataset B. Specifically, the first two rows give the percentage of trials from Datasets B1 and B2 that were predicted correctly (after training on Datasets A1 and A2 with the final feature sets, excluding data from Participant 3). The composite accuracy (third row) was calculated by combining the Stage 1 and Stage 2 percentages, weighted by the number of trials in each class. Additional figures delineating the results of the model for testing on Experiment B (i.e., confusion matrices and scatter plots) are provided in Supplementary Material Figs. C2 and C3 for reference. For comparison, Fig. 3.6 reports the confusion matrix for each stage when using swing

(a)

	Predicted Initially Elevating	Predicted Lowering	Total
Actual Initially Elevating	165	0	165
Actual Lowering	2	21	23
Total	167	21	188

(b)

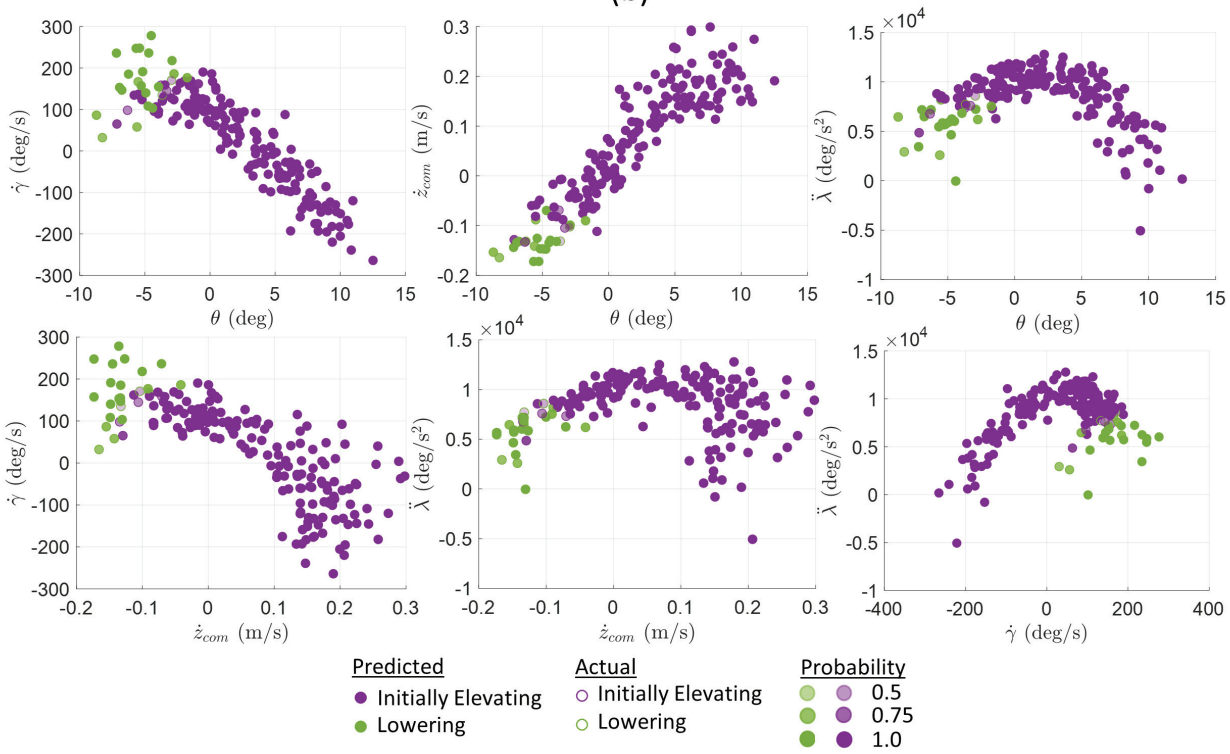

Figure 3.4: (a) The confusion matrix of prediction results and (b) scatter plots of the datasets as a function of features used for Stage 1 of the strategy selection process. For Stage 1, the scatter plot depicts contralateral foot to body COM (CF-to-COM) angle (θ), knee angular velocity ($\dot{\gamma}$), body COM vertical velocity ($\dot{z}_{com}$), and foot angular acceleration ($\ddot{\lambda}$) at the time of perturbation for each of the 188 trials. Refer to Fig. 2 for diagrams of these physical quantities. Purple indicates Initially Elevating, while green indicates Lowering. Marker outline color represents the actual strategy used, while marker fill color represents the model's prediction. Shading of the marker fill indicates the probability of being that strategy as indicated by the logistic regression model, in which the gradient from transparent to opaque indicates a probability of 0.5 to 1.0, respectively.

percentage as the feature set.

3.5 Discussion

Unlike using the conventional swing percentage criterion for describing stumble recovery strategy selection, the RTMM provides a physically implementable model (i.e., employs real-time measurable, physical quantities as inputs), and better accuracy.

For Stage 1 (Initially Elevating or Lowering), the model correctly predicts 99.0% of the strategy selection observed in Experiment A with the feature set of contralateral foot to body COM (CF-to-COM) angle (θ), knee angular veloc-

(a)

	Predicted Elevating	Predicted Delayed Lowering	Total
Actual Elevating	120	6	126
Predicted Delayed Lowering	4	35	39
Total	124	41	165

(b)

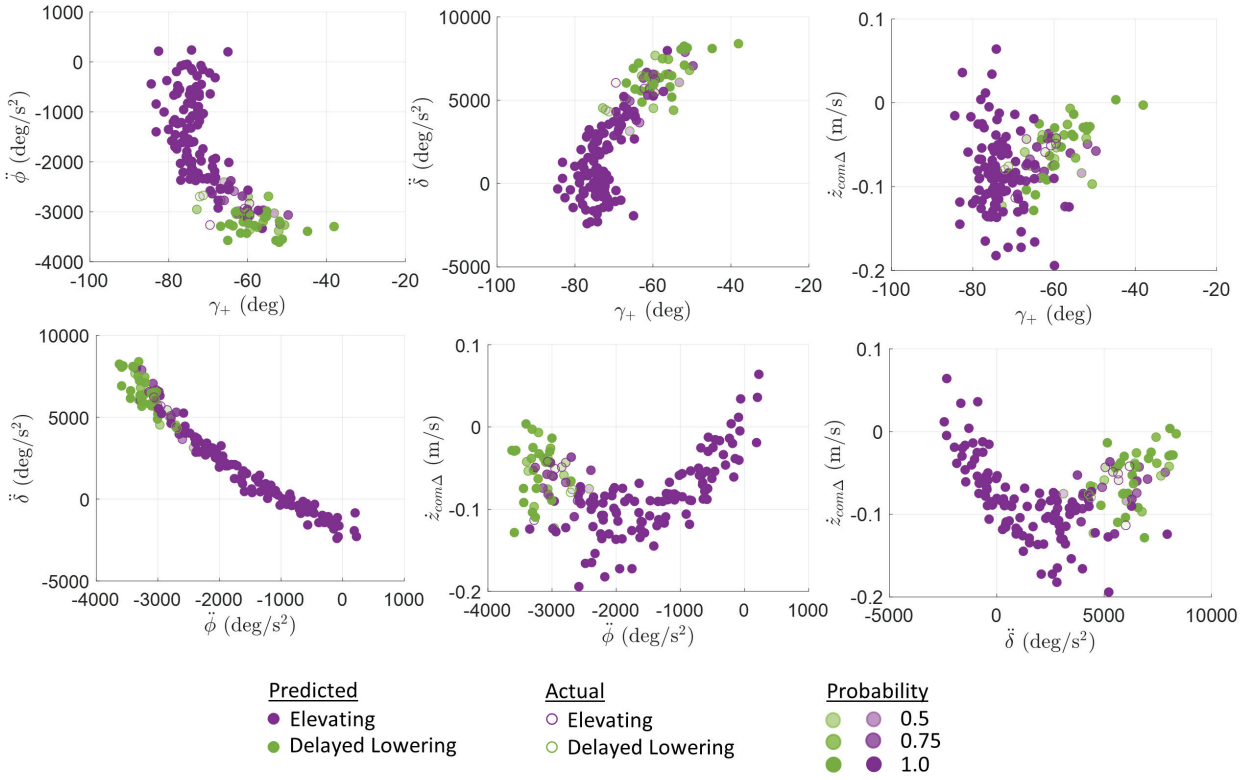

Figure 3.5: (a) The confusion matrix of prediction results and (b) scatter plots of the datasets as a function of features used for Stage 2 of the strategy selection process. For Stage 2, the scatter plot depicts the ipsilateral foot to body COM (IF-to-COM) angular acceleration ($\ddot{\phi}$) and shank angular acceleration ($\ddot{\delta}$) at the time of perturbation, knee angle 60 ms after the perturbation (γ_+), and change in body COM vertical velocity ($\dot{z}_{com\Delta}$) for each of the 165 trials. Note that the "+" indicates that the feature is the measurement taken 60 ms after perturbation, and that the "Δ" indicates that the feature is the change in value from the instant of perturbation to 60 ms after the perturbation. Refer to Fig. 3.2 for diagrams depicting each physical quantity. Purple indicates Elevating while green indicates Delayed Lowering. Marker outline color represents the actual strategy used, while marker fill color represents the model's prediction. Shading of the marker fill indicates the probability of being that strategy as indicated by the logistic regression model, in which the gradient from transparent to opaque indicates a probability of 0.5 to 1.0, respectively.

ity ($\dot{\gamma}$), body COM vertical velocity($\dot{z}_{com}$), and foot angular acceleration ($\ddot{\lambda}$) at the time of perturbation, compared to 93.7% when using swing percentage. Note that CF-to-COM angle captures how far the contralateral foot leads (anterior to) or trails (posterior to) the body's COM at the time of perturbation. As shown in Fig. 3.4(b), as the contralateral foot becomes more posterior to the COM at perturbation (i.e., more negative angle), the more likely a Lowering strategy is used (i.e., the incidence of Lowering strategies increases). Knee angular velocity captures the mass-normalized momentum of the perturbed limb at perturbation. The faster the knee is extending at perturbation (i.e., more positive angular velocity), the more likely a Lowering strategy is used. Body COM vertical velocity captures the mass-normalized momentum of the whole body. As the velocity becomes more positive at perturbation, the

Table 3.2: Classification accuracy for the RTMM and SPM for each stage of the strategy selection process as well as composite accuracy for Dataset A. Specifically, the first two rows give the total classification accuracy from the cross-validation process for Datasets A1 and A2 (i.e., the average of the percentage of correctly predicted trials from each participant/fold). The composite accuracy (third row) was calculated by combining the Stage 1 and Stage 2 classification accuracies, weighted by the number of trials in each class.

Dataset	RTMM Classification Accuracy	SPM Classification Accuracy
A1 (Stage 1)	99.0%	93.7%
A2 (Stage 2)	94.0%	85.6%
Composite	93.8%	81.3%

(a)

	Predicted Initially Elevating	Predicted Lowering	Total
Actual Initially Elevating	160	5	165
Actual Lowering	7	16	23
Total	167	21	188

(b)

	Predicted Elevating	Predicted Delayed Lowering	Total
Actual Elevating	116	10	126
Actual Delayed Lowering	13	26	39
Total	129	36	23

Figure 3.6: The confusion matrix of prediction results for (a) Stage 1 and (b) Stage 2 of the strategy selection process when using swing percentage as the feature set.

Table 3.3: Classification accuracy for the RTMM and SPM for each stage of the strategy selection process as well as composite accuracy for Dataset B. Specifically, the first two rows give the percentage of trials from Datasets B1 and B2 that were predicted correctly (after training on Datasets A1 and A2 with the final feature sets, excluding data from Participant 3). The composite accuracy (third row) was calculated by combining the Stage 1 and Stage 2 percentages, weighted by the number of trials in each class.

Dataset	RTMM Classification Accuracy	SPM Classification Accuracy
B1 (Stage 1)	100.0%	92.3%
B2 (Stage 2)	95.7%	91.3%
Composite	96.2%	85.2%

more likely an Elevating strategy is used. In effect, the body tends to initially opt for a strategy that allows it to continue in the direction it is moving (i.e., avoid a change in momentum). Lastly, the foot angular acceleration captures the instantaneous change in the ipsilateral foot's angular velocity (i.e., change in mass-normalized angular momentum, or angular impulse). When coupled with the other features, a distinct region forms in which the Lowering strategy is more common. For example, the Lowering strategy has higher incidence when the contralateral foot is well behind the COM with lower foot accelerations.

For Stage 2 (Elevating or Delayed Lowering), the model correctly predicts 94.0% of the strategy selection observed in Experiment A with the feature set IF-to-COM angular acceleration ($\ddot{\phi}$) and shank angular acceleration ($\ddot{\delta}$) at the

time of perturbation, knee angle 60 ms after the perturbation (γ_+), and change in body COM vertical velocity ($\dot{z}_{com\Delta}$), compared to 85.6% when using swing percentage. IF-to-COM angular acceleration captures the instantaneous change in the body's angular velocity (i.e., change in mass-normalized angular momentum, or angular impulse). Shank angular acceleration similarly captures the instantaneous change in the tripped limb's angular velocity at perturbation. As shown in Fig. 3.5(b), the body is more likely to abandon Elevating as the magnitudes of these angular impulses increase. Knee angle captures the tripped limb's configuration state 60 ms after the perturbation. Change in body COM vertical velocity captures the body's mass-normalized change in momentum in the vertical direction. Combinations of these four features create distinct regions in which the Delayed Lowering strategy is more likely; for example, regions of less knee flexion (less negative knee angle) and higher angular acceleration magnitude tend to produce Delayed Lowering strategies.

Overall, the classification accuracy of the RTMM for Stage 2 is lower than for Stage 1; this suggests that there is some piece of Stage 2 that is not captured with the physical quantities used (e.g., there may be something intrinsic to each participant that might influence the Stage 2 strategy selection that is not represented by this dynamic model). To investigate this, an additional feature set of participant-specific properties was generated, which included the following: height, mass, sex, average swing time, average stride time, limb tripped, and minimum foot height in swing phase. However, none of these features increased the classification accuracy for Stage 1 or Stage 2 of the strategy selection process, suggesting that neither stage was dependent on these factors (or, at least, not any more than the other features used). Thus, in Stage 2, factors that have not been captured in the present dynamic model (or captured by the participant properties) may be contributing to the selection of Elevating or Delayed Lowering. Such factors might be psychological and/or based on physical fitness, coordination, or strength. Collectively, these findings suggest that the initial reaction (Stage 1) of the strategy selection process is dominated by the physics (i.e., the dynamic conditions at the moment of perturbation, which are the quantities that were extracted and tested in this work), whereas Stage 2 may additionally be influenced by a participant's ability or other factors (that were not tested in this work), which vary participant-to-participant.

It is notable that the feature sets used in the RTMM perform well on trials at different walking speeds (Experiment B), and again outperform swing percentage, as shown in Table 3.3. Supplementary Material Figs. C2 and C3 support and expand upon these results, showing that the features maintain the same trends as from Experiment A. Thus, the RTMM may be robust and not limited to just one speed or cadence.

Table 3.4 shows the RTMM classification accuracy results (using the final feature sets with the same cross validation and hyperparameter tuning procedures as discussed previously) for only trials that occurred between 40-70% swing phase (89 trials in total: 40 Elevating, 37 Delayed Lowering, 12 Lowering) versus SPM. The RTMM outperforms swing percentage in predicting strategies chosen, even in mid-swing, which was the region most in question (see Introduction, Fig. 3.3, [101, 106, 30]).

Table 3.4: Classification accuracy for the RTMM and SPM for each stage of the strategy selection process as well as composite accuracy for Dataset A for only perturbations that occurred between 40 and 70% swing phase. Specifically, the first two rows give the total classification accuracy from the cross-validation process (i.e., the average of the percentage of correctly predicted trials from each participant/fold). The composite accuracy (third row) was calculated by combining the Stage 1 and Stage 2 classification accuracies, weighted by the number of trials in each class.

Dataset	RTMM Classification Accuracy	SPM Classification Accuracy
A1 (Stage 1)	97.8%	88.8%
A2 (Stage 2)	87.0%	71.4%
Composite	86.8%	66.8%

The authors note that if an individual is walking with a stationary (i.e., periodically invariant) gait, as was the case for the treadmill trials used in this analysis, the swing percentage of perturbation can be estimated in real-time using the average swing time of previous strides. The accuracy with which swing percentage can predict strategy selected is reported here, and such an approach may be suitable for predicting strategy selection, depending on (1) availability of biomechanical data, (2) walking conditions, and (3) level of accuracy desired. However, the results reported herein indicate that RTMM approaches offer improved accuracy. Such a model is important in order to provide: 1)

physiological insight into the human body's responses to swing-phase perturbations and 2) a basis on which various applications/interventions requiring real-time stumble recovery strategy selection could be implemented, both of which are discussed below.

As previously explained, the feature set used in the RTMM includes measurements that are related to either the configuration or normalized kinetic state of the human body at and just after perturbation. Given their real-time nature, these signals (or neurophysiological proxies for these signals) could be what the body is utilizing to reflexively respond. Each feature can be thought of as a signal sensed in a physiologically-relevant process, such as a sensory neuron involved in spinal and long-loop reflexes. For example, muscle spindles are sensory neurons that sense limb velocity via muscle length and rate of change; thus, knee angular velocity is information potentially captured by these biological sensors. Similarly, Golgi tendon organs sense load on a limb, and so foot angular acceleration could be accessed and used by these sensory neurons. And more broadly, the configuration states such as CF-to-COM angle are information perceived by the vestibular system along with fusion of various proprioceptors.

The real-time nature of these features is not only important with regard to a potential link to relevant physiological systems, but also in the capacity to be accessed from wearable sensors for various applications. For example, given that these signals are used in the strategy selection process to successfully recover from a stumble, it may be advantageous to monitor these values in a fall prevention program or study. Additionally, for individuals with a higher propensity for falling, such as the elderly, stroke patients, or lower-limb prosthesis users, these signals might be incorporated into fall prevention controllers in assistive devices. Supplementary Material Tables B3 and B4 report classification accuracy results for feature sets that include only quantities measurable from a lower-limb knee prosthesis as an example.

Note that the goal here was to find the best feature sets considering all potential features, so the authors did not place any limits on which of the potential features could be used in the wrapper method; however, for various applications or research questions there may be constraints on what number or type of features can be used (e.g., only features that are measurable from the ipsilateral limb are available, or only two features can be measured at a time). Thus, various other scenarios were considered and results are tabulated in Supplementary Material Tables B3 and B4 for reference. The authors recognize that one approach could have been to initially filter out features with high correlation values to reduce the set of potential features and thus number of potential subsets; however, because the authors had the computational bandwidth to try all combinations (up to 4 features in a subset), and the focus was on finding a set with the best performance (and not with interpreting coefficients), all features were kept in order to maximize opportunities for highest model performance. This is likely why many feature sets performed similarly (as indicated in Results); the authors chose to report the best feature sets in the main text but tabulate other top-performing sets in the Supplementary Material to inform readers on which other features worked well for reference.

There are several limitations to this work. First, for classification problems it is ideal to have an even distribution of classes, which was not the case for this study; this issue is addressed in this work in several ways. Experimentally it is possible to control the timing of perturbation [50], but not to control the recovery strategy employed by the participant. The goal was to elicit perturbations at a range of points in swing phase, which was accomplished (see Fig. 3.3). The authors contend that the class distribution is more representative of real-life occurrences (i.e., the natural response from perturbations at a range of points in swing phase), and thus building a model from this distribution may better reflect the expected instances of these strategies in daily life. The authors do note that the distribution of swing percentage at which the perturbation occurred was not perfectly even; approximately 20% more of the perturbations occurred in the earlier half of swing phase (10-47.5% swing), but given experimental constraints some imperfection is expected. Nevertheless, as explained above, the model was re-run for trials only between 40-70% swing phase, which removed 86 elevating trials (the strategy with the most instances in the full dataset), and results still showed improved accuracy. Additionally, the authors report the overall confusion matrix for each stage in Figs. 3.4 and 3.5 so that supplementary performance metrics can be calculated [43]. Furthermore, Table 3.5 reports the balanced accuracy score for each stage for Datasets A and B, which accounts for the class imbalance by taking the average of the true positive rate (sensitivity/recall) and true negative rate (specificity); the RTMM still outperforms SPM using this metric. Regardless, for both the RTMM and SPM the same set of trials was used; thus, the comparison is fair and consistent, and it still holds that the RTMM outperforms the SPM. Finally, note that a simple majority classification strategy, consisting of always choosing the majority class (initially elevating) for Stage 1, would result in a classification accuracy score of 87.8% for Experiment A and 88.5% for Experiment B, and always choosing the majority class (elevating) for Stage 2 would be 76.4% for Experiment A and 60.9% for Experiment B, and the RTMM results show accuracies substantially

higher than these values.

Table 3.5: Balanced accuracy for the RTMM and SPM for each stage of the strategy selection process for testing with Dataset A and Dataset B. Balanced accuracy is calculated as the average of the true positive rate (sensitivity/recall) and true negative rate (specificity). Specifically, the first two rows give the average of the balanced accuracies from each participant/fold in the cross-validation process for Datasets A1 and A2. The last two rows give the balanced accuracy from testing on Datasets B1 and B2 (after training on Datasets A1 and A2 with the final feature sets, excluding data from Participant 3).

Dataset	RTMM Balanced Accuracy	SPM Balanced Accuracy
A1 (Stage 1)	97.1%	84.2%
A2 (Stage 2)	92.1%	82.3%
B1 (Stage 1)	100%	66.7%
B2 (Stage 2)	96.4%	88.9%

Second, an argument could be made that the increased classification accuracy with the RTMM is expected considering multiple features are included, compared to just one feature with the SPM. The authors agree with this assertion, but point out that limiting to one feature was not in the scope of the overall objective of the work. However, it is worth noting there were several individual features that independently outperformed swing percentage, as indicated in Results and expanded upon in Supplementary Material Tables A1 and A2.

Third, one could argue that limiting the number of features in the final set could limit the performance of the final model. However, the authors contend it was reasonable to use the dimension that accounts for 80% of the variance of the dataset. This not only reduces the computational intensity but also limits the complexity of the model which is important for moderating model variance and thus performance on new data.

Fourth, the authors recognize that Experiment B is a limited dataset and only represents a single participant. Proving that this model extends across speeds was not a main objective of this work; rather, these results provide an initial indication that the RTMM represents the strategy selection process at multiple walking speeds. Note that the authors took care to remove Participant 3's trials from the single-speed training set (Dataset A), and as such the test set is a good indicator of the model's performance on new trials. More trials with additional participants would be ideal to confirm this observation in a future experiment.

Lastly, one could argue that the participants in this study are not representative of the general population. Recall that the objective of this work was to create a model for healthy stumble recovery. Now that such a model has been proposed, valuable future work would be to repeat this process with mobility-impaired populations, such as the elderly, stroke patients, or individuals with lower-limb amputation. Understanding how these feature sets and strategies might differ may give insight into the deficiencies of the recoveries of these populations, informing areas for intervention and improvement.

3.6 Conclusion

In order to better characterize the nature of the stumble recovery strategy selection process, a set of features that are physical and measurable in real-time were identified that predict observed strategy selection with better accuracy than the conventional swing percentage criterion. For Stage 1 (Initially Elevating or Lowering), the model correctly predicts 99.0% of the strategies used with the feature set of CF-to-COM angle, knee angular velocity, COM vertical velocity, and foot angular acceleration at the time of perturbation, compared to 93.7% when using swing percentage. For Stage 2 (Elevating or Delayed Lowering), the model correctly predicts 94.0% of the strategies selected using the feature set of IF-to-COM angular acceleration and shank angular acceleration at the time of perturbation, knee angle 60 ms after the perturbation, and change in body COM vertical velocity, compared to 85.6% when using swing percentage. For Stage 1, the body tends to choose a strategy that prevents a change in momentum, as evidenced by trends seen in knee angular velocity and body COM vertical velocity. For Stage 2, the body tends to abandon the Elevating strategy (Delayed Lowering) in situations of high angular impulse, as evidenced by trends in IF-to-COM

angular acceleration and shank angular acceleration. These feature sets also perform better than swing percentage on a dataset of trials at additional speeds, suggesting that the model may be robust to multiple walking speeds. The increased accuracy of Stage 1 predictions compared to Stage 2 suggest that while the initial reaction (Stage 1) of the strategy selection process is dominated by the physics, Stage 2 may be additionally influenced by participant-specific factors that were not collected, which may be further informed by future studies. These new findings inform both physiological understanding of healthy stumble recovery as well as interventions for those at fall risk.

CHAPTER 4

Powered knee exoskeleton stumble recovery intervention

4.1 Part 1: Design and implementation of a stumble recovery controller for a knee exoskeleton

4.1.1 Part 1 Summary

This paper presents a stumble recovery controller for a knee exoskeleton that detects a stumble perturbation; selects an anticipated recovery strategy; and provides appropriate recovery assistance. In order to assess the efficacy of the controller in providing an assistive response to a stumble perturbation, the controller was implemented in a knee exoskeleton and evaluated in a single healthy adult participant against several other controller reactions, and against the participant's response without an exoskeleton. Results show that the stumble recovery controller successfully detected the perturbation and correctly selected the strategy that matched the participant's response for all 29 trials in which the exoskeleton was used. Further, results show improvements in stumble recovery metrics when using the exoskeleton with the stumble recovery controller, compared to the control cases of: 1) no change in the nominal controller when stumble is detected; 2) turning off exoskeleton torque when a stumble is detected; and 3) not wearing an exoskeleton.

4.1.2 Introduction

The research and development of powered lower limb exoskeletons to assist and augment performance for impaired and healthy individuals, respectively, have grown rapidly in the last decade [125]. Such devices are typically designed, controlled, and optimized for various locomotion activities, such as walking. These controllers, however, do not typically consider or account for common unexpected disturbances, such as tripping over obstacles; an exoskeleton, due to its added mass and/or its insufficient controller, could potentially increase the likelihood of falling and subsequent injury in the event of a stumble. Thus, consideration of the stumble event is important for exoskeletons to ultimately be wearable in daily life. The issue of stumble response in lower limb exoskeletons has received little attention to date in the literature, and many recent review papers have highlighted this knowledge gap [105, 91, 39, 124, 13]. Among the open questions in this regard are: How can tripping be reliably detected? What type of active assistance, if any, should be provided following a stumble, and how is that decision made? Will the human accept active, external device behavior in a scenario that is reflexively driven?

A few papers have investigated recovery from external disturbances while wearing a powered lower limb exoskeleton. Two looked at treadmill belt-slip perturbations while walking with a hip exoskeleton [67, 63]. One investigated treadmill belt-slip perturbations while standing with an ankle exoskeleton [9]. Only one paper has studied obstacle perturbations (more akin to stumble events in real life, vs. belt-slip perturbations), but no active, stumble-specific controller was implemented; rather, the conditions of continuing assistance or stopping assistance were investigated [1]. Thus, it remains to be examined whether an active stumble recovery controller (i.e., one that provides stumble-specific assistance) would improve, impede, or maintain an individual's ability to respond.

While exoskeleton controllers have focused both on augmentation of healthy individuals and on assisting movement for impaired individuals [2], this paper considers an exoskeleton intended for a healthy adult exoskeleton user, and specifically focuses on the extent to which an exoskeleton might help, hurt, or maintain a user's ability to recover from a stumble perturbation. For a healthy individual, the authors contend that there are three main responses to a stumble perturbation that could be employed in a lower limb exoskeleton: 1) the device could simply have no stumble recovery feature (i.e., it could ignore the perturbation); 2) the device could detect the perturbation and subsequently turn off all exoskeleton assistance until the user has recovered; or 3) the device could detect the perturbation and subsequently provide active assistance to the individual to aid in the stumble recovery. This third approach has the potential to improve stumble recovery by providing movement assistance in the human's response and potentially responding sooner than the human would. This approach, however, is greatly complicated by the role that reflexes play in how healthy individuals respond to stumbles; typically, healthy adults select one of three responses following a stumble

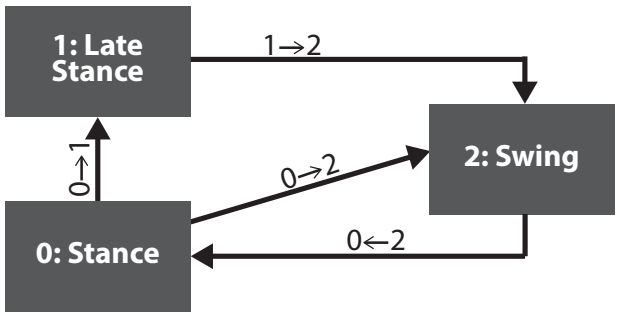

Figure 4.1: Finite-state machine for walking controller.

perturbation – an elevating, lowering, or delayed lowering recovery strategy [50, 102, 107, 24, 101, 27, 22]. As such, providing active recovery assistance with the exoskeleton carries the risk of worsening the response if the exoskeleton selects a recovery response that is inconsistent with the one selected by the user. In other words, in instances of stumble, it remains to be known if an exoskeleton can reliably select the "correct" response, and if it can, to what extent might it aid or hinder the user's ability to mitigate the stumble perturbation.

In order to examine these questions, this paper: 1) leverages prior work by the authors to propose a stumble recovery controller for a knee exoskeleton, which anticipates and assists the user's recovery response; and 2) experimentally examines the response to stumble perturbations for different exoskeleton controllers, including no change to the control action, turning off assistance upon detection, and employing stumble-specific assistance (i.e., employing the stumble recovery controller). The experiments, conducted on a single healthy adult, also included the case with no exoskeleton for reference. The experimental results are discussed with respect to: 1) the extent to which the proposed stumble recovery controller can successfully and repeatably select the correct recovery strategy; and 2) the extent to which the controller improved, impeded, or maintained the participant's ability to recover from stumble perturbations, compared to the other experimental cases.

4.1.3 Controller Development

4.1.3.1 Walking Controller

There is not a clear standard in the literature for a powered knee exoskeleton control method to assist healthy individuals during normal level (unperturbed) walking. However, the field of lower limb exoskeletons has, in general, been converging on the use of torque-pulse control (or phase-based oscillator control), as opposed to other methods such as trajectory control, for movement assistance in healthy individuals (e.g., [113, 127]), presumably because this scheme assists movement without substantially restricting it. Here the authors propose a knee exoskeleton controller that incorporates stance-knee support in stance phase and employs torque-pulse control in swing phase, intended to facilitate walking on level ground for healthy individuals. The finite-state machine for this level walking controller (shown in Fig. 4.1, with state transition conditions given in Table 4.1) consists of three states: stance, late stance, and swing. Stance phase assistance is intended to prevent knee buckling during initial loading by resisting knee flexion during initial stance; late stance behavior removes resistance to flexion during late stance to facilitate initiation of swing phase; and swing-phase behavior supplements swing phase movement with torque pulses that encourage healthy, inertial lower-limb dynamics during swing phase.

More specifically, knee angle (θ) is regulated during the stance state to an equilibrium angle (set as the angle when user is wearing the exoskeleton and standing upright) with the following equation:

$$\tau = k_{p,stance}(\theta_{eq} - \theta) + k_{d,stance}(\dot{\theta}_{desired} - \dot{\theta}) \tag{4.1}$$

Table 4.1: State transition conditions for walking controller

Transition	Condition
$0 \rightarrow 1$	Foot Switch Heel $==0$
$1 \rightarrow 2$ $0 \rightarrow 2$	Foot Switch Toe $==0$ && Foot Switch Heel $==0$ && Thigh Angular Velocity <0 deg/s
$2 \rightarrow 0$	Foot Switch Heel $==1$ $\|\|$ Foot Switch Toe $==1$

where τ is the commanded torque, θ_{eq} is the equilibrium knee angle, θ is current knee angle, $\theta_{desired}$ is 0 deg/s, $\dot{\theta}$ is current knee angular velocity, and $k_{p,stance}$ and $k_{d,stance}$ are experimenter-defined proportional and derivative gains, respectively.

During the late stance state, $k_{p,stance}$ and $k_{d,stance}$ are decreased, so that the user can initiate swing phase. During the swing state, a torque-pulse control scheme is implemented, where the torque pulses are phased with the nominal expected angular acceleration of the knee joint in order to complement the human lower limb's inertial mechanics during swing. Specifically, the nominal knee angle was modeled as a negative cosine in time, vertically shifted by one amplitude; assuming a primarily inertial dynamics, the assistive torque profile is given by the second derivative of the angle, with magnitude determined by a gain η_{swing}, according to the following equation:

$$\tau = \eta_{swing} cos(2\pi/T) \tag{4.2}$$

where t is the time in the swing state and T is the total duration of swing phase, determined by a swing-stance ratio value (tunable by experimenter) and the stance time measured during the current stride. Note that the start of the torque profile is blended from the preceding state to avoid an abrupt increase in torque at the onset of swing. Likewise, commanded torque is blended when transitioning from swing to stance.

4.1.3.2 Reflex Stumble Recovery Controller

The primary objective of this work is to propose and evaluate a stumble recovery controller for a knee exoskeleton. Although a specific implementation of a knee exoskeleton is described subsequently in the experimental implementation section, the controller assumptions regarding the exoskeleton are fairly standard. Specifically, the authors assume the exoskeleton includes an IMU located on the thigh segment; a knee angle sensor; and both heel and toe foot switches. The goal of this controller is to reliably detect a perturbation during swing phase and subsequently implement assistance for whichever recovery strategy the individual employs. As such, the controller involves three components: (1) perturbation detection, (2) recovery strategy decision, and (3) recovery strategy assistance, each described below.

Perturbation Detection

Based on data recorded from a large dataset of stumble responses, obtained using the experimental apparatus described in [50], the authors determined that stumble can reliably be detected using the angular acceleration of the thigh, measured by differentiation of the sagittal-plane gyroscope in the thigh IMU. Specifically, a stumble perturbation could be reliably detected during swing phase when the thigh angular acceleration exceeded a threshold of 9500 deg/s2.

Recovery Strategy Decision

After a stumble, healthy individuals perform one of three strategies – an elevating, lowering, or delayed lowering strategy. In the elevating strategy, upon contacting the obstacle the individual reflexively lifts his/her foot up and over the obstacle to clear it in the same step. For the lowering strategy, upon contacting the obstacle the individual

Table 4.2: Final feature sets for each decision stage of the strategy selection model, with corresponding classification accuracies from the cross-validation procedure for the multi-participant dataset.

Stage	Feature Set	Classification Accuracy
1	θ_p and $\dot{\gamma}_p$	97.4%
2	θ_p , γ_p, and $\dot{\gamma}_p$	88.3%

immediately terminates that step behind the obstacle and instead clears it in the following step. Finally, in the delayed lowering strategy, the individual starts to elevate his/her foot, but ultimately lowers behind the obstacle [50, 102, 107, 24]. Moreover, these responses (elevating vs. lowering) require the opposite initial knee action (flexion vs. extension); since an exoskeleton performing a strategy opposing that of the human may increase fall risk, it is important that the decision be made correctly (i.e., the exoskeleton correctly predicts which recovery strategy the human will select, and provides corresponding assistance). However, though strategy selection is often associated with the swing percentage at which the perturbation occurs, it has been concluded in previous literature [107, 101, 27, 22, 30] that the timing of the perturbation alone cannot predict strategy selection with full accuracy (i.e., the transition from elevating to lowering varies inter- and intra-individual and is not a matter of a simple threshold).

The authors have previously conducted a multi-participant stumble experiment [50] and from it developed a 2-stage strategy selection model using dynamic factors associated with human movement to predict strategy selection with substantially better accuracy compared to using swing percentage alone [27]. In the first stage, the model predicts whether the individual initially begins elevating or lowers (lowering); in the second stage, if initially elevating was selected, the model predicts whether he/she either continues elevating (elevating) or abandons elevating and instead lowers (delayed lowering). The optimal set of inputs to this model, however, requires measurements not available on a typical lower limb exoskeleton. As such, a variation on that predictive algorithm, which uses real-time sensor information available to a typical exoskeleton, was employed here. Specifically, feature selection methods from [27] were repeated on the multi-participant dataset considering strictly real-time measurements available to a knee exoskeleton: knee angle θ, knee angular velocity $\dot{\theta}$, knee angular acceleration $\ddot{\theta}$ (from encoder), thigh angle γ, thigh angular velocity $\dot{\gamma}$, and thigh angular acceleration $\ddot{\gamma}$ (from IMU) at the instant of perturbation detection. A machine-learning wrapper method and cross-validation procedure was used to find the subset of features that produced the highest total classification accuracy for each decision stage. See [27] for methodological details. The feature subsets that produced the highest total classification accuracy for each decision stage are reported in Table 4.2. These feature subsets from each trial in the multi-participant dataset were then fit to a logistic regression model with Ridge regularization (regularization strength value of 10, from hyperparameter tuning process described in [27]) for each stage. The resulting equations were used for the decision algorithm and are enumerated below:

$$P(Lowering) = \frac{1}{1+e^{-(\alpha_0+\alpha_1\theta_p+\alpha_2\dot{\gamma}_p)}} \tag{4.3}$$

$$P(DelayedLowering) = \frac{1}{1+e^{-(\beta_0+\beta_1\theta_p+\beta_2\gamma_p+\beta_3\dot{\gamma}_p)}} \tag{4.4}$$

where θ_p, γ_p, and $\dot{\gamma}_p$ are the knee angle, thigh angle, and thigh angular velocity values at the instant of perturbation detection, respectively, and coefficient values are given in Table 4.3. Note that these are not participant-specific values, but rather are intended to be valid for a general population. The finite-state machine for the reflex stumble recovery controller is given in Fig. 4.2, with state transition conditions enumerated in Table 4.4. As stated in Table 4.4, if the result of (4.3) is greater than 0.5, the result is lowering; if the result of (4.3) is less than 0.5, (4.4) is computed; if the result of (4.4) is greater than 0.5, the result is delayed lowering; if less than 0.5, the result is elevating.

Recovery Strategy Assistance

Table 4.3: Coefficient values for (3) and (4)

Stage 1 (3)		**Stage 2 (4)**	
Coefficient	*Value*	*Coefficient*	*Value*
α_0	4.4281	β_0	0.0005
α_1	0.0831	β_1	0.1230
α_2	5.4624	β_2	-0.2690
		β_3	0.0359

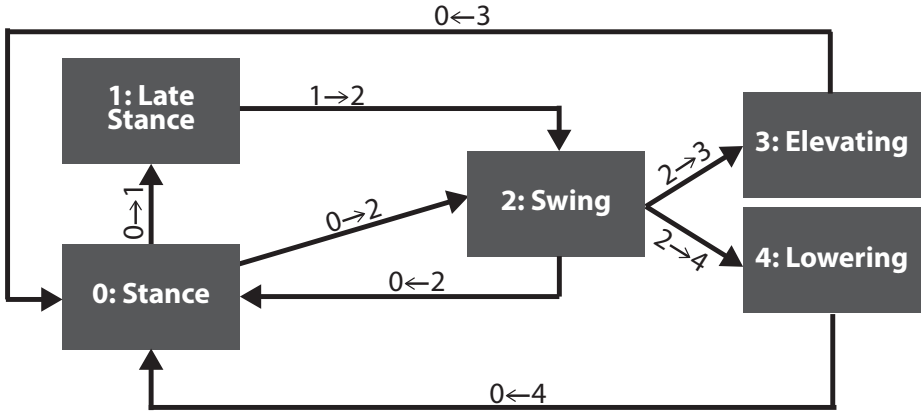

Figure 4.2: Finite-state machine for reflex stumble recovery controller.

For the elevating strategy, a feedforward torque pulse is commanded, like that of swing phase in the walking controller, but the gain and timing of the pulse are increased to facilitate the exaggerated step. For both lowering and delayed lowering strategies, knee angle is regulated to equilibrium angle (as in (4.1)). In the following step, η_{swing} is increased in order to facilitate greater knee flexion for clearing the stumble obstacle.

4.1.4 Experimental Validation

In order to provide a preliminary examination and validation of the proposed reflex stumble recovery controller, and to assess the extent to which it might help or hinder recovery, the proposed assistive walking controller with reflex behavior (i.e., Fig. 4.2) was implemented in a powered knee exoskeleton and tested on a single healthy adult participant in a series of stumble experiments (pictured in Fig. 4.3). In particular, stumble recovery responses were elicited while wearing the exoskeleton, and various stumble recovery metrics were recorded under several different exoskeleton con-

Table 4.4: State transition conditions for reflex stumble recovery controller

Transition	**Condition**
$2 \rightarrow 3$	Thigh Angular Acceleration >9500 deg/s2 && P(Lowering) <=0.5 && P(Delayed Lowering) <= 0.5
$2 \rightarrow 4$	Thigh Angular Acceleration >9500 deg/s2 && (P(Lowering) >0.5 || (P(Lowering) <=0.5 && P(Delayed Lowering) >0.5))
$3 \rightarrow 0$ $4 \rightarrow 0$	Foot Switch Toe == 1 || Foot Switch Heel == 1

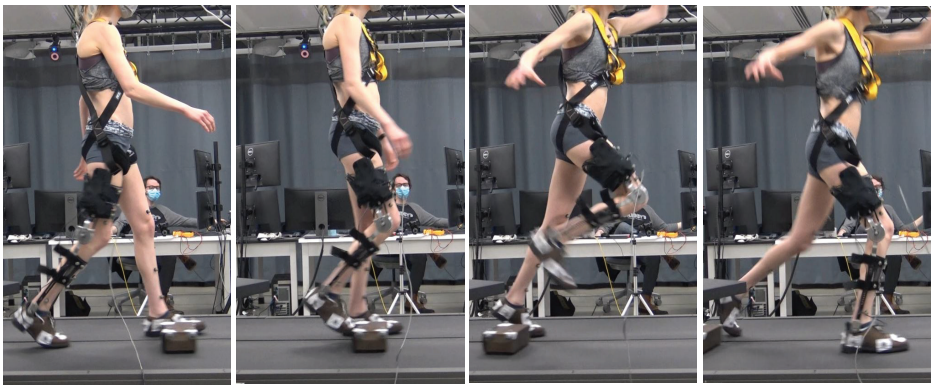

Figure 4.3: Stumble perturbation experiment. A video corresponding to these experiments is provided in the supplementary material.

troller variations. These responses were also compared to the same experiments without the use of the exoskeleton. For these stumble experiments, five experimental cases were compared as follows: 1) stumble response without wearing the exoskeleton (No Exo case); 2) with the exoskeleton providing walking assistance (i.e., walking controller), but without detection of the stumble event (No Change); 3) with the exoskeleton providing walking assistance, where the controller turns off assistance during the stumble event (Turn Off); 4) with the exoskeleton providing walking assistance, with the reflex stumble recovery controller active (Reflex); and 5) with the exoskeleton providing walking assistance, with the reflex stumble recovery controller active, but where the reflex controller intentionally provides the opposite reflex control action to that determined by the decision algorithm (Opposite). For each case, the participant was stumbled multiple times while walking on a treadmill, while her response to the perturbation was recorded with motion capture instrumentation. The order of presentation of each case was as follows: 1) No Change case; 2) Turn Off case; 3) Reflex and Opposite cases, randomly presented; and finally, 4) No Exo case. The experiments are described in more detail as follows.

4.1.4.1 Knee Exoskeleton Hardware

The knee exoskeleton, shown in Fig. 4.4, is a knee-ankle-foot orthosis (KAFO) with a powered knee module in place of a standard knee joint. An articulated ankle-foot-orthosis (AFO) with no compliance was used at the ankle, which was included to prevent the orthosis from sliding down the leg, and to provide a mounting surface for a pair of force sensing resistors (FSRs). The FSRs were mounted on the heel and toe of the AFO, respectively, and provided measurement of heel and/or toe contact. The thigh segment of the exoskeleton is supported by bilateral uprights, while the shank segment is supported by a single lateral upright with adjustable height. The knee joint on the medial aspect is a standard passive hinge joint, while the knee joint on the lateral aspect is actuated by a brushless motor (Allied Motion Technologies MF0076008-A0X) and two-stage chain-drive transmission, which is packaged separately from the knee joint and located on the lateral aspect of the thigh, and actuates the knee joint remotely through a pair of Bowden cables. The actuation unit is powered by a lithium-ion battery pack consisting of six 18650 cells (INR18650-30Q) in series, providing nominal 25.2 V and 72 W-hrs at full charge, with a maximum continuous current capacity of 15 A. The total mass of the knee exoskeleton including the actuation unit, KAFO structure, and battery is 2.95 kg.

In addition to the FSRs, exoskeleton sensing includes an encoder in the knee actuation unit, which measures knee angle, and a nine-axis IMU that provides thigh angle and angular velocity measurements. The actuation unit includes an embedded system that runs all low-level control, including brushless motor current control, and also includes a CAN interface that enables high-level control prototyping and data collection from a laptop computer via the real-time interface provided by MATLAB/Simulink at a sampling rate of one kHz. For the walking controller, thigh angle is calculated via a standard complementary filter sensor fusion that combines accelerometer and gyroscope measurements, with a cross-over frequency of 0.5 Hz. For the decision algorithm, the thigh angle is calculated in the same way, but with a cross-over frequency of 0.1 Hz. Thigh angular velocity is calculated via a standard first-order

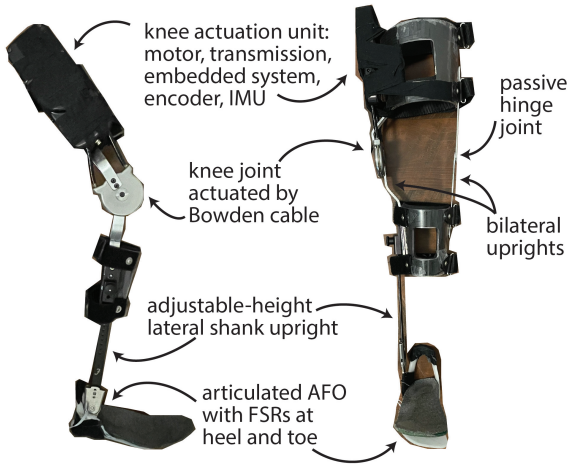

Figure 4.4: Lateral side (left) and front (right) of exoskeleton

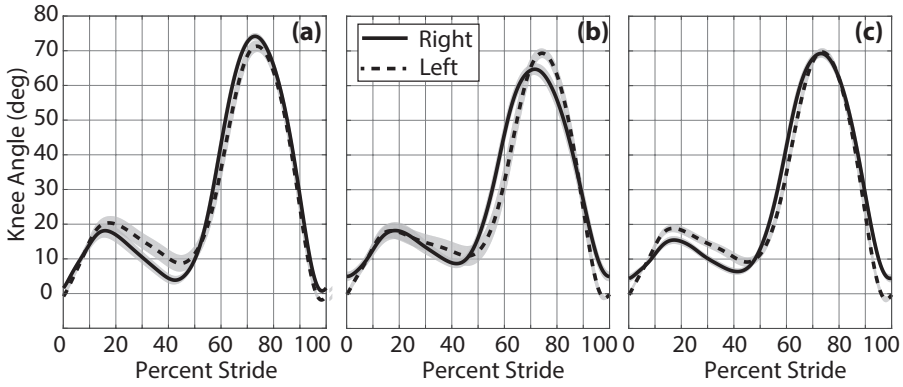

Figure 4.5: 30-stride average (with standard deviation band in gray) left vs. right knee trajectory when participant was (a) not wearing the exoskeleton, (b) wearing the exoskeleton on right limb with assistance turned off, and (c) wearing the exoskeleton on right limb with walking controller enabled.

low-pass filter with a cutoff frequency of 10 Hz for the walking controller and 30 Hz for the decision algorithm.

4.1.4.2 Walking Controller

The walking controller was implemented in the right-legged knee exoskeleton described in the previous section and evaluated for efficacy in providing walking assistance. Fig. 4.5 shows the 30-stride average (with standard deviation in shaded gray) of left and right knee angle trajectories when the participant was (a) not wearing the exoskeleton, (b) wearing the exoskeleton on right limb with assistance turned off, and (c) wearing the exoskeleton on right limb with the walking controller enabled. As shown, the walking controller promotes a healthy knee trajectory. Compared to (b), the right knee trajectory in (c) better matches the participant's right knee trajectory when not wearing the exoskeleton (a) in both phase and magnitude, and it is more symmetric in phase and magnitude to the left knee trajectory.

The ratio of right-to-left swing time (30-stride average) was computed for each of the three cases (i.e., a ratio of one would indicate that the average left and right swing times were equal). For (a), the ratio was 1.067; for (b), the ratio was 1.129; for (c), the ratio was 1.057. Thus, the walking controller promoted approximately the same level of right-left symmetry that the participant employed without wearing the exoskeleton; however, when the exoskeleton was

not providing assistance, the participant's asymmetry increased. Moreover, these results validate that the proposed walking controller promotes typical, healthy walking kinematics and step metrics. A video showing the participant walking for all three discussed cases is including in the supplemental material submitted with this paper.

4.1.4.3 Stumble Experiments

In order to provide a preliminary test of efficacy of the reflex stumble recovery controller, a single participant underwent a series of stumble perturbation experiments, involving 37 stumble perturbations. The stumble perturbation system and protocol used are described in [50]. The experiments were approved by the Vanderbilt Institutional Review Board, and the participant gave written informed consent. The perturbations were targeted at 30, 40, 50, and 60% swing (region of swing phase in which all strategies could occur [27]) for each of the following cases:

- No Exo: The participant does not wear the exoskeleton for these trials, which serve as a measure for how the participant would recover typically. All other trials are conducted while wearing the exoskeleton.
- No Change (Fig. 4.1): Walking controller implemented with perturbation detection turned off. This serves as a measure of how the participant would recover while wearing an exoskeleton without a stumble recovery control feature.
- Turn Off: Walking controller implemented with perturbation detection turned on, and joint torque is zeroed upon detection until the next stance phase is triggered. This serves as a measure of how the participant would recover if controller assistance is turned off after perturbation detection.
- Reflex (Fig. 4.2): Reflex stumble recovery controller implemented. This serves as a measure of how the participant would recover if recovery assistance is provided after perturbation detection.
- Opposite: Reflex stumble recovery controller with opposite decision. The strategy opposite of that indicated by the decision algorithm is selected and corresponding assistance is provided. This serves as a measure of how the participant would respond to the exoskeleton making the incorrect strategy decision.

Note that sensory occlusion techniques and obstacle delivery apparatus design choices precluded the participant from perceiving (hearing, seeing, or feeling) the obstacle prior to contact, as detailed in [50]. Additionally, the swing percentage of the perturbation was randomized and unknown to the participant. When testing the Reflex and Opposite cases, the participant was not told which case the controller would be implementing. A video of representative trials is provided with the supplementary material submitted with this paper.

For all trials, ground reaction force (GRF) data were collected under each foot at one kHz via a force-instrumented split-belt treadmill (Bertec, Columbus, USA). Lower-limb and trunk kinematic data (including foot, shank, thigh, pelvis, and trunk segments) were recorded at 200 Hz via an infrared motion capture system (Vicon, Oxford, GBR). GRF and motion capture data were processed with a zero-phase, third order, Butterworth low-pass filter at a cutoff frequency of 15 and 6 Hz, respectively. Inverse dynamics were computed using Visual 3D (C-Motion, Germantown, USA) to estimate lower-limb and trunk kinematics for each trial. These data were used for assessment purposes only (i.e., were not used for the controller operation).

For each stumble event, the swing percentage of perturbation, recovery strategy used as well as the recovery strategy chosen by the decision algorithm (note that the decision algorithm was run for all trials, even if reflex stumble recovery controller was not enabled) were recorded. Because both the delayed lowering strategy and lowering strategy involve ultimately lowering the foot behind the stumble obstacle, and as such if selected by the decision algorithm were prescribed the same knee controller action for the Reflex case (to facilitate landing behind the stumble obstacle), both strategies were reported as lowering in this work. Knee angle trajectories following the perturbation were computed in order to compare the resulting elevating and lowering strategy trajectories of each case. In addition, sagittal-plane trunk angle (deviation from vertical) following the perturbation was computed, as trunk angle deviations have been reported to be indicators of increased likelihood of falling [81, 18].

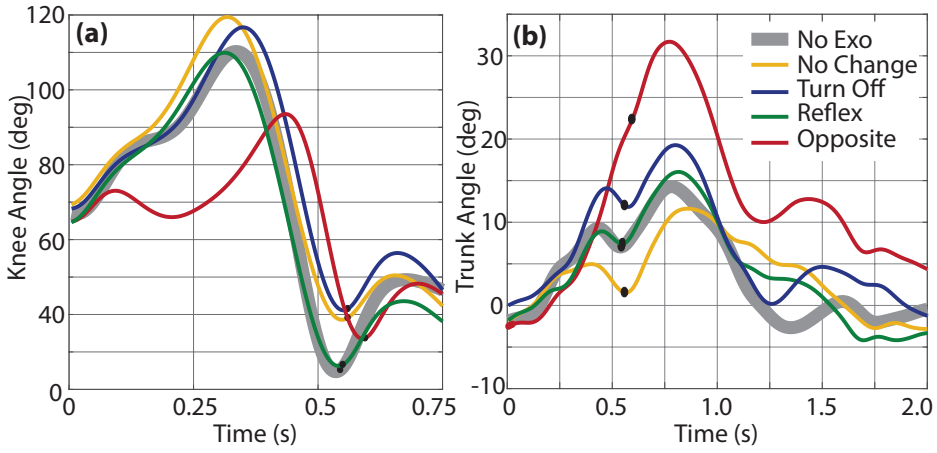

Figure 4.6: Sagittal-plane knee angle (a) and trunk angle (b) following perturbation for a representative elevating strategy for each case. Time 0 indicates the instant of perturbation, and the black filled circle indicates first foot-strike.

4.1.4.4 Experimental Results & Discussion

Overall, the participant experienced a total of 37 obstacle perturbations ranging from 29% to 66% swing. The breakdown of trial case, swing percentage of perturbation, algorithm outputs, and strategy employed is given in Table 4.5.

Perturbation detection

All 21 perturbations from relevant trials (i.e., Turn Off, Reflex, and Opposite cases) were successfully detected. Out of approximately 600 steps (25-35 steps prior to perturbation per trial) there were no false positives.

Decision Algorithm

Table 4.5 gives the probability computed from each logistic regression equation in the decision algorithm, final algorithm decision, and human decision for each trial. Recall that the decision algorithm was run in the background for all trials even if not used in a particular trial, and that both lowering and delayed lowering strategies were reported as lowering. As shown, the algorithm decision matched the human decision for all 29 relevant trials. Note that for two of the Reflex case trials, the perturbation occurred at the exact same percentage of swing phase (43%), but the human chose opposite strategies (lowering and elevating). This further substantiates the idea that strategy selection is not simply a matter of implementing a threshold on the timing of the perturbation; rather, it is important to monitor the dynamic factors of the human body, as the decision algorithm does. Notably, the decision algorithm correctly selected the strategies chosen for both trials.

Elevating Assistance

Fig. 4.6a plots the knee angle trajectories following the perturbation for a representative elevating strategy for when the participant was not wearing the exoskeleton (No Exo) and for all cases while wearing the exoskeleton. An effort was made to compare perturbations of similar initial conditions, so elevating strategies with similar initial knee angles θ_p were chosen. The trials plotted in Figs. 4.6 and 4.7 are shaded gray in Table 4.5.

After the perturbation and prior to initial foot-strike, the participant's knee angle in the Reflex case most closely matches the timing and magnitude of the knee angle trajectory of the No Exo case (Fig. 4.6a). Specifically, in the Reflex case the participant landed with a more extended knee (26.6° flexion) compared to the other cases (38.8°, 41.5°, 33.6° for the No Change, Turn Off, and Opposite cases, respectively), which is a potentially more stable, safe landing position (and closely resembles how the participant responded in the No Exo case, landing at 25.2°). The delayed and decreased peak knee flexion in the Opposite case is due to the participant's actions opposing the implemented lowering

Table 4.5: Stumble experiment outcomes.

Case	% Swing	P(L) Eq. 3	P(DL) Eq. 4	Algorithm Decision	Human Decision
No Exo	29	N/A	N/A	N/A	Elevating
No Exo	46	N/A	N/A	N/A	Lowering
No Exo	39	N/A	N/A	N/A	Elevating
No Exo	51	N/A	N/A	N/A	Lowering
No Exo	28	N/A	N/A	N/A	Elevating
No Exo	48	N/A	N/A	N/A	Lowering
No Exo	42	N/A	N/A	N/A	Elevating
No Exo	55	N/A	N/A	N/A	Lowering
No Change	54	5.20E-11	0.941	Lowering	Lowering
No Change	33	1.40E-06	0.358	Elevating	Elevating
No Change	47	1.33E-05	0.720	Lowering	Lowering
No Change	35	8.17E-09	0.177	Elevating	Elevating
No Change	36	7.21E-06	0.204	Elevating	Elevating
No Change	37	5.27E-08	0.165	Elevating	Elevating
No Change	60	4.45E-04	0.917	Lowering	Lowering
No Change	53	1.92E-06	0.708	Lowering	Lowering
No Change	46	6.61E-07	0.681	Lowering	Lowering
No Change	34	2.89E-06	0.102	Elevating	Elevating
Turn Off	39	6.18E-07	0.304	Elevating	Elevating
Turn Off	53	1.10E-02	0.841	Lowering	Lowering
Turn Off	48	2.72E-07	0.712	Lowering	Lowering
Turn Off	36	2.23E-07	0.164	Elevating	Elevating
Turn Off	63	3.48E-03	0.855	Lowering	Lowering
Turn Off	38	3.14E-07	0.187	Elevating	Elevating
Reflex	48	3.10E-06	0.786	Lowering	Lowering
Reflex	55	5.36E-03	0.698	Lowering	Lowering
Reflex	38	3.37E-06	0.195	Elevating	Elevating
Reflex	43	6.41E-03	0.693	Lowering	Lowering
Reflex	32	1.81E-08	0.105	Elevating	Elevating
Reflex	43	6.42E-06	0.399	Elevating	Elevating
Reflex	54	8.20E-04	0.933	Lowering	Lowering
Opposite	51	5.12E-02	0.746	Lowering	Lowering
Opposite	66	4.23E-05	0.951	Lowering	Lowering
Opposite	42	1.61E-05	0.571	Lowering	Lowering
Opposite	30	2.28E-09	0.078	Elevating	Elevating
Opposite	40	6.29E-07	0.437	Elevating	Elevating
Opposite	36	1.24E-07	0.255	Elevating	Elevating

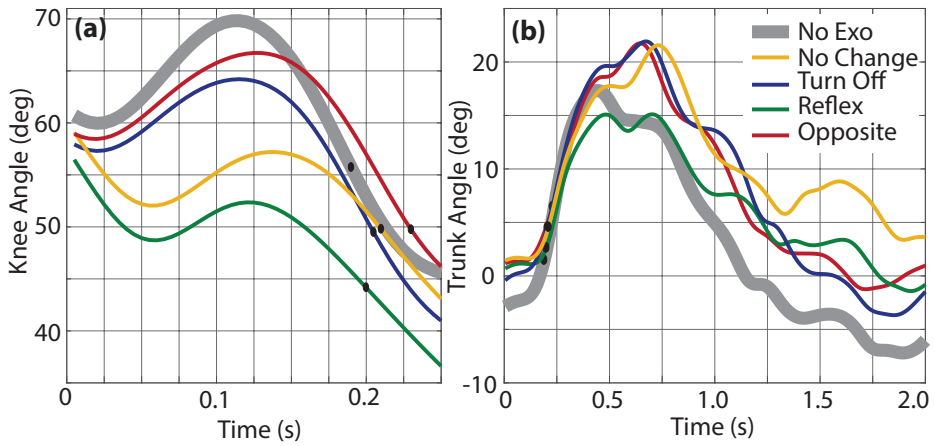

Figure 4.7: Sagittal-plane knee angle (a) and trunk angle (b) following perturbation for a representative lowering strategy for each case. Time 0 indicates the instant of perturbation, and the black filled circle indicates first footstrike.

strategy (i.e., exoskeleton knee is trying to extend for lowering, while human knee is trying to flex for elevating).

Fig. 4.6b plots the trunk angle following the perturbation for the same trials as Fig. 4.6a. As shown, the Opposite case resulted in substantially larger trunk flexion (17.4° more peak flexion than the No Exo case) following the perturbation, further substantiating that a controller choosing the wrong strategy could increase fall risk of the exoskeleton user. The other cases resulted in comparable peak trunk flexion to the No Exo case, with the Reflex case closest to the No Exo case at 1.8° higher, the No Change case at 1.7° lower, and the Turn Off case at 5.0° higher.

Overall, for elevating strategies, the Reflex case maintained the user's ability to recover as compared to the No Exo case in both knee angle trajectory and trunk angle metrics. The Opposite case inhibited the user's ability to recover as compared to the No Exo case in both knee angle trajectory (landed more flexed) and trunk angle (higher peak flexion). The No Change and Turn Off cases inhibited the user's ability to recover in knee angle trajectory (landed more flexed), but did not substantially affect trunk kinematics.

Lowering Assistance

Fig. 4.7a plots the knee angle trajectories following the perturbation for a representative lowering strategy when the participant was not wearing the exoskeleton (No Exo) and for all cases while wearing the exoskeleton. An effort was made to compare perturbations of similar initial conditions, so lowering strategies with similar initial knee angles θ_p were chosen.

After the perturbation and prior to initial foot-strike, the knee flexed the least in the Reflex case (Fig. 4.7a). This could be considered an improvement to the No Exo case, in which the knee flexes 9° more than its value at perturbation before extending to lower (whereas in Reflex case the knee does not flex more than its value at perturbation). In other words, in the No Exo case the participant initially elevated but then abandoned that strategy in favor of lowering (i.e., delayed lowering); with the decision algorithm instantly choosing and implementing lowering strategy assistance in the Reflex case, the delayed lowering strategy and associated hesitation is eliminated. The Reflex case also resulted in the most extended knee at foot-strike (11.6° more extended than No Exo case, and 5° more extended than the other cases), which again could be considered a safer landing position. Note that the Opposite case showed the greatest knee flexion and most delayed foot-strike compared to the other Exo cases (due to the knee controller activating elevating assistance); however, the participant was still able to overcome the opposing controller assistance and lower.

Fig. 4.7b plots the trunk angle following the perturbation for the same trials as Fig. 4.7a. While the Reflex case resulted in the least peak trunk flexion, in all cases peak trunk flexion was within 5° of that of the No Exo case.

Overall, for lowering strategies, the Reflex case improved the user's ability to recover as compared to other cases in terms of knee flexion after perturbation (less hesitation) and knee flexion at foot-strike (landed more extended). The Opposite case inhibited the user's ability to recover as compared to other modes in terms of knee angle and timing of foot-strike, but the participant was not substantially affected in terms of trunk angle. In the No Change case, the participant initially flexed less than Turn Off, but in both the participant landed with approximately the same knee flexion; likewise, trunk flexion was similar for both cases.

The authors note that both the No Change and Turn off cases did not substantially hinder the user in terms of fall risk (trunk angle), and thus these may be adequate responses for healthy exoskeleton users; however, the Reflex case did provide benefits over these cases as enumerated above. Also note that the exoskeleton employed here is relatively small and lightweight; for a bulkier, heavier exoskeleton (e.g., hip-knee-ankle), the effects of these cases may be more prevalent.

The authors note that results analyzed here are for a single participant; thus, all results suggest potential benefits and/or drawbacks of the various cases. Future work will test this controller on more participants to evaluate to what extent these insights hold.

4.1.5 Conclusions

The authors proposed a stumble recovery controller for a knee exoskeleton that acts in concert with the healthy individual's own reflexive strategy decision. For all attempted experimental trials with the exoskeleton, the swing-phase perturbation was successfully detected by the exoskeleton and the strategy selected matched that of the participant. For elevating, the assistance provided by the exoskeleton maintained the participant's ability to recover compared to not wearing the exoskeleton, and improved the participant's ability to recover vs. other cases; for lowering, the assistance provided potentially improved the participant's ability to recover compared to not wearing the exoskeleton and other cases. This controller can be implemented in any lower-limb exoskeleton with control of the knee joint and offers a promising approach to addressing stumble recovery for lower limb exoskeletons.

4.2 Part 2: Development and assessment of real-time, exoskeleton-based stumble detection and recovery strategy identification algorithms

4.2.1 Part 2 Summary

Powered lower-limb exoskeletons have been shown to benefit the human wearer as both assistive and augmenting devices, but their application in the real world is limited in that they do not account for unexpected disturbances, such as a trip or stumble. Ideally, a lower-limb exoskeleton would have the capability to (i) detect a stumble event and (ii) select an anticipated stumble recovery strategy in order to provide appropriate stumble recovery assistance. However, to date algorithms that have explored stumble detection and recovery strategy identification have been limited for real-time implementation due to their detection/classification performance, signals required, and/or testing approach. Therefore, five young, healthy adults wearing a knee exoskeleton underwent a stumble obstacle perturbation experiment in order to collect an exoskeleton sensor dataset of stumbles throughout swing phase. First, this dataset was used to develop a stumble detection algorithm, which ultimately employed thresholds on IMU frequency and magnitude content to detect stumbles with 100% accuracy and no false positives out of 109 stumble events and 109 normal (i.e., unperturbed) swing phases with a mean detection latency of 18 ms. Second, a recovery strategy identification algorithm built from a previously-collected motion capture dataset of stumbles was tested on the exoskeleton sensor dataset of stumbles. The best-performing feature set predicted strategy selected with 96% classification accuracy (105/109 strategies predicted correctly). Overall, the detection and identification algorithms provide improved accuracy with fewer required sensors relative to previous works, and were tested on the largest exoskeleton sensor stumble dataset to date, showing the feasibility of such algorithms for real-time implementation. Such efforts provide the crucial first step in developing lower-limb assistive devices that are robust to stumbles.

4.2.2 Introduction

Powered lower-limb exoskeletons show promise as rehabilitation devices for walking-impaired users (e.g., [64]) and performance augmentation devices for healthy users (e.g., [128]). However, for such devices to be safe and ultimately adopted in the real world, their function needs to be robust to unexpected perturbations, such as a trip or stumble [91, 124, 105, 39].

The response of healthy adults to stumbles (i.e., the event in which the swing foot unexpectedly encounters an obstacle and must clear that obstacle to recover) has been relatively well characterized, offering insights into how a lower-limb exoskeleton might behave. Upon contact with an obstacle, the healthy adult reacts with biceps femoris or rectus femoris response latencies of about 60 ms (among other muscle responses) [101]. These muscle responses commence one of three primary recovery strategies: the elevating, lowering, or delayed lowering strategy [24, 101]. In the elevating strategy, the tripped limb elevates up and over the obstacle, clearing the obstacle in the same step. In the lowering strategy, the tripped limb lowers to the ground posterior to the obstacle, prematurely terminating the step, and the contralateral limb subsequently completes a recovery step; the tripped limb then clears the obstacle in the following step. In the delayed lowering strategy, the tripped limb initially elevates, but ultimately elevation is abandoned and the limb is lowered posterior to the obstacle akin to the lowering strategy. Note that the elevating strategy is characterized by tripped limb knee and hip flexion (to elevate over the obstacle), while the lowering and delayed lowering strategies are characterized by tripped limb knee and hip extension (to terminate the step posterior to the obstacle).

Thus, in order to provide appropriate stumble recovery assistance, a lower-limb exoskeleton ideally would have the following behaviors: (i) the reliable and quick detection of a swing-phase perturbation and (ii) the correct recovery strategy decision (i.e., elevating or lowering). Regarding (i), studies have taken various approaches to investigate potential stumble detection algorithms for powered lower-limb assistive devices, which have provided meaningful insights for this work. Zhang et al. 2011 [126] used anterior-posterior foot acceleration from motion capture data and lower-limb electromyography (EMG) data to detect perturbations; while they achieved high detection accuracy, they reported that further research is needed to improve the false positive rate and detection response time. Additionally, their perturbation study involved treadmill belt accelerations and decelerations (rather than swing-phase obstacle perturbations) which may not accurately represent real-life stumbles [50]; moreover, using motion capture and EMG data may not be representative of sensor data for assistive device applications. Shirota et al. 2014 [106] considered tripped limb kinematics from motion capture data in their linear discriminant analysis classifier when participants were tripped

via a rope-blocking apparatus on a treadmill. While all stumbles were detected, the authors also encouraged further research to decrease false positives. Lawson et al. 2010 [55] used a Fast Fourier Transform (FFT) approach to detect stumbles from participants wearing IMUs during overground obstacle perturbations, which yielded 100% accuracy with a 50 ms detection delay and no false positives. However, three inertial measurement units (IMUs) were employed on three leg segments, which may not be available in some lower-limb devices. Furthermore, a larger test set (19 stumbles were included in this work) would give a better indication of efficacy. Monaco et al. 2017 [67] detected balance loss during treadmill belt acceleration perturbations when participants were wearing a powered hip exoskeleton by comparing actual hip angle to those predicted by a pool of adaptive oscillators with an average detection delay of 350 ms, which is much longer than that observed in the healthy human response (e.g., [101]). A few other studies have explored stumble detection with a single IMU during obstacle perturbations and achieved high detection accuracy [21, 42]; however, these algorithms were intended for more clinical applications analyzing patient stumble rate over an extended period of time, and as such do not detect quick enough for real-time exoskeleton assistance.

Regarding (ii) – making the correct recovery decision – only two studies have specifically investigated the development of a real-time stumble recovery strategy selection algorithm for lower-limb wearable assistive devices, which have given important direction for this work. Shirota et al. 2014 [106] used a linear discriminant analysis classifier to classify elevating or lowering strategies and achieved 92% median classification accuracy. The algorithm, however, used motion capture kinematics from multiple joints/segments, which limits real-world use in an assistive device. Additionally, accuracy was reported based on leave-one-out cross-validation; an entirely new test set (or, at least, testing and training on separate participants) may provide a better assessment of accuracy. Finally, the rope-blocking perturbation technique does not involve a physical obstacle to clear, which may alter recovery strategy selection compared to real-life stumbles. Lawson et al. [55] found a threshold on the RMS of thigh acceleration 50 ms prior to detection that separated elevating from lowering strategies. However, their overground stumble apparatus limited the ability to implement stumbles across swing phase, and therefore it is unclear if mid swing stumbles were tested. Additionally, further testing with more stumbles (19 were tested in this work) would provide a more complete validation of this approach.

Considering these previous works, a stumble detection algorithm and stumble recovery identification algorithm that (1) use sensors typical of a lower-limb exoskeleton, (2) detect stumble and select an anticipated recovery strategy within the human muscle response latency for stumbles, (3) offer high stumble detection accuracy and recovery strategy identification classification accuracy without false positives, and (4) are tested on many (more than 20) swing-phase obstacle perturbations (i.e., real-life stumble scenario) throughout swing phase would build upon prior research and address the problem in a manner that is closer to real-world application.

The authors have previously developed a stumble detection algorithm and recovery strategy identification algorithm for a knee exoskeleton that was evaluated on one healthy adult [26]. The detection algorithm used a simple threshold on thigh acceleration. The recovery strategy identification algorithm implemented a two-stage decision model with logistic regression equations fit from previously collected healthy adult motion capture stumble data [27]. While these approaches yielded 100% detection and classification accuracy for the single participant, the extent to which these approaches might extend across multiple participants has not been tested and is critical for robustness analysis and implementation in the real world. Therefore, the objective of this work is to develop a new stumble detection algorithm and recovery strategy identification algorithm with the aforementioned criteria and evaluate their accuracy on experimental stumble data from multiple healthy adults wearing a knee exoskeleton.

4.2.3 Methods

The following approach was taken to address the proposed objective: First, an experiment was conducted with healthy participants wearing a knee exoskeleton to establish an extensive dataset of exoskeleton sensor data during stumble events. This dataset was used to develop a stumble detection algorithm. Next, a previously-generated dataset of stumbles from different participants was used to train a recovery strategy identification algorithm. This algorithm was then tested on the new exoskeleton stumble experiment dataset.

4.2.3.1 Exoskeleton Stumble Experiment

A swing-phase obstacle perturbation stumble experiment was conducted with five healthy adult participants (one female, 4 males; mean age: 28 +/- 4 years; mean height: 1.8 +/- 0.04 m; mean mass: 80 +/- 17 kg) wearing a unilateral knee exoskeleton to collect sensor data with which to develop the stumble detection algorithm and test the recovery strategy identification algorithm. All experimental protocols were approved by the Vanderbilt Institutional Review Board, and all participants gave their written informed consent.

Knee Exoskeleton Hardware

The unilateral knee exoskeleton used in these experiments is a standard knee-ankle-foot orthosis (KAFO). Sensor data from the device were used to develop the detection and identification algorithms. Specifically, a cassette attached to the thigh segment houses a nine-axis IMU as well as an encoder to measure knee angle. Force-sensing resistors (FSRs) are mounted to the toe and heel of the AFO to detect heel-strike and toe-off events. Note that the cassette also included a motor and transmission to actuate the lateral-side knee joint via a pair of Bowden cables, but this feature was not used in the experiments described here.

Experimental Protocol

Each participant was introduced to a series of stumbles using a custom obstacle perturbation system [50]. The protocol was consistent with previous works using this setup [27, 26, 28], namely: the participant, while wearing the knee exoskeleton, walked on a force-instrumented treadmill at 1.1 m/s. After a random number of steps, an obstacle was released onto the treadmill belt at a random percentage of swing phase to unexpectedly obstruct the swing foot, inducing a stumble and requiring a stumble recovery response. Participants listened to white noise, wore noise-cancelling headphones and wore inferior vision-blocking goggles to occlude auditory and visual cues of obstacle release to limit expectation of the perturbation. Additionally, the obstacle delivery apparatus was designed such that the obstacle's entry onto the treadmill belt was imperceptible [50]. Finally, participants performed Serial Sevens (counting backwards by intervals of seven) as a cognitive distraction task to further limit expectation and/or anticipation of the perturbation. The obstacle perturbation system and experimental setup are pictured in Fig. 4.8.

Data Collection

For each stumble trial (which included steps leading up to the stumble and the stumble itself), raw signals from the exoskeleton knee encoder and thigh IMU were collected via a CAN interface with MATLAB/Simulink at a sampling rate of one kHz. Additionally, ground-reaction forces (GRFs) were collected from the split-belt, force-instrumented treadmill (Bertec, Columbus, USA) at one kHz to compute swing percentage of each perturbation. Signal processing is detailed in the subsections discussing each algorithm.

The recovery strategy of each stumble trial was reported as elevating (if their foot cleared obstacle and landed anterior to obstacle in the same step) or lowering (if their foot lowered posterior to obstacle prior to clearing it). The swing percentage of each stumble was calculated as the time of perturbation relative to the preceding toe-off event divided by the average swing time of 20 strides prior to the perturbation.

4.2.3.2 Stumble Detection Algorithm

Algorithm Development

IMU data (gyroscope signals in three directions and accelerometer signals in three directions) collected during the exoskeleton stumble experiment (109 stumble trials) were used for algorithm development. Each trial was parsed from the toe-off immediately prior to the perturbation to one second after the toe-off (i.e., post-perturbation), yielding 109 perturbation events. Additionally, the swing phase prior to the perturbed swing phase was parsed from each trial, yielding 109 normal swing phases. Originally, in [26], a singular threshold on thigh acceleration was used for detection. However, when tested on all perturbation events and normal swing phases from this study's dataset, this threshold was not robust across multiple participants; instead, each participant required their own threshold. A

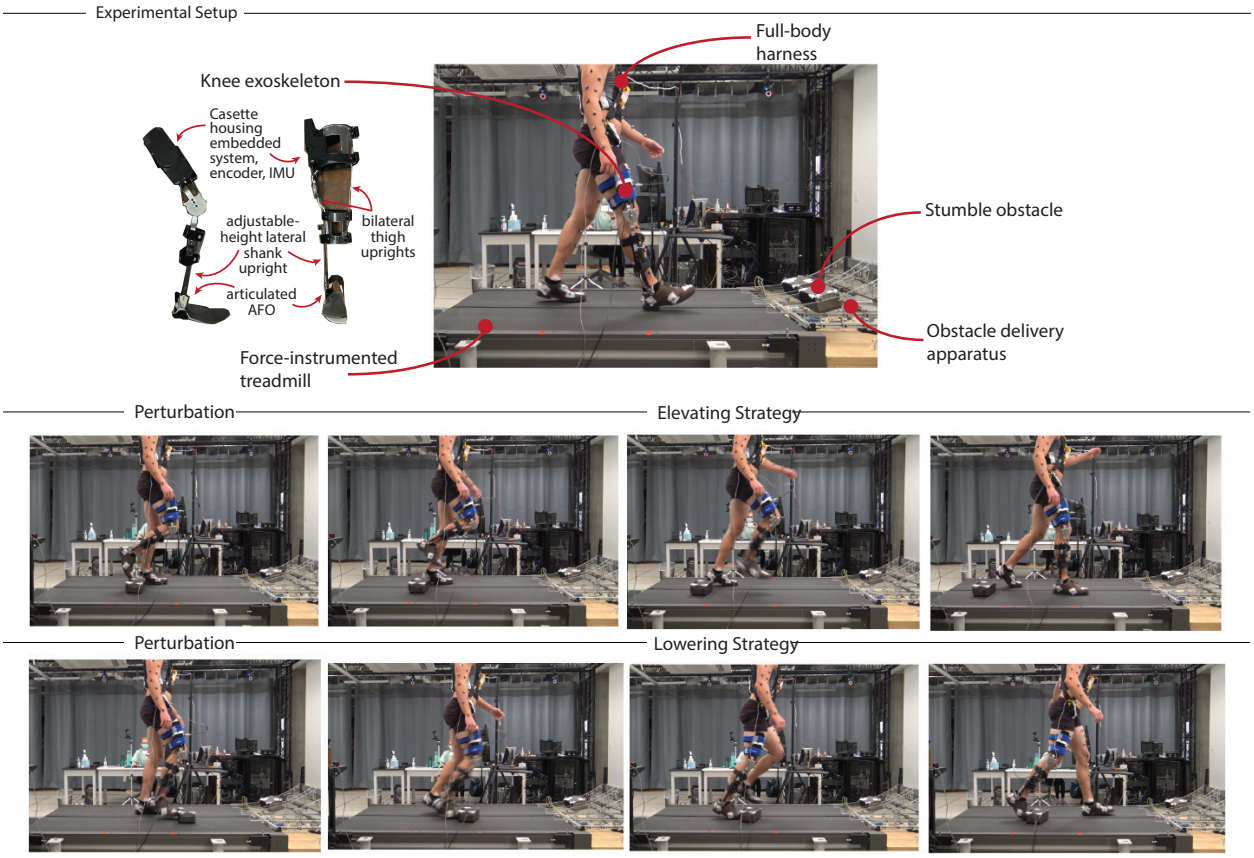

Figure 4.8: Experimental Setup

threshold approach was explored for the remaining available signals, but no universal threshold (or combination of thresholds) could be found that provided accurate detection without false positives. This was consistent with other works which used threshold or outlier-based detection methods [126, 106]. Second, the FFT method from [55] was considered; however, this approach alone also produced many false positives in both the perturbation events (prior to perturbation) and normal swing phases. Therefore, a combined approach that considers both frequency and magnitude information was explored.

The final detection algorithm checks whether the frequency content and magnitude of thigh IMU data has crossed certain thresholds. The algorithm is detailed in Fig. 4.9. Specifically, every 10 ms the FFT of the raw thigh acceleration in the y-direction from the accelerometer is computed for the previous 50 ms. If the power at frequencies of 20, 40, 60, or 80 Hz (i.e., higher than the typical walking frequency of 1-2 Hz) is greater than a threshold, then that instant in time is flagged as a potential perturbation. If flagged, the 10-ms backward difference of the thigh acceleration in the y-direction (normal to thigh segment) from the accelerometer (Thigh Jerk Y in Fig. 4.9(b)) and the 10-ms backward difference of thigh angular velocity from the gyroscope (Thigh Angular Acceleration in Fig. 4.9(b)) are computed. If both signals exceed certain thresholds in the previous 30 ms, that instant is time is marked as a perturbation.

Outcome Metrics

Detection accuracy was computed as the percentage of perturbation events in which the perturbation was successfully detected. False positive rate was computed as the number of false detections that occurred in total out of the 109 perturbation events and 109 normal swing phases. Finally, detection delay for each of the perturbation events was computed as the time difference between the true perturbation index (identified post-hoc as the first peak in the Thigh Acceleration Y signal, indicated in Fig. 4.9(b)) and the perturbation detection index (identified with the detection

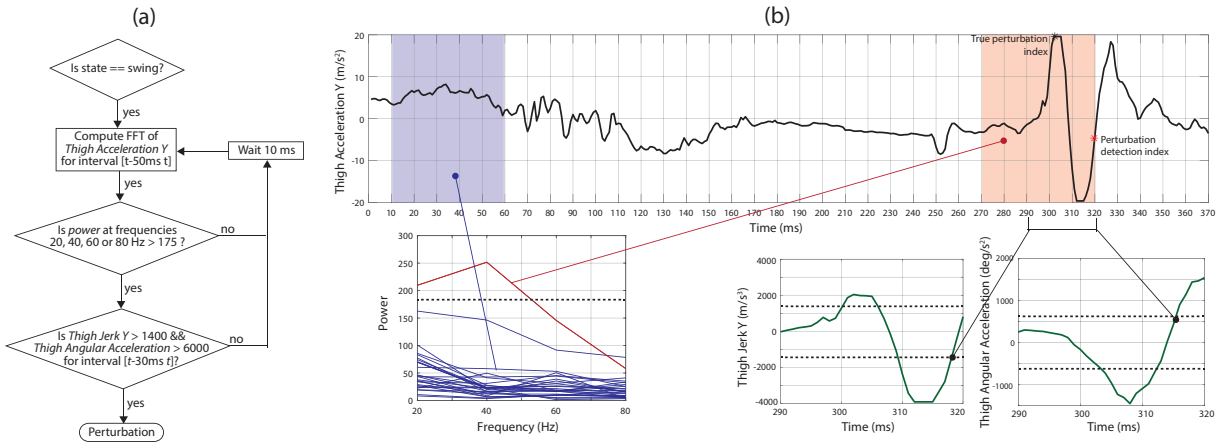

Figure 4.9: (a) Stumble detection algorithm flow chart (b) Example of algorithm implementation on perturbation event

algorithm, indicated in Fig. 4.9(b)).

4.2.3.3 Recovery Strategy Identification Algorithm

The overarching approach to strategy identification algorithm development for this work was to use a previously collected kinematic dataset of 188 stumbles from seven healthy adults [50] to build a strategy selection model, and then to test this model on the kinematic dataset of 109 stumbles from the exoskeleton stumble experiment described above. Note that both experiments employed the same experimental setup and protocol. A two-stage modelling approach was used, which was previously found to best predict recovery strategies: a first decision between initially elevating and lowering (Stage 1), and, if elevating, a second decision between elevating and delayed lowering (Stage 2) [27]. For this model, only kinematic features easily computed from the sensors onboard the exoskeleton were considered: thigh angle, thigh angular velocity, knee angle, and knee angular velocity.

Data Pre-processing & Organization

Motion Capture Dataset For the previously collected healthy adult stumble study, lower-limb kinematics were recorded at 200 Hz via an infrared motion capture system and processed with a zero-phase, third-order, Butterworth low-pass filter at a cutoff frequency of 6 Hz. Inverse kinematics were computed using Visual3D (C-Motion, Germantown, USA) to estimate joint-level kinematics for each trial. The potential inputs (thigh angle, thigh angular velocity, knee angle, and knee angular velocity) were computed at the instant of perturbation, and the recovery strategy was labeled for each stumble. Position inputs (thigh angle, knee angle) were normalized to the value at full extension in the previous step. The trials were split into two datasets for training/validation: the Stage 1 Motion Capture Dataset included all 188 trials labeled as initially elevating or lowering, and the Stage 2 Motion Capture Dataset included the 165 initially elevating trials labeled as elevating or delayed lowering.

Exo Sensor Dataset For the exoskeleton stumble study, lower-limb kinematics were recorded at 1000 Hz via the knee encoder and thigh IMU. Specifically, thigh angle was computed with complementary filter sensor fusion that combines accelerometer and gyroscope measurements with a crossover frequency of 0.1 Hz. Thigh angular velocity was computed via a standard first-order low-pass filter with a cutoff frequency of 30 Hz. Position inputs were normalized to the value at full extension in the previous step. The potential inputs were computed at the true perturbation index, as well as 5, 10 and 15 ms prior to the true perturbation index, and recovery strategy was labeled for each stumble comprising one Exo Sensor Dataset. Exo Sensor Dataset trials were labeled either elevating (all elevating strategies) or lowering (all lowering and delayed lowering strategies). Because both the delayed lowering strategy and lowering strategy involve ultimately lowering the foot behind the stumble obstacle, and would thus require the same

exoskeleton knee assistance, it was not necessary to differentiate between the two in the actual application. Note that these pre-processing steps can be applied in real-time on the exoskeleton, so the testing process represents real-time implementation of the algorithm.

Algorithm Development

Initially, the Motion Capture Dataset was explored for insight into which feature subsets best predicted strategy selection. Similar to the approach in [27, 26], a wrapper method with cross-validation by participant and hyperparameter tuning was used to find the total classification accuracy (computed as the average of the classification accuracies of each participant's set of trials) for each of the 15 possible feature subsets shown in Fig. 4.10. This process was completed for both the Stage 1 and Stage 2 Motion Capture Dataset.

Because no feature subset emerged as substantially best in the cross-validation process for either stage (all performed relatively well, with a classification accuracy range of 88%-97% for Stage 1, and 81%-88% for Stage 2), all 15 feature subsets were considered for model fitting and algorithm testing (i.e., in order to examine to what extent these feature subsets also perform well on the Exo Sensor Dataset) with the following procedure, which is outlined in Fig. 4.10.

For each feature subset for each stage, the Motion Capture Dataset was fit to a logistic regression model with Ridge regularization (using the hyperparameter that maximized classification accuracy for the corresponding feature set in cross-validation process). The logistic regression equations for Stage 1 (Eq. 4.5) and Stage 2 (Eq. 4.6) are given below:

$$P(Lowering) = \frac{1}{1+e^{-(\alpha_0+\alpha_1\gamma+\alpha_2\dot{\gamma}+\alpha_3\theta+\alpha_4\dot{\theta})}} \tag{4.5}$$

$$P(DelayedLowering) = \frac{1}{1+e^{-(\beta_0+\beta_1\gamma+\beta_2\dot{\gamma}+\beta_3\theta+\beta_4\dot{\theta})}} \tag{4.6}$$

Where P(L) is the probability of a lowering strategy vs. an initially elevating strategy, P(DL) is the probability of a delayed lowering strategy vs. an elevating strategy, γ is knee angle, $\dot{\gamma}$ is knee angular velocity, θ is thigh angle, and $\dot{\theta}$ is thigh angular velocity, and α_{0-4} and β_{0-4} are the equation coefficients generated from the model fitting. Note that coefficients have a value of 0 for the features not included in the subset, as indicated in Fig. 4.10.

Fig. 4.10 diagrams the final recovery strategy identification algorithm: If the probability of lowering (calculated from Eq. 4.5) is greater than 0.5, then the strategy is predicted to be lowering. If it is less than 0.5, the strategy is predicted to be initially elevating, and Eq.4.6 (probability of delayed lowering) is computed. If the probability of delayed lowering is greater than 0.5, then the strategy is predicted to be lowering. If it is less than 0.5, the strategy is predicted to be elevating.

For each combination of feature set and stage (15 feature sets for each of two stages = 15^2 combinations), the recovery strategy identification algorithm was applied to each trial in the Exo Sensor Dataset to predict recovery strategy for each trial. This was completed for features computed at the true perturbation index as well as 5, 10, and 15 ms prior. Classification accuracy was computed as the percentage of trials in which recovery strategy was successfully predicted. The combination of Stage 1 feature set, Stage 2 feature set, and perturbation time that produced the highest classification accuracy with the least number of features was chosen as the final algorithm.

Outcome Metrics

The logistic regression equation coefficients and perturbation timing used in the final algorithm are reported. Classification results using this final algorithm are also reported, including a confusion matrix, as well as classification accuracy broken down by participant and by swing phase at which the perturbation occurred.

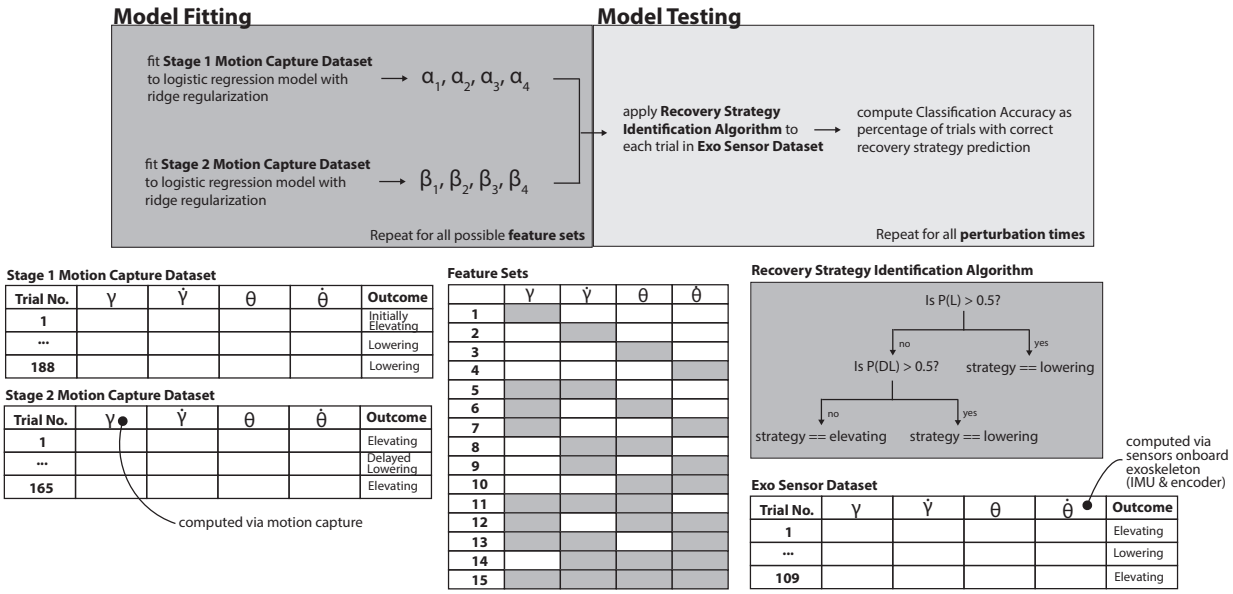

Figure 4.10: Recovery strategy identification algorithm development and testing

Table 4.6: Coefficients for equations in recovery strategy identification algorithm

Eq. 4.5		Eq. 4.6	
Coefficient	Value	Coefficient	Value
α_0	-5.839	β_0	-2.575e-05
α_1	0.266	β_1	0.083
α_2	0.042	β_2	0
α_3	-0.265	β_3	-0.102
α_4	0	β_4	0

4.2.4 Results

4.2.4.1 Stumble Detection Algorithm

Out of 109 perturbation events, the stumble detection algorithm achieved 100% detection accuracy with no false positives. Out of 109 normal swing phases, the stumble detection algorithm yielded no false positives. The average detection delay was 18 +/- 6 ms (range 6-42 ms).

4.2.4.2 Recovery Strategy Identification

The final recovery strategy identification algorithm used the input set computed at 5 ms prior to the true perturbation index. The coefficients from model fitting for each stage are given in Table 4.6.

Out of 109 perturbation events, 105 trials were predicted with the correct recovery strategy, yielding a total classification accuracy of 96%. For three of five participants, the classification accuracy for their trials was 100%, and for the remaining two participants it was 86-88%. Table 4.7 gives a confusion matrix of prediction results, Table 4.8 breaks down classification accuracy by participant, and Fig. 4.11 provides classification results as a function of swing percentage of perturbation.

Table 4.7: Confusion matrix for recovery strategy identification algorithm results

	Predicted Elevating	**Predicted Lowering**	**Total**
Actual Elevating	55	2	57
Actual Lowering	2	50	52
Total	57	52	109

Table 4.8: Classification accuracy for each participant's trials

Participant	**Classification Accuracy**
P1	100% (21/21)
P2	100% (21/21)
P3	88% (15/17)
P4	100% (36/36)
P5	86% (12/14)

As shown, all perturbations in early swing (<40%) and all perturbations in late swing (>60%) were predicted correctly. The confusion matrix of mid swing (40-60%) perturbations is given in Table 4.9.

4.2.5 Discussion

The proposed stumble detection algorithm yielded 100% detection accuracy without false positives, considering 109 perturbation events and 109 normal swing phases. By combining the IMU signal FFT and magnitude threshold approaches, this new algorithm builds upon previous works and addresses the previously reported limitations of high false positive rates.

Aside from the improved detection accuracy and false positive rate, this algorithm offers other advantages. First, the algorithm requires a single IMU attached to the thigh segment of a lower-limb exoskeleton, decreasing the number of sensors needed. Previous works used kinematic data from multiple lower-limb segments for their detection algorithm [106, 55], and one used motion capture and EMG data rather than IMU data; while this is an adequate and necessary approach for exploring detection techniques, ideally the final application would use the actual signals from typical sensors of lower-limb exoskeletons. Furthermore, the detection accuracy using a thigh IMU (rather than shank or foot) is notable considering this location is two segments removed from the perturbation. Second, this algorithm detects with the fastest response latency compared to other works. The average detection delay out of 109 perturbations was 18 ms, and even the maximum delay (42 ms) is well before the average lower-limb muscle response latencies reported in Schillings et al. 2000 [101]. This short detection delay would allow an assistive to device to react as quickly (or potentially, faster) than the human response, providing the best opportunity for optimal recovery strategy assistance. Finally, the detection and false positive rates were evaluated on 109 stumbles throughout swing phase from five participants, which is the most comprehensive obstacle perturbation stumble dataset used for this application to date.

The stumble recovery identification algorithm predicted recovery strategy with 96% accuracy on a separate test set of 109 stumbles using just three signals from sensor data available in a lower-limb exoskeleton. The algorithm can

Table 4.9: Classification accuracy for each participant's trials

	Predicted Elevating	**Predicted Lowering**	**Total**
Actual Elevating	16	2	18
Actual Lowering	2	24	26
Total	18	26	44

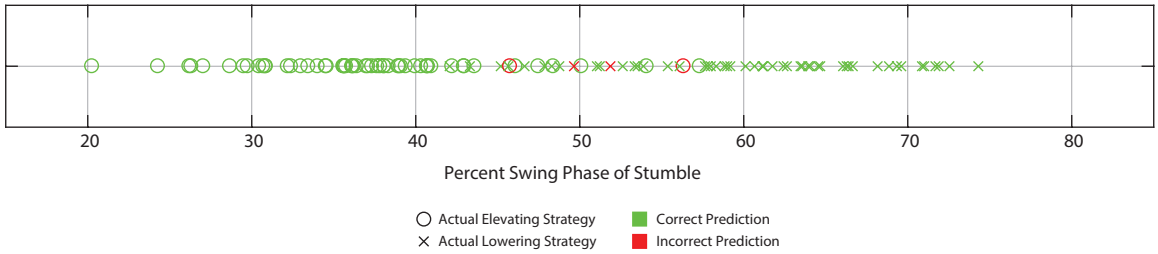

Figure 4.11: Recovery strategies used in exoskeleton stumble experiment as a function of swing percentage at which the perturbation occurred

be easily implementable in real-time on any lower-limb exoskeleton with ability to estimate knee angle, knee angular velocity, and thigh angle (e.g., with a knee encoder and thigh IMU). The only other study to evaluate a recovery strategy algorithm on stumbles from a range of points in swing phase achieved 92% median accuracy, but used motion capture data in their algorithm and evaluated accuracy based on a leave-one-out cross-validation procedure [106]. While this approach provided important insight for this work, ideally an algorithm would be evaluated with a separate test set of data measured from the sensors in an actual assistive device. One other study reported 100% classification accuracy, but their trial set included fewer (19) stumbles, and swing percentage of each stumble was not reported [56].

In total there were four stumbles incorrectly classified: two elevating strategies (Participant 3) and two lowering strategies (Participant 5). These occurred in the mid swing region where, based on studies of healthy participants (e.g., [101, 15, 107, 50, 27]), either strategy could be selected, and either could be successful. Despite the misclassifications, the algorithm still achieved 91% (40/44) accuracy in mid swing; note that the best threshold on swing percentage yields 77% (34/44) accuracy, substantiating the use of real-time, physical quantities as inputs to the model rather than a phase variable [27]. Of note, with Participants 1, 2 and 4 the stumble recovery identification algorithm achieved 100% accuracy.

There are several limitations to this work. First, all stumble trials were completed at a single walking speed. While the two-stage modelling approach for strategy identification has yielded classification results suggesting robustness across walking speeds [27], detection may potentially require a speed-dependent threshold on signal magnitude. Future work could test this detection scheme on additional walking speeds, and potentially a sliding scale of thresholds based on walking speed could be used. The magnitude threshold may also be influenced by the form factor and weight of the exoskeleton worn; in this work the exoskeleton was relatively light, but a heavier exoskeleton may provide a low-pass effect on sensor data that would need to be considered. Additionally, the exo sensor stumble dataset was used for detection algorithm development and testing, and as such there is potential for overfitting; however, the authors contend that the thresholds chosen were qualitatively not overly strict and thus should be generalizable, especially considering the nature of the dataset used, which included an extensive number of stumbles throughout swing phase from multiple participants. The intent was to find thresholds that worked well for this extensive dataset of stumbles, and the authors invite future work to explore the extent to which this detection algorithm extends to more participants, including multiple types/weights of assistive devices. Regarding the recovery strategy identification algorithm, an approach to better matching the filtering of the motion capture training data to the testing sensor data may have improved classification accuracy; however the authors posit that 96% accuracy is quite high considering (1) the different measurement modalities, which further shows the algorithm's robustness and (2) that strategy selection in mid-swing has been shown to be non-unique. This non-uniqueness raises the question: How important is decision accuracy in this region? In the case of an impaired user, perhaps selection of either strategy in this regime would be effective. In the case of a healthy user, would the decision of the exoskeleton influence the selection of the user? Hopefully future works will help to inform these questions. Additionally, the intent for this work was to develop and report the recovery strategy identification algorithm that performed best on a new exoskeleton sensor dataset of stumbles after considering various input options; the authors encourage future work that tests this algorithm with

new stumble datasets to verify its effectiveness on new data. Finally, the results of this work reflect the efficacy of a stumble detection and recovery strategy identification algorithm for the specific type of perturbation tested: a swing-phase, obstacle perturbation. While falling due to stumbles is a common cause of injury [117, 57], and the test setup best replicates this real-life stumble event compared to other systems [50], research regarding detection and response selection for other types of perturbations (i.e., slips, postural perturbations) are needed and could be a topic for future work.

4.2.6 Conclusion

This work develops algorithms for the exoskeleton-based real-time detection of stumble during walking, and also for the real-time identification of stumble recovery strategy, and evaluates these algorithms on a relatively large stumble dataset. Stumbles were detected with 100% accuracy without false positives, and the recovery strategy was identified with 96% classification accuracy out of 109 obstacle perturbation trials occurring throughout swing phase. These algorithms use minimal sensor data (single thigh IMU for detection, thigh IMU and knee encoder for recovery strategy identification) while detecting and identifying strategy quicker than the human reaction time. These algorithms provide the crucial first step in developing lower-limb assistive devices that are robust to the common daily event of a trip or stumble, which has the potential to not only improve safety of these devices but also reduce fall risk for fall-prone individuals.

4.3 Part 3: Efficacy of knee exoskeleton assistance in improving an impaired stumble recovery response

4.3.1 Part 3 Summary

Falls due to stumbles are a major cause of injury for many populations, and as such interventions to reduce fall risk have been a key focus of rehabilitation research. However, the use of powered lower-limb exoskeleton assistance has yet to be explored as a fall mitigation intervention, which could serve two important use cases: (1) a safety mechanism for existing exoskeleton wearers, who may be less capable of recovering from stumbles due to added weight or joint impedance of the device; (2) an external stumble recovery aid for fall-prone populations, such as the elderly or stroke survivors. Thus, three young, healthy adults were recruited for a stumble recovery experiment to test the efficacy of knee exoskeleton assistance in improving an impaired stumble recovery response. Leg weights were attached unilaterally to the participants' shank to simulate a walking and stumble recovery impairment, and a unilateral powered knee exoskeleton was worn on the same leg for walking and stumble recovery assistance. Ultimately, knee exoskeleton assistance served to improve participants' elevating limb kinematics (i.e., increase thigh and knee motion) and reduce overall fall risk (i.e., reduce trunk motion and increase step length) during responses relative to their impaired response (i.e., with the leg weights and no assistance). This initial exploration provides a first indication that knee exoskeleton assistance is a viable approach to improving an impaired stumble recovery response, which may enhance the safety of lower-limb exoskeletons and reduce fall risk for fall-prone populations.

4.3.2 Introduction

Falls are a major cause of injury for many populations [117, 4]. Often falls occur because of a trip or stumble [9, 61, 60, 73]. The stumble event (i.e., foot unexpectedly encountering an obstacle in swing phase that must be cleared to recover) is a common daily-life occurrence that requires a recovery response to avoid a fall. Much rehabilitation research has been devoted to improving stumble recovery and mitigating subsequent injury, particularly for fall-prone populations (e.g., elderly [33], stroke survivors [45], lower-limb prosthesis users [65], etc.).

Several works have characterized stumble recovery and identified the key factors in recovering from a stumble. Ultimately, an individual needs to restore trunk control (arrest forward angular momentum induced by the perturbation) with a sufficient and timely stepping response to recover successfully. Previous works have highlighted the role of both the recovery limb (limb that clears the obstacle) and the support limb (contralateral limb) in recovery success. Pijnappels et al. [87, 88] concluded that the reactive torques of the support limb of healthy adults enable the necessary push-off reaction, thus reducing the forward angular momentum of the body and providing more time for the elevating step. However, in a study with older adults with less adequate push-off responses [85], they found that the participants compensated with better positioning of the recovery (elevating) limb (i.e., longer stride). They propose that improving the forward swing of the recovery limb, which also works to counter induced forward angular momentum, could be a target for fall prevention training. Grabiner et al. 1993 [38] also highlighted the role of the recovery limb. Knee flexion reduces the moment of inertia of the leg, which increases hip flexion velocity; hip flexion and knee extension velocities are integral in providing a sufficient stepping response to recover. Thus, an intervention at the knee joint of the recovery limb (flexion/extension assistance) has the potential to improve recovery responses.

So far, interventions for stumble recovery assistance have primarily involved training protocols. Muscle strength training has been proposed as a means to improve both the support limb's ability to provide counteracting torques and the recovery limb's ability to provide sufficient obstacle clearance [90, 82]. Similarly, exercise and balance-focused training (e.g., Tai Chi [59]) has been proposed as a means to enhance postural stability, lower-limb strength, and flexibility to improve responses to stumble perturbations. Finally, task-specific perturbation training (via sessions involving repeated treadmill acceleration perturbations) has been shown to not only reduce falls and improve stumble recovery during a laboratory-induced trip for various populations [35, 77] but also to mitigate real-world falls [99]. In these works, the authors attribute a learned/trained reduction of trunk motion (flexion, flexion velocity) and increased step length to the improved responses. While these works provide promising and effective interventions, and also identify improvable recovery metrics, these extensive, repeated training protocols may not be feasible (i.e., considering cost, time, ability) for many individuals; furthermore, the long-term effects of such trainings have yet to be determined.

Wearable assistive technology has the potential to improve responses to stumbles without repeated training sessions

by providing immediate assistance to the recovery and/or support limb. In fact, such behavior is important not only as a fall prevention intervention for fall-prone populations, but also as a safety factor for any lower-limb exoskeleton that provides walking assistance. However, exoskeleton assistance during stumbles has been sparingly considered in the field thus far. While some works have explored stumble detection and identification techniques [55, 126, 106, 26], only a few have investigated the effect of exoskeleton assistance on stumble recovery. Hip [67] and ankle [23, 5] exoskeleton assistance during treadmill acceleration perturbations (e.g., slip perturbations) have been shown to improve stability against balance loss and reduce effort to maintain balance, respectively. However, no study has considered exoskeleton assistance during swing-phase obstacle perturbations (i.e., trip/stumble perturbations). Recall that an intervention at the knee joint of the recovery limb may improve responses via (1) knee flexion assistance, which reduces the moment of inertia of the recovery limb, allowing for easier hip flexion and thereby assisting with angular momentum reduction, and (2) knee extension assistance, which aids in the speed and length of the recovery step. Previous preliminary results suggest that knee exoskeleton assistance can be coordinated with the user to improve the recovery limb response [26]; however, this was only tested on a single healthy individual, so the extent to which it improves an impaired response for multiple participants has not been demonstrated.

Therefore, the objective of this work is to examine the extent to which powered knee exoskeleton assistance (applied unilaterally to the recovery limb) can potentially improve an impaired stumble recovery response. In this work, early swing perturbations that require an elevating strategy to recover (i.e., the tripped limb is the recovery limb) are considered. Before introducing such an intervention to fall-prone populations (e.g., elderly, stroke survivors, post-polio patients), who may be less suited for the physical demand of an exploratory study requiring many stumbles, the authors deemed it important to first test this type of intervention in able-bodied individuals. Consequently, to perform this study it was necessary to first impair the healthy individuals' ability to recover, in order to approximate the gait and recovery response of a mobility-impaired population. In order to do so, leg weights were added unilaterally to the participants' shank (i.e., the recovery limb wearing the exoskeleton) in an effort to (1) induce a walking impairment and (2) require more effort in the stepping response during stumble recovery.

This work therefore examines the following three questions: (1) Does weight added to the shank impair gait in a manner reflective of a target impaired population, and can the user coordinate with the exoskeleton walking controller to improve the impaired gait? (2) Does weight at the shank impair the elevating limb response during a stumble event, and does this also extend to impaired fall risk? (3) Does an exoskeleton stumble recovery controller improve the impaired elevating limb response, and does this also extend to reduced fall risk?

4.3.3 Methods

4.3.3.1 Interventional Device

A modified unilateral powered knee exoskeleton (Fig. 4.12(a)) was used as both the impairment technique and improvement technique in this study, discussed subsequently. The exoskeleton is a standard knee-ankle-foot orthosis (KAFO) modified with a non-standard powered knee module, which is actuated by a pair of Bowden cables driven by a brushless motor and a two-stage chain-drive transmission with a transmission ratio of 11.2. The transmission, embedded system, and sensors (nine-axis inertial measurement unit (IMU) to measure thigh motion and encoder to measure knee motion) are housed in a cassette attached to the thigh segment. Two force-sensing resistors (FSRs) are attached to the foot: one under the heel of the shoe insole (for swing/stance determination), and one externally on the toe structure of the shoe (for stumble detection). For purposes of the experiments conducted here, the device was powered with an off-board linear power supply (Kepco BOP36-12M) that supplied up to 10A of current, which corresponded to 14.5 Nm of joint torque. An embedded system runs all low-level control, including brushless motor current control, and also includes a CAN interface that enables high-level control prototyping and data collection from a laptop computer via the real-time interface provided by MATLAB/Simulink at a sampling rate of one kHz. Thigh angular velocity is measured from the IMU with a first-order low-pass filter with a cutoff frequency of 10 Hz. Thigh angle is calculated via a standard complementary filter sensor fusion that combines measurements from the accelerometer and gyroscope measurements, with a crossover frequency between the two measurements of 0.5 Hz.

Impairment Method

To impair walking gait as well as the elevating limb recovery response, 12-14 lb leg weights were attached to the shank segment of the knee exoskeleton, as pictured in Fig. 4.12(a). Methods for evaluating the efficacy of these weights in impairing walking gait and stumble recovery are discussed subsequently.

Improvement Method

A closed-loop walking controller was designed to assist the knee joint during level ground walking (Fig. 4.12(b)), with the intent of correcting or reducing the simulated impairment introduced by the leg weights. The controller is comprised of a finite-state machine that transitions between two states: stance and swing. To prevent knee buckling during initial stance, knee angle is regulated to zero degrees using the following PD controller:

$$\tau = k_p(\theta_{desired} - \theta) + k_d(\dot{\theta}_{desired} - \dot{\theta}) \tag{4.7}$$

where τ is the commanded torque, $\theta_{desired}$ is 0 deg, θ is the current knee angle, $\dot{\theta}_{desired}$ is 0 deg/s, $\dot{\theta}$ is current knee angular velocity, and k_p and k_d are experimenter-defined proportional and derivative gains, respectively. This assistance is removed 300 ms into stance to facilitate initiation of swing phase by allowing knee flexion. To assist swing-phase motion, a position controller tracks a predefined knee angle trajectory (shown in Fig. 4.12(b)) using Eq. 4.7, where $\theta_{desired}$ and $\dot{\theta}_{desired}$ are the desired knee angle and knee angular velocity from the spline and its derivative at the current time in swing phase. The elapsed time of the swing state is determined by a swing-stance ratio and the stance time of the current stride. State transitions are determined by heel FSR loading and thigh angular velocity thresholds (Fig. 4.12(b)). The following variables were tunable for each user: $k_{p,stance}$, $k_{d,stance}$, $k_{p,swing}$, $k_{d,swing}$, peak swing knee angle, swing-stance ratio, and thigh angular velocity threshold.

A stumble recovery controller was designed to assist the knee in the execution of the elevating strategy. Upon detection of a stumble indicated by contact with the obstacle recorded from the toe FSR, a feedforward torque pulse intended to assist the flexion and subsequent extension of the elevating response is implemented. Specifically, the pulse is a 450-ms (approximate length of elevating strategies from a previous stumble study conducted at the same walking speed [50]) spline with approximately 14.5 Nm peak applied torque in flexion and extension (Fig. 4.12(b)).

4.3.3.2 Stumble Recovery Experiment

Experimental Protocol

Six young, healthy adult participants were recruited to participate in the exoskeleton stumble recovery experiment. The protocol involved sessions on two separate days, an acclimation day and a testing day. All experimental protocols were approved by the Vanderbilt Institutional Review Board, and all participants gave their written informed consent.

During the acclimation day, the knee exoskeleton was fit to the participant's right leg. Specifically, a thigh segment, shank segment, AFO and shoe were selected that best fit the participant, and the height of the lateral shank upright was adjusted such that the center of the exoskeleton knee joint best approximated the axis of rotation of their biological knee. Then the participant walked on the treadmill at 1.1 m/s while the experimenter tuned the walking controller. Finally, the participant was introduced to a few stumbles (setup and protocol discussed subsequently) in order to be familiarized with the experimental protocol prior to testing day.

On testing day, the participant underwent a series of stumble trials using a custom obstacle perturbation system [50]. The experimental setup and protocol are pictured in Fig. 4.13. For each trial, participants walked on a force-instrumented treadmill at 1.1 m/s. After a random number of steps, a 35-lb steel block was released from the obstacle delivery apparatus onto the treadmill belt such that it contacted the participant's foot at an experimenter-defined percentage of swing phase. Note that various sensory occlusion techniques (e.g., noise-cancelling headphones and inferior vision-blocking goggles) and a cognitive distraction task (Serial Sevens) were employed to limit expectation of the stumble. Additionally, the obstacle delivery apparatus was shown to deliver the obstacle without perception of the participants in a previous validation study. See [50] for full protocol and system details. For this experiment, pertur-

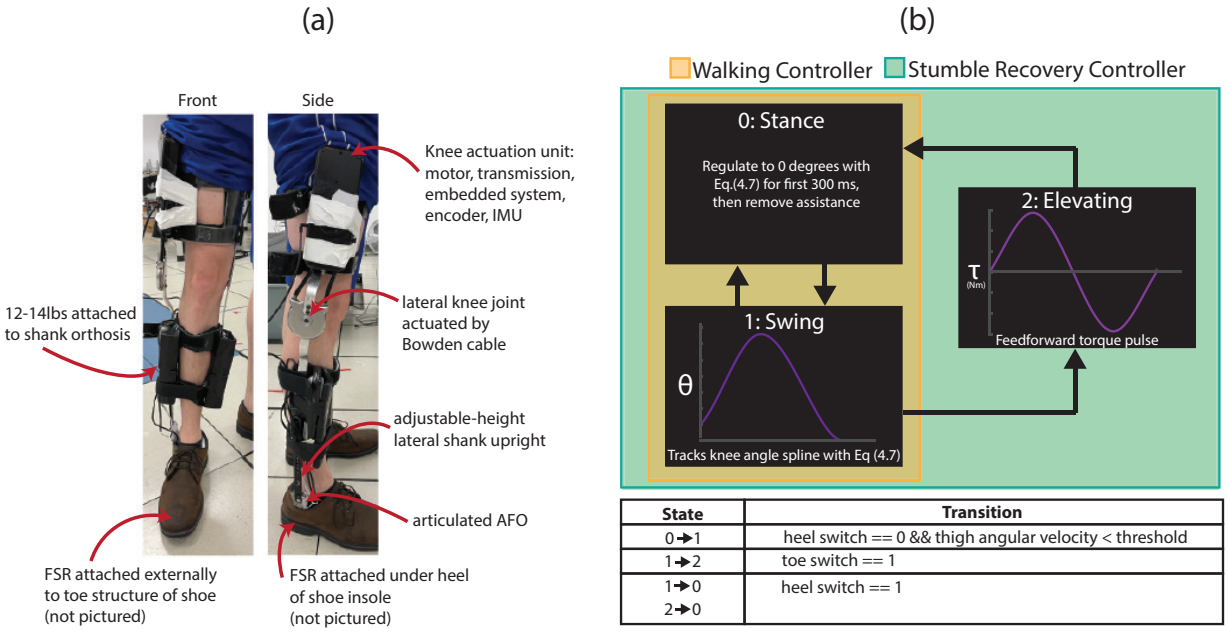

State	Transition
0→1	heel switch == 0 && thigh angular velocity < threshold
1→2	toe switch == 1
1→0 2→0	heel switch == 1

Figure 4.12: Interventional device and controllers

bations were targeted to occur in early swing phase (20-40% swing) such that elevating strategies would be employed to recover. Handrails were removed from the treadmill so they could not be used to recover, but participants wore a full-body harness to prevent contacting the treadmill in the event of a fall.

The stumble perturbations were introduced for four experimental cases: (1) without wearing the exoskeleton (Control); (2) wearing the weighted-shank exoskeleton without the controllers enabled (Baseline); (3) wearing the weighted-shank exoskeleton with the walking controller enabled (Walk Only); and (4) wearing the weighted-shank exoskeleton with the stumble recovery controller enabled (Stumble Recovery). The Control case was intended to capture how an unimpaired, young, healthy adult responds to early-swing perturbations, which served as the healthy control response. The Baseline case was intended to capture the response of the participant impaired by the weighted-shank exoskeleton without device assistance, which served as the baseline response of the impaired individual. The Walk Only case was intended to capture how an impaired individual responded if they were wearing an exoskeleton that assisted walking but did not have a stumble recovery feature. Finally, the Stumble Recovery case was intended to capture how an impaired individual responded if they were wearing an exoskeleton that assisted walking and also provided stumble recovery assistance when detected. The Control trials were conducted first. The order of exoskeleton trials (Baseline, Walk Only, Stumble Recovery), as well as trials in which the left limb (i.e., limb not wearing exoskeleton) was stumbled, were randomized. The participant was not informed of the case of each trial. Each participant was introduced to 3-6 trials for each case.

Additionally, before and after the stumble perturbation trial sets, 60-second walking trials (without perturbation) were conducted for the Control, Baseline, and Walk Only cases.

Data Collection & Processing

For each trial, ground reaction forces (GRFs) were collected at 1000Hz via a lateral, split-belt, force-instrumented treadmill (Bertec, Columbus, USA). Full-body kinematic data were collected at 200Hz via infrared motion capture, which included feet, shank, thigh, pelvis, trunk, forearm, and upper arm segments. GRF and motion capture data were filtered with a zero-phase, 3rd order, low-pass Butterworth filter with cut-off frequencies of 15 and 6 Hz, respectively. Inverse kinematics were computed using Visual3D (C-Motion, Germantown, USA) to estimate joint-level kinematics for each trial.

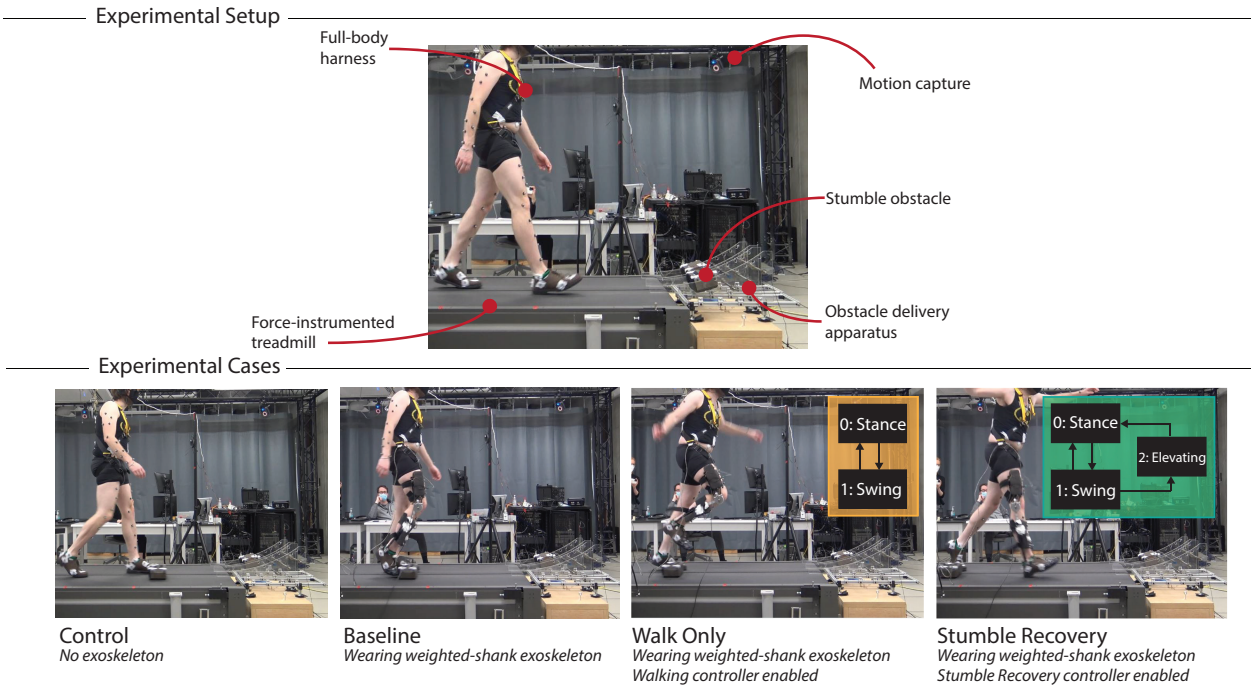

Figure 4.13: Experimental Setup & Protocol

Data Analysis

Trials were excluded from analysis based on a few criteria. First, if the participant stepped on the obstacle or over the obstacle (i.e., missed targeting), the trial was not deemed a swing-phase perturbation and was excluded. Second, if the participants' foot hit the obstacle substantially medially, this caused the block to rotate which is an outlier relative to remaining stumbles (i.e., perturbation impulse is altered, and in some cases block rotated enough such that it did not need to be cleared); thus, if the block rotated more than 45 degrees about the vertical axis after contacting the participants' foot, the trial was excluded from the analysis.

For each trial, the perturbation event was identified as the instant at which the foot contacted the obstacle, which was determined via a transient peak in the anterior-posterior GRF measured by the treadmill. The swing percentage of each perturbation was estimated as the time from the toe-off immediately preceding the perturbation to the instant of perturbation, relative to the average of 20 swing times prior to the perturbation.

To address the first question posed in this paper (to what extent does adding weight to the leg approximate a gait impairment, and to what extent can the exoskeleton address that impairment), overall temporal symmetry was computed using gait information from the average of 20 strides during the walking trials for each case. Overall temporal symmetry is defined here as the ratio of the right limb's temporal swing-stance symmetry to the left limb's temporal swing-stance symmetry [78]. Temporal swing-stance symmetry is defined as the ratio of swing time to stance time for a given limb, where swing time is the time from toe-off to foot-strike, and stance time is the time from foot-strike to toe-off. In a study examining the gait asymmetry of community-ambulating stroke survivors, the normative range for overall temporal symmetry was defined as 0.9 to 1.1, mild asymmetry was defined to be 1.1 to 1.5, and severe asymmetry defined as greater than 1.5 (with a value over 1.0 indicating a preference to rely on the non-paretic limb) [78]. Note that gait asymmetry has been identified as a factor for predicting falls for stroke patients [123]. These ranges were used to determine if the participants were adequate candidates for the impairment and improvement techniques chosen for this study. Specifically, if the Baseline case induced an asymmetry in the mild range, and the asymmetry was restored to the normative range with Walk Only case, then the participant was considered to be (1) substantially

impaired with the weighted-shank exoskeleton, and (2) responsive to controller assistance and thus considered for stumble trials. This was the case for three participants (one female, two males; mean height; 1.77 m, mean mass: 77.9 kg; mean age: 26 years). Additionally, the average knee angle and angular velocity from 20 strides for each walking trial were computed to compare the knee range of motion and velocity range of each experimental case.

To address the second and third questions (to what extent does weight impair a stumble response, and to what extent can an exoskeleton stumble controller mitigate that impairment), various outcome metrics were computed to assess the extent to which the weighted-shank exoskeleton and stumble recovery controller respectively impaired and improved the stumble recovery response. Both local (elevating limb kinematics) and global (overall fall risk) metrics were considered. These outcome metrics are diagrammed in Fig. 4.14 along with representative trajectories. To evaluate local impairment/improvement, the range in knee angle, knee angular velocity, thigh angle, and thigh angular velocity from the instant of perturbation to the first foot-strike of the recovery limb was computed for each trial. To evaluate global impairment/improvement, trunk angle and trunk angular velocity at recovery foot-strike were computed (calculated relative to the value at perturbation). Additionally, the elapsed time from perturbation to the instant at which trunk angular velocity reversed direction from forward rotation to backward rotation (i.e., how soon induced forward angular momentum was arrested) was computed. These trunk metrics reflect the participants' ability to restore trunk motion during the recovery. Finally, the recovery foot anterior-posterior center-of-mass (COM) position relative to the pelvis anterior-posterior COM position at recovery foot-strike (calculated relative to the value at perturbation) was computed for each trial. Trunk angle, trunk angular velocity, and foot positioning at recovery foot-strike have previously been reported to discriminate falls from recoveries [81, 74, 35, 77] and many works cite trunk control and stepping response as keys to successful recovery [38, 85, 101, 24, 30]; thus changes in these metrics can be used as indicators of fall risk or improved recovery.

To examine the extent of stumble response impairment, the local and global outcome metrics from Baseline trials were compared to Control trials. Since stumble recovery responses vary depending on when in swing phase the perturbation occurs [24, 101, 107, 27], it was important to compare outcome metrics from like perturbations (i.e., occurring at the same swing percentage, or as close as possible). Thus, trials that were closest in swing percentage were paired using the following procedure: each successful Baseline trial was paired with a Control trial that was closest in swing percentage. If there were no Control trial within 3% swing of said Baseline trial, then that Baseline trial was not used in analysis. Conversely, if there were more than one Control trial within 1% swing of said Baseline trial, then both (or more) Control trials were paired with the Baseline trial to comprise two (or more) comparison pairs. For each comparison pair, the difference in each outcome metric (Baseline relative to Control) was computed.

To examine the extent of stumble recovery improvement, the identical comparison pair approach was used for (i) Stumble Recovery relative to Baseline and (ii) Stumble Recovery relative to Walk Only.

4.3.4 Results

The weighted-shank exoskeleton substantially impaired walking gait, and this impairment was restored or considerably improved with the walking controller for the three participants. The overall temporal symmetry, as well as the phase plane of knee angle versus knee angular velocity for each participant for each case (Control, Baseline, and Walk Only) are shown in Fig. 4.15.

After removing trials due to (1) the participant stepping on the obstacle, (2) the obstacle rotating greater than 45 degrees about the vertical axis, or (3) the trial timing being deemed unsuitable for comparison to other trials (i.e., no other trials within 3% swing), 31 trials were available for analysis. Figures 4.16, 4.17, and 4.18 plot the difference in local and global outcome metrics for Baseline relative to Control comparison pairs (i.e., assessing impairment), Stumble Recovery relative to Baseline comparison pairs (i.e., assessing improvement), and Stumble Recovery relative to Walk Only comparison pairs (i.e., assessing improvement). Impairments were determined by less knee angle/angular velocity range, less thigh angle/angular velocity range, less anterior foot position relative to pelvis (i.e., negative difference) and more trunk angle, more trunk angular velocity, and longer time to trunk angular velocity reversal (i.e., positive difference), which are indicated by red shading in Figs. 4.16, 4.17, and 4.18. Green shading indicates improvement (positive difference for knee, thigh and foot position metrics, and negative difference for trunk metrics).

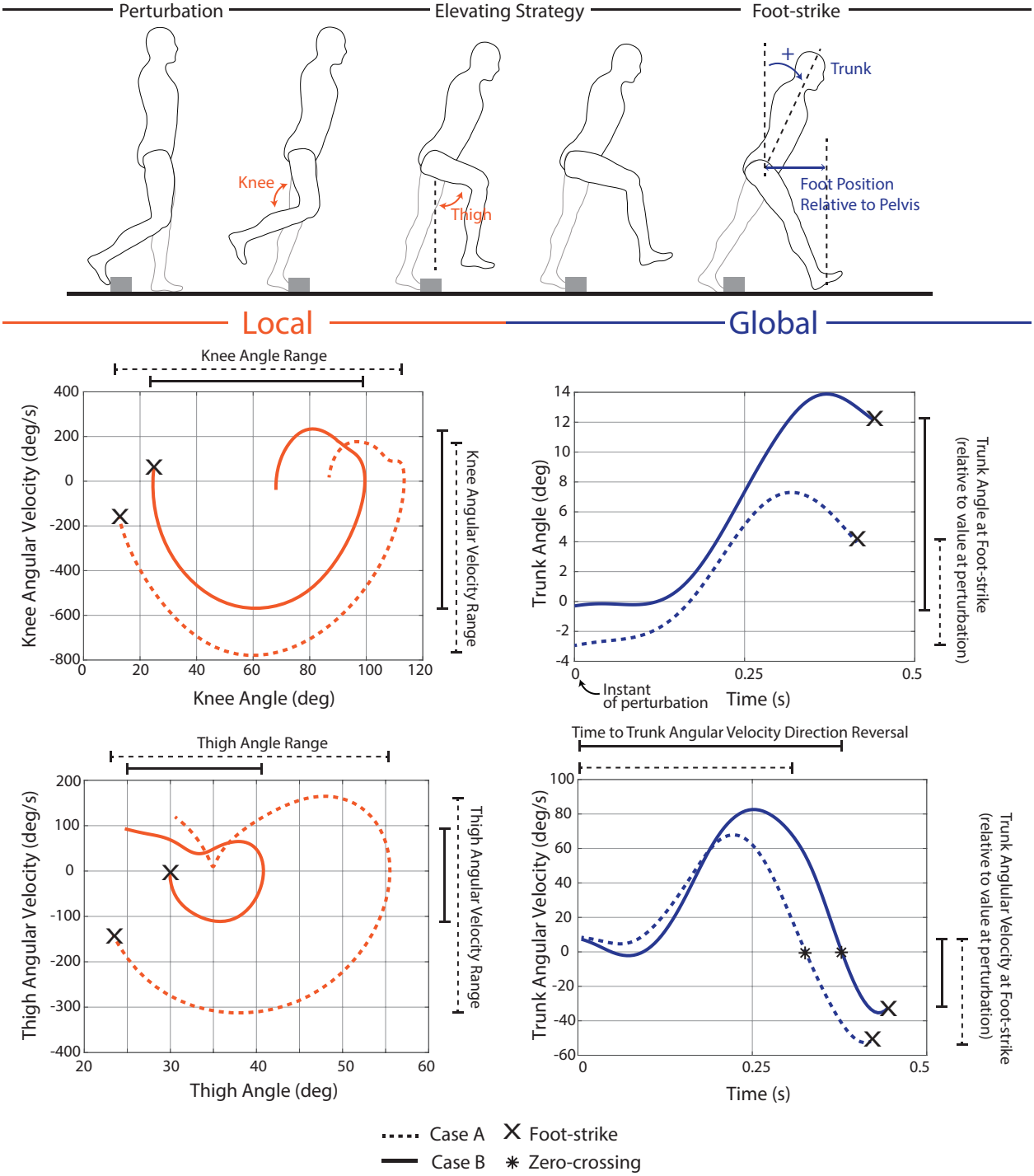

Figure 4.14: Outcome metrics to assess local and global impairment/improvement. Data from a representative comparison pair (Case A and Case B) are plotted. The difference in each metric (Case A relative to Case B) was computed for each trial compared for analysis.

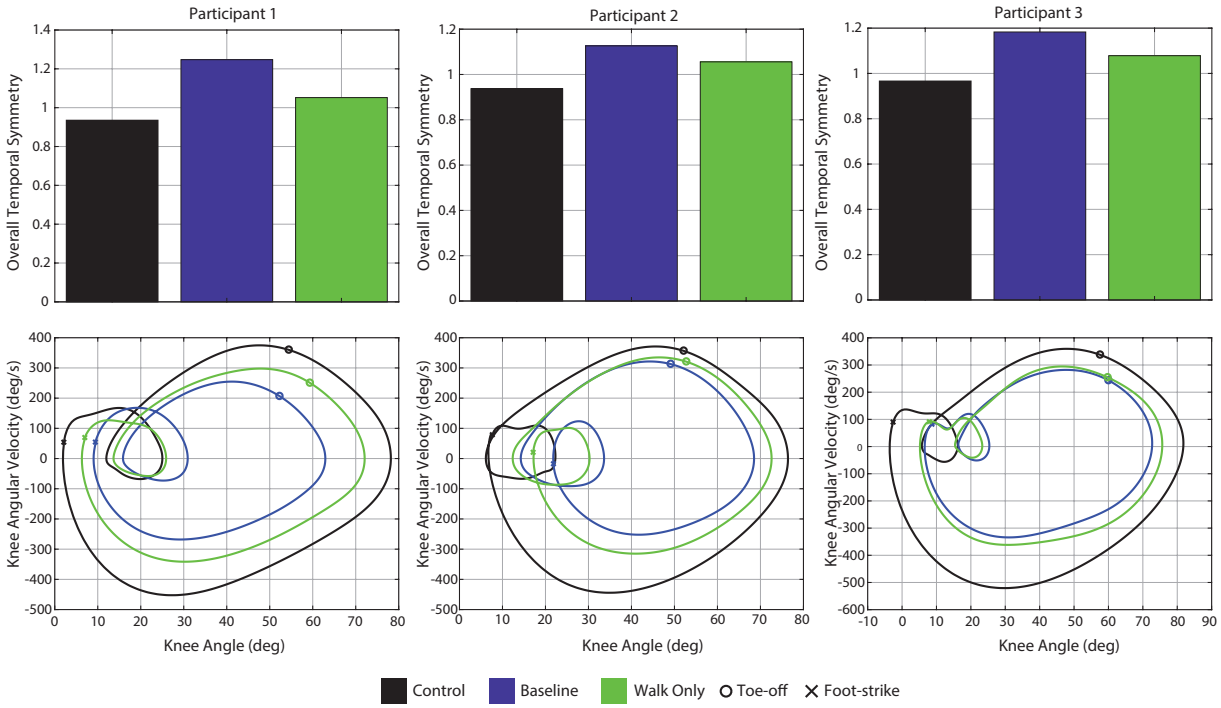

Figure 4.15: Overall temporal symmetry and knee motion for walking trials

4.3.5 Discussion

4.3.5.1 Approximation of walking impairment: Weights attached to shank impair gait, exoskeleton walking controller improves it

Weights attached to the shank segment of the exoskeleton substantially impaired the three participants' walking gait in terms of temporal asymmetry and knee motion. The weights increased participants' right-side swing time and thus increased their right-side swing-stance ratio, as participants took longer to move their right limb due to its added mass. As shown in Fig. 4.15 (top), this resulted in increased overall asymmetry values for the Baseline case (all in mild asymmetry range) compared to their Control trials (all in normative asymmetry range). Furthermore, these Baseline overall temporal asymmetry values reached levels akin to the mild asymmetry experienced by stroke survivors, and thus may approximate gait abnormalities exhibited by those at higher fall risk [78, 123]. Additionally, the added weight to the participants' shank segment hindered their ability to flex and extend their knee joint, as evidenced by a decrease in knee motion (angle and angular velocity) for the Baseline case relative to Control (Fig. 4.15, bottom).

The exoskeleton walking controller improved walking gait (symmetry and knee motion) for the three participants. The trajectory-tracking controller provided the assistance to complete a faster (more symmetrical) swing time. Specifically, flexion assistance at toe-off helped initiate swing phase and reach more normative knee flexion during swing, while the extension assistance helped to complete swing phase in a timely manner. While overall temporal asymmetry was not fully restored to Control values, it was reduced for each participant below the mild asymmetry threshold of 1.1 to the normative range (Fig. 4.15, top). Similarly, knee range metrics for the Walk Only case increased relative to Baseline, though not to Control values (Fig. 4.15, bottom). A knee exoskeleton with greater control authority may have served to fully restore symmetry and knee motion (i.e., the device used here was torque-limited, particularly relative to the increased leg inertia associated with the added leg weights).

These outcomes were important validations that weights attached to the shank segment of an exoskeleton could reasonably approximate impaired gait, and that an exoskeleton knee controller could improve it, which were important

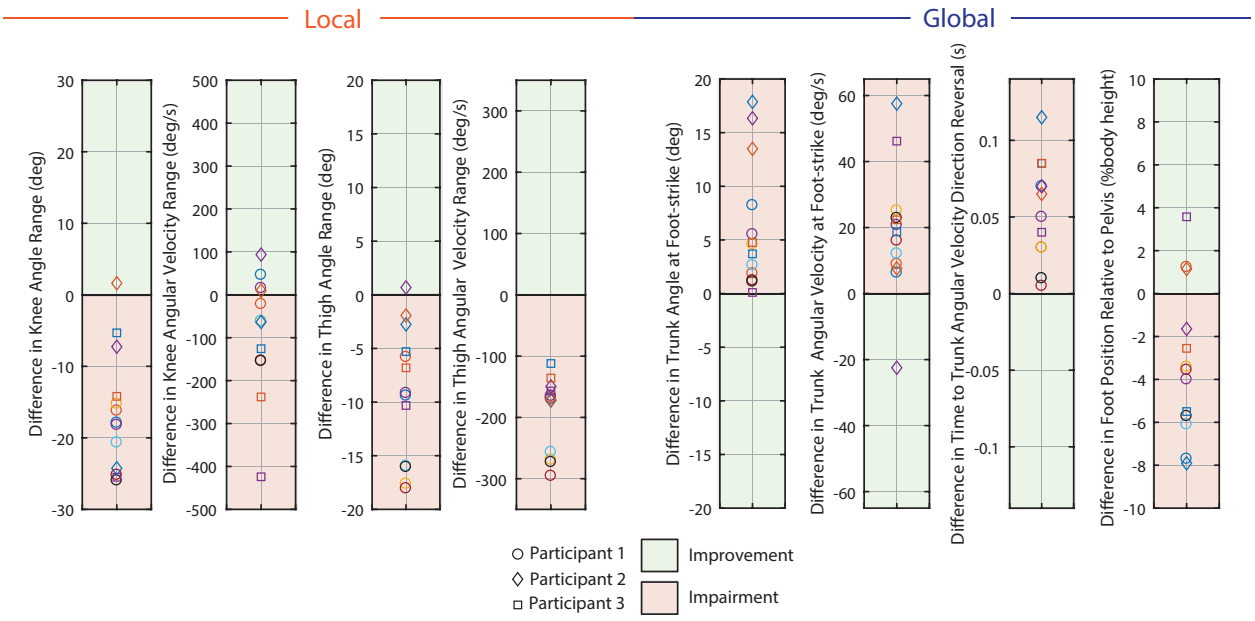

Figure 4.16: Baseline relative to Control. Overall, leg weights attached to the shank impaired elevating limb response (local) and increased fall risk (global) relative to responses when not wearing the leg weights.

preliminary validations for the stumble assessment. However, these walking outcomes do not assess the extent to which weights might impair a stumble response, or the extent to which an exoskeleton might improve it.

4.3.5.2 Assessment of stumble recovery impairment: Weights attached to shank impair elevating limb response and increase fall risk

Overall the recovery limb was substantially impaired when elevating over the obstacle due to the added weight at the shank. This was evidenced by comparing the elevating kinematics of the participants' right limb when wearing the weighted exoskeleton (Baseline) to their kinematics when not wearing an exoskeleton (Control). Twelve of thirteen comparison pairs (see Methods) exhibited a decrease in knee and thigh range of motion during the elevating response for the Baseline case relative to Control. Nine pairs exhibited a decrease in knee velocity range, and all pairs showed a decrease in thigh velocity range (Fig. 4.16).

However, an intervention that impairs locally (where the intervention was applied) does not necessarily imply that the individuals' overall response was impaired. Thus, it was important to also consider global response outcome metrics. As shown in Fig. 4.16, the participants landed their elevating step with more trunk flexion (all pairs) and more trunk flexion velocity (12/13 pairs) in the Baseline case relative to their Control trials. In previous laboratory-induced tripping studies, increases in these two metrics have repeatedly been reported as discriminators between those who fall and those who recover [81, 35, 77]. Furthermore, for all pairs the participants reversed their trunk velocity direction (from forward rotation to backward rotation) later (i.e., longer elapsed time after perturbation) for the Baseline case relative to the Control case. This indicates a delayed ability to control trunk motion and arrest forward momentum, also suggesting a higher risk of falling. Finally, for most trials (10/13) the participants landed with their foot less anterior to their pelvis compared to the Control case (i.e., shorter step). Previous studies report step positioning as a key factor in a successful recovery [35, 77, 74, 18, 44] (i.e., larger step is better).

Therefore, the change in local outcome metrics indicate a deficient elevating limb response, and the change in global outcome metrics indicate that this local impairment extended to an overall increase in fall risk. These results were

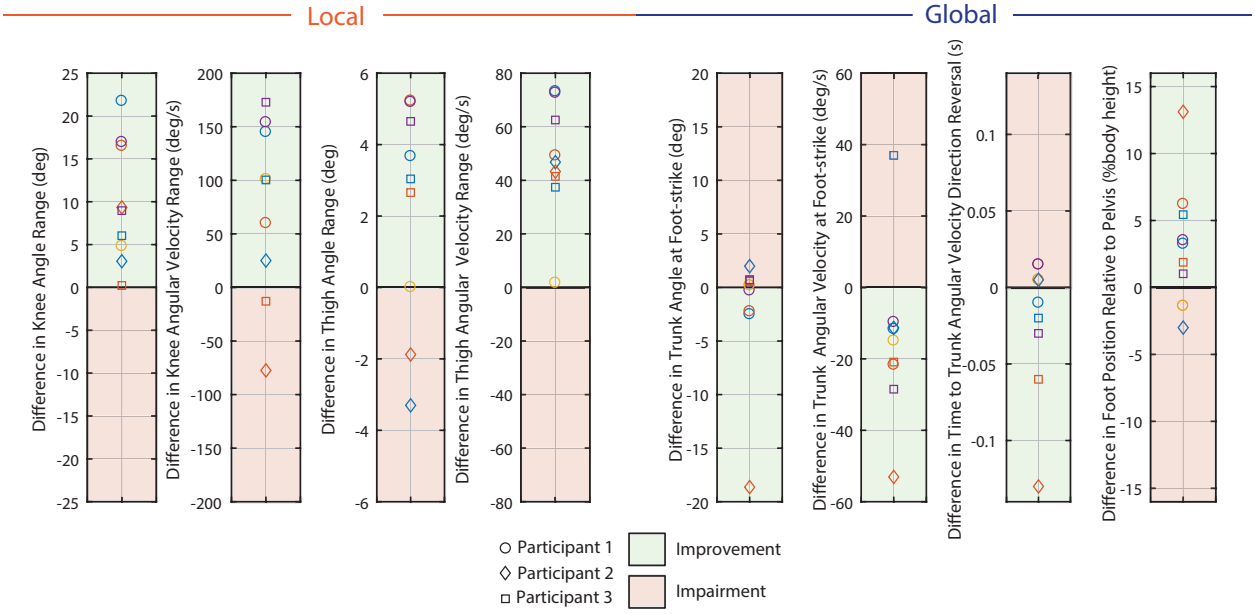

Figure 4.17: Stumble Recovery relative to Baseline. Overall, the stumble recovery assistance improved elevating limb response (local) and reduced fall risk (global) relative to responses when impaired with leg weights without assistance.

important for ultimately addressing the main objective – Can a knee exoskeleton stumble recovery controller improve an impaired stumble recovery response? Additionally, these results further bolster the hypotheses from prior studies that the recovery limb plays a crucial role in recovery [85, 38, 29].

4.3.5.3 Assessment of stumble recovery improvement: Exoskeleton stumble recovery controller improves elevating limb response and reduces fall risk

Ultimately, the objective of this work was to determine the extent to which a powered knee exoskeleton stumble recovery controller could improve an impaired stumble recovery response. This question was assessed by comparing the participants' response to perturbations with the stumble recovery controller enabled (Stumble Recovery) to their Baseline (i.e., impaired) response. For all nine comparison pairs, the participants' knee range of motion during the elevating response increased when the stumble recovery controller was enabled, and knee velocity range increased for seven of those pairs (Fig. 4.17). Thus the knee flexion/extension torque served to successfully assist the knee, providing a response more akin to their Control trials. Furthermore, thigh range of motion and thigh velocity range also increased for seven and nine pairs, respectively. Thus this assistance at the knee not only improved knee motion, but also facilitated a better thigh response, both of which are key components of the elevating step [38, 28].

While previous works have suggested improving the elevating step as a promising target for intervention, it was important to confirm that improvement at the local level (at the site of intervention) also extended to global improvement (i.e., decreased fall risk). As shown in Fig. 4.17, for most comparison pairs the participants landed the elevating step with decreased trunk velocity (8/9 pairs) and a more anterior foot position relative to their pelvis (7/9 pairs), both of which indicate a decrease in fall risk (as discussed previously). Additionally, participants reversed their trunk velocity direction sooner relative to the Baseline case for 5/9 trials, which indicates that they were able to arrest the perturbation's induced forward angular momentum (i.e., control trunk motion) more effectively with the Stumble Recovery Controller. The majority of cases did not see an improvement (decrease) in trunk flexion (4/9); however, note that trunk flexion did not increase more than 3 degrees, so the Stumble Recovery Controller did not substantially increase this fall risk metric.

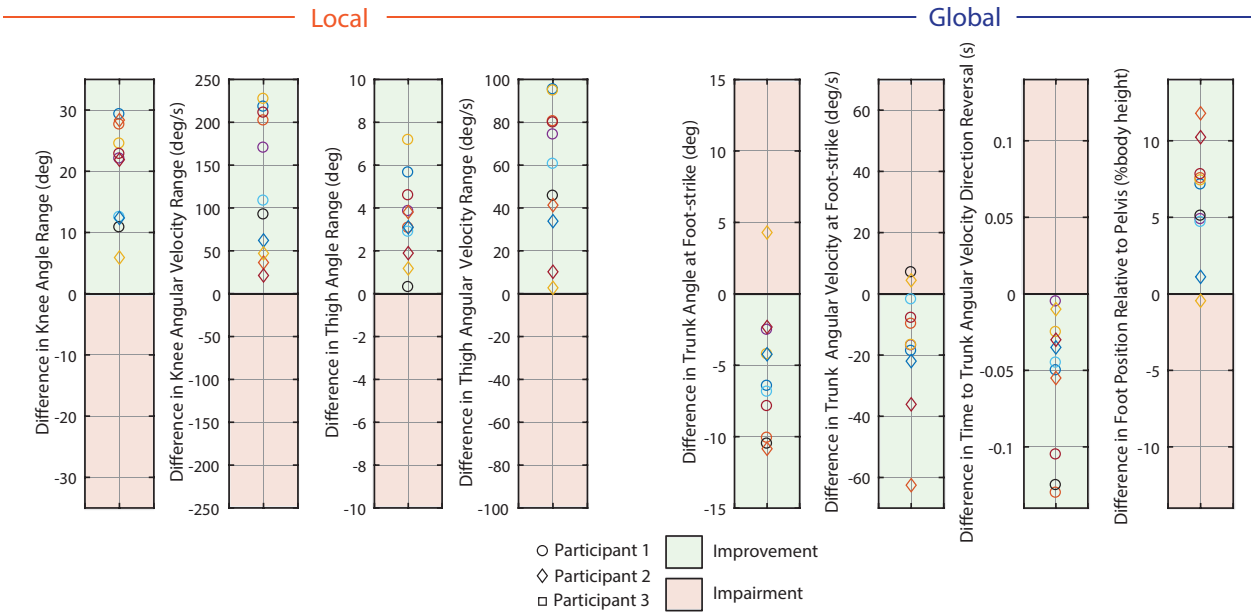

Figure 4.18: Stumble Recovery relative to Walk Only. Overall, the stumble recovery assistance improved elevating limb response (local) and reduced fall risk (global) relative to responses when impaired with leg weights with only walking assistance.

The Stumble Recovery responses were also compared to the Walk Only cases. This shows the difference in responses while wearing a rehabilitation exoskeleton (i.e., one that provides walking assistance) with versus without a stumble recovery feature. As shown in Fig. 4.18, for all 11 comparison pairs the responses with the Stumble Recovery controller exhibited increased knee and thigh angle and velocity ranges relative to the Walk Only cases. Recall that for the walking controller (Walk Only), a knee angle spline was tracked with a closed-loop PD controller in swing phase; thus, when a perturbation happened in swing (and was not detected by the controller), the participant attempted a knee trajectory different from the planned trajectory. Moreover, the controller was trying to drive the knee to its planned swing trajectory while the participant wanted an elevating response trajectory, which is longer and involves substantially more knee flexion. Specifically, when the participant attempted to flex additionally after contacting the obstacle, the knee controller was commanding extension in the knee to complete swing phase. This mismatch in user intent and controller planning restricted the participant's elevating limb kinematics, which ultimately increased the users' fall risk. For most cases, the Stumble Recovery Controller outperformed the Walk Only controller in terms of fall risk, exhibiting less trunk flexion (10/11 pairs) and trunk flexion velocity (9/11) at foot-strike, a quicker reversal of trunk velocity direction (11/11), and a more anterior foot placement relative to the pelvis (10/11).

Therefore, the proposed knee exoskeleton stumble recovery controller successfully improved participants' lower-limb response kinematics and consequently improved fall risk metrics relative to their Baseline responses and Walk Only responses.

This is the first study to show that exoskeleton assistance at the knee could improve an impaired stumble recovery response. This validation with healthy individuals now invites the testing of this approach with fall-prone populations, such as the elderly, stroke survivors, post-polio patients, or multiple-sclerosis patients, who may benefit from exoskeleton knee assistance. Such populations exhibit some of the impairments provided by the weighted shank technique used here (i.e., gait asymmetry, decreased knee/thigh range of motion, decreased muscle response or delayed response time), and thus they may be good candidates for the proposed exoskeleton knee assistance. The authors note, however, that the impairment tested in this work is a coarse approximation of a neuromuscular deficit, and fails to capture many aspects of various gait impairments (e.g., neurological impairment); furthermore, the healthy participants

tested in this work have access to various response mechanisms that may not be available for some fall-prone populations. Therefore, future work is needed to test the extent to which this stumble recovery improvement approach may extend to fall-prone populations. The authors also note that lower-limb exoskeletons are emerging not only as rehabilitation devices for individuals with walking impairment, but also as augmentation devices for healthy individuals (e.g., [128]). Although tripping over obstacles is certainly an eventuality, such devices do not currently account for stumble perturbations. Without an incorporated stumble response, existing mechanical or control features of an exoskeleton (e.g., added weight, joint impedance, or restrictive controller) might limit the ability of the exoskeleton user to react adequately to an unexpected stumble. Since this work has shown the efficacy of knee assistance for stumble recovery for healthy individuals, and the impairment technique used in this work could also approximate the effect of a heavier exoskeleton, implementing this or a similar intervention into existing exoskeletons may reduce an individual's fall risk while wearing a lower limb exoskeleton.

4.3.6 Limitations

There are several limitations to this work. First, in this study the improvement intervention was limited by the specifications of the knee exoskeleton device available. The maximum knee torque for given recovery speeds was applied to the participants; however, a device with higher torque and speed capacity would likely have improved responses. Second, in this work only one type of assistance was explored (i.e., a feedforward torque flexion-extension pulse). Results proved that assistance at the knee helps; however, future works could explore different types and levels of assistance to optimize response outcomes, such as assistance magnitude, timing, and control strategy. Third, this work compared the Stumble Recovery case to both the Baseline and Walk Only cases to show Stumble Recovery improvement; however, note that the Walk Only case results are specific to the type of walking controller used, and as such other walking controllers may have yielded different results. Similarly, there are other behaviors that could be implemented after perturbation that were not tested in this work, and warrant further investigation. Fourth, only stumble recovery responses using the elevating strategy were tested in this work. Efficacy for assistance during the lowering strategy (the other primary stumble recovery strategy) warrants exploration; however, the lowering strategy also involves quick knee flexion and extension of the recovery limb, and so a similar approach could be feasible. Finally, more trials from more participants would further support these results; however, considering the taxing nature of this protocol, and that the same trends were seen across all three participants, the authors contend that these results provide the initial validation needed to confirm the promise of this intervention method and motivate the development of this approach for the applications discussed previously.

4.3.7 Conclusion

A knee exoskeleton stumble recovery controller successfully improved participants' elevating stumble recovery response at both the local level (i.e., improved recovery limb kinematics) and global level (i.e., decreased fall risk) in an obstacle perturbation experiment in which healthy participants were impaired (locally and globally) with weights attached to the shank. Ultimately, this initial exploration indicates that providing similar assistance to individuals with walking impairment might improve recovery responses and reduce the likelihood of falling, although that assertion must of course be substantiated with future work. Nonetheless, this preliminary work provides a crucial first step in investigating the potential efficacy of wearable lower-limb devices in stumble recovery roles, and substantiates the potential promise of such stumble recovery assistance in eventually enhancing the safety and adoption of lower-limb exoskeletons and mitigating falls in fall-prone populations.

CHAPTER 5

Factors leading to falls in transfemoral prosthesis users: A case series of sound-side stumble recovery responses

5.1 Chapter Summary

Transfemoral prosthesis users' high fall rate is related to increased injury risk, medical costs, and fear of falling. Better understanding how stumble conditions (e.g., participant age, prosthesis type, side tripped, and swing phase of perturbation) affect transfemoral prosthesis users could provide insight into response deficiencies and inform fall prevention interventions. Six unilateral transfemoral prosthesis users experienced obstacle perturbations to their sound limb in early, mid, and late swing phase. Fall outcome, recovery strategy, and kinematics of each response were recorded to characterize (1) recoveries versus falls for transfemoral prosthesis users and (2) prosthesis user recoveries versus healthy adult recoveries. Out of 25 stumbles, 13 resulted in falls with five of six transfemoral prosthesis users falling at least once. By contrast, in a previously published study of seven healthy adults comprising 214 stumbles using the same experimental apparatus, no participants fell. The two oldest prosthesis users fell after every stumble, stumbles in mid swing resulted in the most falls, and prosthesis type was not related to strategy/fall outcomes. Prosthesis users who recovered used the elevating strategy in early swing, lowering strategy in late swing, and elevating or lowering with hopping in mid swing, but exhibited increased contralateral (prosthetic-side) thigh abduction and trunk flexion relative to healthy controls. Falls occurred if the tripped (sound) limb did not reach ample thigh/knee flexion to sufficiently clear the obstacle in the elevating step, or if the prosthetic limb did not facilitate a successful step response after the initial sound-side elevating or lowering step. Such responses generally led to smaller step lengths, less anterior foot positioning, and more forward trunk flexion/flexion velocity in the resulting foot-strikes. Introducing training (e.g., muscle strength or task-specific motor skill) and/or modifying assistive devices (e.g., lower-limb prostheses or exoskeletons) may improve responses for transfemoral prosthesis users. Specifically, training or exoskeleton assistance could help facilitate sufficient thigh/knee flexion for elevating; training or prosthesis assistance could provide support-limb counteracting torques to aid in elevating; and training or prosthesis assistance could help initiate and safely complete prosthetic swing.

5.2 Introduction

The transfemoral prosthesis user population experiences a substantially high fall rate and accompanying risk of injury, medical costs, and psychosocial effects. In a study of 17 transfemoral prosthesis users who reported falls after a 4-week period, an average of 1.25 falls (averaging microprocessor and non-microprocessor knee results) were reported per person [41]. In a similar study examining 19 participants over a 60-day period, an average of 2 falls were reported per person [46]. Interestingly,a recent study reports the healthy adult population's fall rate to be just 0.37 falls per person per year, though the authors note this work involved a different study design and population size [120]. Furthermore, more than 60% of transfemoral prosthesis users reported falling at least once in the past year [65, 14, 68].

With higher fall risk comes increased injury incidence and medical costs. In studies of fall-related injury of lower-limb prosthesis users (transfemoral and transtibial), approximately half of the prosthesis users who fell reported an injury that required medical care [65, 14]. Mundel et al. 2017 [68] reported that the six-month costs of falls resulting in hospitalization for transfemoral prosthesis users are similar to those reported in the elderly population.

Aside from physical and financial consequences, lower-limb prosthesis users experience psychosocial effects of this increased fall prevalence. Forty-seven percent of transfemoral prosthesis users reported a fear of falling [65], and 60% of lower-limb prosthesis users reported that falls affected their daily lives with respect to work, leisure, and confidence [53]. In a focus-group study of lower-limb prosthesis users, participants reported that falls trigger emotions of embarrassment, loss of confidence, fear, and depression, and that they limit participation in certain activities due to risk of falling [49].

In order to develop interventions (e.g., prostheses, training) to decrease fall likelihood, and thus alleviate the physical, monetary, and psychosocial burdens resulting from such falls, it is important to understand both the mechanisms that help prevent falls in healthy populations as well as the deficiencies in recoveries of transfemoral prosthesis users. While responses to trips/stumbles (i.e., obstacle perturbations to the foot in swing phase) in healthy adults have been well characterized, a comparable extent of research for the transfemoral prosthesis user population is lacking.

Three primary responses have been identified and characterized as recovery strategies to swing-phase perturbations (i.e., stumbles or trips) for healthy adults: the elevating, lowering, and delayed lowering strategies [101, 24]. Research has highlighted the kinematics of the tripped limb for each recovery strategy [24, 102, 38, 107, 50], the reflexes involved in each recovery strategy [101, 24, 103, 100, 96, 119], the role of the support (contralateral) limb during elevating strategies [87, 86, 88], and the role of arm movements in successfully recovering from stumbles [97, 89].

For healthy adults, such responses have been found to differ as a function of various factors, including (i) swing phase at which the perturbation occurs and (ii) age of the participants. Regarding (i), recovery strategy selected depends on the dynamic state of the human body at the perturbation [27], factors that vary depending on when in swing phase the perturbation occurs. Regarding (ii), older adults fall more often, which has been attributed to delayed and decreased muscle activation in the response [90, 87, 100, 82].

While these factors of (i) swing phase and (ii) age likely also affect transfemoral prosthesis users' stumble recovery responses, they may be additionally influenced by factors that are unique to their population, including: (iii) knee prosthesis type, and (iv) side tripped (i.e., sound limb versus prosthetic limb). Regarding (iii), typically prescribed prosthetic knees have various joint designs and control schemes, aspects that affect their behavior after perturbations that are not under the participant's direct control. A recent study highlighted different rates of falls for wearers of different prosthetic knee models [12]. Regarding (iv), it has been shown that both the tripped (ipsilateral) limb and contralateral limb play crucial roles in recovery (one as recovery limb and the other as support limb, depending on strategy) for healthy adults [86, 87, 88]; thus, depending on whether the tripped limb is the sound or the prosthetic limb, responses may differ for transfemoral prosthesis users (unlike healthy populations with two identical biological limbs).

Relatively little research has been published examining how factors (i)-(iv) affect stumble responses for transfemoral prosthesis users. In a retrospective study of lower-limb prosthesis users, walking was the most commonly reported activity at the time of a fall. Fifty-four percent of falls were attributed to a disruption of the prosthesis user's base of support (as opposed to a disruption to their center of mass), and 22% were due to tripping specifically [48]. However, further details of how prosthesis users fell, such as which foot was disrupted (i.e., sound versus prosthetic side), and what strategy was attempted following the perturbation, have not been documented in retrospective studies. Thus, while retrospective studies provide important information regarding fall prevalence and effects of falling, it is also crucial to study the real-time nature of stumbles in order to better understand the factors that contribute to falling and hopefully provide insight for mitigation or prevention.

To date, two studies have introduced stumble perturbations to both limbs of transfemoral prosthesis users and report varying results related to factors (i)-(iv) [16, 107]. Both studies reported prosthesis user-specific recovery strategies of hopping or skipping after the lowering response. In addition, Crenshaw et al. [17] reported that two out of three sound-side stumbles resulted in a fall (compared to one out of four prosthetic-side stumbles), substantiating the need to study stumbles to the sound limb. They specifically called on future studies to clarify the relationship between stumble features and recovery success. Shirota et al. [107] did not report any falls. Participants in this study were allowed to use handrails, and the rope-blocking perturbation setup did not entail a physical obstacle to clear after stumbling, both factors that may have affected the recovery outcome. However, their results did substantiate Pijnappel et al.'s work that the role of the support limb is critical to recovery [86, 87, 88], further motivating a more comprehensive investigation of sound-side stumble recovery, in which the prosthetic limb is the support limb for elevating strategies.

In order to build upon these prior investigations, and specifically to better understand how different stumble conditions (i.e., participant age, swing phase of perturbation, prosthesis type, and side tripped) affect responses, six transfemoral prosthesis users were recruited to undergo a series of stumble perturbations to both their sound and prosthetic limbs occurring in early, mid, and late swing phase. These experiments elicited substantially different responses depending on which limb was tripped (i.e., sound versus prosthetic), which warranted separate analyses and intervention sugges-

tions. This paper presents the results from tripping the sound limb. Due to limitations in paper length, the results from tripping the prosthetic limb will be presented in a subsequent paper.

Therefore the objective of this work is to examine the responses of transfemoral prosthesis users to sound-side stumble perturbations in order to gain insight into what contributes to falls or facilitates recovery for this population. The primary aim is to characterize their responses by reporting fall outcomes, recovery strategies, and relevant kinematics; the secondary aim is to further analyze these responses to investigate what differentiates recoveries versus falls for transfemoral prosthesis users, as well as what differentiates prosthesis user recoveries from healthy adult recoveries. The intent of this analysis is to provide insights into the deficiencies of transfemoral prosthesis user stumble recovery to better inform fall prevention interventions.

5.3 Methods

5.3.1 Experimental Protocol

Six unilateral transfemoral prosthesis users were recruited for the stumble recovery experiment. Participant details are tabulated in Table 5.1. All participants wore their prescribed passive prostheses. The prosthetic knee models are noted in Table 5.1, and the ankles were all energy storage-and-return type prostheses.

Table 5.1: Participant information

Participant	Age	Sex	Prosthetic Side	Etiology	Years of Prosthesis Use	Prescribed Prosthesis
HC	25	Male	N/A	N/A	N/A	N/A
P1	62	Male	Right	Trauma	49	Ottobock C-Leg
P2	42	Male	Left	Trauma	14	Ottobock 3R80
P3	28	Female	Right	Congenital	27	Ottobock C-Leg
P4	32	Male	Left	Trauma	4	Blatchford KX06
P5	50	Male	Left	Infection	5	Ottobock C-Leg
P6	30	Male	Left	Trauma	12	Ottobock C-Leg

Participants walked on a treadmill at 0.8 m/s and were introduced to a series of obstacle perturbations, targeted to occur in early, mid, and late swing phase ($<$40%, 40-60%, $>$60% swing, respectively) for each limb (i.e., prosthetic-side and sound-side). Specifically, a 35-lb steel block (obstacle) was positioned on a ramp apparatus in front of the treadmill and held in place by an electromagnet; when cued from an onboard targeting algorithm, the electromagnet switches off, releasing the obstacle down the ramp and onto the treadmill belt such that it contacts the participant's foot at the experimenter-defined percentage of swing phase.

The number of steps prior to perturbation, limb stumbled, and swing phase targeted were randomized for each participant. Randomization of trials, apparatus design and targeting algorithm, sensory occlusion techniques, and a distraction task were used to ensure the obstacle was unperceived by the participants prior to perturbation and to limit expectation of the stumble. The stumble perturbation system and experimental protocol employed are described in detail and validated experimentally in [50]. Fig. 5.1 depicts the experimental setup with video frames from representative early, mid, and late swing phase stumbles.

The goal was to capture the response to one early, one mid, and one late swing stumble for each limb for each participant. Recall that for this work sound-side stumble responses are presented, while prosthetic-side stumble responses will be reported separately. Depending on the participant's comfort level, and due to the taxing nature of the protocol, the number of perturbations per session was capped and as such this protocol was completed in either one or two sessions (one session for P2, P3, and P5; two sessions for P1, P4, and P6). Note that the handrails were removed from the treadmill so they could not be used during recovery (in order to mimic a real-life stumble scenario, in which handrails are rarely available), but participants wore a full-body harness to prevent contact with the treadmill in the event of a fall.

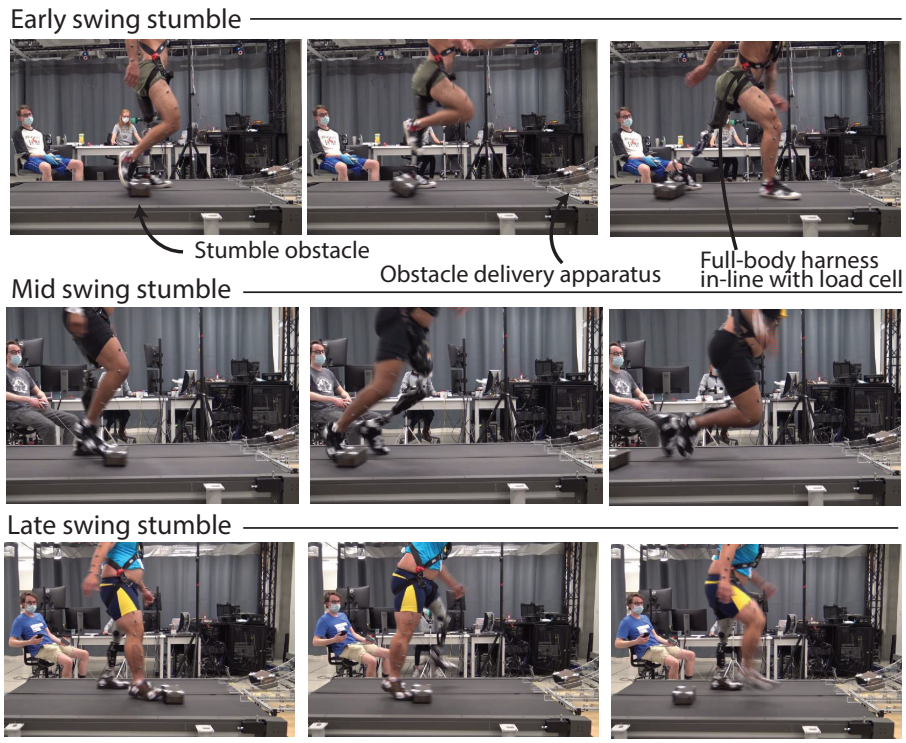

Figure 5.1: Experimental setup for stumble recovery experiments. Perturbations in early swing (top), mid swing (middle), and late swing (bottom) are pictured here. The stumble perturbation system and experimental protocol are detailed in [50]. Video clips of each stumble trial are included in the Additional files 1-3.

Each participant was given the same instructions prior to the stumble trials, namely: walk on the treadmill, perform serial sevens (counting backwards by seven) out loud and monitor visual feedback to stay centered on the treadmill; when the perturbation occurs, try to recover; the treadmill will be stopped to complete the trial when either (1) the participant falls into the harness or (2) the participant recovers and has returned to steady-state walking (qualitatively determined by the experimenters). Participants were given ample time to practice walking on the treadmill without perturbations prior to the stumble trials. All experimental protocols were approved by the Vanderbilt Institutional Review Board, and all participants gave their written informed consent.

5.3.2 Data Collection & Processing

Ground reaction forces (GRFs) were recorded under each foot at a sampling rate of 1 kHz via a lateral split-belt, force-instrumented treadmill (Bertec, Columbus, USA). Full-body kinematic data were collected via synchronized infrared motion capture (Vicon, Oxford, GBR) at a sampling rate of 200 Hz. Passive reflective markers were placed bilaterally over the lower limbs at the anterior/posterior superior iliac spines, medial/lateral femoral epicondyles and malleoli, posterior/medial/lateral calcaneus, 1st and 5th metatarsals, and navicular bone; the arms at the acromion, medial/lateral humeral epicondyles, medial/lateral styloid processes; and the torso at the left and right clavicle, sternum, and C7. Clusters of four markers were placed bilaterally on the thigh, shank, upper arm, and forearm. For the prosthetic-side lower limb, markers were placed on the estimated medial/lateral joint center of the prosthetic knee (i.e., femoral epicondyles) and estimated medial/lateral malleoli and foot anatomical landmarks (i.e., calcaneus, metatarsals, navicular bone) of the prosthetic foot. GRF and motion capture data were filtered with a zero-phase, 3rd order, low-pass Butterworth filter with a cut-off frequency of 15 and 6 Hz, respectively. Inverse dynamics were computed using Visual3D (C-Motion, Germantown, USA) to estimate joint-level kinematics and kinetics for each trial.

5.3.3 Outcome Metrics

Several outcome metrics were computed to characterize each stumble response in order to address the primary aim. First, the swing percentage at which the perturbation occurred was estimated as the time from the preceding toe-off event to the instant of perturbation, relative to the average swing time from 20 strides during the same trial. The perturbation was determined as the instant at which the foot contacted the obstacle, which was identified via a transient peak in the anterior-posterior (AP) GRF measured by the treadmill, as in [50]. Second, each trial was labeled as a fall or a recovery based on the force measured by a load cell in-line with the full-body harness. Specifically, if the load cell measured greater than 50% of the participant's bodyweight, the trial was defined as a fall; otherwise, it was defined as a recovery, similar to [17]. Finally, the recovery strategy used after each perturbation was reported as one of the three previously characterized recovery strategies from healthy adult stumble studies: elevating, lowering, or delayed lowering. Strategies were determined based on the trajectory of the swing foot after perturbation (as in [107, 27, 50]): in the elevating strategy, the foot lifts up and over the obstacle after contact with the obstacle; in the lowering strategy, the foot lowers to the ground behind the obstacle after contact with the obstacle; in the delayed lowering strategy, the foot initially elevates (i.e., shows upward motion) before elevation is abandoned and the foot subsequently lowers to the ground without clearing the obstacle. Refer to the legend of Fig. 5.2 for representative illustrations of each recovery strategy. Previous studies reported prosthesis user-specific strategies in response to perturbations to the sound side: hopping and skipping [17, 108]. Both of these strategies still involve initial tripped limb lowering or delayed lowering, with the hopping or skipping action as a subsequent response. Thus for this work strategies were reported primarily as elevating, lowering, or delayed lowering, and if hopping or skipping was also utilized, this was additionally documented. For each fall, the number of steps from the time of perturbation to harness loading of $>$50% bodyweight was also recorded.

Several time-series kinematic trajectories were computed for further characterization of each response. Specifically, ipsilateral (tripped/sound-side) and contralateral (prosthetic-side) sagittal-plane thigh, knee, and ankle angle were computed to characterize and compare the lower-limb motion after each perturbation. Frontal-plane prosthetic-side thigh angle was also computed to characterize the thigh abduction involved in the subsequent step after the stumble. Additionally, sagittal-plane trunk angle (deviation from vertical) after the perturbation was computed, as trunk angle deviations have been reported to be indicators of increased likelihood of falling [81, 18]. Finally, as previous studies have reported the role of arm movements in recovery of healthy adults [97, 89], the trajectories of the forearm center-of-mass were computed.

Discrete summary metrics were also extracted in order to address the secondary aim (i.e., to further clarify differences in transfemoral prosthesis user recoveries versus falls, and transfemoral prosthesis user recoveries versus healthy control recoveries). First, discrete metrics capturing key lower-limb dynamics during the response were extracted in order to identify lower-limb distinctions between recoveries and falls: peak ipsilateral (sound-side) thigh flexion, peak ipsilateral knee flexion, peak contralateral (prosthetic-side) thigh flexion, peak contralateral knee flexion, and contralateral knee angle at foot-strike. Second, the work of Grabiner et al. has previously identified several metrics that discriminate falls versus recoveries for various populations by capturing the body's state at each of the response foot-strikes [38, 81, 74, 35, 18]. Interventions that improve these variables and decrease fall risk have been subsequently reported [47, 77, 44, 71, 32, 37]. Specifically, time to initial foot-strike, as well as step length (computed as difference in AP position of the stepping foot's center-of-mass (COM) to the remaining foot's COM), AP foot position relative to the body's COM, trunk flexion, and trunk flexion velocity at each of the recovery foot-strikes have been presented. Thus these variables were also computed for this work in order to (1) illustrate the resulting whole-body outcomes of the aforementioned lower-limb kinematic differences, and (2) align this work with previous studies and potential interventions. Finally, peak trunk angle and trunk angular velocity, as well as peak contralateral (prosthetic-side) thigh abduction were computed for all recoveries.

5.3.4 Control Comparison Data

Data from a previous healthy adult stumble study [50, 27] was used for comparison to the responses of transfemoral prosthesis users. Seven healthy adults underwent a similar protocol using the same experimental apparatus, in which each participant experienced approximately 28 obstacle perturbations while walking at 1.1 m/s. These data collectively

represent 86 elevating strategies in early swing, 40 elevating strategies in mid swing, 24 delayed lowering strategies in mid swing, and 38 lowering/delayed lowering strategies in late swing. Although not exactly speed-matched with the experiments described here, these data nonetheless provide insights regarding which metrics correspond to successful recovery responses, and thus better illustrate prospective deficiencies in responses that result in a fall. Another experiment was also conducted in which a single healthy adult participant repeated the protocol at a walking speed of 0.8 m/s [27]. The healthy participants were wearing the same marker set, and motion capture and GRF data were processed identically to the transfemoral prosthesis user dataset. Data from the seven healthy participants, along with (separately identified) data from the single speed-matched healthy control participant (hereafter referred to as HC, details reported in Table 1), is provided as a reference in Figs. 5.4, 5.7, 5.11, and 5.13 below. Data from a representative trial from HC are included in Figs. 5.3, 5.5, 5.6, 5.8, 5.9, 5.10, and 5.12.

5.4 Results

Fifteen out of the 26 stumbles to the sound side of the transfemoral prosthesis users resulted in falls. This is in stark contrast to the healthy participants, in which no falls occurred out of 214 total stumbles.

Of the 26 transfemoral prosthesis user stumble responses, seven were elevating, nine were delayed lowering, and 10 were lowering. Four hopping strategies were used after lowering or delayed lowering strategies. No skipping strategies were observed. Five out of six participants fell at least once. Two participants fell after all perturbations, and three participants only fell after perturbations in mid swing. The breakdown of fall outcomes and strategies used for each participant are reported in Fig. 5.2.

Figures 5.3, 5.6, 5.9, and 5.10 provide time-series kinematic trajectories of the lower limbs, trunk, and arms after each individual perturbation for early, late, and mid swing stumbles. Note that Figs. 5.9 and 5.10 separate the mid swing responses into elevating strategies and lowering/delayed lowering strategies, respectively, for visual clarity. To supplement these figures, textual descriptions of the kinematics of each response are provided, organized by falls and recoveries for early, late, and mid swing stumbles. Videos of each stumble response are also available in Additional files 1-3.

Discrete summary metrics from Figs. 5.3, 5.6, 5.9, and 5.10 are plotted separately in Figs. 5.4, 5.7, and 5.11 to highlight lower-limb kinematic differences in falls versus recoveries among transfemoral prosthesis users. Figs. 5.5, 5.8, and 5.12 plot the resulting foot-strike configuration states to further distinguish falls and recoveries. Finally, Fig. 5.13 plots peak trunk and thigh abduction metrics to highlight differences in transfemoral prosthesis user recoveries from healthy control recoveries.

5.4.1 Early Swing

5.4.1.1 Recoveries

All four recoveries from early swing perturbations were accomplished by the elevating strategy, in which the tripped limb lifted up and over the obstacle in the same step, landing anterior to the obstacle. Refer to the legend of Fig. 5.2 for a representative illustration of this response. These responses (P2, P3, P4 and P6) are characterized by ipsilateral thigh flexion (peak 44-57 deg) and knee flexion (peak 104-121 deg) during the elevating step, trajectories comparable to the HC elevating step (Fig. 5.3, A and C). However, transfemoral prosthesis users exhibited 7-23 deg more contralateral (prosthetic-side) thigh abduction in the following step and substantially more peak trunk flexion and flexion velocity than the HC response (Fig. 5.3, L and K). Also of note, HC used 11 deg contralateral ankle plantarflexion during the elevating step, a position not available to the prosthesis users due to their passive prosthetic ankles (Fig. 5.3, I). Regarding arm movements, transfemoral prosthesis users exhibited similar contralateral forearm trajectories, characterized by initial deviation superior, anterior, and medial to the position at perturbation before returning to that position. HC employed a similar trajectory but with less overall displacement (Fig. 5.3, M-O).

5.4.1.2 Falls

Two of the six participants fell consistently in response to early swing perturbations (Fig. 5.2). Of note, these two participants fell after all perturbations to their sound limb. These early swing falls occurred after one elevating strategy and four delayed lowering strategies. During the elevating strategy, P5b just cleared the obstacle using substantially less thigh and knee flexion than non-fallers (Fig. 5.3, A and C) and landing well before HC, P2, P3, and P6 (as indicated with ipsilateral foot-strike in Fig. 5.3 and Time from Perturbation metric in Fig. 5.5). In his subsequent contralateral (prosthetic-side) step, he did not reach full knee extension and landed with a flexed knee (Fig. 5.3, H). In the remaining early swing stumbles, P1 and P5 initially elevated but ultimately abandoned elevating and lowered without clearing the obstacle (i.e., delayed lowering). P5a fell during the swing phase of his attempted contralateral (prosthetic-side) step that he did not complete, as evidenced by substantially less contralateral thigh flexion (Fig. 5.3, F). In the remaining falls, P5c and P1a,b could not initiate the contralateral step, as evidenced by the lack of contralateral (prosthetic-side) thigh flexion/knee flexion after the delayed lowering step (Fig. 5.3, F). Transfemoral prosthesis user arm trajectories were characterized by initial deviation superior and anterior from initial position but never returned to that position before loading the harness with >50% bodyweight (Fig. 5.3, M-O).

5.4.1.3 Discrete Summary Metrics: Transfemoral prosthesis user recoveries versus falls in early swing

Lower-limb Dynamics As shown in Fig. 5.4, transfemoral prosthesis users who recovered from early swing stumbles exhibited higher thigh and knee flexion in the first ipsilateral (sound-side) step after perturbation. These kinematics indicate employing a successful elevating strategy to clear the obstacle; note this is in contrast to the substantially less thigh/knee flexion used in the single elevating and four delayed lowering strategies that resulted in falls. Additionally, the prosthesis users who recovered used more peak thigh flexion in the contralateral (prosthetic-side) step and landed with an extended knee. These kinematics reflect successfully initiating swing phase on the prosthetic limb and landing in a safe configuration, as opposed to a lack of thigh flexion and/or knee flexion at foot-strike which resulted in falls. Note that data from HC (single healthy participant tripped at 0.8 m/s) and the seven-participant average of early swing responses resemble kinematics used by prosthesis users who recovered.

Foot-strike States As shown in Fig. 5.5, compared to the elevating strategy fall, elevating strategy recoveries involved a longer time from perturbation to first foot-strike, as well as a greater step length and more anterior foot position relative to body COM at the first (sound-side) and second (prosthetic-side) foot-strikes. At the second foot-strike, elevating recoveries also exhibited less trunk flexion and more negative (backward) trunk flexion velocity compared to the elevating fall. Lowering strategies always resulted in falls for early swing stumbles, which were characterized by a positive (forward) trunk flexion velocity at first foot-strike. Only one lowering strategy completed the next ground contact (prosthetic-side, recovery step), which involved substantial trunk flexion, negative trunk angular velocity, a short step length, and foot position posterior to the body COM.

5.4.2 Late Swing

5.4.2.1 Recoveries

All late swing recoveries were accomplished by the lowering strategy, in which the tripped limb was immediately lowered to the ground, terminating that step and initiating a step with the contralateral (prosthetic) limb, followed by another ipsilateral (sound-side) step to clear the obstacle. Refer to the legend of Fig. 5.2 for a representative illustration of this response. Transfemoral prosthesis users exhibited 5-35 deg less knee flexion and 20-23 deg more thigh abduction in contralateral step (Fig. 5.6, G and L) compared to HC. Three transfemoral prosthesis users (P2, P4, P6) exhibited more trunk flexion after the perturbation than HC (Fig. 5.6, K). Transfemoral prosthesis users exhibited similar ipsilateral arm trajectories, characterized by initial deviation superior, anterior, and lateral to the original position before returning to that position. HC employed a similar trajectory but with less overall displacement (Fig. 5.6, M-O).

5.4.2.2 Falls

Two of the six participants fell consistently in response to late swing perturbations (Fig. 5.2). Of note, these two participants fell after all perturbations to their sound limb. The five falls (P1a,b,c,d and P5) were all attempted lowering strategies. P1a,b lowered the tripped (sound) limb to the ground, then attempted to hop off the same limb (hopping) rather than initiate a contralateral step, as evidenced by the ipsilateral thigh and knee flexion after foot-strike and lack of contralateral thigh flexion after the perturbation (Fig. 5.6, A2, C2, F). After P1's remaining two late swing perturbations (P1c,d), P1 fell immediately after lowering the tripped limb to the ground and no other recovery steps were attempted, as shown by lack of initiation of ipsilateral thigh flexion or contralateral thigh and knee flexion (Fig. 5.6, A2, F, G). P5 lowered the tripped limb to the ground and initiated a contralateral step, as evidenced by contralateral thigh flexion, but landed much sooner than the non-fallers' (P2, P3, P4, P6) contralateral step with a more flexed knee, as shown in the timing and knee flexion at contralateral foot-strike (Fig. 5.6, H).

5.4.2.3 Discrete Summary Metrics: Transfemoral prosthesis user recoveries versus falls in late swing

Lower-limb Dynamics As shown in Fig. 5.7, transfemoral prosthesis users who recovered exhibited substantially higher contralateral (prosthetic-side) thigh flexion and landed with a more extended knee. These kinematics reflect successfully initiating swing phase on the prosthetic limb and landing in a safe configuration, as opposed to a lack of thigh flexion and/or knee flexion at foot-strike which resulted in falls. Additionally, prosthesis users who recovered reached higher thigh and knee flexion in the subsequent ipsilateral step. These kinematics reflect successfully clearing the obstacle, as opposed to lack of thigh/knee flexion exhibited by those who fell after lowering or lowering with hopping. Note that data from HC and the seven-participant average of late swing responses resemble kinematics used by prosthesis users who recovered.

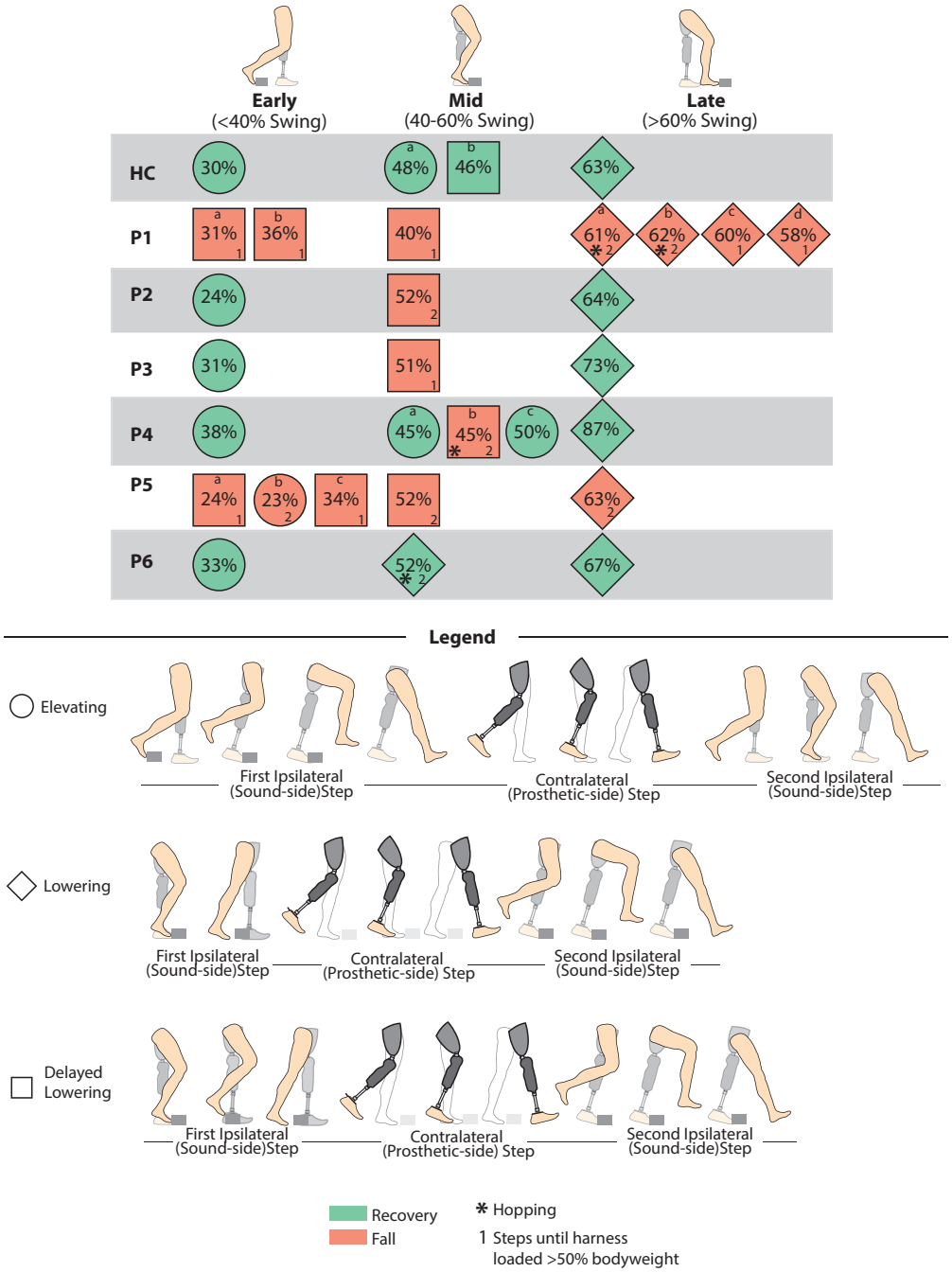

Figure 5.2: Summary of outcomes for each stumble for each participant. Fall versus recovery, recovery strategy attempted, swing percentage of perturbation, and number of steps prior to a fall (i.e., loading the harness with >50% bodyweight) are provided for each stumble. Video clips of each stumble trial are included in the Additional files 1-3. If the participant experienced more than one perturbation in a particular bin of swing phase, it is identified by a lower-case letter which is used in subsequent figures and Additional files 1-3.

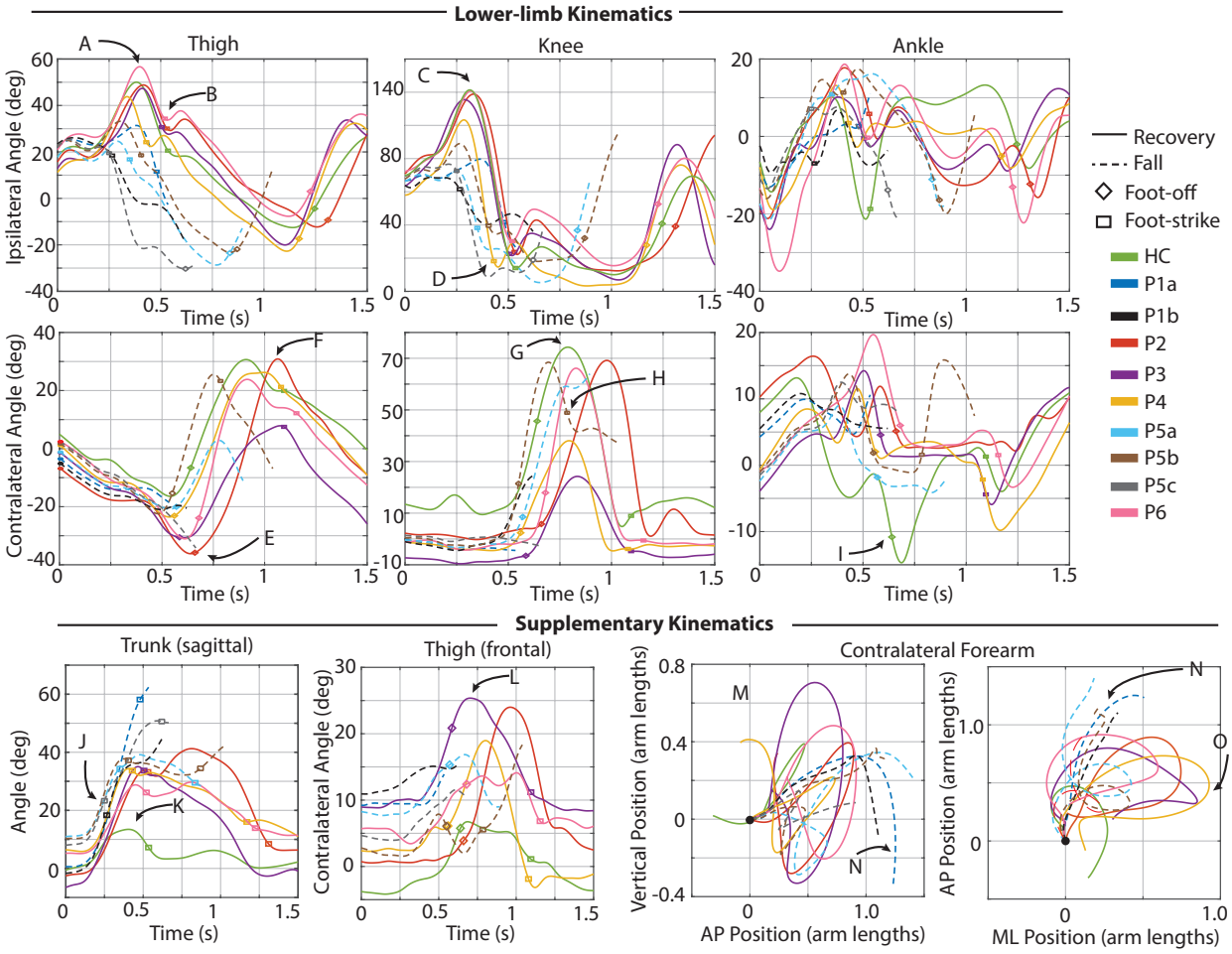

Figure 5.3: Kinematic characterization for early swing perturbations. Lower-limb kinematics: Sagittal-plane thigh, knee, and ankle angle trajectories for the ipsilateral (tripped/sound, top) and contralateral (support/prosthetic, bottom) limbs after the perturbation. Supplementary kinematics, from left to right: sagittal-plane trunk angle, frontal-plane contralateral thigh angle, contralateral forearm center-of-mass trajectory in sagittal and transverse planes. Positive angles indicate sagittal plane joint flexion, frontal plane thigh abduction, and trunk angle forward deviation from vertical. Positive arm positions indicate superior, anterior, and medial to position at perturbation. Arm positions are normalized from the position at perturbation, so trajectories begin at position (0, 0). Lower-limb and trunk trajectories are plotted from the instant of perturbation (Time 0) to either 1.5 seconds after perturbation (recoveries) or until the participant loaded the harness with >50% bodyweight (falls). Arm trajectories are plotted from the instant of perturbation to either one second after perturbation (recoveries) or until the participant loaded the harness with >50% bodyweight (falls).

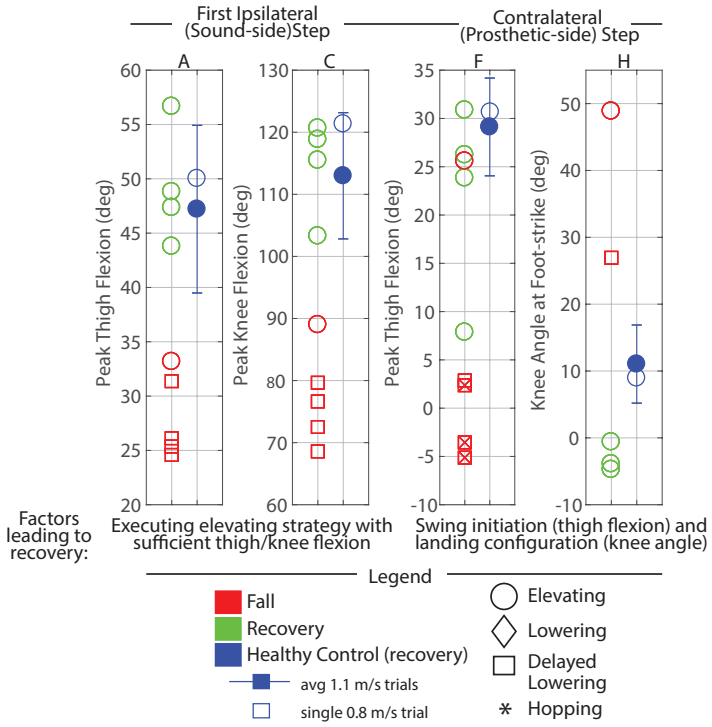

Figure 5.4: Early swing discrete summary metrics: Lower-limb dynamics. These plots highlight the differences in lower-limb motion between transfemoral prosthesis user falls versus recoveries, with healthy control recovery data included as a reference. Peak thigh and knee flexion in the ipsilateral (tripped/sound-side) step were calculated from perturbation to first ipsilateral foot-strike. Peak thigh flexion in contralateral (prosthetic-side) step was calculated from first ipsilateral foot-strike to first contralateral foot-strike or fall, whichever index occurred first. An "x" in a marker indicates the prosthesis user did not toe-off prior to falling. Capital letters above each plot correspond to letters that are marked in Fig. 5.3 for reference.

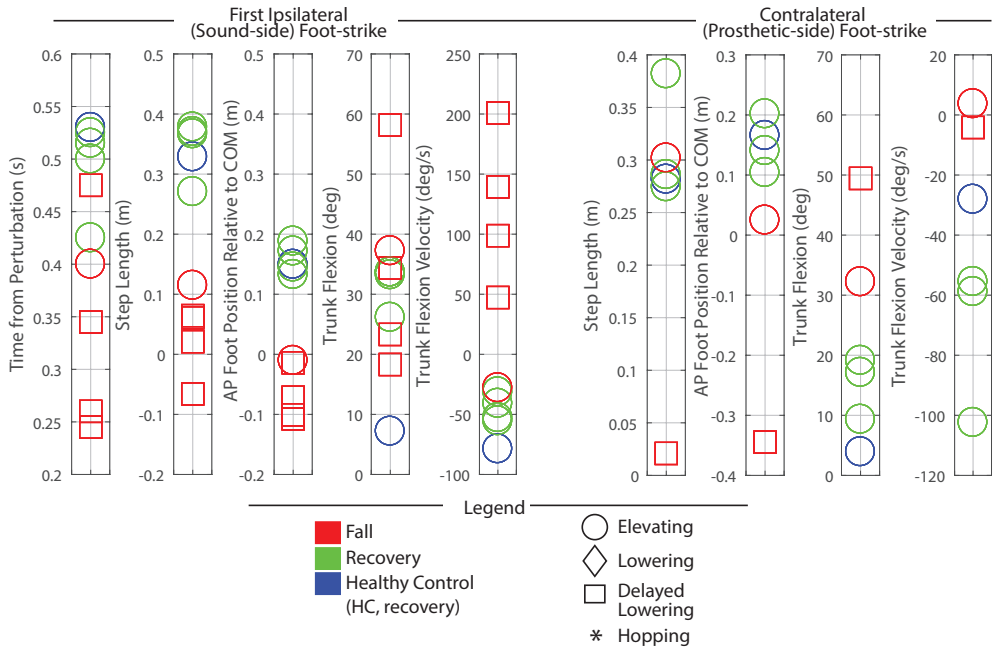

Figure 5.5: Early swing discrete summary metrics: Foot-strike states. These plots capture the body's state at each foot-strike after the perturbation, highlighting the differences in falls vs. recoveries for transfemoral prosthesis users. Each metric was computed at the indicated foot-strike. Positive values indicate anterior position, forward trunk flexion, and forward trunk flexion velocity.

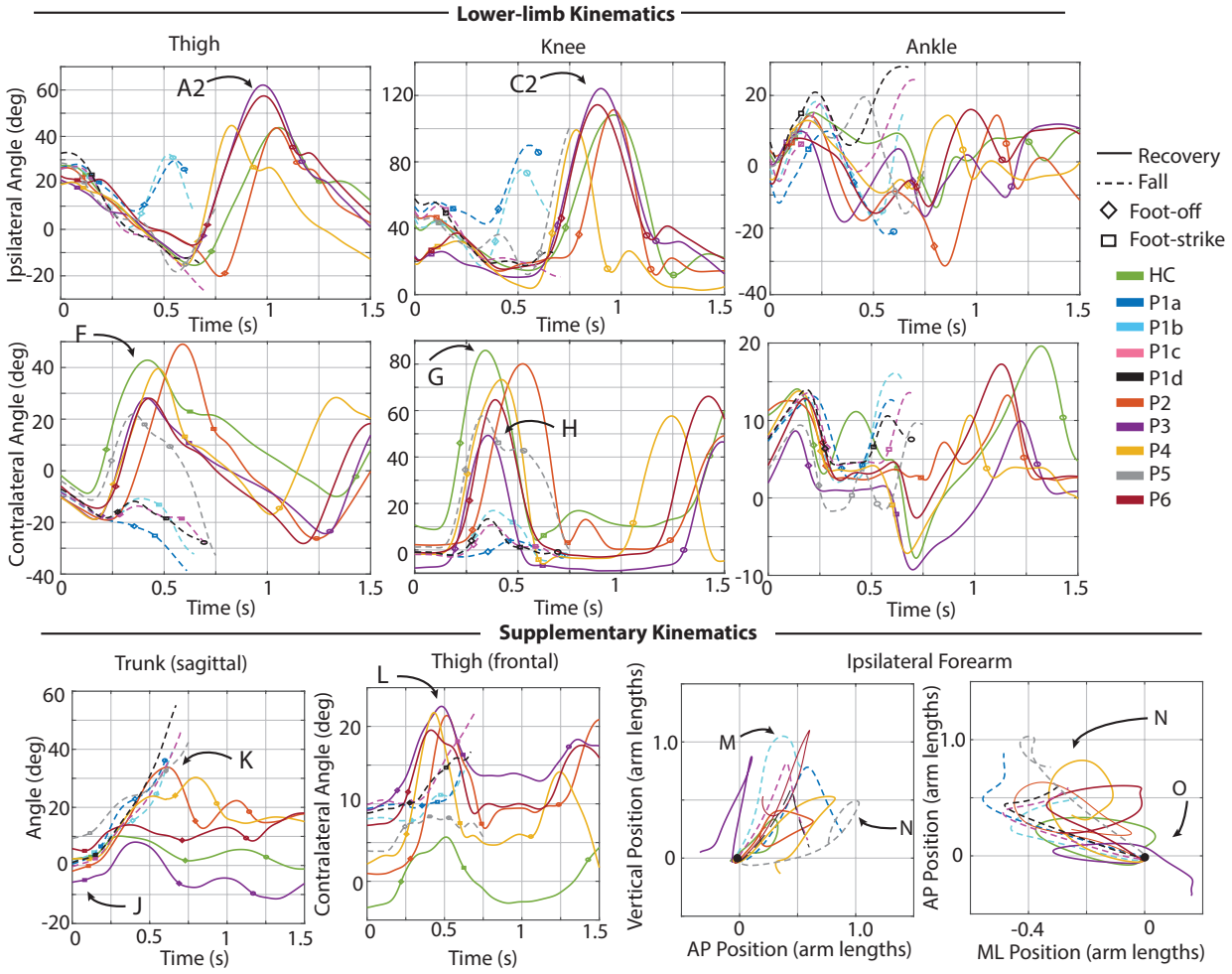

Figure 5.6: Kinematic characterization for late swing perturbations. Lower-limb kinematics: Sagittal-plane thigh, knee, and ankle angle trajectories for the ipsilateral (tripped/sound, top) and contralateral (support/prosthetic, bottom) limbs after the perturbation. Supplementary kinematics, from left to right: sagittal-plane trunk angle, frontal-plane contralateral thigh angle, ipsilateral forearm center-of-mass trajectory in sagittal and transverse planes. Positive angles indicate sagittal plane joint flexion, frontal plane thigh abduction, and trunk angle forward deviation from vertical. Positive arm positions indicate superior, anterior, and medial to position at perturbation. Arm positions are normalized from the position at perturbation, so trajectories begin at position (0, 0). Lower-limb and trunk trajectories are plotted from the instant of perturbation (Time 0) to either 1.5 seconds after perturbation (recoveries) or until the participant loaded the harness with >50% bodyweight (falls). Arm trajectories are plotted from the instant of perturbation to either one second after perturbation (recoveries) or until the participant loaded the harness with >50% bodyweight (falls).

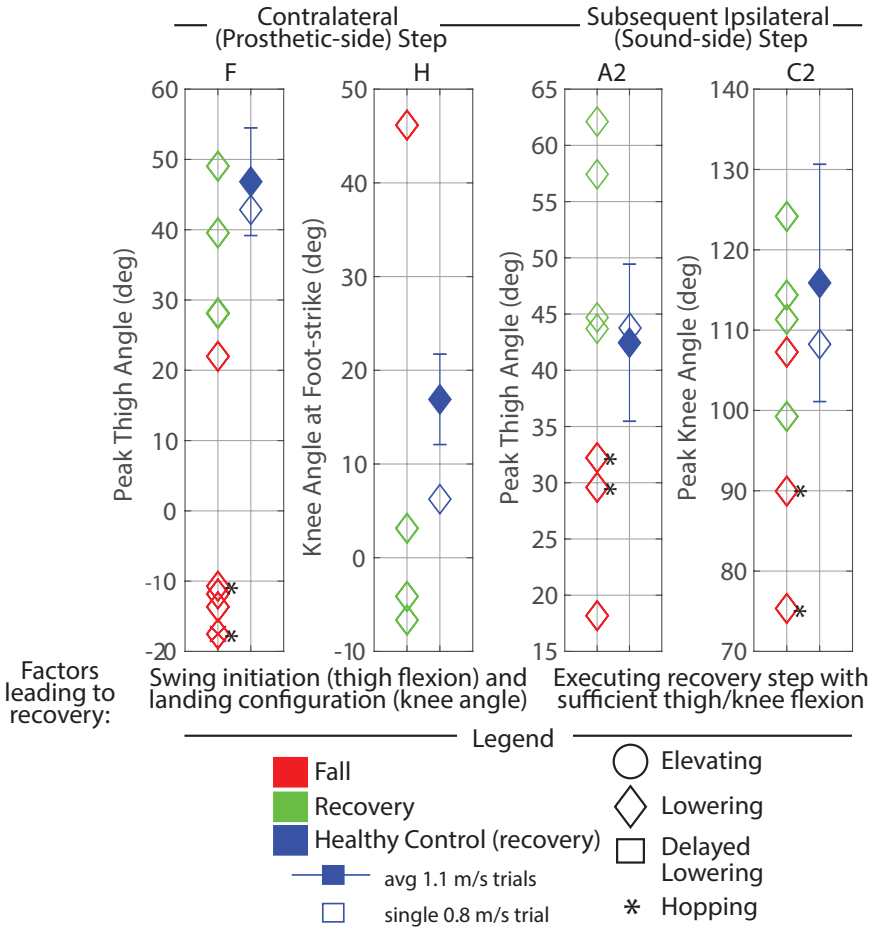

Figure 5.7: Late swing discrete summary metrics: Lower-limb dynamics. These plots highlight the differences in lower-limb motion between transfemoral prosthesis user falls versus recoveries, with healthy control recovery data included as a reference. Peak thigh flexion in contralateral (prosthetic-side) step was calculated from first ipsilateral foot-strike to first contralateral foot-strike or fall, whichever index occurred first. An "x" in a marker indicates the prosthesis user did not toe-off prior to falling. Peak thigh and knee angle in subsequent ipsilateral (sound-side) step were calculated from ipsilateral toe-off after lowering to foot-strike. Metrics are only plotted if they occurred before the participant loaded the harness with >50% bodyweight (fall). Capital letters above each plot correspond to letters that are marked in Fig. 5.6 for reference.

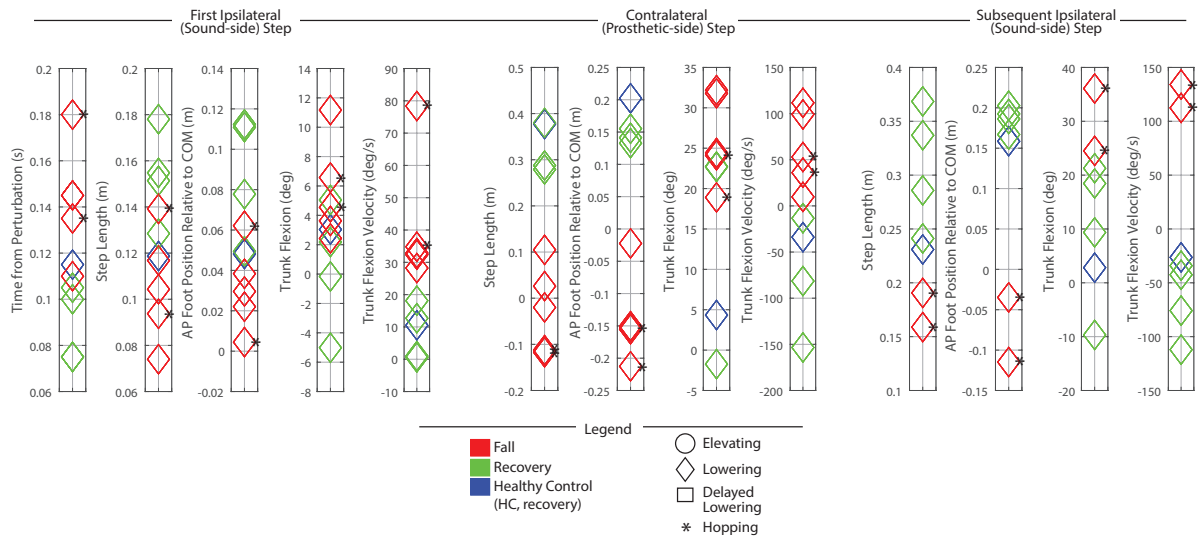

Figure 5.8: Late swing discrete summary metrics: Foot-strike states. These plots capture the body's state at each foot-strike after the perturbation, highlighting the differences in falls vs. recoveries for transfemoral prosthesis users. Each metric was computed at the indicated foot-strike. Positive values indicate anterior position, forward trunk flexion, and forward trunk flexion velocity.

Foot-strike States As shown in Fig. 5.8, compared to lowering strategy falls, lowering strategy recoveries generally involved less time from perturbation to first foot-strike, greater step length, more anterior foot position relative to COM, less trunk flexion, and more negative (backward) flexion velocity at first foot-strike (initial sound-limb loading), the next foot-strike (prosthetic-side recovery step), and the subsequent sound-side foot-strike.

5.4.3 Mid Swing

5.4.3.1 Recoveries

Recoveries in mid swing were accomplished by two elevating strategies (P4a,c) and one lowering strategy with hopping (P6a). As shown in Fig. 5.9, during the elevating strategies (P4) the tripped limb lifted up and over the obstacle in the same step, landing anterior to the obstacle, as HCa did. However, HC exhibited substantially higher peak thigh and knee flexion during the elevating step (10 deg and 20 deg more, respectively) and landed later than P4 (Fig. 5.9, A-D). During the subsequent contralateral (prosthetic-side) step, P4 exhibited substantially more thigh extension in the sagittal plane (Fig. 5.9, E) and abduction in the frontal plane (Fig. 5.9, L), less knee flexion (Fig. 5.9, G), less ankle plantarflexion (Fig. 5.9, I), and more trunk flexion (23-30 deg, Fig. 5.9, K) than HC. Contralateral arm motion followed similar trajectories to that of the early swing elevating strategies of transfemoral prosthesis users, with HC again using less overall arm displacement (Fig. 5.9, M-O).

As shown in Fig. 5.10, P6 recovered using a lowering with hopping strategy; specifically, upon contacting the obstacle he immediately terminated his step and lowered behind the obstacle, but subsequently hopped off of his ipsilateral (sound) limb. During the hop the contralateral (prosthetic-side) limb swung laterally (substantial thigh abduction without knee flexion) to facilitate the following step and landed just before the second ipsilateral step (versus a $\sim$500 ms difference between foot-strikes with HCb, indicated by foot-strike marker in Fig. 5.10). HCb exhibited substantially more thigh and knee flexion and ankle plantarflexion in the contralateral step (Fig. 5.10, F, G, I), then landed with a more extended thigh and knee in the subsequent ipsilateral step (Fig. 5.10 B2, D2). HC also exhibited 13 deg less peak trunk flexion and 15 deg less thigh abduction after the perturbation (Fig. 5.10 K, L).

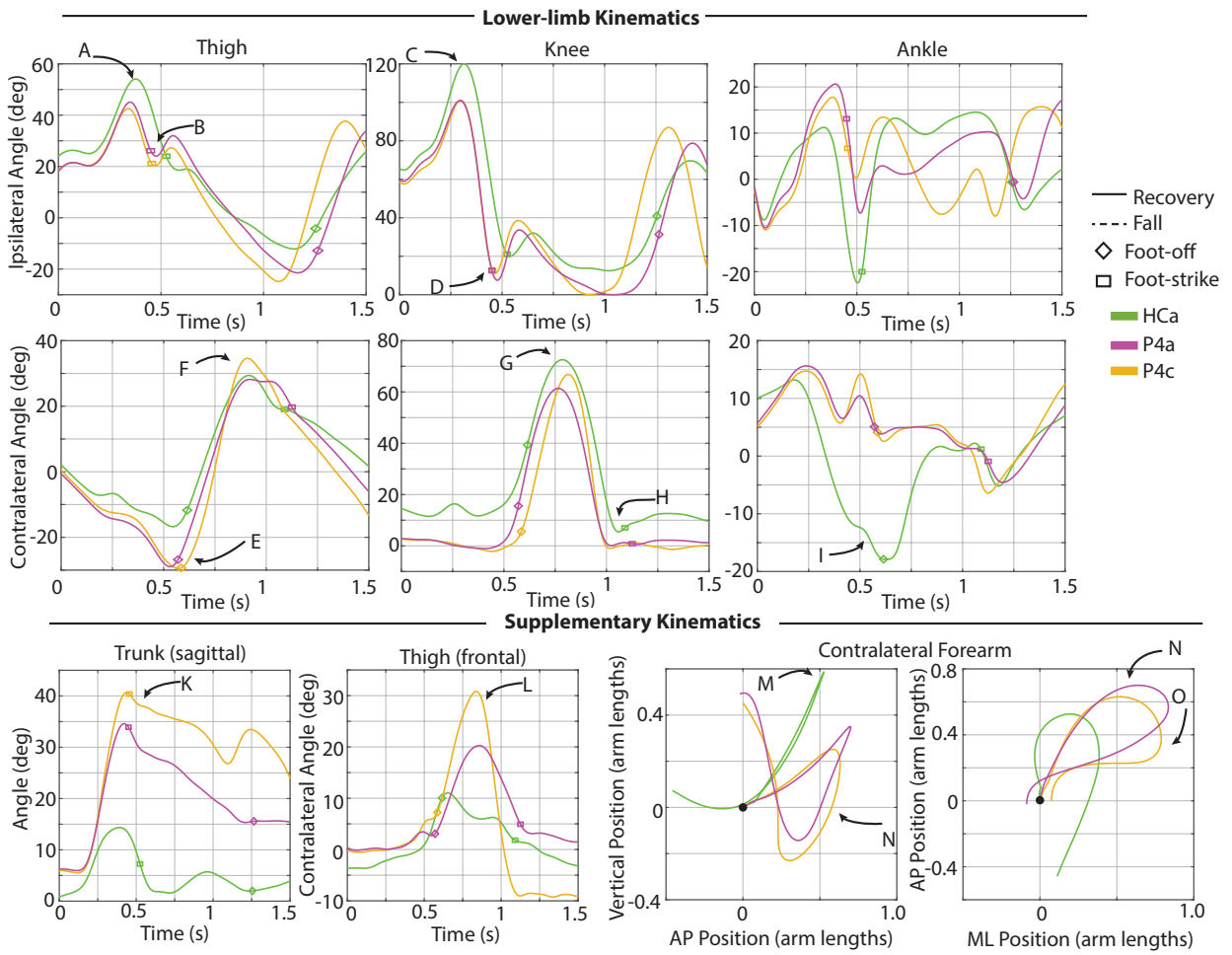

Figure 5.9: Kinematic characterization for elevating strategies after mid swing perturbations. Lower-limb kinematics: Sagittal-plane thigh, knee, and ankle angle trajectories for the ipsilateral (tripped/sound, top) and contralateral (support/prosthetic, bottom) limbs after the perturbation. Supplementary kinematics, from left to right: sagittal-plane trunk angle, frontal-plane contralateral thigh angle, contralateral forearm center-of-mass trajectory in sagittal and transverse planes. Positive angles indicate sagittal plane joint flexion, frontal plane thigh abduction, and trunk angle forward deviation from vertical. Positive arm positions indicate superior, anterior, and medial to position at perturbation. Arm positions are normalized from the position at perturbation, so trajectories begin at position (0, 0). Lower-limb and trunk trajectories are plotted from the instant of perturbation (Time 0) to either 1.5 seconds after perturbation (recoveries) or until the participant loaded the harness with >50% bodyweight (falls). Arm trajectories are plotted from the instant of perturbation to either one second after perturbation (recoveries) or until the participant loaded the harness with >50% bodyweight (falls).

5.4.3.2 Falls

Five of the six participants fell during mid swing perturbations. P4 attempted a delayed lowering with hopping strategy, in which upon contacting the obstacle he initially elevated but ultimately terminated his step and lowered behind the obstacle, then subsequently hopped but experienced substantial trunk flexion just as he landed and loaded the harness with >50% bodyweight. P4 landed with his prosthetic-side thigh substantially more extended than P6, as evidenced by contralateral thigh angle at foot-strike (Fig. 5.10, J). P2 attempted a delayed lowering strategy, in which he initially elevated upon contacting the obstacle, but ultimately lowered behind the obstacle, followed by a contralateral step, but did not succeed in landing, experiencing substantial trunk flexion before loading the harness with

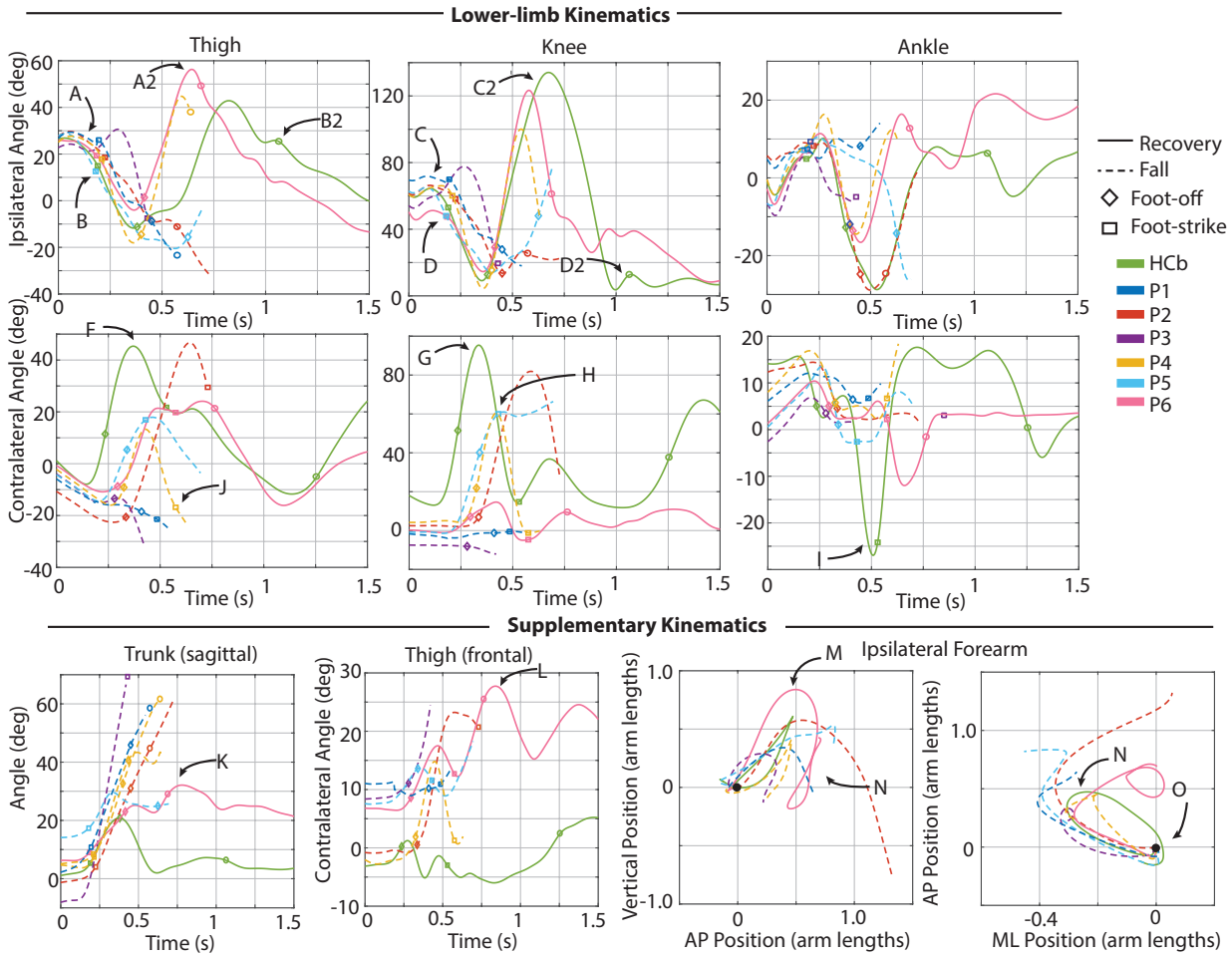

Figure 5.10: Kinematic characterization for lowering/delayed lowering strategies after mid swing perturbations. Lower-limb kinematics: Sagittal-plane thigh, knee, and ankle angle trajectories for the ipsilateral (tripped/sound, top) and contralateral (support/prosthetic, bottom) limbs after the perturbation. Supplementary kinematics, from left to right: sagittal-plane trunk angle, frontal-plane contralateral thigh angle, ipsilateral forearm center-of-mass trajectory in sagittal and transverse planes. Positive angles indicate sagittal plane joint flexion, frontal plane thigh abduction, and trunk angle forward deviation from vertical. Positive arm positions indicate superior, anterior, and medial to position at perturbation. Arm positions are normalized from the position at perturbation, so trajectories begin at position (0, 0). Lower-limb and trunk trajectories are plotted from the instant of perturbation (Time 0) to either 1.5 seconds after perturbation (recoveries) or until the participant loaded the harness with >50% bodyweight (falls). Arm trajectories are plotted from the instant of perturbation to either one second after perturbation (recoveries) or until the participant loaded the harness with >50% bodyweight (falls).

>50% bodyweight. P5 also attempted a delayed lowering strategy and initiated a contralateral (prosthetic-side step), but landed with substantial knee flexion, as evidenced in contralateral knee angle at foot-strike (Fig. 5.10, H), which buckled the knee and led to a fall. Finally, P1 and P3 attempted delayed lowering strategies but were unable to initiate a contralateral (prosthetic-side) step after the lowering step before falling, as evidenced by lack of contralateral thigh flexion (Fig. 5.10, F). Fallers' ipsilateral arm motions were characterized by arm motion superior, anterior, and lateral to position at perturbation (Fig. 5.10, M-O).

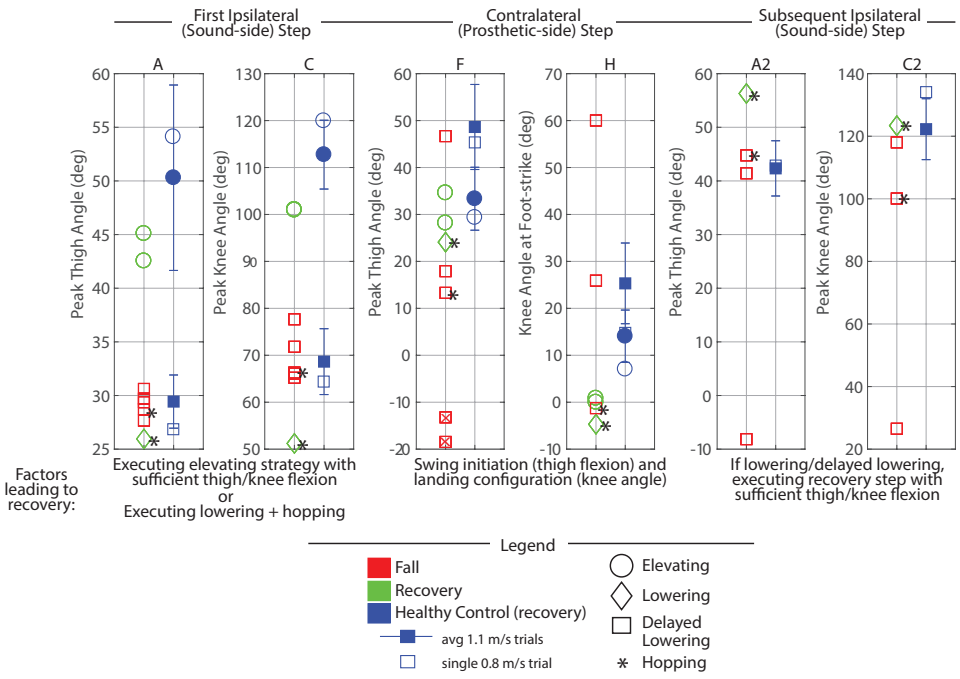

Figure 5.11: Mid swing discrete metrics: Lower-limb level. These plots highlight the differences in lower-limb motion between transfemoral prosthesis user falls versus recoveries, with healthy control recovery data included as a reference. Peak thigh and knee flexion in the ipsilateral (tripped/sound-side) step were calculated from perturbation to first ipsilateral foot-strike. Peak thigh flexion in contralateral (support/prosthetic-side) step was calculated from first ipsilateral foot-strike to first contralateral foot-strike or fall, whichever index occurred first. An "x" in a marker indicates the prosthesis user did not toe-off prior to falling. Peak thigh and knee angle in subsequent ipsilateral (sound-side) step were calculated from ipsilateral toe-off after lowering to foot-strike. Metrics are only plotted if they occurred before the participant loaded the harness with >50% bodyweight (fall). Capital letters above each plot correspond to letters that are marked in Fig. 5.9 and 5.10 for reference.

5.4.3.3 Discrete Summary Metrics: Transfemoral prosthesis user recoveries versus falls in mid swing

Lower-limb Dynamics Transfemoral prosthesis users who recovered after mid swing stumbles either elevated or lowered with hopping. Thus kinematics that differentiate falls versus recoveries (Fig. 5.11) reflect the description/trends noted for early swing elevating strategies from Fig. 5.4 (sufficient thigh/knee flexion in first ipsilateral step, and sufficient thigh flexion and knee extension at foot-strike in contralateral step), or late swing lowering strategies from Fig. 5.7 (sufficient thigh flexion and knee extension at foot-strike in contralateral step after lowering, and sufficient thigh/knee flexion in next ipsilateral step to clear obstacle). Recall that for the successful lowering strategy in mid swing, a hopping strategy was also employed. Note that data from HC (single healthy participant tripped at 0.8 m/s) and the seven-participant average of early swing responses resemble kinematics used by prosthesis users who recovered.

Foot-strike States The mid swing elevating strategy recoveries involved step times, step lengths, foot positions relative to COM, trunk flexion, and trunk flexion velocities comparable to early swing elevating strategies. Compared to mid swing lowering strategy falls, the mid swing delayed lowering strategy recovery involved a more anterior foot position relative to center of mass at first sound-side foot-strike, as well as a greater step length, more anterior foot position relative to COM, and less trunk flexion in the next contralateral (prosthetic-side) foot-strike.

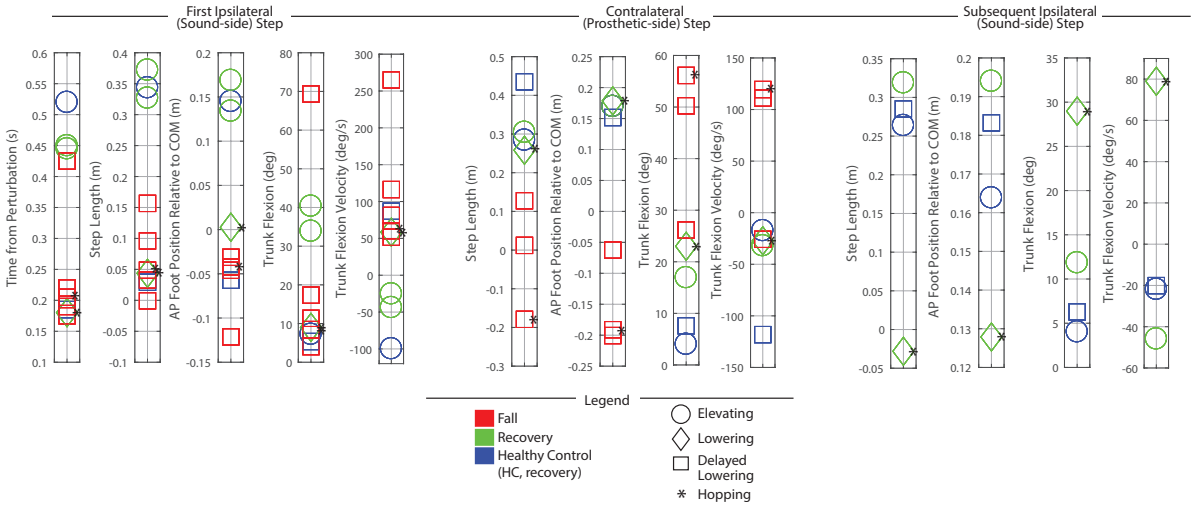

Figure 5.12: Mid swing discrete metrics: Foot-strike states. These plots capture the body's state at each foot-strike after the perturbation, highlighting the differences in falls vs. recoveries for transfemoral prosthesis users. Each metric was computed at indicated foot-strike. Positive values indicate anterior position, forward trunk flexion, and forward trunk flexion velocity.

5.4.4 Discrete Summary Metrics: Transfemoral prosthesis user recoveries versus healthy control recoveries in early, mid, and late swing

As shown in Fig. 5.13, early and mid swing perturbations induced approximately double the effect on transfemoral prosthesis users (versus healthy participants) in terms of peak trunk flexion and flexion velocity. The majority of prosthesis user late swing stumble responses also involved more peak trunk flexion and flexion velocity than HC (single 0.8 m/s trial). Additionally, for early, mid, and late swing stumbles, prosthesis users employed substantially more thigh abduction in the contralateral (prosthetic-side) step during recovery compared to healthy control data (7-19 deg for early, 10-20 deg for mid, and 15-19 deg for late).

Note that relative to HC, the prosthesis users who recovered with an elevating strategy used a comparable step length and foot positioning at first foot-strike, but landed with more trunk flexion and more forward trunk flexion velocity (Figs. 5.5 and 5.12). During lowering/delayed lowering strategies, HC took a larger contralateral step with more anterior foot positioning relative to COM than the majority of prosthesis user recoveries (Figs. 5.8 and 5.12).

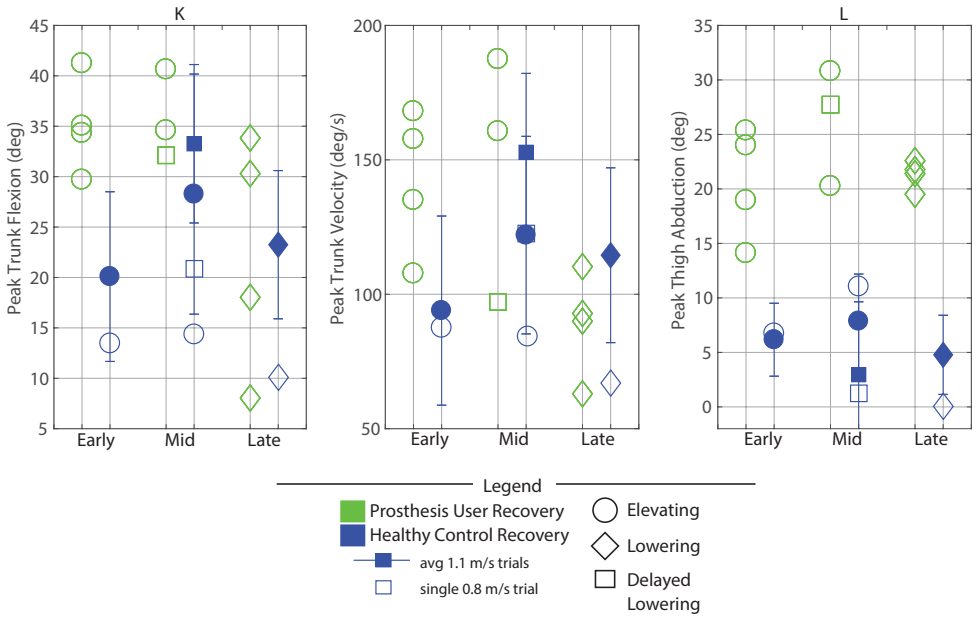

Figure 5.13: Discrete summary metrics comparing transfemoral prosthesis user versus healthy control recoveries. Peak trunk flexion and flexion velocity were calculated as the peak value from perturbation to 1.5 seconds after the perturbation. Peak prosthetic-side thigh abduction was calculated as peak frontal-plane thigh angle from contralateral toe-off to contralateral foot-strike. Capital letters above each plot correspond to letters that are marked in Figs. 5.3, 5.6, 5.9, and 5.10 for reference.

5.5 Discussion

Five of the six transfemoral prosthesis users fell at least once in this study, while none of the seven healthy control participants fell in [50, 27]. These results substantiate the high fall prevalence relative to healthy adults reported in retrospective studies [53, 41, 46, 114, 120, 65], highlighting that stumbles to the sound limb should not be overlooked when considering interventions for fall prevention.

The following subsections provide an in-depth discussion of results with respect to the stumble conditions of (i) swing phase, (ii) participant age, and (iii) prosthesis type, as well as a commentary on arm motion. Finally, based on these observations, several interventions for improving recovery and mitigating falls for the transfemoral prosthesis user population are considered.

5.5.1 Considering Swing Phase

5.5.1.1 Early

Transfemoral prosthesis users who recovered in early swing (P2, P3, P4, P6) used an elevating strategy, as HC did. This was accomplished via substantial sound-side thigh and knee flexion to complete the elevating step, and a successful initiation (thigh flexion) and completion (extended knee angle) of the next prosthetic-side step (Fig. 5.4); this lower-limb motion allowed prosthesis users to land with a greater step length, more anterior foot position relative to COM, less trunk flexion, and more negative trunk velocity at each of the recovery foot-strikes (Fig. 5.5), aligning with the work of Grabiner et al. which has shown that an improvement in these metrics (i.e., trending in the direction described) indicates a decreased fall risk [81, 74, 35, 99, 18].

However, transfemoral prosthesis users who recovered exhibited more support limb (prosthetic-side) thigh abduction in the next step and increased trunk flexion and flexion velocity compared to healthy control data (Fig. 5.13). Thigh abduction is likely a compensation mechanism in order to facilitate swing phase during the non-cyclic activity of stumble recovery (see Considering Prosthesis Type subsection). Increased trunk flexion has been reported as an indicator of increased fall likelihood [81, 18] and may be due to lack of moment generation of the prosthetic limb joints (See Considering Age, Commentary on Arm Motion, and Interventions for Consideration subsections). Likewise, contralateral ankle plantarflexion employed by HC during the elevating step (not observed for prosthesis users) may have helped reduce forward angular momentum and thus limit trunk flexion during recovery [88, 70, 110] (see Considering Age and Interventions for Consideration subsections).

Transfemoral prosthesis users who fell in early swing (P1, P5) either inadequately performed the elevating strategy or attempted a delayed lowering strategy but could not successfully initiate a contralateral (prosthetic-side) step. In the seven-participant healthy adult study, all 86 stumbles that occurred before 40% swing phase resulted in elevating strategies (i.e., none abandoned elevating to perform the delayed lowering strategy) [27, 50]. In this study, the transfemoral prosthesis users who used the delayed lowering strategy (i.e., abandoned elevating) exhibited substantially high forward trunk flexion velocity at initial sound-side foot-strike, and only one could complete the second prosthetic-side step, suggesting that employing the delayed lowering strategy in early swing may increase the body's forward angular momentum enough to contribute to falls. This increase in trunk flexion and forward trunk flexion velocity at recovery foot-strikes aligns with the work of Grabiner et al. [38, 81, 74, 35, 99, 18, 37], which has used these metrics as fall indicators for other populations.

These early swing findings are inconsistent with the only other study of sound-side, early swing perturbations with transfemoral prosthesis users, in which majority lowering strategies and no falls were reported [108]. This may be due to the ability of participants in that study to use the handrails and/or to the lack of a physical obstacle to clear in the rope-blocking apparatus.

Collectively these results suggest that properly performing the elevating strategy is key for recovering from early swing stumbles.

5.5.1.2 Late

Transfemoral prosthesis users who recovered in late swing (P2, P3, P4, P6) used a lowering strategy, as HC did. This was accomplished via substantial thigh flexion and safe landing configuration for the prosthetic-side step as well as substantial sound-side thigh and knee flexion in the subsequent step to clear the obstacle (Fig. 5.4); this lower-limb motion allowed users to land with a larger step length, more anterior foot position relative to COM, and more negative trunk flexion velocity at the prosthetic-side foot-strike and subsequent sound-side foot-strike (Fig. 5.8), again aligning with trends seen in [81, 74, 35, 99, 18, 47, 44, 71, 76, 32, 37].

However, lowering strategy recoveries involved more trunk flexion and more support limb (prosthetic-side) thigh abduction compared to healthy controls (Fig. 5.13) likely in part due to deficiencies in stance release of their prescribed knee prosthesis (see Considering Prosthesis Type subsection).

The transfemoral prosthesis users who fell in late swing (P1, P5) all attempted a lowering strategy but could not initiate and/or complete the next (prosthetic-side) step. This was evidenced by the lack of prosthetic-side thigh flexion or flexed knee at prosthetic-side foot-strike (Fig. 5.4), which contributed to the smaller step length, posterior foot position relative to COM, and more forward trunk flexion velocity at prosthetic-side foot-strike (Fig. 5.8), metrics that agree with previously reported fall indicators. Note that these lowering strategy falls were also characterized by a longer time to initial loading (first sound-side foot-strike), which is consistent with findings of [81].

These late swing findings are mostly consistent with Shirota et al. [108], who also observed lowering strategies, as well as with Crenshaw et al. [17], who observed one elevating (fall), one lowering with hopping (recovery), and one lowering (fall), and suggested that lack of knee control contributed to the difficulty of executing the recovery step with the prosthetic limb.

Collectively these results suggest that properly initiating swing after the lowering step, landing in a safe (i.e., extended knee) configuration on the prosthetic limb, and using sufficient thigh/knee flexion to clear the obstacle in the subsequent sound-side step are key for recovering from late swing stumbles.

5.5.1.3 Mid

Transfemoral prosthesis users who recovered in mid swing (P4, P6) used an elevating or lowering with hopping strategy. The trends observed in early swing elevating strategies and late swing lowering strategies extend to mid swing regarding lower-limb dynamics (Fig. 5.11) and foot-strike states (Fig. 5.12).

These mid swing findings are mostly consistent with Shirota et al. [108] in terms of strategy selection. However, while Shirota et al. observed no falls, this mid swing region presented the highest likelihood of falls across participants (i.e., five of six fell) in the present study, suggesting that this region may warrant particular attention when considering interventions. The lowering with hopping response was qualitatively similar to the hopping strategy discussed in previous works [17, 108]. Crenshaw et al. 2013 [17] notes that this strategy may be difficult for individuals with plantarflexion weakness; indeed, in this study only one participant successfully recovered in this way.

Collectively these results suggest that either properly performing the elevating strategy or properly initiating prosthetic-side swing after the lowering step (for a more normative, without hopping, lowering/delayed lowering strategy) is key for recovering from mid swing stumbles.

5.5.2 Considering Age

It is notable that the two oldest participants in this case series (P1 and P5) were the only two participants to fall after every perturbation. These results are consistent with several studies of healthy (non-prosthesis user) older and younger adults, in which the older adults fell more [87, 114] which was attributed to delayed and/or diminished muscle responses [87, 100]. Pijnappels et al. [90] highlights that older adults have problems meeting the requirements for adequate balance recovery, since muscle strength, reaction time, and coordination decline with age. Specifically,

Pijnappels et al. [87] reported significantly longer rise times of electromyography (EMG) amplitudes of the biceps femoris, gastrocnemius medialis, and soleus muscles in the support limb of the older adults, which reduces rate of force generation. This finding is likely compounded in the present study by the fact that in the case of elevating strategies, the support limb is the prosthetic limb, in which these three muscles have been altered or removed due to amputation/congenital limb difference (discussed more in the Commentary on Arm Motion and Interventions for Consideration sections). Pijnappels et al. and others conclude that a combination of resistance/strength training and task-specific motor skill training has the potential to improve responses [35, 90], which are discussed in the Interventions for Consideration section.

Pavol et al. 1999 [79] reported in their overground stumble study of older adults that the participants who took more rapid steps had significantly increased likelihood of falling after a trip. Additionally, gait asymmetry metrics have been used to determine and quantify gait pathologies [122]. Thus the cadence and prosthetic-to-sound limb swing time symmetry were computed for each participant. P5 walked with a substantially increased cadence (i.e., more rapid steps, at 115 steps/min) compared to the remaining participants (87-97 steps/min). P1 and P5 also walked with higher swing-time asymmetry (ratio of 1.52 and 1.41, respectively) compared to the remaining participants (1.23-1.31). Therefore, age of participant may be a proxy for other step metrics that indicate higher fall risk.

5.5.3 Considering Prosthesis Type

Four of the transfemoral prosthesis user participants wore an Ottobock C-Leg (P1, P3, P5, P6), which is a hydraulic-based microprocessor-controlled knee (MPK). Two participants wore hydraulic non-MPKs: P2 wore an Ottobock 3R80, a single-axis, rotary-hydraulic knee; P4 wore a Blatchford KX06, a four-bar, hydraulic knee. All six are hydraulic knees with stance control function (i.e., high resistance against flexion during stance). Stance resistance against flexion is initiated at heel-strike in the non-MPKs, while it is initiated during swing extension in the C-leg. The C-leg and 3R80 are both single-axis knees, while the KX06 employs 4-bar kinematics that increase toe clearance during swing phase and also enhance stability during stance phase.

For early and late swing perturbations, there was no clear trend in prosthesis type contributing to falls versus recoveries. Recall that the two transfemoral prosthesis users who fell were also the oldest participants, which was discussed in the Considering Age section. However, the transfemoral prosthesis users who recovered (regardless of prosthesis type) used substantial thigh abduction during the subsequent prosthetic-side step (Fig. 5.13), likely to help initiate swing at a time when the prescribed device was not in the proper mode. Both non-MPKs and MPKs rely on various sensing thresholds to allow for stance release, which is reliable during the cyclic motion of walking; however, these prostheses do not account for the interruption of inertial swing dynamics that occurs during sound-side stumbles.

For mid swing perturbations, the participant who recovered using an elevating strategy wore a non-MPK (P4 with KX06). The participant who recovered using a lowering strategy wore an MPK (P6 with C-Leg). However, it is unclear whether the devices themselves helped facilitate recovery; especially in the case of P6, the C-Leg's lack of stance release likely led to the hopping response after lowering that required substantial thigh abduction to facilitate swing and involved increased trunk flexion. Thus, the recoveries in mid swing are potentially attributed to the ability of the prosthesis user rather than the prosthesis itself. For the delayed lowering responses (all falls), the non-MPK users (P2 and P4) were able to initiate a subsequent step with their prosthetic side after the lowering step (Fig. 5.10), while the MPK users could not initiate this subsequent step. Thus, the non-MPKs may have some advantage at more quickly initiating swing; however, their capabilities were not robust enough to successfully complete the step.

There was one instance of prosthetic knee buckling, in which P5 did not take a full prosthetic-side step after his delayed lowering step and landed with the knee substantially flexed (Figs. 5.10 and 5.11).

From these observations, for sound-side stumble recovery there does not seem to be a clear advantage of knee prosthesis type. Instead, both demonstrated similar deficits: namely, the inability to initiate swing and/or complete swing during the recovery step. All participants wore similar energy storage-and-return type prosthetic feet, and all showed similar deficits in terms of lack of active plantarflexion and less range of motion compared to HC. The effect of prosthetic foot model was beyond the scope of this work but could be investigated in future studies.

5.5.4 Commentary on Arm Motion

Roos et al. 2008 [97] concluded that arm movements contribute to stumble recovery for healthy adults by both elevating the body's center of mass and reducing its forward angular momentum, which provide more time for the positioning of the recovery limb. Pijnappels et al. 2010 [89] concluded that arm responses counteracted transverse plane body rotation which helped with recovery foot positioning. For all three strategies, but particularly with elevating, transfemoral prosthesis user recoveries were characterized by substantially more vertical, anterior, and medial/lateral deviation of the forearm from its position at perturbation (prior to returning to that position) as well as increased trunk flexion compared to HC (Figs. 5.3, 5.6, 5.9, 5.10, and 5.13). As discussed in the Considering Swing Phase and Interventions for Consideration sections, Pijnappels et al. [88] conclude that the reactive torques of the support limb of healthy adults enable the necessary push-off reaction, thus reducing the forward angular momentum of the body and providing more time for positioning of the elevating limb. Given that the support limb was the prosthetic limb (i.e., no active ankle or knee power and compromised muscles) for elevating strategies in this study, perhaps the exaggerated arm motion observed among transfemoral prosthesis users is necessary to counter the lack of moment generation of the support limb, allowing for reduced forward angular momentum and/or better foot placement to avoid falling.

Interestingly, the transfemoral prosthesis users who fell after every perturbation were the two oldest participants, and they employed arm motion similar to those found in the older participants of Roos et al. 2008 [97]; described as a more "protective" strategy, these arm movements were characterized by more anterior displacement (a forward reaching-like motion that suggested bracing themselves for an expected fall), rather than the "preventive" strategy employed by younger adults to counteract loss of balance (Figs. 5.3, 5.6, 5.9, and 5.10).

Interventions for Consideration

5.5.4.1 What causes falls?

In this case series, fall incidence was related to swing percentage (the mid swing stumbles resulted in the most falls) and age (the oldest prosthesis users fell after every stumble), but not with prosthesis type (MPK versus non-MPK), as discussed in the previous discussion subsections.

Falls for this population can be attributed to two main deficiencies in the transfemoral prosthesis users' responses after a stumble. First, falls occurred if the tripped (sound) limb did not reach ample thigh and knee flexion to sufficiently clear the obstacle in the elevating step (Fig. 5.4 and 5.11, A and C). The inability to perform the elevating strategy may come from a decrease in strength or reaction time of the tripped (sound) limb (see Considering Age section), and/or a lack of counteracting moment generation in the support (prosthetic) limb (see Considering Swing Phase and Commentary on Arm Motion sections). Recall that even the elevating strategy recoveries involved more trunk flexion, forward trunk flexion velocity, and arm motion than healthy controls, also likely due to these two factors.

Second, falls occurred if the prosthetic limb did not facilitate a successful step response (Fig. 5.7 and 5.11, F and H) after the initial elevating or lowering sound-side step; specifically, either prosthetic swing was not initiated (as evidenced by lack of thigh flexion before falling) or swing was initiated but the prosthesis landed in an unsafe configuration (i.e., knee flexed). The inability to perform this prosthetic-side step is likely due to their prescribed prostheses' control scheme that does not decrease flexion resistance until stance-release thresholds are met, as well as its passive behavior that relies on ballistic coordination with the thigh for full swing phase motion, both of which are compromised when the cyclic motion of gait is interrupted during a stumble (see Considering Prosthesis Type subsection). Recall that even the elevating and lowering strategy recoveries involved more thigh abduction in the prosthetic-side step, also likely due to this factor.

Both of these deficiencies in lower-limb dynamics (highlighted in Figs. 5.4, 5.7, and 5.11) overall led to shorter steps, less anterior foot placement relative to COM, and more trunk flexion/flexion velocity at each of the response footstrikes (highlighted in Figs. 5.5, 5.8, and 5.12) for fallers compared to non-fallers, confirming that these previously reported metrics [38, 81, 74, 35, 18, 47, 77, 44, 71, 32] translate to the transfemoral prosthesis user population.

These observations suggest that appropriate interventions to decrease fall risk for transfemoral prosthesis users may be

to assist in properly performing the elevating strategy and/or to assist in initiating and safely completing the prosthetic-side step. Such interventions could be accomplished with some combination of training and external assistance, discussed below.

5.5.4.2 Training interventions

Strength training and/or task-specific motor skill training may help prosthesis users recover by targeting the two aforementioned deficiencies.

First, strength training targeted at the sound (tripped) limb's hip and knee flexors may improve success in elevating over the obstacle. (Note one could potentially also accomplish this with a powered exoskeleton on the sound limb.) Training targeted at the prosthetic-side (support limb) hip flexors could also help by providing counteracting torques during the elevating step; however, transfemoral prosthesis users still may lack in the necessary knee or ankle torques due to their passive prostheses. Additionally, training targeted at the prosthetic-side hip could help initiate swing phase; however, the transfemoral prosthesis users who recovered in this study employed substantial thigh abduction to accomplish the step due to prosthesis constraints, likely necessitating external interventions discussed subsequently. Strength training has shown potential for improving responses for fall-prone populations [90]; future work is needed to investigate the feasibility of such training for prosthesis users for sound-side stumbles.

Second, a task-specific training protocol in the form of repeatedly introduced treadmill acceleration disturbances that require a stepping response may also improve recovery outcomes. In particular, the work of Grabiner et al. has shown that this task-specific training can improve the metrics at response foot-strikes linked to increase fall risk reported in Figs. Figs. 5.5, 5.8, and 5.12, and ultimately reduce fall incidence [35, 99]. Future work is needed to investigate the feasibility of such training for transfemoral prosthesis users for sound-side stumbles.

5.5.4.3 Prosthesis interventions

Powered prostheses (e.g., [56, 3, 58]) may reduce fall risk by addressing the deficiencies of the typically prescribed passive prosthetic knees in responses to stumbles.

First, a powered prosthesis could improve the sound limb elevating response by providing the necessary counteracting ankle plantarflexion and/or knee flexion torques in the support limb, allowing for a more normative push-off to facilitate the elevating step and reduce the body's forward angular momentum [87, 108].

Second, a powered prosthesis could presumably sense a stumble and initiate powered swing phase for the subsequent step without requiring ballistic coordination with the thigh, as passive prostheses do. In other words, users could more easily initiate and complete swing phase in the following step, addressing one of the leading causes of falls among study participants. Additionally, powered prostheses can provide robust stance support even if the prosthesis lands with a flexed knee. Some energetically passive knees could provide robust stance support as well, although in general, any prosthesis that does so must implement this as a stumble-specific behavior, since otherwise doing so would interfere with stance knee yielding during slope or stair descent.

Such improvements in the lower-limb deficiencies observed may improve the body's state at prosthetic-side foot-strike (i.e., larger step length, more anterior foot placement, less trunk flexion, and more negative trunk flexion velocity).

These suggestions may not only reduce falls but also generally improve responses for transfemoral prosthesis users who did not fall. For example, transfemoral prosthesis users still exhibited responses that indicated increased risk of falling (increased trunk flexion/flexion velocity) and compensation mechanisms (increased thigh abduction and arm motion); thus, training and/or assistive device interventions may improve these metrics, ultimately helping to reduce the need to abduct and help control forward angular momentum to reduce these deficiencies.

Despite this potential for improvement, to date there have been no prosthetic interventions developed or tested to address sound-side stumbles for transfemoral prosthesis users. Future work is needed to investigate the feasibility of

such interventions.

5.5.5 Limitations

There are several limitations to this work. First, a sample size of more participants would have improved the confidence of the observations enumerated here. More non-MPK users would have improved the discussion on the effect of prosthesis type. Regardless, given the inherent heterogeneity of the prosthesis user population (i.e., varying ages, activity levels, comorbidities, years of prosthesis use, prosthesis types), a case series characterization such as that presented here is arguably more representative than one in which a singular averaged result is reported [54].

Second, while substantial efforts were made experimentally to ensure the obstacle was not perceived prior to contacting the participant's foot (see Methods and Results of [50]), the participants did know that they would be stumbled at some point during the trial.

Third, there is potential that requiring a cognitive task during the trials may alter balance outcomes; however, a recent stumble study found that performing Serial Sevens (i.e., the cognitive task chosen in this work) did not alter the participants' recovery response [75]. Furthermore, in the real world tripping often occurs when individuals are distracted/not paying attention [69, 19], so the task is not entirely unlike real-life situations.

Fourth, rest was not standardized across participants; instead, participants were given the opportunity to rest as much as desired in between each stumble based on their own comfort and energy levels. This rest period was based on personal preference rather than physiological monitoring, so there is potential that fatigue could have affected responses. However, there were no observed trends in fall/recovery outcomes with order of trials (e.g., no evidence that more falls occurred towards the end of a session) across participants.

Finally, the authors note that there are other factors that may have played a role in responses: socket attachment, residual muscle condition, and physical fitness level. Though this type of analysis was beyond the scope of the present work, future studies investigating these factors are encouraged.

5.6 Conclusion

This study presents a case series of sound-side stumble responses to obstacle perturbations in early, mid and late swing phase for six transfemoral prosthesis users of various ages and prosthesis types. Five out of six participants fell at least once – in contrast to a similar study of seven healthy participants in which none fell – highlighting the importance of studying sound-side stumbles and considering appropriate interventions. Stumbles elicited in mid swing resulted in the most falls (five out of six participants fell), suggesting a potential region of focus for intervention design. The two oldest participants were the only two to fall after every stumble, highlighting age-related differences in muscle strength and control and consequently ability to recover. Prosthesis type (specifically MPK versus non-MPK) did not relate to strategy or fall outcomes among the six participants studied; rather, both prosthesis types exhibited similar deficits regarding inability to initiate and/or complete swing phase.

Strategies that resulted in recoveries for transfemoral prosthesis users matched those used by the healthy control participant; namely the elevating in early swing, the lowering in late swing, and either the elevating or the lowering (with hopping) in mid swing. However, these recoveries still showed kinematic variations from the control participant, characterized by increased prosthetic-side thigh abduction, increased trunk flexion and flexion velocity, and exaggerated arm motions. Thigh abduction is likely a compensation performed to help initiate swing phase on the prosthetic side. Trunk and arm responses are likely affected by the nature of the passive prosthetic support limb, which cannot generate the counteracting torques typically generated by healthy musculature. Those who fell inadequately performed these recovery strategies, evidenced by lower-limb deficiencies in executing the elevating step and/or in initiating and completing the prosthetic-side step, which led to a shorter step length, less anterior foot placement relative to COM, more trunk flexion, and more forward trunk flexion velocity at each foot-strike, metrics that have been previously reported as fall indicators.

These observations suggest that interventions via training (e.g., muscle strength or task-specific motor skill) and/or assistive devices (e.g., lower-limb prostheses or exoskeletons) may address the main response deficiencies that led to falls for transfemoral prosthesis users. Specifically, training or exoskeleton assistance could help facilitate sufficient thigh/knee flexion for the elevating strategy; training or prosthesis assistance could provide counteracting torques in the support limb to facilitate elevating; and training or prosthesis assistance could help initiate and safely complete prosthetic swing.

CHAPTER 6

Powered knee prosthesis stumble recovery intervention

6.1 Part 1: Efficacy of a powered knee prosthesis with closed-loop walking controller in reducing falls and recovery deficiencies after sound-side stumbles

6.1.1 Part 1 Summary

Transfemoral prosthesis users experience a high fall rate, which leads to injury and fear of falling. Previous works have reported that stumbles to the sound limb incur a similar fall rate and comparable recovery deficiencies (e.g., increased trunk motion and thigh abduction relative to healthy controls) as stumbles to the prosthetic limb, though to date no intervention has been tested to mitigate these effects. Thus, in this work three unilateral transfemoral prosthesis users experienced stumble obstacle perturbations to their sound limb in early, mid and late swing phase while wearing a powered knee prosthesis intervention with a closed-loop walking controller (i.e., impedance control in stance, trajectory control in swing). Fall outcome, recovery strategy, as well as trunk and thigh kinematics were recorded in order to compare responses with the powered prosthesis intervention to responses with their prescribed, passive prosthesis. Intra-participant fall rate did not change with the powered prosthesis intervention relative to their prescribed prosthesis after early and late swing stumbles, but fall rate improved slightly for two participants after mid swing stumbles, promoting the elevating strategy. Overall, recoveries with the powered prosthesis intervention involved less trunk flexion, less trunk flexion velocity, and less prosthetic-side thigh abduction, reducing deficiencies relative to recoveries with their prescribed passive prostheses. The robust stance support and powered swing phase of the powered knee prosthesis intervention, features that are unavailable to typically prescribed passive knee prostheses, served to (1) help counter induced forward angular momentum and aid in the control of trunk motion during elevating strategies, (2) prevent knee buckling during recoveries, and (3) reduce compensatory thigh motion in the prosthetic-side step. Incorporating this intervention with task-specific training, muscle strength training, and/or a powered ankle may improve upon benefits observed in this work.

6.1.2 Introduction

Transfemoral prosthesis users experience a high stumble and fall rate [41, 46], which is linked to increased injury risk [14, 68] and fear of falling [65, 53, 49] relative to healthy controls. Research exploring interventions to improve recovery from stumbles (i.e., obstacle perturbations to the foot in swing phase) and reduce fall risk may benefit this population.

A few works have performed stumble experiments with transfemoral prosthesis users to characterize stumble recovery strategies and identify deficiencies in responses, ultimately providing insight into fall risk interventions [108, 17, 28]. Intriguingly, the two studies to date that tripped both limbs and incurred falls reported a similar fall rate from sound-side stumbles relative to prosthetic-side stumbles. Crenshaw et al. [17] reported 2/3 falls from sound-side stumbles versus 1/4 falls from prosthetic-side stumbles; likewise, Eveld et al. [28] reported 15/26 falls from sound-side stumbles versus 13/24 stumbles from prosthetic-side stumbles. Stumble response results from Shirota et al.[108] also highlighted that sound-side stumbles should not be overlooked, given that both limbs play an integral role to successful recoveries. For the cases in which prosthesis users avoided falling, recoveries exhibited increased forward trunk flexion and trunk flexion velocity relative to healthy controls [17, 28]. The ability to control trunk motion (i.e., limit flexion and flexion velocity) after stumbles has been identified as integral to successful recoveries and a target for intervention in previous works to reduce falls [37, 35, 36]. Additionally, prosthesis users employed substantial thigh abduction in the subsequent prosthetic-side step, which was not observed in healthy controls when recovering from similar stumble perturbations and can be attributed to prosthesis shortcomings [28]. Though stumbles to the sound-limb are a clear safety risk for transfemoral prosthesis users, to date no intervention has been designed or tested to address sound-side stumbles for this population.

Previous works suggest (among other interventions, such as task-specific training [35]) the potential utility of a powered knee prosthesis in addressing fall rate and recovery deficiencies after sound-side stumbles [28, 17]. Indeed, active flexion and extension provided by powered prosthetic knees (e.g., [56, 58, 3]) have been shown to be beneficial for non-ballistic behaviors such as stair climbing and other activities of daily living; however, research in the area of stumble recovery for powered prosthetic knees is limited. Relative to typically prescribed passive prostheses, a powered prosthesis with a standard walking controller (i.e., closed-loop impedance and trajectory controllers for stance and swing, respectively) could help the aforementioned response deficits. First, robust stance support may provide the active torques necessary to counter the perturbation-induced forward angular momentum and help control trunk motion during elevating strategies [88, 87, 108, 28]. Additionally, load-based stance support may limit unintended buckling of the prosthetic limb, potentially reducing falls and increasing user trust in loading the device. Finally, a powered swing phase, in which the knee self-generates motion, may help initiate and complete swing phase with more normative knee flexion, particularly during a disrupted stride, eliminating the need for thigh abduction or other compensatory actions [28].

Despite the potential to reduce falls and improve recovery responses, a powered knee prosthesis has yet to be tested as an intervention with transfemoral prosthesis users during sound-side stumbles. Thus the objective of this work is to evaluate the extent to which a powered knee prosthesis with a closed-loop walking controller may mitigate (i) fall rate and (ii) recovery deficiencies (e.g., forward trunk motion and thigh abduction) for transfemoral prosthesis users relative to their prescribed passive prostheses following sound-side stumbles. This work is in essence a brief follow-up study from [28], investigating one of the primary interventions proposed in that paper, which will provide insight into the potential efficacy of a powered knee intervention and inform future research directions.

6.1.3 Methods

6.1.3.1 Interventional Device: Powered Knee Prosthesis

Hardware

The device used in this experiment is the powered knee unit of the robotic leg prosthesis described in [56] and pictured in Fig. 6.1. Briefly, the knee unit includes a brushless DC motor with a three-stage belt/chain speed reduction (176:1) transmission that can generate approximately 85 Nm of active torque with a range of motion of 5 deg hyperextension to 115 deg flexion. The device houses a six-axis IMU in the shank as well as encoders at the knee joint and motor to measure shank and knee angles and angular velocities. Additionally, a load cell in the knee unit senses axial load in the shank. Although the prosthesis as described in [56] includes both a powered knee and ankle, the prosthesis employed in the studies described here include only the experimental powered knee unit, along with a conventional (passive) prosthetic foot unit.

Walking Controller

The walking controller finite-state machine (developed by Shane King and Leo Vailati) for the powered knee is depicted in Fig. 6.2 with state transition conditions given in Table 6.1.

During walking, the knee transitions among four states: pre-stance, stance, late stance, and swing. During the stance states, an impedance control approach is used with the following control law:

$$\tau = k_{p,stance}(\theta_{eq} - \theta) + k_{d,stance}(\dot{\theta}) \tag{6.1}$$

where τ is commanded torque, $k_{p,stance}$ is the proportional gain or stiffness, θ is the joint angle, θ_{eq} is the desired joint angle equilibrium position, $k_{d,stance}$ is the damping coefficient, and $\dot{\theta}$ is the joint angular velocity. In pre-stance, $k_{p,stance}$ is low to enable some give immediately after swing; in stance, $k_{p,stance}$ is high to support the user; in late stance, there is no resistance to flexion to facilitate swing initiation.

Figure 6.1: Powered knee prosthesis

Figure 6.2: Finite-state machine for powered knee prosthesis closed-loop walking controller.

Table 6.1: State transition conditions for powered knee prosthesis closed-loop walking controller.

Transition	Condition
0 to 2	Knee angle threshold
1 to 2	Load threshold
2 to 3	Shank angle threshold Load threshold Load rate threshold
3 to 4	Shank angle threshold Load threshold
3 to 2	Load threshold Shank angle threshold Time limit
4 to 1	Completion of trajectory
4 to 2	Load threshold

During swing, a PD controller is used to track a knee angle trajectory spline modeled after healthy walking data with the following control law:

Table 6.2: Participant information. Participant numbering is consistent with [28]

Participant	Age	Prosthetic side	Sex	Etiology	Years of prosthesis use	Prescribed Prosthesis
P1	62	Right	Male	Trauma	49	Ottobock C-Leg
P3	28	Right	Female	Congenital	27	Ottobock C-Leg
P4	30	Left	Male	Trauma	4	Blatchford KX06

$$\tau = k_{p,swing}(\theta_{desired} - \theta) + k_{d,swing}(\dot{\theta}_{desired} - \dot{\theta}) \tag{6.2}$$

where $\theta_{desired}$ and $\dot{\theta}_{desired}$ are the desired knee angle and knee angular velocity from the spline and its derivative at the current time in swing, and $k_{p,swing}$ and $k_{d,swing}$ are proportional and derivative gains, respectively.

Note that the features of (1) active stance support and (2) powered swing with primarily load-based initiation are unique to the interventional device (i.e., relative to the participants' passive prescribed prostheses) and based on previous results from [17, 108, 28] have the potential to provide stumble recovery benefits.

6.1.4 Experimental Protocol

In a previous study, six transfemoral prosthesis users underwent a stumble recovery experiment using their prescribed, passive knee and ankle prostheses [28]. Three of those participants (Fig. 6.2) returned to repeat this testing protocol while wearing the powered knee prosthesis intervention.

First, participants were invited for prosthesis fitting, walking controller tuning, and familiarization. Specifically, they were fitted with the powered knee prosthesis with matched height and consistent alignment to their prescribed prosthesis. For two participants, the device was attached to their prescribed ankle/foot prosthesis. For one participant (P4), the build height of the powered knee did not accommodate his current ankle prosthesis, so a lower-profile foot was selected for testing. All three participants wore the same socket and suspension system as with the prescribed prosthesis. Next, participants were familiarized with the powered knee for level-ground walking. The walking controller parameters (gains and state transition thresholds) were tuned while participants walked on a treadmill at 0.8 m/s until they were sufficiently comfortable walking in the device.

On a separate day, participants returned for the obstacle perturbation stumble experiment. Details of the experimental setup and protocol are given in [50, 28]. Briefly, participants walked on a treadmill at 0.8 m/s. After a random number of steps, a 16-kg (35-lb) steel obstacle was released from the obstacle delivery apparatus and onto the treadmill such that it contacted the participant's swing foot at an experimenter-specified percentage of swing phase. Participants wore a full-body harness to prevent contact with the treadmill in the event of a fall. Various experimental techniques were employed to ensure the obstacle's entry onto the treadmill was imperceptible, including sensory occlusion [50]. Participants were instructed to count backwards by intervals of seven as a cognitive distraction task, and they were stumbled on both their sound and prosthetic limb to limit expectation of the stumble. Stumbles were targeted to occur in early, mid, and late swing phase. Figure 6.3 depicts the experimental setup with video frames of an early swing stumble trial for both the prescribed and powered prosthesis condition.

6.1.4.1 Data Collection & Processing

Ground reaction forces (GRFs) were recorded under each foot at a sampling rate of one kHz via a lateral split-belt, force-instrumented treadmill (Bertec, Columbus, USA). Full-body kinematic data were collected via synchronized infrared motion capture (Vicon, Oxford, GBR) at a sampling rate of 200 Hz. GRF and motion capture data were filtered with a zero-phase, 3rd order, low-pass Butterworth filter with a cut-off frequency of 15 and 6 Hz, respectively. Inverse kinematics were computed using Visual3D (C-Motion, Germantown, USA) to estimate joint-level kinematics

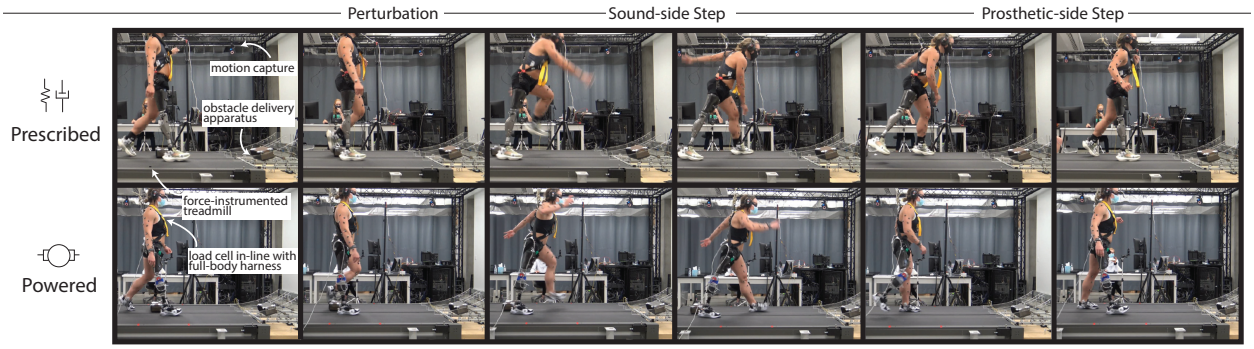

Figure 6.3: Video frames depict an elevating strategy after an early swing perturbation for one participant (P3) using her prescribed passive prosthesis (top) and the powered prosthesis intervention (bottom).

for each trial. Bodyweight assistance by the harness was measured via an in-line load cell during each trial.

6.1.4.2 Data Analysis

For this work, only trials in which the sound limb was tripped were analyzed. Trials were excluded if the participant stepped over the obstacle or onto it (i.e., not a stumble perturbation). The swing percentage of each perturbation was estimated as in [50].

To address objective (i), the fall outcome and recovery strategy attempted were recorded for each trial. A fall was determined based on the bodyweight assisted by the harness after the stumble: If the load cell measured more than 50% bodyweight and sustained a load for more than 500 ms, the trial was considered a fall, similar to [17, 28]. The recovery strategy was defined as elevating, lowering, or delayed lowering, based on previously published definitions [108]. Hopping or skipping after lowering or delayed lowering was also noted (defined in [17, 108]).

To address objective (ii), several outcome metrics were computed to quantify recovery deficiencies for both prescribed and powered prosthesis recoveries. First, peak (sagittal-plane) trunk flexion and flexion velocity after the stumble perturbation were calculated. Second, peak thigh abduction in the prosthetic-side step was calculated. Since recovery responses differ depending on when in swing phase the perturbation occurs [107, 101, 27], each prescribed prosthesis recovery was paired with a powered prosthesis recovery that was closest in swing percentage for comparison in order to interpret the effect of the powered prosthesis intervention with other perturbation factors controlled.

For reference, the same outcome metrics were computed from a previously collected dataset of stumbles from one healthy adult walking at 0.8 m/s using the same experimental setup, protocol, and data processing techniques [27].

6.1.5 Results

Overall, seven out of 22 sound-side stumbles resulted in falls (32%) with the powered prosthesis intervention, compared to nine out of 15 (60%) with the prescribed prostheses. To address objective (i), the full breakdown of fall outcomes and recovery strategies attempted for each trial in early, mid, and late swing phase is reported in Fig. 6.4 (i) for each participant. To address objective (ii), recovery deficiency metrics (peak trunk flexion, peak trunk flexion velocity, and peak prosthetic-side thigh abduction) are reported in Fig. 6.4 (ii) to compare powered versus prescribed recoveries from similar perturbations (i.e., trials at similar swing percentages).

Results from a single healthy control participant are included in Fig. 6.4 (ii) for reference. For early swing, the black line plots the average value from four trials that occurred at 30-32% swing. For mid and late swing, the black lines plot the values from the single mid swing elevating strategy (48% swing) and single late swing lowering strategy (73%

swing) in the dataset.

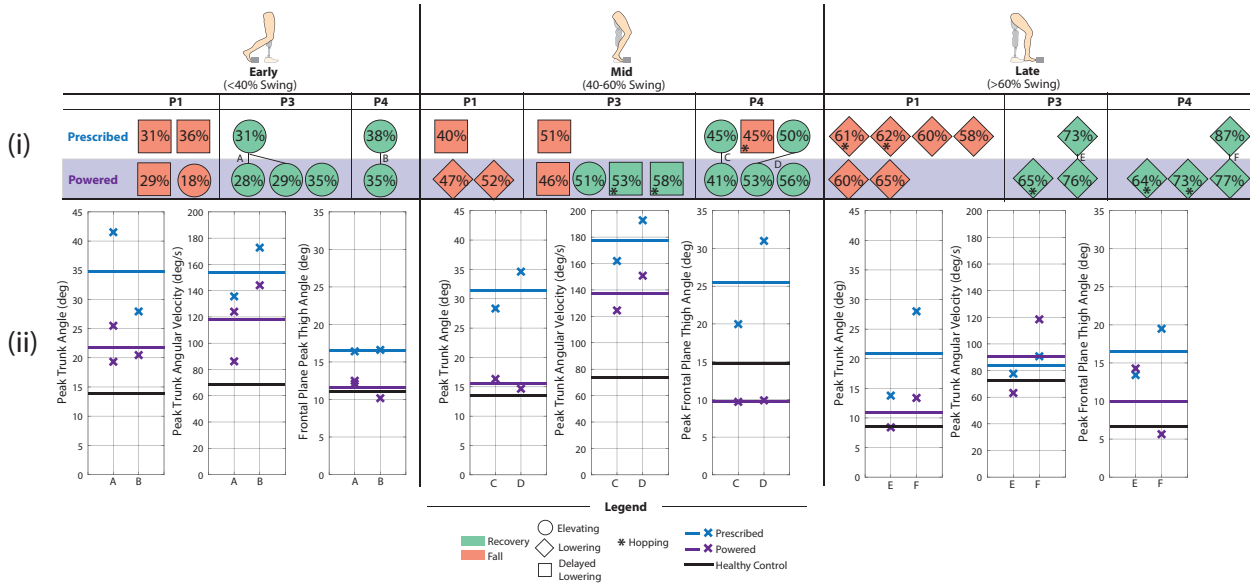

Figure 6.4: (i) Recovery strategy and fall outcomes and (ii) recovery deficiency metrics for early, mid, and late swing stumbles for each participant when wearing their prescribed prosthesis and the powered prosthesis intervention. An "x" represents a single data point, and a line is the average of trials in that category (prescribed, powered, or healthy control). Overall, recoveries with the powered prosthesis intervention (purple) involved less trunk flexion, less trunk flexion velocity, and less prosthetic-side thigh abduction relative to recoveries with prescribed passive prostheses (blue), and reached values closer to that of the healthy control (black), indicating better trunk control and less compensation during recoveries.

6.1.6 Discussion

6.1.6.1 Early swing

For early swing stumbles, the intra-participant fall rate did not change with the powered prosthesis intervention; P1 fell after every stumble in both the prescribed and powered prosthesis, while P3 and P4 recovered after every stumble. However, P1's responses were closer to recovery with the powered prosthesis. For one trial (18% swing), P1 completed the elevating strategy, clearing the obstacle and landing anterior to it, but fell after foot-strike. This was the only time P1 performed the elevating strategy after early swing sound-side stumbles, which has been previously suggested as key to recovering from early swing perturbations [28]. Likewise, for the second trial (29%), though he ultimately abandoned elevating and fell, his tripped limb's hip and knee flexed such that his foot elevated 6 and 11.5 cm higher than his two attempts when using his prescribed prosthesis (a substantial improvement considering the obstacle was 7.5 cm tall). This improvement in elevating the tripped limb is visually represented in Fig. 6.5.

Comparing P3 and P4's successful elevating strategies from similar perturbations (A and B in Fig. 6.4), recoveries using the powered prosthesis intervention involved less peak trunk flexion and trunk flexion velocity. Since controlling forward trunk motion has been considered integral to successful recovery, a reduction in these metrics can be considered an overall improvement in recovery, as this reflects the participants' ability to counter the forward angular momentum induced by the perturbation [38, 36]. This may be due to the counteracting torque of the powered prosthetic knee as the support limb, which is not available with typically prescribed passive prostheses [87, 88, 108]. Furthermore, the robust stance support of the powered knee allowed participants to trust loading the device (without risk of buckling) after the perturbation, which likely helped facilitate the execution of the elevating strategy. This decrease in trunk motion with the powered prosthesis intervention is visually represented in Fig. 6.6.

Additionally, P3 and P4 exhibited less thigh abduction in the next prosthetic-side step while using the powered pros-

thesis intervention. Initiating a step in non-cyclic scenarios (e.g., steps after stumble perturbations) is difficult with a passive device; thus, participants compensate by swinging their limb out laterally to initiate and complete a step with enough toe clearance to avoid scuffing [28]. However, with the powered prosthesis, unloading the device initiates the powered swing phase (active knee flexion and extension), which provides sufficient toe clearance without the need to abduct the thigh. This decrease in thigh abduction corresponding to active knee flexion is visually represented in Fig. 6.6.

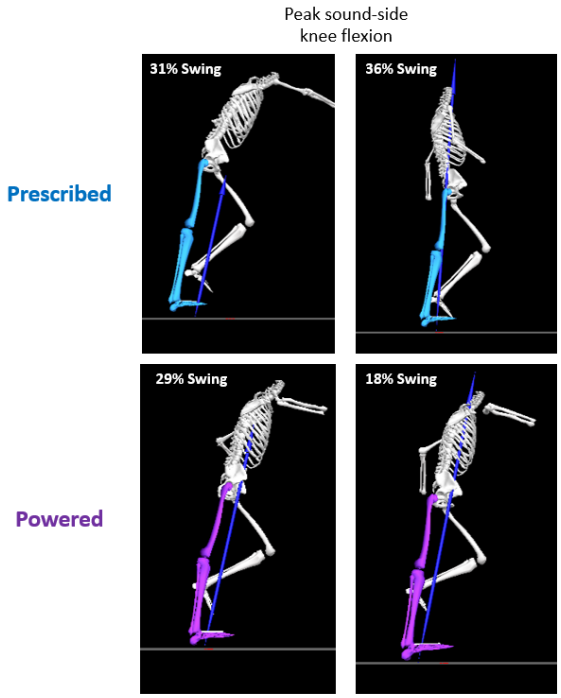

Figure 6.5: Motion capture 3D renderings of P1 at peak sound-side knee flexion after early swing stumbles. These frames visually depict the greater knee flexion and foot height achieved (recovery limb, white) after stumbles with the powered prosthesis intervention (support limb, purple) versus his prescribed passive prosthesis (support limb, blue). The robust stance support and active torques may have helped control trunk motion and increased user trust in loading the device, which promoted the elevating strategy approach.

6.1.6.2 Mid swing

For mid swing perturbations, the intra-participant fall rate did not change for P1 (fell after all stumbles), but improved for P3 and P4. P3 fell after the single mid swing stumble in her prescribed device, but recovered from 3/4 stumbles in the powered prosthesis intervention. Notably, for perturbations at the same swing percentage (51%), she fell with a delayed lowering strategy in her prescribed device but recovered using an elevating strategy with the powered device. Similarly, P4 fell after a delayed lowering strategy and recovered with two elevating strategies in his prescribed device, but recovered from all three perturbations with elevating strategies in the powered device. As suggested in the early swing subsection, the powered prosthesis intervention may promote successful execution of the elevating strategy. This is especially important for mid swing stumbles, which previously resulted in the highest fall rate with prescribed prostheses [28].

For P4's recoveries with elevating strategies from similar perturbations (C and D in Fig. 6.4), he exhibited less trunk flexion, trunk flexion velocity and thigh abduction during the recoveries with the powered prosthesis intervention, which as discussed earlier is considered an improvement in terms of fall risk and compensation techniques required to recover.

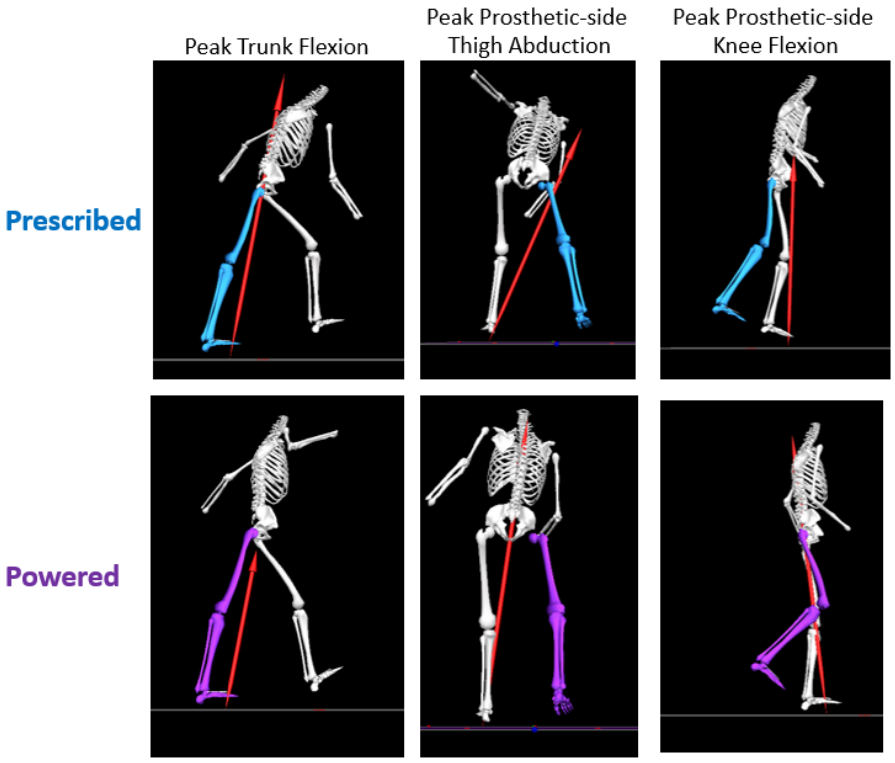

Figure 6.6: Motion capture 3D renderings of P3 at peak trunk flexion during the sound-side elevating step, and at peak prosthetic-side thigh abduction and knee flexion in the next prosthetic-side step. These frames visually depict less trunk flexion, less thigh abduction, and more knee flexion during the recovery with the powered prosthesis intervention (purpose) compared to her prescribed passive prosthesis (blue).

6.1.6.3 Late swing

For late swing stumbles, the intra-participant fall rate did not change with the powered prosthesis intervention; P1 fell after every stumble in both the prescribed and powered prosthesis, while P3 and P4 recovered after every stumble. Comparing similar perturbations from P3 and P4 (E and F in Fig. 6.4), peak trunk flexion was reduced with the powered prosthesis for both participants, peak trunk flexion velocity was reduced for P3 and peak thigh abduction was reduced for P4.

Note that in mid and late swing, P3 and P4 used lowering/delayed lowering with hopping to successfully recover with the powered prosthesis intervention; in these scenarios the knee maintained extension (i.e., did not buckle) during the landing, which allowed them to safely load both limbs and recover.

6.1.6.4 Limitations

There are several limitations to this work. Ideally, the study design would have accommodated an even number of trials, and more trials, per participant per condition (prescribed versus powered prosthesis). However, due to the involved experimental setup and taxing nature of the protocol, this was not possible for all participants. Similarly, an ABA testing style would be preferable for this study; however, due to participant availability it was not reasonable or possible for some participants to return for more multi-hour sessions.

6.1.6.5 Future Directions

Based on the results from this study, the authors recommend several directions for future work. First, for this study the powered prosthetic knee did not have any stumble detection feature; rather, its behavior was dictated by a simple walking controller. It is noteworthy that improvements in fall rate, trunk motion, and thigh abduction were seen with this simple intervention; however, introducing a stumble detection feature that increases swing time after a lowering strategy may further improve recovery metrics for late swing perturbations. Second, in this study participants were informed of the powered knee's key behaviors that might help them during stumbles (i.e., it can be loaded without buckling, and it will take a step when unloaded), but they were not introduced to stumbles until the actual data collection. It is again noteworthy that improvements were seen given the limited time on the device prior to the stumble experiments, highlighting that features of a simple closed-loop walking controller can provide recovery benefits; however, more time with the interventional device and some familiarization with stumbling on the device may have helped participants trust the device more and further improve responses. Finally, only the knee joint was powered with this intervention; including a powered ankle joint may (1) increase the counteracting torques as the support limb during an elevating strategy and help further reduce forward angular momentum and (2) help jump-start a step after the lowering strategy, which may have benefited P1 (who was older and potentially less able to control prosthetic-side thigh motion).

Aside from improvements to the powered knee prosthesis intervention alone, incorporating other interventions may benefit prosthesis users. Previous works have suggested the benefit of muscle strength training [90] and compensatory step training [35] for transfemoral prosthesis users. These interventions have yet to be tested for this population, and incorporating these trainings with the powered prosthesis may maximize stumble recovery improvement.

6.1.6.6 Conclusion

This is the first study to show the effects of a powered knee prosthesis with closed-loop walking controller in transfemoral prosthesis users when responding to sound-side stumbles. Observations from the testing indicated that the robust stance support of the powered prosthesis served to help counter perturbation-induced forward angular momentum and control trunk motion during elevating strategy recoveries and prevent knee buckling during recovery, evidenced by reduced trunk flexion and flexion velocity during recoveries and fewer falls in mid swing. Additionally, the powered swing phase served to reduce compensatory thigh abduction in the next step of recovery. Incorporating task-specific training with the powered prosthesis intervention, along with muscle strength and coordination exercise protocols, may further improve recoveries for transfemoral prosthesis users.

6.2 Part 2: Efficacy of a powered knee prosthesis with closed-loop walking controller and stumble recovery assistance in reducing falls and recovery deficiencies after prosthetic-side stumbles

6.2.1 Part 2 Summary

Transfemoral prosthesis users' high stumble and fall rate leads not only to injuries and related medical expenses but also to loss of confidence due to fear of falling. Previous works have identified deficiencies in typically-prescribed, passive prostheses that lead to falls and recovery deficiencies such as increased trunk motion and thigh abduction. Powered prosthetic knees have the potential to address these deficiencies, but to date such an intervention has not been tested with transfemoral prosthesis users. Thus, three unilateral, transfemoral prosthesis users underwent a stumble obstacle perturbation experiment, in which they were introduced to stumbles to their prosthetic limb in early, mid and late swing phase while wearing a powered knee prosthesis intervention. The powered knee prosthesis employed a closed-loop walking controller (i.e., impedance control in stance and trajectory control in swing) as well as a stumble recovery controller (i.e., detected stumble and performed elevating or lowering strategy assistance). Fall outcome, recovery strategy, as well as trunk and thigh kinematics were recorded in order to compare responses with the powered prosthesis intervention to responses with their prescribed, passive prosthesis. For trials in which the device's and user's strategy selection matched, the powered prosthesis intervention overall improved the fall rate relative to responses with prescribed, passive prostheses (though there was an uneven number of trials for each case). Additionally, overall responses with the powered prosthesis intervention involved less trunk flexion, trunk flexion velocity, and prosthetic-side thigh abduction relative to responses with prescribed prostheses, indicating better trunk control and a reduction in compensation techniques. These results provide initial indications that this type of powered knee prosthesis is a viable intervention for reducing falls and recovery deficiencies for this population, which may be attributed to its robust stance support, powered swing phase, and active elevating strategy.

6.2.2 Introduction

Chapters 1, 5, and 6 (Part 1) highlight the high stumble and fall rate of transfemoral prosthesis users, which necessitates prosthetic interventions to address response deficiencies. Previous chapters focused on interventions for mitigating falls and recovery deficiencies of sound-side stumbles. In this work, a powered prosthesis intervention to address prosthetic-side stumbles is explored.

Several previous works have studied transfemoral prosthesis user responses to prosthetic-side interventions. These studies reported elevating, lowering, and delayed lowering strategies, as defined in previous works [101, 24], as well as hopping or skipping strategies. Crenshaw et al. [17] stumbled transfemoral prosthesis users in mid to late swing phase in an overground obstacle perturbation setup. One out of four stumbles resulted in a fall, which was attributed to knee buckling upon lowering after perturbation. Shirota et al. [108] stumbled transfemoral prosthesis users throughout swing phase but did not report any falls; however, the experimental setup included handrails and the perturbation did not involve a physical obstacle to clear, which may account for the differences in recovery strategy and fall outcomes.

King et al. 2022a [52] tripped transfemoral prosthesis users throughout swing phase in an obstacle perturbation setup and concluded that four key prosthesis deficiencies contributed to falls after prosthetic-side stumbles: (1) buckling in stance phase, (2) poor extension in swing phase, (3) poor swing initiation after perturbation, and (4) the lack of ability to perform the elevating strategy. First, in this study transfemoral prosthesis users experienced knee buckling upon landing the initial lowering or elevating step due to insufficient stance limb flexion resistance. Second, poor swing extension assistance during the initial elevating or lowering step led to delayed or shorter steps and further biased the prosthesis towards buckling in stance phase. Third, insufficient swing initiation in subsequent recovery steps led to falls or required substantial thigh abduction to recover. Fourth, the lack of ability to perform the elevating strategy (which requires coordinated hip and knee flexion and extension to clear the obstacle in the same step) in early swing often resulted in falls. All of these deficits led to increased trunk flexion and flexion velocity during recoveries relative to healthy control recoveries, which indicates an increased fall risk [37, 35, 36].

There have been some attempts to incorporate behaviors into prosthetic knees that would reduce the risk of falling due to perturbations in swing phase. For example, the Ottobock C-Leg (a commonly prescribed microprocessor-controlled knee) includes functionality that increases the resistance to flexion in late swing phase (during extension), with the

aim to promote safe loading of the leg in the event of a stumble [8]. While studies have shown this feature to improve stumble recovery with respect to falls and compensation techniques compared to other passive prosthetic knees on the market [11, 8, 7, 12], the stumble behavior still proves deficient. Falls still occurred in these studies, and recoveries still required compensation techniques (e.g., thigh abduction) to clear the obstacle after the lowering step. Moreover, this approach does not provide any active response to the stumble due to lack of power, so the elevating strategy for recovery still cannot be employed.

Given the inability of microprocessor-controlled knees to account for the aforementioned deficiencies, powered knee prostheses have the potential to fill this gap. Several works have suggested the potential for powered prosthetic knees to help in addressing the deficits of typically prescribed passive devices and consequently reduce fall likelihood [17, 108, 34, 115, 52]. Indeed, powered prosthetic knees (e.g., research devices ([56, 58, 3]) and devices on the market (Ossur Power Knee, Reboocon Bionics IntelLeg Knee)) have the potential to address all four deficiencies outlined in [52]. Specifically, powered knees can provide robust stance support with load-based stance initiation and impedance control, addressing deficiency (1). Second, powered swing phase with load-based initiation and a trajectory-tracking controller may help initiate and complete a full swing phase without the need to abduct the thigh, addressing deficiencies (2) and (3). Finally, the ability to provide active flexion and extension could enable the elevating strategy for early swing stumbles, addressing deficiency (4).

Despite this potential for stumble recovery improvement, only a few studies have explored a powered knee prostheses for stumbles. Gordon et al. 2019 [34] proposed and validated an obstacle avoidance controller which uses prosthetic limb kinematics to predict the user's intent to avoid an obstacle and correspondingly alters the trajectory of the limb to clear the obstacle. While this is an interesting and useful feature for a prosthetic limb to have, it does not address the event of unexpectedly stumbling; rather, it requires the volitional intent of the user to avoid stumbling. Thatte et al. 2019 [116] presented a controller that uses a laser sensor and IMU to predict a stumble event and correspondingly alter the leg trajectory to avoid falling, the first stumble controller to incorporate visual feedback. This controller has been tested on one able-bodied user with an artificially induced stumble event (user-initiated scuff) so far, and future work was suggested to test on transfemoral prosthesis users and explore other optimization techniques for further impact. Thatte et al. 2016 [115] proposed and tested a hybrid neuromuscular control policy and analyzed its response to unexpected disturbances during swing, which successfully responded with an elevating strategy after early swing disturbances and a lowering strategy after late swing disturbances. This controller was tested on one able-bodied user with a simulated disturbance to the knee joint, and future work was suggested to test on transfemoral prosthesis users at faster walking speeds and address mid swing stumbles. Other works have investigated methods for stumble detection, stumble type classification, and recovery strategy classification [55, 126] but have not implemented them in a powered knee. Thus, the efficacy of a powered knee in mitigating falls after prosthetic-side stumbles for transfemoral prosthesis users has yet to be comprehensively evaluated.

Therefore, the objective of this work is to evaluate the extent to which a powered knee prosthesis with a closed-loop walking controller and active stumble recovery responses may mitigate (i) fall rate and (ii) recovery deficiencies (e.g., increased trunk motion and thigh abduction) for transfemoral prosthesis users relative to their prescribed prosthesis following prosthetic-side stumbles.

6.2.3 Methods

6.2.3.1 Interventional Device: Powered Knee Prosthesis

Hardware

Readers are referred to Chapter 6, Part 1 for device hardware details.

Walking Controller

The readers are referred to Chapter 6, Part 1 for walking controller details.

Note that the features of active stance support and powered swing with load-based initiation are unique to the inter-

ventional device (i.e., versus participants' passive prescribed prostheses) and have the potential to address deficiencies (1-3).

Stumble Recovery Controller

The stumble recovery controller used for this experiment is depicted in Fig. 6.7 below and designed by Shane King, detailed in [51]. Briefly, the approach looks at the shank-thigh angle configuration space trajectory immediately after impact with the obstacle, compared to the configuration space of a typical gait cycle (i.e., prior to the perturbation), to decide whether to implement the elevating strategy or the lowering strategy. For the elevating strategy, the knee tracks a spline similar to swing phase, with a greater peak knee flexion angle. For the lowering strategy, the knee enters the stance state to facilitate the lowering step, then increases flexion in its subsequent swing phase in order to clear the obstacle.

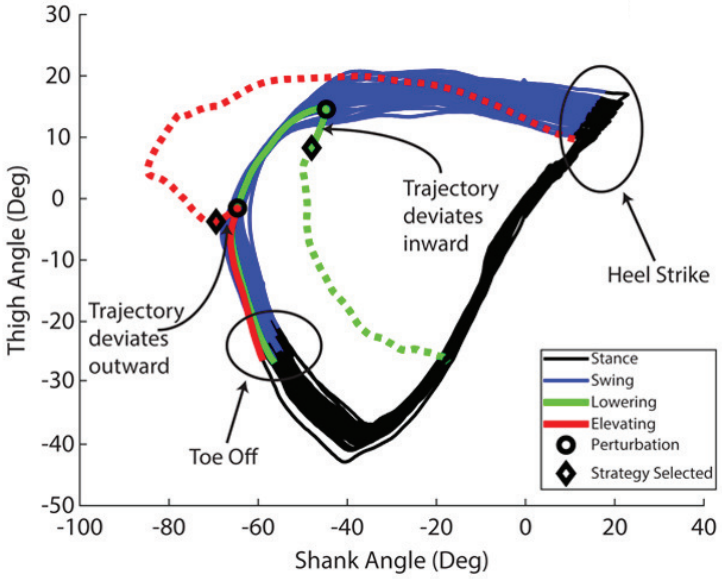

Figure 6.7: Diagram of approach for the powered knee stumble recovery controller. The shank-thigh configuration space for a typical gait cycle (stance in black, swing in blue) is superimposed with the configuration space trajectories of a representative elevating strategy (red) and lowering strategy (green). The stumble recovery controller looks at the configuration space immediately after the perturbation (20 ms, from circle to diamond) to determine whether to implement the elevating or lowering strategy. If the trajectory deviates outward from the typical swing path, elevating is implemented, as shown by the dotted red line; if the trajectory deviates inward, lowering is implemented, as shown by the dotted green line. (Figure courtesy of [52]]

Note that this active response to the perturbation is unique to the powered knee prosthesis intervention and not available in typically prescribed passive prostheses, potentially addressing deficiency (4).

6.2.3.2 Experimental Protocol & Data Analysis

The experimental protocol and data analysis for this study are identical to Chapter 6, Part 1, with two exceptions: (1) prosthetic-side stumbles are analyzed rather than sound-side stumbles; (2) participants underwent a training protocol that introduced the active recovery strategies provided by the powered prosthesis intervention prior to testing, as detailed in the following subsection.

Stumble Recovery Strategy Training

After prosthesis fitting and walking controller familiarization and tuning, the participant was introduced to the elevating strategy. They were coached to continue swinging their limb upon contact with the obstacle and trust that

the powered knee would quickly bend and straighten to clear the obstacle. They were repeatedly introduced to early swing perturbations in an incremental fashion until they could comfortably coordinate their response with the device's response. Specifically, they first were allowed to watch the obstacle encounter the prosthesis and use the handrails to recover. Then they were advised to wear the sensory occlusion equipment (i.e., white noise in earbuds, noise-cancelling headphones, inferior vision-blocking goggles) but still had access to the handrails. Finally, the handrails were removed (in some cases, one at a time).

Next, the participant was re-introduced to the lowering strategy (a strategy more familiar to them, as this is the typical response of passive prosthetic knees). They were incrementally introduced to this perturbation in the same manner as the elevating strategy.

Finally, the participant was introduced to the elevating and lowering strategies in random order, first with then without the handrails and sensory occlusion equipment. Once the participant successfully coordinated with the prosthesis response in this setup, they were considered to have passed the training segment.

Note that controller performance will be comprehensively analyzed in a separate work; however, the intent of this work is to assess how correct stumble recovery assistance affected responses. Thus only trials in which the device's and user's strategy selection matched were included in the analysis.

6.2.4 Results

Overall, three out of 31 successful stumble trials resulted in falls (10%) with the powered prosthesis intervention, compared to four out of 13 trials (32%) with the prescribed prostheses. Trials were grouped into early swing (<35% swing), mid swing (35-55% swing) and late swing (>55% swing) for analysis. To address objective (i), the full breakdown of fall outcomes and recovery strategies attempted for each trial in early, mid and late swing phase is reported in Fig. 6.8 (i) for each participant. To address objective (ii), recovery deficiency metrics (peak trunk flexion angle, peak trunk flexion velocity, and peak prosthetic-side thigh abduction) are reported in Fig. 6.8 (ii) to compare powered versus prescribed recoveries. As in Chapter 6 (Part 1), results from a single healthy control participant are included in Fig. 6.8 (ii) for reference, which plots the average values from six early swing elevating strategies, two mid swing delayed lowering strategies, and three late swing lowering strategies.

6.2.5 Discussion

6.2.5.1 Early Swing

For early swing stumbles, the intra-participant fall rate improved for P3 and P4 (fell after 50% of prescribed prosthesis stumbles, but recovered from all powered prosthesis stumbles). P1 recovered from his single prescribed prosthesis trial; however, this recovery involved a full-body transverse plane 90-degree turn upon initial loading of the prosthetic limb, followed by hopping on the sound limb and substantial side-stepping before returning to steady-state forward walking gait. P1 recovered from five of six stumbles with the powered prosthesis intervention. In all cases he successfully completed the elevating strategy, clearing the obstacle in the same step which allowed him to avoid turning and side-stepping. For one of P1's powered prosthesis trials, he completed the elevating strategy but lost his footing after several steps and ultimately fell. However, overall using the elevating strategy (which was not possible for five of six prescribed prosthesis trials) resulted in a higher recovery rate.

Comparing P1 and P3's recoveries, using the powered prosthesis intervention with the elevating strategy involved less peak trunk flexion and trunk flexion velocity compared to their delayed lowering strategies on their prescribed prosthesis. This suggests that implementing the elevating strategy when appropriate helps control trunk motion, which has been identified as a key component of successful stumble recovery [36, 87, 88]. A reduction in trunk flexion metrics was not observed with P4's powered prosthesis trials compared to prescribed prosthesis trials, as he used the elevating strategy in both cases.

For all three participants, thigh abduction was reduced with the powered prosthesis intervention relative to prescribed

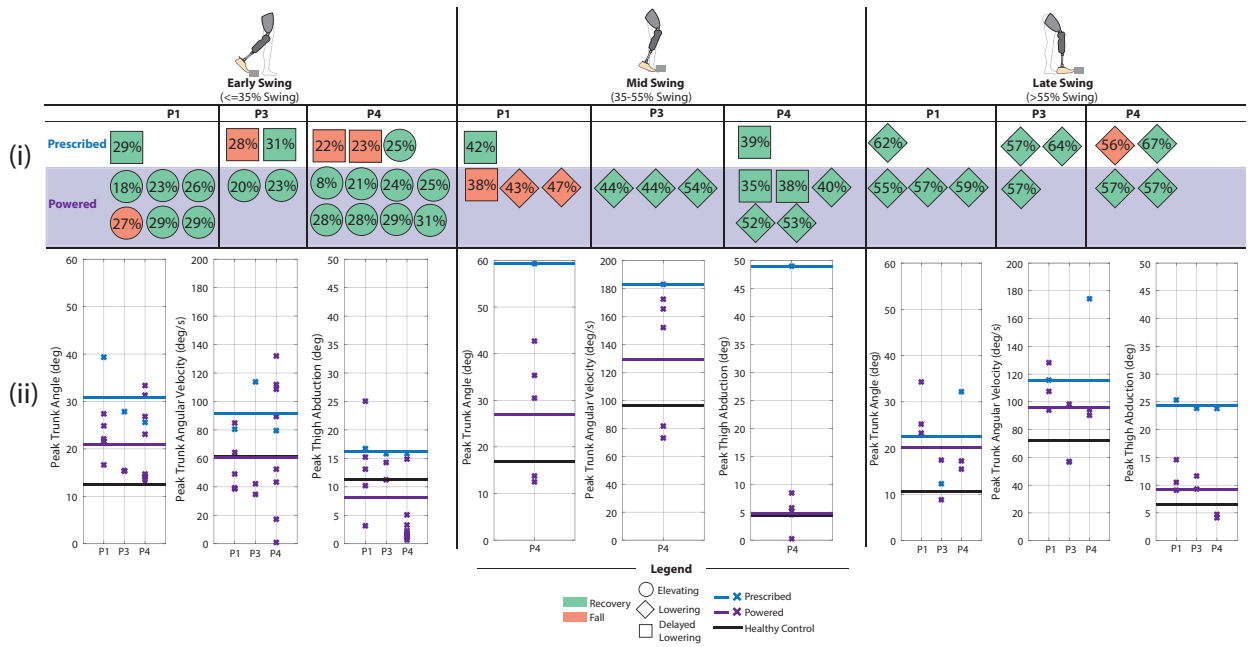

Figure 6.8: (i) Recovery strategy and fall outcomes and (ii) recovery deficiency metrics for early, mid, and late swing stumbles for each participant when wearing their prescribed prosthesis and the powered prosthesis intervention after prosthetic-side stumbles. An "x" represents a single data point, and a line is the average of trials in that category (prescribed, powered, or healthy control). Overall, recoveries with the powered prosthesis intervention (purple) involved less trunk flexion, less trunk flexion velocity, and less prosthetic-side thigh abduction relative to recoveries with prescribed passive prostheses (blue), and reached values closer to that of the healthy control (black), indicating better trunk control and less compensation during recoveries.

prostheses for all but one trial. The powered prosthesis provides load-based swing initiation and powered swing motion (i.e., active flexion and extension), which reduced the thigh abduction compensation technique used with prescribed prostheses to initiate and complete swing phase with enough toe clearance.

6.2.5.2 Mid swing

For mid swing perturbations, the intra-participant fall rate worsened for P1 and did not change for P4. P1 recovered from his single mid swing perturbation with his prescribed prosthesis, but he fell after all three mid swing perturbations with the powered prosthesis intervention. However, P1's recovery on his prescribed prosthesis still involved deficiencies: he used substantial thigh abduction with a hopping strategy before turning 90 degrees and side-stepping for approximately 10 steps prior to returning to a steady-state, forward walking gait. During P1's stumbles with the powered prosthesis, the knee's quick, active extension to implement the lowering strategy appeared to drive rapid thigh extension that induced forward trunk flexion which limited his recovery step and resulted in a fall. Perhaps a modification to the lowering strategy control action (e.g., extend over a longer period of time, or lock joint at its loaded angle rather than extend) would have reduced this trunk flexion and helped P1 recover. P4 recovered from all mid swing perturbations.

Comparing P4's mid swing recoveries, he exhibited less peak trunk flexion, flexion velocity, and thigh abduction with the powered prosthesis intervention relative to his prescribed prosthesis. During the recovery with his prescribed prosthesis, he initially elevated but abandoned elevating, lowering behind the obstacle with substantial trunk flexion and a quick sound-side step. He then hopped from his sound limb while swinging his prosthetic limb laterally to complete the prosthetic-side step. During the powered prosthesis trials, the device's quick stumble detection and implementation of the lowering strategy (active extension) allowed P4 to land behind the obstacle (initial loading)

quicker than with his prescribed prosthesis (which involved a delayed reaction time likely due to lack of proprioception and required hip extension to extend the passive prosthesis). This quicker initial loading allowed more time to execute a longer recovery step with the sound limb, reducing trunk motion compared to the prescribed prosthesis trials. The powered prosthesis then completed the lowering strategy with a powered swing phase in the next step to clear the obstacle. This active knee flexion and extension eliminated the need to abduct (i.e., swing entire leg out laterally) in order to initiate swing phase and clear the obstacle, as P4 did with the prescribed prosthesis.

6.2.5.3 Late swing

For late swing perturbations, the intra-participant fall rate did not change for P1 or P3 (recovered after all stumbles) but improved for P4. P4 fell after one of two stumbles with his prescribed prosthesis but recovered from all four stumbles on the powered prosthesis intervention. During the late swing fall, P4's prescribed knee prosthesis flexed upon contact with the obstacle and landed behind the obstacle still flexed such that it buckled upon loading. The robust stance support with the powered knee prosthesis eliminates the possibility of buckling while loaded.

Comparing recoveries from like perturbations, P4's peak trunk flexion and flexion velocity decreased with the powered prosthesis intervention relative to his prescribed prosthesis, but this trend was not observed for P1 or P3. This may reflect the participants' core strength in their response to the rapid knee extension in the powered knee's lowering strategy, which may have induced trunk flexion, as discussed in P1's mid swing stumble responses.

However, for all three participants thigh abduction was decreased with the powered prosthesis relative to prescribed prostheses, due to the active flexion and extension provided by the powered swing phase that eliminates the need to abduct to initiate swing phase and/or clear the obstacle.

6.2.6 Limitations

There are several limitations to this work. First, ideally this comparison would have comprised an even number of trials for each case (prescribed versus powered prosthesis), and preferably an ABA study design. Unfortunately due to the taxing nature of this protocol, stumbles were capped per session to prevent fatigue, and participant availability was limited for multiple multi-hour sessions. As such, this work was intended to provide a preliminary analysis of the effect of the powered prosthesis intervention and insights for future innovation, which were accomplished.

Second, one could argue that allowing training for the powered prosthesis intervention biased results for that case. However, the intent of this work was to compare how individuals typically respond with their prescribed prosthesis (which they have previously been fit to and trained on extensively) versus how they respond when properly using a new powered intervention. It would have been unfair to not introduce the individuals to the new powered prosthesis behaviors prior to testing; rather, the authors contend that this training is akin to typical and necessary learning of how to use a new type of prosthesis.

6.2.7 Future Directions

The promising results of this work invite future studies to build upon these findings. First, testing this powered prosthesis intervention on more individuals may help bolster the results presented in this work. Additionally, the inclusion of more outcome metrics (e.g., steps to steady-state walking, frontal and transverse plane trunk metrics, etc.) to quantify recovery deficiency would provide more insight into prosthesis user responses. In future experiments, modifications to the lowering strategy (as highlighted in Discussion) may further improve outcome metrics.

The authors note that a powered prosthesis is not the only possible intervention to reduce falls for prosthetic-side stumbles for this population; future works could explore its combination with task-specific training and/or muscle strength training [35, 90]. Additionally, some behaviors provided by the powered prosthesis (e.g., more robust stance support) may be implementable in passive or quasi-powered prostheses.

6.2.8 Conclusions

Overall, the results of this work provide preliminary evidence of the efficacy of a powered knee prosthesis as an intervention for stumble recovery for transfemoral prosthesis users. The active elevating strategy reduced falls and trunk motion after early swing stumbles, the robust stance support eliminated buckling and subsequent falls, and the powered swing phase reduced compensatory thigh abduction relative to prescribed prosthesis stumble outcomes. Such behaviors offer promising solutions towards improving stumble recovery and ultimately reducing falls and the effects of falling for this population.

CHAPTER 7

Conclusion

7.1 Conclusions

The results of this dissertation address a crucial gap in the current development of lower-limb wearable assistive devices: accounting for stumble perturbations. Understanding what behaviors might improve stumble recovery and how to implement them had received little exploration thus far in the field. In this work, stumble recovery behaviors were proposed based on experimental insights, designed for real-time use, and implemented into a robotic knee prosthesis and exoskeleton with favorable fall risk outcomes. This thesis comprises the most complete examination to date of how stumble recovery behaviors might be implemented into lower limb exoskeletal and prosthetic knee devices, and to what extent they might be effective in reducing the likelihood of falls.

Regarding exoskeletons, the three key elements of a stumble recovery controller were designed and tested in a powered knee exoskeleton: stumble detection, stumble recovery strategy identification, and stumble recovery strategy assistance. Detection and identification algorithms yielded high detection and classification accuracies when tested with real-time exoskeleton sensor data from a substantial dataset of stumbles – the critical first steps in implementing any exoskeleton assistance. Elevating strategy assistance was shown to improve elevating limb kinematics and reduce fall risk metrics for three healthy adults whose recovery was impaired due to leg weights attached to the shank – the first study to show recovery limb exoskeleton assistance to be a viable intervention for mitigating fall risk. These works offer promising approaches to account for stumble perturbations in exoskeletons, which may ultimately contribute to increased exoskeleton user safety and improved stumble recovery for fall-prone populations.

Regarding prostheses, several active behaviors were incorporated into a powered knee prosthesis as a stumble recovery intervention. Primarily, sound-side stumbles were considered, which was a completely unexplored area of research. Thus behaviors were designed based on deficiencies identified from stumble experiments with participants wearing their prescribed passive prosthesis – the most comprehensive analyses of swing-phase obstacle perturbation responses for transfemoral prosthesis users to date. An active closed-loop walking controller was shown to decrease trunk motion (i.e., fall risk) and thigh abduction (i.e., compensation technique to initiate and complete swing phase) during recoveries, which was attributed to robust stance support and load-initiated, powered swing phase. Additionally, stumble recovery assistance following prosthetic-side stumbles was tested. Incorporating a powered elevating strategy reduced falls in early swing and reduced trunk motion (i.e., fall risk), and powered swing phase again reduced thigh abduction. Collectively these works offer promising approaches to improving stumble recovery for transfemoral prosthesis users by considering trips to both the sound and prosthetic limb, which may ultimately contribute to a decrease in fall risk and associated effects of falling, a major issue for this population.

These promising innovations in robotic lower-limb prostheses and exoskeletons were tested using a custom obstacle perturbation system and informed by the healthy adult response to stumble perturbations. First, this novel experimental setup and protocol is the only system to date shown to introduce obstacle perturbations during treadmill walking that were realistic, unexpected, targetable, and allowed for biomechanics evaluation. The system proved invaluable in the iterative design process required to develop these stumble recovery interventions. Second, the healthy adult response had previously been characterized in numerous works, but the phenomenon of strategy selection remained unanswered. A machine learning approach applied to a dataset of healthy adult stumbles elucidated this decision process, ultimately forming the foundation for the exoskeleton recovery strategy identification algorithm.

In conclusion, this work uses novel experimental techniques and comprehensive biomechanics analyses to propose and test robotic knee prosthesis and exoskeleton interventions for stumble recovery. In the end, knee assistance at both the recovery and support limb yielded promising results for improving stumble recovery and ultimately reducing fall risk for many populations.

7.2 Future Directions

The work presented in this dissertation offers exciting opportunities for future innovation. Since the implementation of stumble recovery behaviors was a new and underexplored field, it was necessary in this work to start with a narrow investigation space as a first attempt at designing and testing interventions. However, with this foundation in place, approaches that broaden the scope of these suggested applications would certainly contribute to the overarching goal of reducing fall risk and improving safety of lower-limb prostheses and exoskeletons.

To start, the obstacle perturbation system and protocol can be used to characterize stumble recovery for many additional populations with high fall risk. Similar to transfemoral prosthesis users, for many populations (e.g., elderly, stroke survivors, post-polio patients, individuals with cerebral palsy or multiple sclerosis) retrospective studies report high fall rates relative to healthy controls, but relatively little research has been done to actually study and identify deficiencies in their responses. Such studies would help develop further interventions to reduce their fall risk. Additionally, the obstacle perturbation system could be used to test other obstacle perturbation scenarios. For example, stumble recovery during sloped walking or at various speeds has yet to be explored.

Second, there are several open questions regarding how to best design the assistance profile. This work shows that when coordinated with the user's intent, knee recovery strategy assistance can improve stumble recovery outcomes; however, the recovery strategy identification algorithm developed in this work correctly predicted the user's intent for 96% of stumbles. Therefore, the field would benefit from a more comprehensive examination of the following questions: Should the assistance be bimodal (i.e., make a decision between two strategies) or unimodal (only perform one strategy)? More specifically, to what extent can a bimodal response coordinate with the user's intent, and what are the implications of implementing assistance contrary to the user's intent? Are there situations in which either strategy is sufficient? Ultimately, which type of response is safest for the user? Furthermore, there are opportunities to optimize the assistance provided: the timing, magnitude, and control scheme could be explored to maximize recovery benefit. Additionally, future studies could consider assisting the hip or ankle joint in addition to the knee, as well as bilateral interventions that provide assistance to both limbs during stumble recovery.

Third, the interventions tested here were applied to transfemoral prosthesis users and healthy adults with a simulated impairment. Future work could assess the extent to which these behaviors apply to other fall-prone populations (and to what extent these conclusions are population- or pathology-specific).

Finally, the interventions proposed and tested here focus on a specific type of unexpected perturbation: a stumble. However, other perturbations, such as slips or postural disturbances also warrant future research to ultimately reduce fall risk in prostheses and exoskeletons.

This work has set the foundation for the future of stumble recovery in assistive devices by (1) studying and characterizing stumble recovery, (2) using insights from experiments to design and test interventions, and (3) suggesting successful and feasible robotic knee exoskeleton and prosthesis behaviors. Future work can broaden the scope of work with the same approach.

CHAPTER 8

Appendix

The following are included as supplementary files to this dissertation:

Chapter 2

- Additional file 1: A compilation video of a single subject recovering from a range of variously timed perturbations throughout swing phase. The subject is walking at 1.1 m/s. Elevating, lowering, and delayed lowering strategies are demonstrated.
- Additional file 2: CAD files detailing the design of the Obstacle Delivery Apparatus in full (ramp, block, and magnet). McMaster-Carr part numbers are included in the properties for applicable parts.
- Additional file 3: A script containing the essential functions to the operation of the Predictive Targeting Algorithm. Intended as a guide for similar systems.

Chapter 3

- Supplementary material: The purpose of this Supplementary Material is to provide intermediate/extended results such that readers with similar but slightly diverging research questions or potential applications can better understand what signals and approaches may work best for their purposes. Sections A and B provide additional results from the feature exploration and feature selection processes, respectively. Section C provides additional figures from Experiment B to help visualize results. Section D provides feature selection results from alternate strategy selection frameworks.

Chapter 4, Part 1

- Supplementary material: This video shows implementation of the stumble recovery controller in a knee exoskeleton worn by a healthy adult participant. Both walking and stumble trials are presented.For walking trials, three conditions are shown: a) not wearing the exoskeleton; b) wearing the exoskeleton with assistance turned off; and c) wearing the exoskeleton with walking controller enabled (Fig. 4.5).For stumble trials, five experimental cases are shown, as described in detail in the paper: 1) No Exo; 2) No Change; 3) Turn Off; 4) Reflex; 5) Opposite. Note that only one recovery strategy (elevating) is shown here (Fig. 4.6).

Chapter 5

- Additional file 1: A compilation video of each participant's stumble responses in early swing ($<$40% swing phase). If a participant experienced more than one perturbation in early swing, it is identified by a lower-case letter which is used in the main text and figures. Refer to Fig. 5.2 for fall/recovery outcome, strategy, and swing percentage of each stumble.
- Additional file 2: A compilation video of each participant's stumble responses in mid swing (40-60% swing phase). If a participant experienced more than one perturbation in mid swing, it is identified by a lower-case letter which is used in the main text and figures. Refer to Fig. 5.2 for fall/recovery outcome, strategy, and swing percentage of each stumble.
- Additional file 3: A compilation video of each participant's stumble responses in late swing ($>$60% swing phase). If a participant experienced more than one perturbation in late swing, it is identified by a lower-case

letter which is used in the main text and figures. Refer to Fig. 5.2 for fall/recovery outcome, strategy, and swing percentage of each stumble.

References

[1] Y. Akiyama, Y. Fukui, S. Okamoto, and Y. Yamada. Effects of exoskeletal gait assistance on the recovery motion following tripping. *PLOS ONE*, 15(2):e0229150, Feb. 2020.

[2] N. Aliman, R. Ramli, and S. Haris. Design and development of lower limb exoskeletons: A survey. *Robotics and Autonomous Systems*, 95:102–116, Sept. 2017.

[3] A. F. Azocar, L. M. Mooney, J.-F. Duval, A. M. Simon, L. J. Hargrove, and E. J. Rouse. Design and clinical implementation of an open-source bionic leg. *Nature Biomedical Engineering*, 4(10):941–953, Oct. 2020. Bandiera_abtest: a Cc_license_type: cc_by Cg_type: Nature Research Journals Number: 10 Primary_atype: Research Publisher: Nature Publishing Group Subject_term: Biomedical engineering;Electrical and electronic engineering;Mechanical engineering;Medical research Subject_term_id: biomedical-engineering;electrical-and-electronic-engineering;mechanical-engineering;medical-research.

[4] S. P. Baker and A. H. Harvey. Fall Injuries in the Elderly. *Clinics in Geriatric Medicine*, 1(3):501–512, Aug. 1985.

[5] C. Bayón, A. Q. L. Keemink, M. van Mierlo, W. Rampeltshammer, H. van der Kooij, and E. H. F. van Asseldonk. Cooperative ankle-exoskeleton control can reduce effort to recover balance after unexpected disturbances during walking. *Journal of NeuroEngineering and Rehabilitation*, 19(1):21, Feb. 2022.

[6] M. Belanger and A. E. Patla. Phase-dependent compensatory responses to perturbation applied during walking in humans. *Journal of Motor Behavior*, 19(4):434–453, Dec. 1987. Publisher: Routledge _eprint: https://doi.org/10.1080/00222895.1987.10735423.

[7] M. Bellmann, T. M. Köhler, and T. Schmalz. Comparative biomechanical evaluation of two technologically different microprocessor-controlled prosthetic knee joints in safety-relevant daily-life situations. *Biomedical Engineering / Biomedizinische Technik*, 64(4):407–420, Aug. 2019. Publisher: De Gruyter Section: Biomedical Engineering / Biomedizinische Technik.

[8] M. Bellmann, T. Schmalz, and S. Blumentritt. Comparative biomechanical analysis of current microprocessor-controlled prosthetic knee joints. *Archives of Physical Medicine and Rehabilitation*, 91(4):644–652, Apr. 2010.

[9] W. P. Berg, H. M. Alessio, E. M. Mills, and C. Tong. Circumstances and consequences of falls in independent community-dwelling older adults. *Age and Ageing*, 26(4):261–268, 1997.

[10] S. Blumentritt, H. W. Scherer, J. W. Michael, and T. Schmalz. Transfemoral Amputees Walking on a Rotary Hydraulic Prosthetic Knee Mechanism: A Preliminary Report. *JPO: Journal of Prosthetics and Orthotics*, 10(3):61–70, July 1998.

[11] S. Blumentritt, T. Schmalz, and R. Jarasch. The Safety of C-Leg: Biomechanical Tests:. *JPO Journal of Prosthetics and Orthotics*, 21(1):2–15, Jan. 2009.

[12] J. H. Campbell, P. M. Stevens, and S. R. Wurdeman. OASIS 1: Retrospective analysis of four different microprocessor knee types. *Journal of Rehabilitation and Assistive Technologies Engineering*, 7:2055668320968476, Jan. 2020. Publisher: SAGE Publications Ltd STM.

[13] M. Cenciarini and A. M. Dollar. Biomechanical considerations in the design of lower limb exoskeletons. In *2011 IEEE International Conference on Rehabilitation Robotics*, pages 1–6, June 2011.

[14] S. Chihuri and C. K. Wong. Factors associated with the likelihood of fall-related injury among people with lower limb loss. *Injury Epidemiology*, 5:42, Nov. 2018.

[15] A. F. Cordero, H. J. F. M. Koopman, and F. C. T. van der Helm. Mechanical model of the recovery from stumbling. *Biological Cybernetics*, 91(4):212–220, Oct. 2004.

[16] J. R. Crenshaw, K. R. Kaufman, and M. D. Grabiner. Compensatory-step training of healthy, mobile people with unilateral, transfemoral or knee disarticulation amputations: A potential intervention for trip-related falls. *Gait & Posture*, 38(3):500–506, July 2013.

[17] J. R. Crenshaw, K. R. Kaufman, and M. D. Grabiner. Trip recoveries of people with unilateral, transfemoral or knee disarticulation amputations: Initial findings. *Gait & Posture*, 38(3):534–536, July 2013.

[18] J. R. Crenshaw, N. J. Rosenblatt, C. P. Hurt, and M. D. Grabiner. The discriminant capabilities of stability measures, trunk kinematics, and step kinematics in classifying successful and failed compensatory stepping responses by young adults. *Journal of Biomechanics*, 45(1):129–133, Jan. 2012.

[19] E. Decullier, C. M. Couris, O. Beauchet, A. Zamora, C. Annweiler, P. Dargent-Molina, and A.-M. Schott. Falls' and fallers' profiles. *The journal of nutrition, health & aging*, 14(7):602–608, Aug. 2010.

[20] J. Dems ˇ ar, T. Curk, A. Erjavec, J. Demsar, T. Curk, A. Erjave, C. Gorup, T. Hocevar, M. Milutinovic, M. Mozina, M. Polajnar, M. Toplak, A. Staric, M. Stajdohar, L. Umek, L. Zagar, J. Zbontar, M. Zitnik, and B. Zupan. Orange: Data Mining Toolbox in Python. *Journal of Machine Learning Research*, 14:2349–2353, 2013.

[21] D. den Hartog. The Stumblemeter: Design and validation of a system that detects and classifies human stumbling during gait. 2021.

[22] J. Duysens and A. Forner-Cordero. Walking with perturbations: a guide for biped humans and robots. *Bioinspiration & Biomimetics*, 13(6):061001, 2018.

[23] A. R. Emmens, E. H. F. van Asseldonk, and H. van der Kooij. Effects of a powered ankle-foot orthosis on perturbed standing balance. *Journal of NeuroEngineering and Rehabilitation*, 15(1):50, June 2018.

[24] J. J. Eng, D. A. Winter, and A. E. Patla. Strategies for recovery from a trip in early and late swing during human walking. *Experimental Brain Research*, 102(2):339–349, Dec. 1994.

[25] J. J. Eng, D. A. Winter, and A. E. Patla. Intralimb dynamics simplify reactive control strategies during locomotion. *Journal of Biomechanics*, 30(6):581–588, June 1997.

[26] M. Eveld, S. King, K. Zelik, and M. Goldfarb. Design and implementation of a stumble recovery controller for a knee exoskeleton. In *2021 IEEE/RSJ International Conference on Intelligent Robots and Systems (IROS)*, pages 6196–6203, Sept. 2021. ISSN: 2153-0866.

[27] M. E. Eveld, S. T. King, L. G. Vailati, K. E. Zelik, and M. Goldfarb. On the Basis for Stumble Recovery Strategy Selection in Healthy Adults. *Journal of Biomechanical Engineering*, Feb. 2021.

[28] M. E. Eveld, S. T. King, K. E. Zelik, and M. Goldfarb. Factors leading to falls in transfemoral prosthesis users: A case series of sound-side stumble recovery responses. *Journal of NeuroEngineering and Rehabilitation*, 2022.

[29] A. Forner-Cordero, H. Koopman, and F. van der Helm. Mechanical model of the recovery reaction from stumbling: effect of step length on trunk control. *Journal of the Brazilian Society of Mechanical Sciences and Engineering*, 36(3):491–500, May 2014.

[30] A. Forner Cordero, H. F. J. M. Koopman, and F. C. T. van der Helm. Multiple-step strategies to recover from stumbling perturbations. *Gait & Posture*, 18(1):47–59, Aug. 2003.

[31] A. Forner Cordero, H. J. F. M. Koopman, and F. C. T. van der Helm. Energy analysis of human stumbling: the limitations of recovery. *Gait & Posture*, 21(3):243–254, Apr. 2005.

[32] K. C. Foucher, M. L. Pater, and M. D. Grabiner. Task-specific perturbation training improves the recovery stepping responses by women with knee osteoarthritis following laboratory-induced trips. *Journal of Orthopaedic Research*, 38(3):663–669, 2020. _eprint: https://onlinelibrary.wiley.com/doi/pdf/10.1002/jor.24505.

[33] G. F. Fuller. Falls in the Elderly. *American Family Physician*, 61(7):2159–2168, Apr. 2000.

[34] M. Gordon, N. Thatte, and H. Geyer. Online Learning for Proactive Obstacle Avoidance with Powered Transfemoral Prostheses. In *2019 International Conference on Robotics and Automation (ICRA)*, pages 7920–7925, May 2019. ISSN: 2577-087X.

[35] M. D. Grabiner, M. L. Bareither, S. Gatts, J. Marone, and K. L. Troy. Task-specific training reduces trip-related fall risk in women. Dec. 2012.

[36] M. D. Grabiner, S. Donovan, M. L. Bareither, J. R. Marone, K. Hamstra-Wright, S. Gatts, and K. L. Troy. Trunk kinematics and fall risk of older adults: Translating biomechanical results to the clinic. *Journal of Electromyography and Kinesiology*, 18(2):197–204, Apr. 2008.

[37] M. D. Grabiner and K. Kaufman. Developing and establishing biomechanical variables as risk biomarkers for preventable gait-related falls and assessment of intervention effectiveness. *Frontiers in Sports and Active Living*, 3, 2021.

[38] M. D. Grabiner, T. J. Koh, T. M. Lundin, and D. W. Jahnigen. Kinematics of recovery from a stumble. *Journal of Gerontology*, 48(3):M97–102, May 1993.

[39] M. Grimmer, R. Riener, C. J. Walsh, and A. Seyfarth. Mobility related physical and functional losses due to aging and disease - a motivation for lower limb exoskeletons. *Journal of NeuroEngineering and Rehabilitation*, 16(1):2, Jan. 2019.

[40] I. Guyon and A. Elisseeff. An Introduction to Variable and Feature Selection. page 26.

[41] B. J. Hafner, L. L. Willingham, N. C. Buell, K. J. Allyn, and D. G. Smith. Evaluation of function, performance, and preference as transfemoral amputees transition from mechanical to microprocessor control of the prosthetic knee. *Archives of Physical Medicine and Rehabilitation*, 88(2):207–217, Feb. 2007. Publisher: Elsevier.

[42] N. Hajj Chehade, P. Ozisik, J. Gomez, F. Ramos, and G. Pottie. Detecting stumbles with a single accelerometer. In *2012 Annual International Conference of the IEEE Engineering in Medicine and Biology Society*, pages 6681–6686, Aug. 2012. ISSN: 1558-4615.

[43] E. Halilaj, A. Rajagopal, M. Fiterau, J. L. Hicks, T. J. Hastie, and S. L. Delp. Machine learning in human movement biomechanics: Best practices, common pitfalls, and new opportunities. *Journal of Biomechanics*, 81:1–11, Nov. 2018.

[44] C. F. Honeycutt, M. Nevisipour, and M. D. Grabiner. Characteristics and adaptive strategies linked with falls in stroke survivors from analysis of laboratory-induced falls. *Journal of Biomechanics*, 49(14):3313–3319, Oct. 2016.

[45] L. Jørgensen, T. Engstad, and B. K. Jacobsen. Higher Incidence of Falls in Long-Term Stroke Survivors Than in Population Controls. *Stroke*, 33(2):542–547, Feb. 2002. Publisher: American Heart Association.

[46] J. T. Kahle, M. J. Highsmith, and S. L. Hubbard. Comparison of nonmicroprocessor knee mechanism versus C-Leg on Prosthesis Evaluation Questionnaire, stumbles, falls, walking tests, stair descent, and knee preference. *Journal of Rehabilitation Research & Development*, 45(1):1–14, Jan. 2008. Publisher: Department of Veterans Affairs.

[47] K. R. Kaufman, M. P. Wyatt, P. H. Sessoms, and M. D. Grabiner. Task-specific Fall Prevention Training Is Effective for Warfighters With Transtibial Amputations. *Clinical Orthopaedics and Related Research®*, 472(10):3076–3084, Oct. 2014.

[48] J. Kim, M. J. Major, B. Hafner, and A. Sawers. Frequency and circumstances of falls reported by ambulatory unilateral lower limb prosthesis users: A secondary analysis. *PM&R*, 11(4):344–353, 2019. _eprint: https://onlinelibrary.wiley.com/doi/pdf/10.1016/j.pmrj.2018.08.385.

[49] J. Kim, C. L. McDonald, B. J. Hafner, and A. Sawers. Fall-related events in people who are lower limb prosthesis users: the lived experience. *Disability and Rehabilitation*, 0(0):1–12, Mar. 2021. Publisher: Taylor & Francis _eprint: https://doi.org/10.1080/09638288.2021.1891467.

[50] S. T. King, M. E. Eveld, A. Martínez, K. E. Zelik, and M. Goldfarb. A novel system for introducing precisely-controlled, unanticipated gait perturbations for the study of stumble recovery. *Journal of NeuroEngineering and Rehabilitation*, 16(1):69, June 2019.

[51] S. T. King, M. E. Eveld, L. G. Vailati, K. E. Zelik, and M. Goldfarb. Development and evaluation of a powered knee stumble recovery controller for transfemoral prosthesis users, American Society of Biomechanics Conference, Aug. 2020.

[52] S. T. King, M. E. Eveld, K. E. Zelik, and M. Goldfarb. A case series of early swing perturbation recovery strategies in transfemoral prosthesis users, International Society of Biomechanics Conference, Aug. 2021.

[53] J. Kulkarni, S. Wright, C. Toole, J. Morris, and R. Hirons. Falls in patients with lower limb amputations: prevalence and contributing factors. *Physiotherapy*, 82(2):130–136, Feb. 1996.

[54] E. P. Lamers, M. E. Eveld, and K. E. Zelik. Subject-specific responses to an adaptive ankle prosthesis during incline walking. *Journal of Biomechanics*, 95:109273, Oct. 2019.

[55] B. E. Lawson, H. Atakan Varol, F. Sup, and M. Goldfarb. Stumble detection and classification for an intelligent transfemoral prosthesis. *Conference proceedings: ... Annual International Conference of the IEEE Engineering in Medicine and Biology Society. IEEE Engineering in Medicine and Biology Society. Annual Conference*, 2010:511–514, 2010.

[56] B. E. Lawson, J. Mitchell, D. Truex, A. Shultz, E. Ledoux, and M. Goldfarb. A robotic leg prosthesis: Design, control, and implementation. *IEEE Robotics Automation Magazine*, 21(4):70–81, Dec. 2014.

[57] T. Leamon and P. Murphy. Occupational Slips and Falls: More than a Trivial Problem. *Ergonomics*, 38:487–98, Apr. 1995.

[58] T. Lenzi, M. Cempini, L. Hargrove, and T. Kuiken. Design, development, and testing of a lightweight hybrid robotic knee prosthesis. *The International Journal of Robotics Research*, 37(8):953–976, July 2018. Publisher: SAGE Publications Ltd STM.

[59] F. Li, P. Harmer, K. J. Fisher, E. McAuley, N. Chaumeton, E. Eckstrom, and N. L. Wilson. Tai Chi and fall reductions in older adults: a randomized controlled trial. *The Journals of Gerontology. Series A, Biological Sciences and Medical Sciences*, 60(2):187–194, Feb. 2005.

[60] W. Li, T. H. Keegan, B. Sternfeld, S. Sidney, C. P. Quesenberry, and J. L. Kelsey. Outdoor Falls Among Middle-Aged and Older Adults: A Neglected Public Health Problem. *American Journal of Public Health*, 96(7):1192–1200, July 2006. Publisher: American Public Health Association.

[61] S. R. Lord, J. A. Ward, P. Williams, and K. J. Anstey. An epidemiological study of falls in older community-dwelling women: the Randwick falls and fractures study. *Australian Journal of Public Health*, 17(3):240–245, 1993. _eprint: https://onlinelibrary.wiley.com/doi/pdf/10.1111/j.1753-6405.1993.tb00143.x.

[62] A. Mansfield, J. S. Wong, J. Bryce, S. Knorr, and K. K. Patterson. Does perturbation-based balance training prevent falls? Systematic review and meta-analysis of preliminary randomized controlled trials. *Physical Therapy*, 95(5):700+, May 2015. Section: 700.

[63] D. Martelli, F. Vannetti, M. Cortese, P. Tropea, F. Giovacchini, S. Micera, V. Monaco, and N. Vitiello. The effects on biomechanics of walking and balance recovery in a novel pelvis exoskeleton during zero-torque control. *Robotica*, 32(8):1317–1330, Dec. 2014.

[64] A. Martínez, C. Durrough, and M. Goldfarb. A Single-Joint Implementation of Flow Control: Knee Joint Walking Assistance for Individuals With Mobility Impairment. *IEEE Transactions on Neural Systems and Rehabilitation Engineering*, 28(4):934–942, Apr. 2020. Conference Name: IEEE Transactions on Neural Systems and Rehabilitation Engineering.

[65] W. C. Miller, M. Speechley, and B. Deathe. The prevalence and risk factors of falling and fear of falling among lower extremity amputees. *Archives of Physical Medicine and Rehabilitation*, 82(8):1031–1037, Aug. 2001.

[66] A. F. Mohammad, K. A. Khan, L. Galvin, O. Hardiman, and P. G. O'Connell. High Incidence of Osteoporosis and Fractures in an Aging Post-Polio Population. *European Neurology*, 62(6):369–374, 2009. Publisher: Karger Publishers.

[67] V. Monaco, P. Tropea, F. Aprigliano, D. Martelli, A. Parri, M. Cortese, R. Molino-Lova, N. Vitiello, and S. Micera. An ecologically-controlled exoskeleton can improve balance recovery after slippage. *Scientific Reports*, 7(1):46721, May 2017. Number: 1 Publisher: Nature Publishing Group.

[68] B. Mundell, H. Maradit Kremers, S. Visscher, K. Hoppe, and K. Kaufman. Direct medical costs of accidental falls for adults with transfemoral amputations. *Prosthetics and Orthotics International*, 41(6):564–570, Dec. 2017. Publisher: SAGE Publications Ltd STM.

[69] N. M. Nachreiner, M. J. Findorff, J. F. Wyman, and T. C. McCarthy. Circumstances and consequences of falls in community-dwelling older women. *Journal of Women's Health*, 16(10):1437–1446, Dec. 2007. Publisher: Mary Ann Liebert, Inc., publishers.

[70] R. R. Neptune and C. P. McGowan. Muscle contributions to whole-body sagittal plane angular momentum during walking. *Journal of Biomechanics*, 44(1):6–12, Jan. 2011.

[71] M. Nevisipour, M. D. Grabiner, and C. F. Honeycutt. A single session of trip-specific training modifies trunk control following treadmill induced balance perturbations in stroke survivors. *Gait & Posture*, 70:222–228, May 2019.

[72] P. H. Nieuwenhuijzen, A. M. Schillings, G. P. Van Galen, and J. Duysens. Modulation of the startle response during human gait. *Journal of Neurophysiology*, 84(1):65–74, July 2000.

[73] P. W. Overstall, A. N. Exton-Smith, F. J. Imms, and A. L. Johnson. Falls in the elderly related to postural imbalance. *BMJ*, 1(6056):261–264, Jan. 1977.

[74] T. M. Owings, M. J. Pavol, and M. D. Grabiner. Mechanisms of failed recovery following postural perturbations on a motorized treadmill mimic those associated with an actual forward trip. *Clinical Biomechanics*, 16(9):813–819, Nov. 2001.

[75] I. Paran, H. Nachmani, and I. Melzer. A concurrent attention-demanding task did not interfere with balance recovery function in standing and walking among young adults - An explorative laboratory study. *Human Movement Science*, 73:102675, Oct. 2020.

[76] M. L. Pater, N. J. Rosenblatt, and M. D. Grabiner. Expectation of an upcoming large postural perturbation influences the recovery stepping response and outcome. *Gait & Posture*, 41(1):335–337, Jan. 2015.

[77] M. L. Pater, N. J. Rosenblatt, and M. D. Grabiner. Knee osteoarthritis negatively affects the recovery step following large forward-directed postural perturbations. *Journal of Biomechanics*, 49(7):1128–1133, May 2016.

[78] K. K. Patterson, I. Parafianowicz, C. J. Danells, V. Closson, M. C. Verrier, W. R. Staines, S. E. Black, and W. E. McIlroy. Gait Asymmetry in Community-Ambulating Stroke Survivors. *Archives of Physical Medicine and Rehabilitation*, 89(2):304–310, Feb. 2008.

[79] M. J. Pavol, T. M. Owings, K. T. Foley, and M. D. Grabiner. Gait characteristics as risk factors for falling from trips induced in older adults. *The Journals of Gerontology: Series A*, 54(11):M583–M590, Nov. 1999.

[80] M. J. Pavol, T. M. Owings, K. T. Foley, and M. D. Grabiner. The sex and age of older adults influence the outcome of induced trips. *The Journals of Gerontology: Series A*, 54(2):M103–M108, Feb. 1999.

[81] M. J. Pavol, T. M. Owings, K. T. Foley, and M. D. Grabiner. Mechanisms leading to a fall from an induced trip in healthy older adults. *The Journals of Gerontology. Series A, Biological Sciences and Medical Sciences*, 56(7):M428–437, July 2001.

[82] M. J. Pavol, T. M. Owings, K. T. Foley, and M. D. Grabiner. Influence of lower extremity strength of healthy older adults on the outcome of an induced trip. *Journal of the American Geriatrics Society*, 50(2):256–262, 2002.

[83] F. Pedregosa, G. Varoquaux, A. Gramfort, V. Michel, B. Thirion, O. Grisel, M. Blondel, P. Prettenhofer, R. Weiss, V. Dubourg, J. Vanderplas, A. Passos, and D. Cournapeau. Scikit-learn: Machine Learning in Python. *MACHINE LEARNING IN PYTHON*, page 6.

[84] B. Peirce. *A system of analytic mechanics*. Boston : Little, Brown and Company, 1855.

[85] M. Pijnappels, M. F. Bobbert, and J. H. v. Dieën. Push-off reactions in recovery after tripping discriminate young subjects, older non-fallers and older fallers. *Gait & Posture*, 21(4):388–394, June 2005.

[86] M. Pijnappels, M. F. Bobbert, and J. H. van Dieën. Contribution of the support limb in control of angular momentum after tripping. *Journal of Biomechanics*, 37(12):1811–1818, Dec. 2004.

[87] M. Pijnappels, M. F. Bobbert, and J. H. van Dieën. Control of support limb muscles in recovery after tripping in young and older subjects. *Experimental Brain Research*, 160(3):326–333, Jan. 2005.

[88] M. Pijnappels, M. F. Bobbert, and J. H. van Dieën. How early reactions in the support limb contribute to balance recovery after tripping. *Journal of Biomechanics*, 38(3):627–634, Mar. 2005.

[89] M. Pijnappels, I. Kingma, D. Wezenberg, G. Reurink, and J. H. van Dieën. Armed against falls: the contribution of arm movements to balance recovery after tripping. *Experimental Brain Research*, 201(4):689–699, Apr. 2010.

[90] M. Pijnappels, N. D. Reeves, C. N. Maganaris, and J. H. van Dieën. Tripping without falling; lower limb strength, a limitation for balance recovery and a target for training in the elderly. *Journal of Electromyography and Kinesiology*, 18(2):188–196, Apr. 2008.

[91] D. Pinto-Fernandez, D. Torricelli, M. d. C. Sanchez-Villamanan, F. Aller, K. Mombaur, R. Conti, N. Vitiello, J. C. Moreno, and J. L. Pons. Performance Evaluation of Lower Limb Exoskeletons: A Systematic Review. *IEEE Transactions on Neural Systems and Rehabilitation Engineering*, 28(7):1573–1583, July 2020. Conference Name: IEEE Transactions on Neural Systems and Rehabilitation Engineering.

[92] Z. Potocanac, J. de Bruin, S. van der Veen, S. Verschueren, J. van Dieën, J. Duysens, and M. Pijnappels. Fast online corrections of tripping responses. *Experimental Brain Research*, 232(11):3579–3590, Nov. 2014.

[93] Z. Potocanac and J. Duysens. Online adjustments of leg movements in healthy young and old. *Experimental Brain Research*, 235(8):2329–2348, 2017.

[94] Z. Potocanac, M. Pijnappels, S. Verschueren, J. van Dieën, and J. Duysens. Two-stage muscle activity responses in decisions about leg movement adjustments during trip recovery. *Journal of Neurophysiology*, 115(1):143–156, Nov. 2015.

[95] D. Potvin. Enabling Factors Related to Prosthetic Use by People With Transtibial and Transfemoral Amputation. 80:8, 1999.

[96] S. Rietdyk and A. E. Patla. Context-dependent reflex control: some insights into the role of balance. *Experimental Brain Research*, 119(2):251–259, Feb. 1998.

[97] P. E. Roos, M. P. McGuigan, D. G. Kerwin, and G. Trewartha. The role of arm movement in early trip recovery in younger and older adults. *Gait & Posture*, 27(2):352–356, Feb. 2008.

[98] P. E. Roos, M. P. McGuigan, and G. Trewartha. The role of strategy selection, limb force capacity and limb positioning in successful trip recovery. *Clinical Biomechanics*, 25(9):873–878, Nov. 2010.

[99] N. J. Rosenblatt, J. Marone, and M. D. Grabiner. Preventing trip-related falls by community-dwelling adults: A prospective study. *Journal of the American Geriatrics Society*, 61(9):1629–1631, 2013. _eprint: https://onlinelibrary.wiley.com/doi/pdf/10.1111/jgs.12428.

[100] A. M. Schillings, T. Mulder, and J. Duysens. Stumbling over obstacles in older adults compared to young adults. *Journal of Neurophysiology*, 94(2):1158–1168, Aug. 2005.

[101] A. M. Schillings, B. van Wezel, T. Mulder, and J. Duysens. Muscular responses and movement strategies during stumbling over obstacles. *Journal of Neurophysiology*, 83(4):2093–2102, Apr. 2000.

[102] A. M. Schillings, B. M. Van Wezel, and J. Duysens. Mechanically induced stumbling during human treadmill walking. *Journal of Neuroscience Methods*, 67(1):11–17, July 1996.

[103] A. M. Schillings, B. M. Van Wezel, T. Mulder, and J. Duysens. Widespread short-latency stretch reflexes and their modulation during stumbling over obstacles. *Brain Research*, 816(2):480–486, Jan. 1999.

[104] P. H. Sessoms, M. Wyatt, M. Grabiner, J.-D. Collins, T. Kingsbury, N. Thesing, and K. Kaufman. Method for evoking a trip-like response using a treadmill-based perturbation during locomotion. *Journal of Biomechanics*, 47(1):277–280, Jan. 2014.

[105] D. Shi, W. Zhang, W. Zhang, and X. Ding. A Review on Lower Limb Rehabilitation Exoskeleton Robots. *Chinese Journal of Mechanical Engineering*, 32(1):74, Aug. 2019.

[106] C. Shirota, A. M. Simon, and T. A. Kuiken. Recovery strategy identification throughout swing phase using kinematic data from the tripped leg. In *2014 36th Annual International Conference of the IEEE Engineering in Medicine and Biology Society*, pages 6199–6202, Aug. 2014.

[107] C. Shirota, A. M. Simon, and T. A. Kuiken. Trip recovery strategies following perturbations of variable duration. *Journal of Biomechanics*, 47(11):2679–2684, Aug. 2014.

[108] C. Shirota, A. M. Simon, and T. A. Kuiken. Transfemoral amputee recovery strategies following trips to their sound and prosthesis sides throughout swing phase. *Journal of NeuroEngineering and Rehabilitation*, 12:79, Sept. 2015.

[109] C. Shirota, A. M. Simon, E. J. Rouse, and T. A. Kuiken. The effect of perturbation onset timing and length on tripping recovery strategies. In *2011 Annual International Conference of the IEEE Engineering in Medicine and Biology Society*, pages 7833–7836, Aug. 2011.

[110] A. K. Silverman and R. R. Neptune. Differences in whole-body angular momentum between below-knee amputees and non-amputees across walking speeds. *Journal of Biomechanics*, 44(3):379–385, Feb. 2011.

[111] C. Smeesters, W. C. Hayes, and T. A. McMahon. The threshold trip duration for which recovery is no longer possible is associated with strength and reaction time. *Journal of Biomechanics*, 34(5):589–595, May 2001.

[112] A. Smith. The Serial Sevens Subtraction Test. *Archives of Neurology*, 17(1):78–80, July 1967.

[113] T. G. Sugar, A. Bates, M. Holgate, J. Kerestes, M. Mignolet, P. New, R. K. Ramachandran, S. Redkar, and C. Wheeler. Limit Cycles to Enhance Human Performance Based on Phase Oscillators. *Journal of Mechanisms and Robotics*, 7(011001), Feb. 2015.

[114] L. A. Talbot, R. J. Musiol, E. K. Witham, and E. J. Metter. Falls in young, middle-aged and older community dwelling adults: perceived cause, environmental factors and injury. *BMC Public Health*, 5(1):86, Dec. 2005.

[115] N. Thatte and H. Geyer. Toward Balance Recovery With Leg Prostheses Using Neuromuscular Model Control. *IEEE Transactions on Biomedical Engineering*, 63(5):904–913, May 2016. Conference Name: IEEE Transactions on Biomedical Engineering.

[116] N. Thatte, N. Srinivasan, and H. Geyer. Real-Time Reactive Trip Avoidance for Powered Transfemoral Prostheses. In *Robotics: Science and Systems XV*. Robotics: Science and Systems Foundation, June 2019.

[117] M. E. Tinetti, D. I. Baker, G. McAvay, E. B. Claus, P. Garrett, M. Gottschalk, M. L. Koch, K. Trainor, and R. I. Horwitz. A Multifactorial Intervention to Reduce the Risk of Falling among Elderly People Living in the Community. *New England Journal of Medicine*, 331(13):821–827, Sept. 1994. Publisher: Massachusetts Medical Society _eprint: https://doi.org/10.1056/NEJM199409293311301.

[118] A. J. van den Bogert, M. J. Pavol, and M. D. Grabiner. Response time is more important than walking speed for the ability of older adults to avoid a fall after a trip. *Journal of Biomechanics*, 35(2):199–205, Feb. 2002.

[119] J. C. E. van der Burg, M. Pijnappels, and J. H. van Dieën. Out-of-plane trunk movements and trunk muscle activity after a trip during walking. *Experimental Brain Research*, 165(3):407–412, Sept. 2005.

[120] S. K. Verma, J. L. Willetts, H. L. Corns, H. R. Marucci-Wellman, D. A. Lombardi, and T. K. Courtney. Falls and fall-related injuries among community-dwelling adults in the United States. *PLOS ONE*, 11(3):e0150939, Mar. 2016.

[121] D. J. Villarreal, D. Quintero, and R. D. Gregg. A Perturbation Mechanism for Investigations of Phase-Dependent Behavior in Human Locomotion. *IEEE Access*, 4:893–904, 2016.

[122] S. Viteckova, P. Kutilek, Z. Svoboda, R. Krupicka, J. Kauler, and Z. Szabo. Gait symmetry measures: A review of current and prospective methods. *Biomedical Signal Processing and Control*, 42:89–100, Apr. 2018.

[123] T.-S. Wei, P.-T. Liu, L.-W. Chang, and S.-Y. Liu. Gait asymmetry, ankle spasticity, and depression as independent predictors of falls in ambulatory stroke patients. *PLOS ONE*, 12(5):e0177136, May 2017. Publisher: Public Library of Science.

[124] T. Yan, M. Cempini, C. M. Oddo, and N. Vitiello. Review of assistive strategies in powered lower-limb orthoses and exoskeletons. *Robotics and Autonomous Systems*, 64:120–136, Feb. 2015.

[125] A. J. Young and D. P. Ferris. State of the Art and Future Directions for Lower Limb Robotic Exoskeletons. *IEEE Transactions on Neural Systems and Rehabilitation Engineering*, 25(2):171–182, Feb. 2017. Conference Name: IEEE Transactions on Neural Systems and Rehabilitation Engineering.

[126] F. Zhang, S. E. D'Andrea, M. J. Nunnery, S. M. Kay, and H. Huang. Towards Design of a Stumble Detection System for Artificial Legs. *IEEE Transactions on Neural Systems and Rehabilitation Engineering*, 19(5):567–577, Oct. 2011.

[127] J. Zhang, P. Fiers, K. A. Witte, R. W. Jackson, K. L. Poggensee, C. G. Atkeson, and S. H. Collins. Human-in-the-loop optimization of exoskeleton assistance during walking. *Science*, 356(6344):1280–1284, June 2017. Publisher: American Association for the Advancement of Science Section: Report.

[128] A. Zoss, H. Kazerooni, and A. Chu. Biomechanical design of the Berkeley lower extremity exoskeleton (BLEEX). *IEEE/ASME Transactions on Mechatronics*, 11(2):128–138, Apr. 2006. Conference Name: IEEE/ASME Transactions on Mechatronics.